RR Lyrae stars and the Blazhko effect

By

Robert Lipka

Submitted in fulfilment of the requirements for the Degree of Doctor of Philosophy

School of Physics

The University of Tasmania

April 2012

Declaration of Originality

This thesis contains no material which has been accepted for a degree or diploma by the University or any other institution, except by way of background information and duly acknowledged in the thesis, and to the best of my knowledge and belief no material previously published or written by another person except where due acknowledgment is made in the text of the thesis, nor does the thesis contain any material that infringes copyright.

(Robert Lipka)

Acknowledgments

This PhD has been a long journey with breaks and stumbles. I have changed into a different person in the time it took me to complete it. I can honestly say the majority of who I am right now has developed in the same time. The stories are too numerous to tell. In hindsight I would improve how I have done some things but in the now I am very happy to have reached this point and would not go back into the past. The clearest thing in my mind is that in science just like in life we build upon the support we receive from others. Such as it is and irrespective of how hard I may try to succeed alone this thesis would not exist without the support of a large number of people.

I want to thank my parents for all the support given to me in many forms over all these years. The continuing support I have received from Dr John Greenhill has made everything else possible. I want to thank Dr Simon Ellingsen for putting up with me for a number of years. I wish to thank the supervisors whose suggestions directed me in the past: Dr Jean-Philippe Beaulieu, Dr Bob Watson and Dr Raymond Haynes.

The PLANET collaboration provided the data on which I started the thesis. I want to thank all the people involved for the work in gathering it. I am also grateful for the software, information and support I received from within this group. I could not have done a thing without all of this.

I want to thank the OGLE group for giving me access to data and advice without which large parts of my work would be impossible: to Dr Tomasz Mizerski for help with his catalogue; to Professor Andrzej Udalski for his support with obtaining OGLE data; to Professor Igor Soszynski for his work in providing data and for putting up with my questions. All this help is all the more appreciated because it did not have to be provided.

I wish to thank all my friends who remain around me after all these years and who variously kept me either sane or crazy but who supported me at many times: David Stejskal, Cliff Senkbeil and Cheng Han Kea. You guys know most of the stories ☺

Thanks also goes to a little furball now running around on another continent for keeping me happy and grounded on more than one occasion without speaking much. Dogs rule.

ABSTRACT

A survey of RR Lyrae stars in the observations of the PLANET collaboration between the years 1995 and 2005 is presented. An exhaustive search of the data has identified 87 RR Lyrae stars and 10 of them exhibit a detectable Blazhko modulation. Lightcurves of the stars are produced through combining data from all the telescopes contributing to PLANET and the stars are well described in a catalogue format. Attempts to constrain models for the Blazhko effect lead to a comparison of the PLANET data to OGLE microlensing survey observations. It is established that the methods used for identifying the RR Lyrae stars in the PLANET data produce a complete detection of these stars in the areas that were observed. Further, the use of the OGLE data produced results supporting magnetic models for the Blazhko effect.

New equidistant frequency quintuplets have been discovered in the lightcurves of two Blazhko stars. Such frequency quintuplets are a requirement of the magnetic models attempting to explain the Blazhko effect. The Blazhko effect has remained unexplained for over 100 years and represents a well known and persistent puzzle in variable star research. Competing models for explaining this effect have been developed but all lack conclusive support from observations. In recent years only six other detections of a frequency quintuplet in a Blazhko star have been published (Hurta et al 2008, Jurcsik et al 2008, Kolenberg et al 2009, Jurcsik et al 2009, Chadid et al 2010, Kolenberg et al 2011). This work provides additional support for the magnetic model explanation of the Blazhko effect by showing that frequency quintuplets in Blazhko stars are relatively common and are not an analysis or data artefact. Error and significance analysis shows that the detected frequency quintuplets have small amplitudes but are significant and occur very close to the positions required by the magnetic models.

It is shown that the previous absence of frequency quintuplet detections in Blazhko stars was most likely caused by the lack of data suitable for their detection and this has affected the explanation of the Blazhko effect. It can no longer be said that the absence of frequency quintuplets in Blazhko stars is an inconsistency with the magnetic models. Results supporting these theses are given and specific future research is described that in combination with the detection of frequency quintuplets should further constrain which models for the Blazhko effect best agree with observations.

Contents

1 What art thou RR Lyrae star?

1.1 Introduction

1.1.1 Old stars

RR Lyrae stars are stars that have evolved off the main sequence. They are low-mass red giants in the core helium burning stage of their lives and as such they are also old stars (McWilliam 2011 among others). Most belong to Population II. They tend to have high radial velocities, and move fast in a way characteristic of Population II (Smith 1995). Non-trivial differences in age exist among them, demonstrated by metallicity and motion distribution differences. For example some 25 percent of these stars in the galactic disc in the solar neighbourhood are only slightly to moderately metal deficient relative to the Sun, and have rotation speed about the Galactic centre of about 200 km/s (Smith 1995 p 8). These are believed to belong to the thick disc population, part of the vanguard of the younger Population I (Preston 1959, and numerous more recent papers on RR Lyrae metallicity and distribution, Castellani *et al* 1981, Suntzeff 1992, Borkova and Marsakov 2003, Sarajedini *et al* 2006, being a few examples). RR Lyrae stars are the most numerous clearly defined class of variable stars observed so far. More than seven RR Lyrae stars are known for each Cepheid or W Virginis star within the Galaxy (Smith 1995 p 6). Studying RR Lyrae stars defines stellar pulsation research. RR Lyrae stars are involved in all stellar pulsation research at some level. Pulsation principles learned from RR Lyrae stars can be applied to other variable stars.

1.1.2 Radial Pulsation

Over time, as knowledge about RR Lyrae stars accumulates, the known properties of this group alter and expand. The defining feature of RR Lyrae stars is variable light output caused by radial pulsation in their outer layers, occurring in old red giant stars with periods of above ~ 0.2 days and changes in amplitude of above ~ 0.2 mag in V band (Soszynski *et al* 2011). The lower bounds of these two proprties are relatively well delimited by the presence of other types of variable stars, and numerous examples of RR Lyrae stars. The upper bounds are characterised by atypical and much less numerous RR Lyrae variables, and are thus less well defined, but without confusion with other types of variables when all the characteristics of RR Lyrae stars are assessed together. The longest period RR Lyrae stars have periods of a little over 1 day (Schmidt *et al* 1990). The majority of these stars have a period below 0.8 days. The highest luminosity changes for RR Lyraes are around 1 mag (Kinman and Brown 2010), but can go up to around 1.6 mag in the V band (Szczygieł *et al* 2009). These variations are recorded in a lightcurve, a plot of light intensity against time. For the majority of these stars this results in a lightcurve of a characteristic shape, a sinusoid distorted to varying degrees of asymmetry. The same general pattern applies to all the group members, for example see Figure 1.2, but details of the shapes vary considerably. During a pulsation cycle as the star shrinks in radius its luminosity decreases and as it expands it increases. Due to the details of heating, cooling, and the ionisation reactions driving these, the changes in radial size or velocity are not exactly in phase with the changes in light output (for example Smith 1995). There are also suggestions of non-radial pulsation modes contributing significantly to the variations in luminosity at least in some RR Lyrae stars, but this is part of ongoing research (see the "RR Lyrae Pulsation" section).

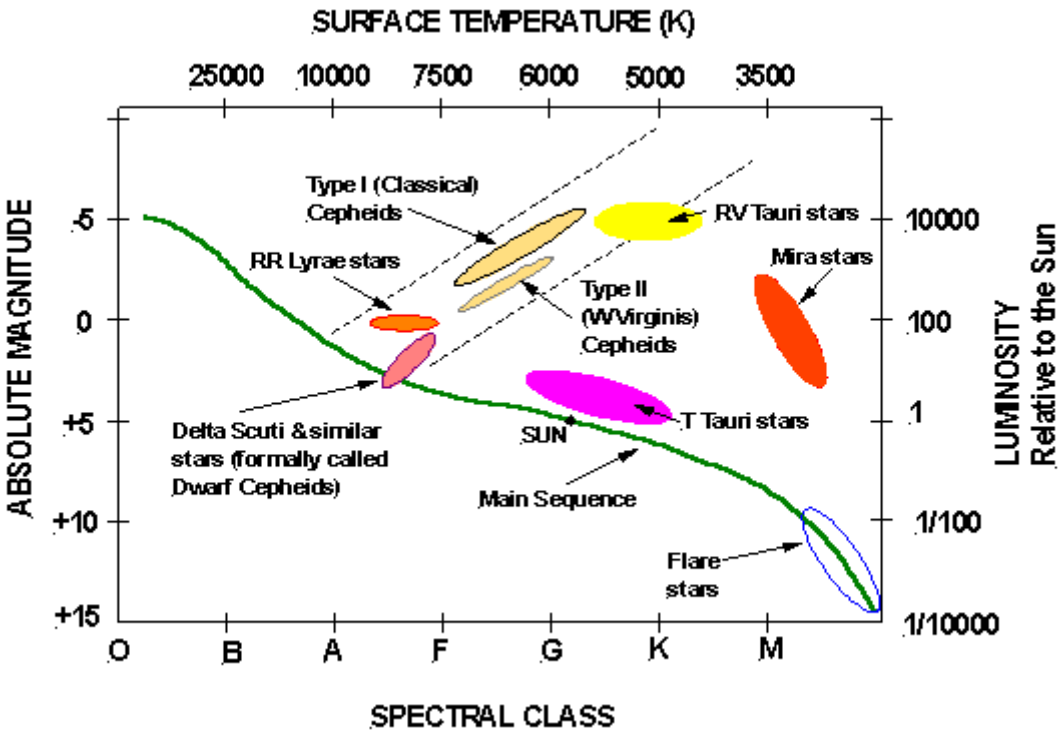

Figure 1.1: An approximate position of RR Lyrae stars in a HR diagram (image obtained from http://webs.mn.catholic.edu.au/physics/emery/hsc_astrophysics_page3.htm).

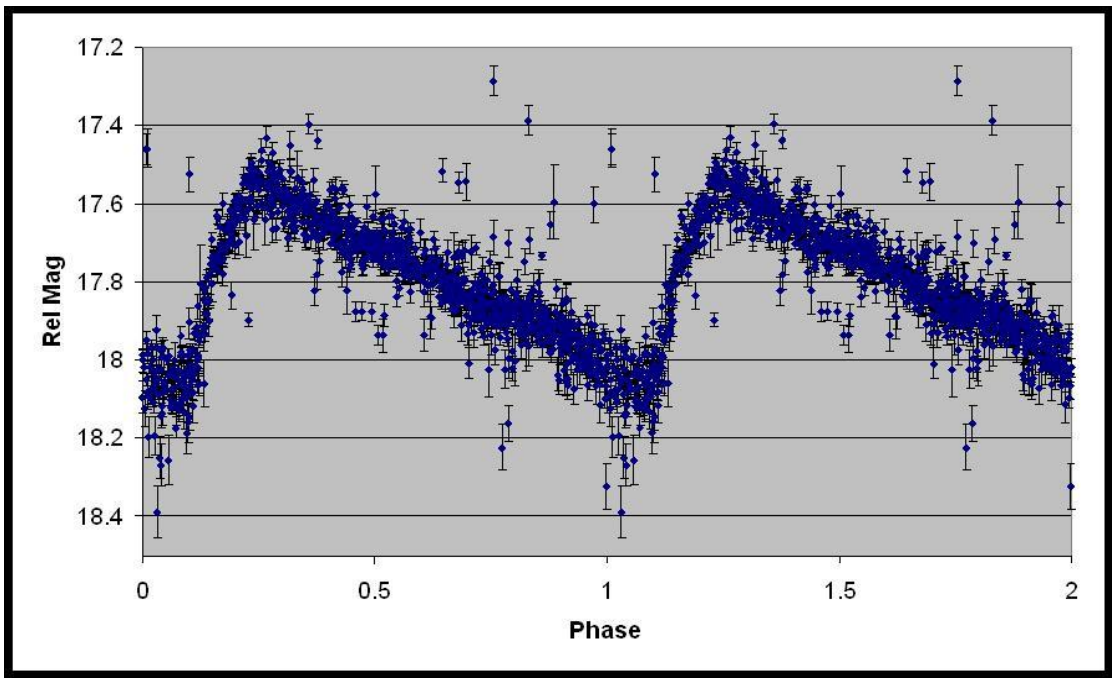

Figure 1.2: An example of type ab RR Lyrae lightcurve plotted over two cycles to emphasise the shape

1.1.3 Curriculum Vitae

Mass is very unequally distributed in RR Lyrae stars – it has a structure typical of a Red Giant. The dense core with a radius of about 5 Earth radii contains ~ 0.5 $M_{\odot}$, while the outer 50 percent of the star's radius is of very low density with little mass, on the order of 0.001 $M_{\odot}$. The mass of an average RR Lyrae star is ~ 0.7 $M_{\odot}$. Their radius varies between 4 – 6 $R_{\odot}$. As the star pulsates the difference between the maximum and minimum radius of a RR Lyrae star is on the order of 15 percent of its mean radius. RR Lyrae stars are bright - luminosity is a few dozen times solar. The average absolute magnitude of these stars is +0.6 ± 0.2 at least for the metal-poor or usually Population II stars, and is in itself uncertain (Smith 1995 pp 8 – 15). The uncertainty in average luminosity of RR Lyrae stars is part of real variations, across a narrow range, in light output among members of the group, rather than purely due to accuracy of measurements. More precise understanding of the structure and light output of these stars is part of the effort behind refining them to become distance indicators (for example, recently, Bono G. 2003, Muzzin *et al* 2004, Jesper 2006, Del Principe *et al* 2006). The relatively metal-rich RR Lyrae stars are less luminous than their metal-poor counterparts, at least according to substantial current evidence. The mean effective temperature varies from 6100 K to 7400 K, with the RRab group (see below) being the coolest, and the RRc group being the hottest. The effective temperature determination varies by up to 300 K between the methods used (for example Smith 1995).

1.2 Where in space are RR Lyrae stars?

1.2.1 Globular clusters

RR Lyrae stars were first identified in globular clusters at the end of the nineteenth century. They were classified as RR Lyraes a little later (Bailey 1902), and over time the definition and

membership of the group evolved towards the current understanding. This type of star was and still is strongly associated with globular clusters. An isolated cluster provides a convenient sample of stars with nearly the same starting composition; this removes some of the variability in the initial conditions of its members, allowing a more constrained assessment of their evolution. This common origin of RR Lyrae stars within a particular globular cluster is precisely how their study has been approached at the beginning, and even currently it remains the standard way of studying these variables. For example, metallicity influences on the properties of RR Lyrae stars, differences in average periods and proportions of variability types in globular clusters, all become clearer (starting with Arp 1955) when correlated with the chemical composition of these clusters and similar ages of stars within a cluster. Most variable stars identified up to today within the globular clusters are still of this type. Nevertheless, today the number of known RR Lyrae stars found outside of globular clusters greatly outnumbers those within.

1.2.2 Galactic Bulge

RR Lyrae stars in the galactic bulge are observed through "windows", areas where the interstellar absorption is reduced. Baade's Window (l = -1°, b = -4°) is perhaps the best known. The emphasis is on the use of RR Lyrae stars in the determination of the distance to the galactic centre and its structure and evolution. It is argued from stellar evolution models that among all the locations the bulge RR Lyrae stars are the oldest. Modelling of the horizontal branch morphology and RR Lyrae stars has shown that these stars are 1.3 ± 0.3 Gyr older than in the Halo (Lee 1992). If the age of halo globular clusters is in the range of 14 – 17 Gyr, and the Bulge stars are even older, this presents a problem for the value of the Hubble constant by putting a lower limit on the age of the Universe of up to 18 Gyr (Smith 1995; Renzini 1999). Thus the Hubble constant is constrained well below 90 km/s/Mpc. This would be in general agreement with the Hubble constant derived from WMAP (Wilkinson Microwave Anisotropy Probe) at the value of 70 km/s/Mpc +2.4/-3.2

(Spergel *et al* 2003), the most recent result with small uncertainties, but straining the agreement with the age of the universe of 13.7 ± 0.2 Gyr from the same source. This is similar to the problem for the ages of RR Lyrae stars determined in globular clusters and the Magellanic Clouds. Thus RR Lyrae stars also provide another constraint to the age of the Universe and results from other fields but some of the results are contradictory (Smith 1995 p p 62 – 63).

1.2.3 Galactic disc

The largest number of observed RR Lyrae stars are found in the galactic disc, also called field RR Lyrae stars. Unlike the case in galactic globular clusters these field stars occur across a mixture of populations, both Population II and Population I, and the finer subdivisions such as the Thick Disc population (among others, Gilmore et al 1990). Furthermore disc RR Lyrae stars are a mixture across metallicity, with stars having up to and even slightly above solar metal content.

1.2.4 Extragalactic

The Large and Small Magellanic Clouds, distant some 50 and 60 kpc, respectively, are the nearest systems to the Milky Way displaying both old stars and ongoing star formation. Since RR Lyrae stars are faint in comparison to standard candles like the Cepheids, it was only in 1951 that the first RR Lyrae stars were discovered in the Large Magellanic Clouds (Thackeray and Wesselink 1953). RR Lyrae stars occur in the Magellanic Clouds in clusters analogous to the galactic globular clusters, and as field stars. In the Magellanic Clouds the youngest cluster RR Lyrae stars seem to be about 12 Gyr old (Smith 1995). This is an indication that the RR Lyrae stars need at least this much time to evolve their characteristic variability. If applicable to our Galaxy, this means that disc stars were forming at least this long ago, assuming that the Galaxy and the Magellanic systems share similar if not exactly the same origins. It is not a definitive proof that younger RR Lyrae type

variables cannot evolve elsewhere under different conditions. Magellanic RR Lyrae stars tend to have parameters slightly different from the Galactic stars, reflecting different environments, different starting metallicities, and perhaps different evolutionary paths. In particular the LMC RR Lyrae stars show a larger fraction undergoing second harmonic pulsation than occurs in the Galaxy. The ratio of periods for double mode RR Lyrae stars, first overtone to fundamental, is below any Galactic RR Lyrae stars. This is however based on only two objects in the LMC. This subclass of RR Lyrae stars is relatively rare in the Galaxy as well. The average period of known RR Lyrae stars is different between the Galaxy and the LMC and has a different distribution for each location (Alcock et al 1996). Currently both Magellanic Clouds are targets of intensive surveys with the aim to detecting more of all types of RR Lyrae stars (Mizerski 2003; Alcock et al 1996).

There are eight dwarf spheroidal galaxies within about 250 kpc of the Milky Way (Smith 1995), plus the more recently discovered Sagittarius Dwarf Elliptical Galaxy (Ibata et al 1994) and the Canis Major Dwarf (Martin et al 2004). The first extragalactic RR Lyrae stars were discovered in Sculptor and Fornax galaxies in 1939 (Baade and Hubble 1939), and thus were known earlier than even the ones in the Magellanic Clouds. RR Lyrae stars have been identified in six of these small galaxies for some time (Smith 1995), and more recently in Leo I (Held E. V. et al 2001), in Fornax through a combination of the colour magnitude diagram, and the correlation of variability between observations in the V and I bands, without specifying individual stars outside of their CMD (Bersier and Wood 1999), and in globular clusters around Fornax (Mackey and Gilmore 2003). Therefore by now RR Lyrae stars have been detected in all the galaxies in the immediate neighbourhood of the Milky Way. As expected these stars are a general feature of stellar evolution and are not specific to the Milky Way, and being plentiful they make desirable distance indicators and evolutionary probes of the Local Group. This application of RR Lyre stars is limited by the uncertainties in their absolute magnitudes, arising mainly from a lack of sufficient knowledge about their behaviour, and not observational accuracies of magnitude measurements.

The detection of RR Lyrae stars in the Andromeda galaxy had to await the use of CCD detectors at large telescopes, around 5 meter class instruments, and later access to the data from the Hubble Space Telescope. Beginning in 1987 a few hundred RR Lyrae stars have been detected in the Andromeda galaxy (Pritchett and Bergh 1987; and more recently for example Brown et al 2004), and its dwarf elliptical companions (Saha and Hoessel 1987). Most of these are found in the companions. However, where available the periods and lightcurves for these are less reliable than in other areas because of the distance. Ultimately with CCD detectors on 4m-class telescopes and with conditions of excellent seeing, RR Lyrae stars can be detected out to a distance of 1 Mpc. With the Hubble Space Telescope photometric observations of RR Lyrae stars will be feasible out to a distance of 3 Mpc (Pritchett 1988), although getting sufficient telescope time for accurate lightcurve determination at these distances is likely to be the main problem.

1.2.5 Numbers

By the 1990s, when for all practical purposes all of the Galactic globular clusters were long surveyed for RR Lyrae stars, there were 27 globular clusters without any identified RR Lyrae star and 77 globular clusters with at least one (Suntzeff *et al* 1991). The number of them within a globular cluster varies from none to around 260, with around 1900 identified in all galactic globular clusters. Assuming a near completion of the RR Lyrae searches in Galactic globular cluster, taking into account the difficulty of identifying variable stars near the centres of globular clusters, and correcting for possible foreground stars, an estimate for the total number of RR Lyrae stars in the globular clusters of the Galaxy is given at 1945 ± 40 (Suntzeff *et al* 1991). As of this time most RR Lyrae stars in Galactic globular clusters have been discovered, with only around 6 percent remaining undiscovered. This conclusion and the stability of the result is confirmed by a literature

review on variable stars in Galactic globular clusters up the year 2001 that identifies approximately 1800 RR Lyrae stars (Clement *et al* 2001), little changed from and in agreement with the older prediction. Similarly most globular clusters around the Milky Way would probably have been discovered by now, and thus the inventory of Galactic globular cluster RR Lyrae stars is nearly complete. In particular, the number of known globular clusters has been slowly increasing in recent times as more sensitive observations are carried out (for example see the summary in Bonatto *et al* 2007), 7 new Galactic globular clusters have been identified since 2003, with further 11 objects being possible globular clusters. By comparison as of 2003 there were 150 known Galactic globular clusters (Harris 1996, 2003 update at http://www.physics.mcmaster.ca/~harris/mwgc.dat). The number of detected field RR Lyrae stars stands at around 7000 – a very small fraction of the RR Lyrae stars that are out there. This includes all the known stars in the Halo, the thick disc, and in the Bulge. One estimate puts the number of these variables at 85,000 in the region between 4 and 25 kpc from the galactic centre (Suntzeff, Kinman, and Kraft 1991), thus excluding the Bulge and the thick disc. The total number of RR Lyraes in the Galaxy, including those in the Galactic Bulge and in the thick disc, is substantially larger still. Thus, unlike in the case of Galactic globular clusters (Suntzeff *et al* 1991, Clement *et al* 2001, see the argument above), everywhere else in the Galaxy most of the RR Lyrae stars are still waiting to be discovered. Accordingly, more recently, 2700 RR Lyrae stars have been identified in OGLE II data in the centre of the Galaxy (Mizerski 2003), effectively in the Bulge. Outside of globular clusters, a convenient package of stars in one location, RR Lyrae identification requires and is limited by survey coverage. As of mid 1990s the number of RR Lyrae stars in the Magellanic clouds was at around two hundred in the clusters, and another couple of hundred of field stars. This changed in a very short period of time. The numbers of known Magellanic RR Lyrae stars grew rapidly with the star surveys in the area. For example by 1996 the number of RR Lyrae stars in the Large Magellanic Cloud alone reached almost eight thousand from the MACHO project alone (Alcock et al 1996), and 7612 RR Lyraes from the OGLE II project (Soszynski et al 2003), although it is not specified in the paper explicitly how many of these stars

are common to both catalogues. It has been estimated that in total the LMC contains about 10^4 type ab RR Lyrae stars (Kinman et al 1991), see the next section for definition. The dwarf spheroidal galaxies associated with the Milky way contain altogether around 1000 identified RR Lyrae stars (Smith 1995, Bersier and Wood 1999, Held E. V. et al 2001, Mackey and Gilmore 2003). The number of RR Lyrae stars in the remaining extragalactic locations is limited only by the observing method, currently the known total is on the order of thousands. This is a dynamic field under multiple investigations, and the numbers of known RR Lyrae stars are increasing constantly.

1.3 The cast

1.3.1 RRab

RR Lyrae stars are subdivided according to the type of pulsation they exhibit, and this is correlated to their lightcurve shapes and other properties. The largest group is the RRab stars (RR Lyrae stars, or RR Lyraes of type ab), or fundamental frequency radial pulsators. The pulsation occurs in the radial direction in layers around the star, and at the fundamental frequency it has only one node in the interior and one antinode at the surface (see the RR Lyrae pulsation section for a more detailed description). Formerly this type was separated into two groups RRa and RRb now recognised as two boundaries of the same process, with the RR Lyraes spanning the full continuum between the two. At the RRa boundary the following properties apply: the amplitude of luminosity variation is near to or greater than 1 magnitude; the average period is about 0.5 day; the lightcurve shows a strong asymmetry. The asymmetry is defined as the ratio of the time occupied by the rising part of the lightcurve to that of the pulsation period. At the RRb boundary the following properties apply: the amplitude of luminosity variation is less at between 0.5-0.8 magnitude; the period longer at ~0.7 days; the lightcurve is more rounded and its asymmetry less marked (Bailey 1902). RRab

stars span the whole range between these two boundaries. Compare Figure 1 and 2 for an example of different asymmetries in RR Lyrae lightcuves.

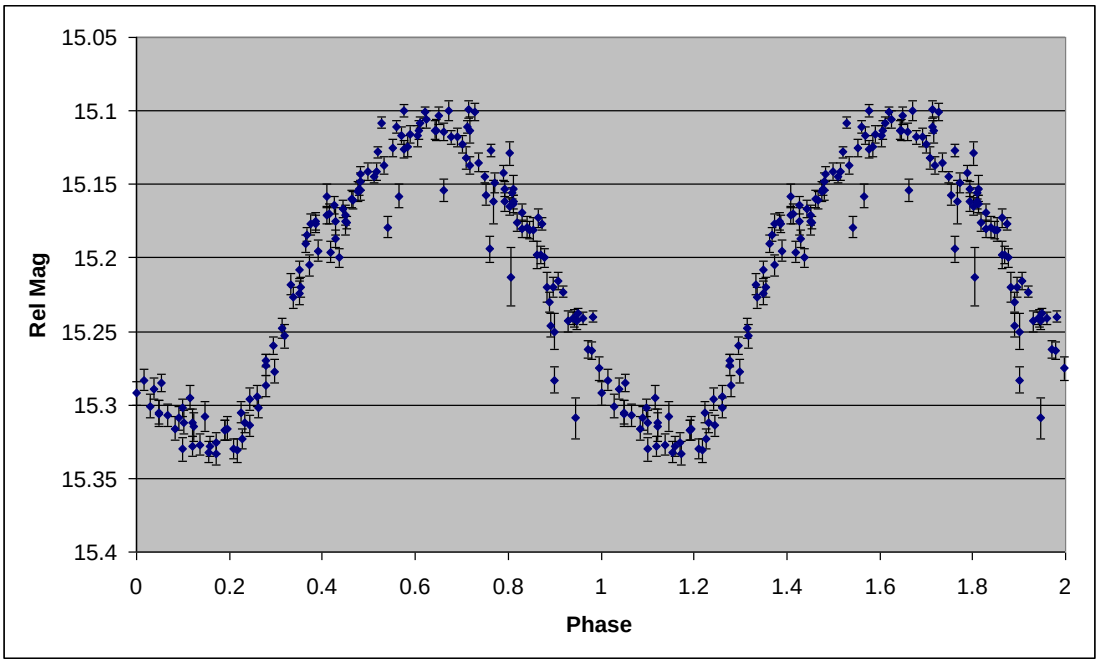

Figure 1: An example of type c RR Lyrae lightcurve plotted over two cycles to emphasise the shape. This lightcurve is an example of a more symmetric, close to sinusoidal shape.

1.3.2 RRc

The RRc stars are first overtone frequency radial pulsators. This is the analogous radial pulsation to that in type ab RR Lyrae stars, but in this case there are two nodes in the interior, and an antinode, plus an antinode at the surface. Their lightcurves have low asymmetry – they are almost sinusoidal with a rounded maximum. The amplitude of luminosity variation is close to 0.5 magnitudes. The average period is relatively short at about 0.3 day. Among known Galactic field RR Lyrae stars, those outside the globular clusters, 91 percent are of type RRab and only 9 percent of the type RRc. However RRc variables have lower pulsation amplitude so they are less likely to

be detected. Hence these figures may be an underestimate of the fraction of RRc stars in the Galactic field (Smith 1995 various pages).

1.3.3 RRd

The RRd stars are double mode pulsators. They exhibit radial pulsation at both the fundamental and first overtone frequencies. Stellar pulsation theory predicts that the first overtone pulsation period is between about 0.74 to 0.75 as long as the fundamental period (Smith 1995), and this is in agreement with observations (for example Klaus and Wils 2006, Clementini *et al* 2004, among the most recent identifications), with possible exceptions down to a ratio of 0.717 for one star (Jerzykiewicz 1995). This results in a beat frequency in the lightcurve of ~1 to 2 days. These stars have only been identified relatively recently (Sandage et al 1981), only a few dozens are known in the Galaxy. As of 1997 the largest number of them has been identified by the MACHO project in the Large Magellanic Cloud, a total of 73 RRd stars among a database 7900 RR Lyrae stars. This gives a fraction of just under 1 percent of RRd stars among all RR Lyrae stars in that sample. Their numbers in the Galaxy are too small and localised to provide a meaningful overall Galactic fraction. In contrast to the LMC the number of RRd stars in the Galactic Bugle is a much smaller fraction. Among the OGLE II RR Lyraes there are only 3 RRd stars out of around 2700, an incidence rate about ten times less than in the LMC (Mizerski 2003). RR d stars are especially useful because the presence of the two oscillation modes in the same star allows the determination of their mass more accurately than other methods, see below.

1.3.4 RRe

The RRe stars are classified as second overtone pulsators. They are the most recently discovered class of RR Lyrae stars. Though, Kovács 1998 suggests that the proposed RRe stars are ordinary

RRc stars at the short-period end of the instability strip. Kovács 1998 summarises the evidence against the existence of this type of RR Lyrae stars under three main arguments: compared to RRc stars the lightcurves of proposed RRe stars do not show any distinguishing features and features predicted by some theoretical models are absent; the periods of RRe candidates in M68 and IC4499 are incompatible with the stars pulsating in the second overtone based on their relative magnitudes and colours; hydrodynamical calculations suggest that the chances of second overtone pulsation occurring in the observed period range are "slim". The existence of RRe stars has been suggested for some time, and recently supported by for example the MACHO survey finding 272 RRe stars (Soszynski et al 2003). The stars in MACHO are classified as RRe through relating their periods to amplitudes and other lightcurve Fourier parameters and all these descriptors overlap to varying amounts for all RR Lyrae types. The RRe stars are a new group with not yet firmly established properties.

1.4 Genesis

1.4.1 Evolution of a low mass star

1.4.1.1 Main sequence

A RR Lyrae begins as a low-mass star of around 0.8 $M_{\odot}$. It spends a long time on the main sequence, perhaps about 15 Gyr, fusing hydrogen to helium in its core. It should be noted that the 15 Gyr figure is in the upper range of possible values and in contradiction to the age of the Universe from other sources. Its radius and luminosity increase somewhat over time, but it remains on the main sequence largely unchanged until core hydrogen becomes exhausted (Smith 1995 p 12).

1.4.1.2 Red giant

Next the stars start fusing hydrogen in a thick shell around its helium core. At this stage its radius increases faster than luminosity and the star reddens in colour, swells, and brightens. As more hydrogen is used up the surface temperatures drop and convection extends deeper into the star's interior. It brightens rapidly. Meanwhile the helium from hydrogen fusion accumulates and the core contracts to such densities that its electrons become degenerate. The star becomes a red giant with a very dense, small, and hot core, and very rarefied, much cooler, large and convection dominated envelope (Caputo 1985).

1.4.1.3 Zero age horizontal branch

Eventually the core accumulates to densities sufficient to initiate helium fusion. The core temperature becomes high enough for helium fusion via the triple alpha process, which begins in the so-called helium flash. This removes the core degeneracy and the star then proceeds to the zero-age horizontal branch and the core helium burning stage of its existence. Its radius and luminosity are much reduced from what it was at the end of its existence as a red giant. It is at this stage that a star of appropriate composition pulsates as a RR Lyrae for about one hundred million years until the helium in its core is depleted (Smith 1995 p 13, Caputo 1985). Thus the RR Lyrae phase of a low mass star is only a very small fraction of its total energy producing lifetime, which is around 10 billion years.

1.4.1.4 Asymptotic red giant branch and exit

As core helium exhaustion approaches the RR Lyrae star leaves the horizontal branch. It swells, cools, and moves onto the asymptotic red giant branch. It burns fuel in a helium and a hydrogen shell around its carbon and oxygen core. In the end the star uses up all of its available hydrogen and helium fuel and ends as a white dwarf (Smith 1995).

1.4.2 The instability strip

The RR Lyrae instability strip is a continuous area in the horizontal branch part of a colour-magnitude diagram where these variables fall. The blue and red edges of the instability strip lie near $(B\text{-}V)_0$=0.18 and 0.40, corresponding to effective temperatures of about 7400 K and 6100 K respectively. Schwarzchild (1940) concluded that a "star which can pulsate does pulsate" and that "in a colour-magnitude diagram one ought not to find any non-variables in a region occupied by variables. Horizontal branch stars within the bounds of the instability strip pulsate as RR Lyrae stars. Horizontal branch stars outside of it, are not variable, or are variables of non RR Lyrae type. The RRc stars are generally bluer than the RRab variables and so help define the blue edge of the instability strip. RR Lyraes near the red edge are of type ab. Thus if a star's evolutionary track crosses the RR Lyrae instability strip, it will pulsate as a RR Lyrae. However, a star may arrive into this instability strip from a part of the horizontal branch outside of it, or even get pushed into it either by mass loss or gain during its lifetime. The star's metallicity will alter how it evolves and when it starts to pulsate. Furthermore the edges of the instability strip are not precisely determined, and are depended on chemical composition and perhaps other variables. Thus the instability strip is not merely defined by colour and magnitude, but more correctly can be thought of as a multidimensional volume based on all parameters affecting it. In other words defining the edges of the instability strip in terms of a HR diagram alone may not account for all the variables affecting

whether a star pulsates and may make the edges of the instability strip transitional rather than sharply defined. The judgment on the universal applicability of Schwarzschild's conclusion is still reserved (Smith 1995) – there are rare cases of non-variable stars in globular clusters apparently belonging to the instability strip. For example a single globular cluster star located well within the instability strip for the cluster has been shown to be non-variable (Smith 1985) in photoelectric observations, but the same star, along with another star in the same situation in the same cluster, are shown to have the expected variability of RR Lyrae type at a small level when measured with a CCD detector (Clement and Rowe 2001). Hence Schwarzchild's conclusion is maintained up to this time.

1.5 Make-up

1.5.1 Metallicity variations and locations

A RR Lyrae star is not simply described by its mass and metallicity. The proportions of the elements making up all stars tend to increasingly differ with greater physical distances between them. Stars forming at different locations will form from different gas and dust. A star's metallicity is an overall measure of heavier elements it contains in the observable portions. Furthermore the star's structure and chemical distribution determines observable light. Two stars with exactly the same average chemical content but different internal distribution of elements would behave differently. For example if for two stars forming in the same area some influence caused different proportions of various elements to end up in the core versus the outer layers, the two stars would be observed as different types. Settling and diffusion of the chemical elements in the star affect the distribution of material within it. Differences in the starting condition of the star, such as higher spin, the presence of companions, induced mass loss or mass gain from outside of it, can affect the

evolution of its properties even in the case of the same starting chemical composition. These possible modifiers will affect the observed metallicities, and the properties of RR Lyrae stars.

In the standard MK spectral classification system stars are assigned a spectral type based on the strength of the lines of their spectra, and a luminosity class ordered by brightness (Morgan and Keenan 1973, and a recent extension Kirkpatrick 2005). The system is flexible in that spectral types and luminosity classes can be added as necessary. The metal rich RR Lyrae stars can be assigned a nearly consistent spectral classification in the MK system (Smith 1995). However, as the metallicity decreases this system breaks down for RR Lyrae stars, and their classification becomes dependent on the absorption line used to establish it. The spectral type of RR Lyrae stars as determined from the hydrogen Balmer lines was often different than the one derived from the Ca II *K*-line. This result points to a difference in the chemical make-up of outer layers of RR Lyrae stars and/or differences in their physical conditions as compared to the more standard stars used to establish the MK system. The difference became the basis for Preston's Δ*S* index (Preston 1959). In particular the difference in spectral type of a RR Lyrae star at minimum light as determined from the hydrogen Balmer lines (Sp(H)), and the Ca II *K*-line at 3933 Å (Sp(K)), is defined as the index Δ*S*. The index is:

$$\Delta S = 10[\mathrm{Sp(H)} - \mathrm{Sp}(K)].$$

This establishes a more consistent spectral classification of RR Lyrae stars. The index has been calibrated by different authors.

Butler (1975): $[\mathrm{Fe/H}] = -0.23 - 0.16\Delta S$

Blanco (1992): $[\mathrm{Fe/H}] = -0.02(\pm 0.34) - 0.18(\pm 0.05)\Delta S$

Suntzeff et al (1991): $[\mathrm{Fe/H}] = -0.408 - 0.158\Delta S$

The ΔS index indicates metal abundance, and is usually calibrated as a linear relation with [Fe/H] of opposite gradient (ΔS increases as metallicity decreases and vice versa). Periods of RR Lyrae stars are correlated to the ΔS index. Periods of RR Lyrae stars and proper motions increase in tandem. The short period RRab variables, of low ΔS, and high metallicity, lie close to the galactic plane, and have small motions relative to the Sun (Smith 1995).

Periods of RRab and RRc RR Lyrae stars increase slightly with decreasing metallicity, similar correlations have been found for these variables in globular clusters and in the galactic field (among others Kemper 1982; Preston 1995). The more metal-poor globular clusters have RR Lyraes which are brighter and of longer period at a given effective temperature. Similarly by location and the usually greater metallicity in the Galactic disc, the shorter period RRab variables lie close to the Galactic plane, they have small motions relative to the Sun and can be termed metal-rich RR Lyraes. The RR Lyrae population in the solar neighbourhood includes a significant metal-rich component, 25% of these RRab stars have [Fe/H] > -0.55. The motion relative to the Sun increases up to the velocities associated with halo stars as one goes to metal-poor RR Lyraes (Smith 1995). Thus the metallicity of RR Lyrae star varies, and their properties depend significantly on it.

Historically globular clusters have been the favourite venue for studying a sample of RR Lyraes formed with the same starting conditions. The stars within a single globular cluster can be regarded as having been formed with a common chemical composition, at essentially a single location, at about the same time. This scenario can be disrupted by changing any of these postulates, but in the Galaxy this seems to have occurred for only one globular cluster, ω Centauri (for example Romano et al 2007). ω Centauri has an unusually large range of metallicites, for a globular cluster, among its stars. This range translates to a larger variation in the properties of its RR Lyrae stars. The relationship of luminosity and metallicity for RR Lyrae stars in ω Centauri is not identical to

that for globular cluster RR Lyraes generally. For almost all globular clusters their RR Lyrae stars tend to have a very similar metallicity reflecting a common origin in an isolated and homogenous material, and common evolutionary paths. These variables occur across a narrow mass range. It follows then that the RR Lyrae stars in a given globular cluster are at a similar evolutionary stage. Differences in evolutionary stage of stars at a single location do occur and can be the result of variation in mass around the RR Lyrae requirement. Random events setting up differences in properties of forming stars like for example the orientation of the magnetic field, or perhaps uneven diffusion and separation of proto-cluster material as its stars are formed, can in turn affect pulsation and mixing within a star. Dispersion in stage of evolution can be due to duration of cluster formation. Different paths for arriving into the instability strip could put a star into an evolutionary stage different from the rest of the RR Lyrae stars. For example mass loss could move a star into the instability strip, as opposed to a star starting out with the required mass (Smith 1995).

The metal-rich RR Lyrae stars have short periods, mostly $P < 0.45$ day. However, there are relatively few of these metal rich RR Lyraes in the relatively metal rich globular clusters, but they do occur in the Galactic field. Galactic Disc stars with solar metal abundance would be blue enough to enter the RR Lyrae instability strip only if they had a mass of about 0.5 $M_{\odot}$. At the current time the progenitor old disc stars turn off stars, going off the main sequence into the horizontal branch and possibly through the instability strip, are expected to have much higher masses, perhaps as high as 1.0 $M_{\odot}$. This requires a normally unrealistically large mass loss before the metal-rich stars of this population can become RR Lyrae stars. In other words the metal rich disc stars are not yet old enough to become RR Lyrae stars, unless other processes intervene (Taam et al 1976). The recent recognition that the metal-rich RR Lyraes belong to thick disc population, older than the disc population, has lowered the masses of the progenitor turn off stars (the stars entering the instability strip) to 0.8 $M_{\odot}$, making the required mass loss more likely. This is a further demonstration that RR

Lyraes are spread across population types and metallicities, a star of this type being the product of correct composition and age.

In the Small Magellanic Cloud the metal-rich RRab stars with periods less than 0.45 day seem to be absent. Similarly, in the large Magellanic Cloud no significant metal-rich population of RR Lyraes exists. This suggests that no metal rich stars sufficiently old to evolve into RR Lyrae exist at these locations. When the current crop of Magellanic RR Lyraes were forming those galaxies were not metal enriched to the same levels as in the disc of the Milky Way (Smith 1995).

At distances from the Galactic centre greater than about the Sun's, the halo field RR Lyraes settle to a constant metallicity <[Fe/H]> = -1.65 with a real dispersion of about 0.30 dex. At smaller distances the metallicities are higher. Recent studies also show that this trend also applies to the distribution of globular clusters. The RR Lyrae stars towards the Baade's Window in the Galactic bulge have metallicity <[Fe/H]> = -1.0 with 0.16 dex dispersion. Thus the RR Lyrae stars towards Baade's window will have a relatively greater metallicity.

1.5.2 Age differences

Broadly taken, globular clusters with intermediate metallicity, around [Fe/H] of -1.5, tend to be richer in RR Lyrae stars. This may be explained in terms of correlation of metallicity with horizontal branch type (or evolutionary stage of the stars). The metal-rich globular clusters have horizontal branches lying entirely to the red side of the instability strip in the colour-magnitude diagram. For the most metal deficient globular clusters, the horizontal branch stars lie mainly to the blue side of the instability strip. In both cases the number of RR Lyrae stars in relation to the cluster size would be small. Large variations in the relative number of RR Lyrae stars in clusters with the same [Fe/H] exist – horizontal branch morphology is not a function of it alone. Cluster age is put

forward as the most likely second parameter: older clusters have bluer horizontal branches at a given metallicity, as RR Lyrae stars evolve blueward.

Farther away from the Galaxy's centre the globular clusters tending to contain more RR Lyrae stars are more metal poor (Suntzeff et al. 1991). At the same time, at a fixed metallicity, the horizontal branches of globular clusters become redder, on average, as distance from the galactic centre increases (i.e. most, or on average, RR Lyrae stars evolve blueward). If metallicity and age determine the frequency of RR Lyrae in a globular cluster, the inner halo clusters tend to be older than those in the outer halo by a few giga years (also see Zinn 1980; Zinn 1985).

Whether a red giant evolves into the instability strip during its horizontal branch lifetime depends upon poorly known quantities such as the amount of mass loss prior to the horizontal branch stage. Hence ages of RR Lyraes vary depending on how they arrived into the instability strip. The Magellanic Clouds contain young as well as old globular-like star clusters. At metallicity near [Fe/H]= - 1.4 a Magellanic Cloud cluster has to be at least 10-12 Gyr old before stars within it have sufficient time to become RR Lyraes. This is an indication of a minimum age of these stars, but younger RR Lyraes could be produced elsewhere under conditions different from those in the Magellanic Clouds. It is argued (Lee 1992) that bulge RR Lyraes are the oldest of their kind, and among the oldest stars of any type in the Galaxy, older than the oldest halo stars by about 1 Gyr.

1.5.3 Nucleosynthesis and mixing

Diffusion and convection may change the photospheric chemical abundance of horizontal branch stars. However, this is not a fully answered question for RR Lyrae stars. In low-mass stars, such as at least some RR Lyrae progenitors, nucleosynthesis of significant amounts of elements heavier than carbon and oxygen is not expected during the lifetime of a RR Lyrae star. The

measured abundance of heavy elements in the photosphere of a RR Lyrae star is believed to reflect the composition of the material from which it formed. Thus RR Lyrae stars are easily recognisable tracers of chemical history of a region. If significant mixing out from the core occurs, the older RR Lyrae stars should show the enrichment of outer layers mainly with helium, and some oxygen and carbon (Korn *et al* 2007, Talon 2007, Vauclair 2003).

1.6 Pulsation Mechanisms

1.6.1 Ionisation zones

1.6.1.1 Helium

An induced pulsation in a star would decay away on the order of thousands of years without an ongoing input of energy. A pulsating star needs a way to add, or store energy in the high temperature part of the pulsation cycle and release it in the low temperature part. The most important mechanism for maintaining pulsation in RR Lyrae stars is the double ionisation of helium. Energy is needed to remove electrons from atoms, and it is returned when the atoms recapture the electron. This way ionisation stores energy directly. However, ionisation drives pulsation through two mechanisms. In areas where an abundant element is being ionised the opacity of the plasma increases with compression, trapping thermal energy in the heated plasma – this is the κ-mechanism. During the compression part of pulsation the energy is absorbed and stored through ionisation of the gas and then released in expansion – this is the γ-mechanism. Therefore thermal and ionisation energy is stored and released in a cyclical way (Smith 1995 pp 21-22, King and Cox 1968).

1.6.1.2 Hydrogen

Ionisation of hydrogen contributes less than ionisation of helium to driving pulsation in RR Lyrae stars, but it is still significant (Christy 1966). It sets up its own κ and γ-mechanisms but in different layers, at different depths.

1.6.2 The temperature, the depth, and RR Lyrae stars

The locations or depths of the helium and hydrogen ionisation layers are determined by the temperatures. The temperature of the helium second ionisation zone is 3×10^4 to 6×10^4 K, and the hydrogen ionisation occurs at temperatures less than 3×10^4 K. The temperature of 6×10^4 K occurs at radii more than 90 percent of the distance from the centre of the star to the surface. The other temperatures occur even closer to the surface. Hence pulsation is set up in the outermost layers of RR Lyrae stars. These temperatures also represent a requirement for the presence of pulsation. If a star is too hot the second helium ionisation zone ends up too high in the atmosphere of the star to set up pulsation. If the star is too cold, convection is stronger and it disrupts pulsation (Smith 1995).

1.7 The mystery of the Blazhko effect

1.7.1 The usual suspects

The Blazhko effect is an umbrella term for RR Lyrae lightcurve modulation with a usual period of a few tens of days, but varying between around 10 to over 500 days (for example Smith 1995). Usually, but not always, the modulation is such that the light output around the maximum is affected more than at the minimum. In addition the luminosity around the maximum is reduced rather than increased. These properties of the Blazhko modulation are compared against the unmodulated RR Lyrae radial pulsation component, which can be derived from frequency decomposition of a Blazhko lightcurve, or simple cycle to cycle comparison as the modulation occurs. The amplitude of the modulation differs between the Blazhko stars, and the Blazhko effect itself can vary over cycles several years long (for example Szeidl 1988). Furthermore some evidence exists for a third regular modulation in Blazhko stars with a period of duration on the

order of a few hundred days, but its long-term stability is uncertain. The Blazhko effect itself can be irregular, sometimes in combination with changes in the primary radial pulsation (see the summary in Smith 1995 pp 107 – 109). The strength of the Blazhko modulation can change from very small to very strong. It can also cease altogether. RR Lyrae stars with the Blazhko effect also often exhibit complicated changes in their primary periods. The lightcurves of some RR Lyrae stars exhibit additional scatter on their descending branches, possibly without the presence of the standard Blazhko modulation. These variations occur in addition to the main radial pulsation and the Blazhko modulation; it is not well known whether they are connected or independent effects. By the mid-1990s there were only about 40 Blazhko stars with well-established periods. Within the last ten years or so this has grown to many hundreds of Blazhko stars with well established characteristics. This increase in number of known Blazhko stars is the result of variable stars searches in data from large surveys. OGLE II has found over 500 Blazhko stars (Mizerski 2003), MACHO identified around 260 Blazhko stars in the LMC alone (Alcock *et al* 2000), and more recently ASAS (All Sky Automated Survey) has found 122 Blazhko stars in its initial observing stages (Szczygiel and Fabrycky 2007), among others. In the past the Blazhko effect was commonly detected by noting an increased scatter in a lightcurve folded by the dominant period, which opened the possibility of contaminating the detections with other effects and variability types. The more recent Blazhko detections take advantage of the wealth of survey data to produce well described lightcurves, and well specified component periods structure and amplitude details for these stars. Approximately between 20 to 30 percent of type ab RR Lyrae stars exhibit the Blazhko effect. The exact fraction of the Blazhko stars among type ab RR Lyraes varies in the given range depending on location and thus the chemical and evolutionary details of the given sample of stars. The fractional occurrence of Blazhko effect among the RRc stars is not determined due to the smaller numbers of the RRc subtype, but is much less than for RRab stars in all the survey samples. The RRc stars may or may not exhibit the same Blazhko effect as the RRab stars. It is possible that there are distinct processes

involved in causing RR Lyrae lightcurve modulations on these time scales, maybe even among the RRab stars themselves.

There are numerous suggestions for an explanation of the Blazhko effect, some going in and out of favour. For example the oblique magnetic pulsator model (Sibahashi 2000) was being supplanted by models based on the resonance between radial and non-radial pulsation modes (for example Dziembowski and Mizerski 2004), but recently a quintuplet frequency structure has been detected in the Blazhko star RV UMa (Hurta *et al* 2007) providing support again for the oblique magnetic pulsator explanation for at least some Blazhko stars. According to for example Kovács (1995) there are currently three main sufficiently developed possibilities. One is the oblique magnetic pulsator model, which assumes that the Blazhko stars have a magnetic field oblique to the pulsation axis. The radial pulsation is deformed (mainly by the Lorentz force) to have additional non-radial components symmetric around the magnetic axis. It is assumed that the magnetic axis is inclined ("oblique") to the rotation axis of the star. As the star rotates, the aspect angle of the non-radial components varies and then these components manifest themselves as the long-term modulation of the luminosity variation of RR Lyrae stars. The second explanation involves a dynamical interaction between the radial fundamental mode and a resonant non-radial mode, the currently favoured explanation (beginning with Van Hoolst *et al* 1998). In the course of this non-linear interaction a periodic amplitude modulation may occur when the two pulsation modes overlay and produce a beat period modulation. The closely spaced frequency structures consistent with this model, doublets and triplets, have been shown to exist in hundreds of Blazhko stars in multiple studies (for example Mizerski 2003). The third explanation is a steady or stationary resonant pulsation in the radial fundamental mode together with a non-radial mode of low spherical degree with almost the same period (as for example described in Kovács 1995, or Chadid *et al* 1999). Contrary to the dynamical interaction there is only a weak interaction between the two excited modes (almost resonant) and they keep constant amplitudes and phases. The amplitude

modulation is caused by the rotation of the non-radial surface patterns in analogous way to the oblique pulsator model, and the amplitude is model dependent. These are broad categories of accepted models and refinements within them can create more distinct explanations. The first two explanations for the Blazhko effect are the currently favoured ones, with the most research concentrating on them.

1.7.2 Case unsolved

Present models for explaining the Blazhko effect are based on the presence of non-radial pulsation in some form. The explanation of the effect requires placing the non-radial modes in the correct setting. The idea that the Blazhko effect involves the interaction of two radial modes has been abandoned (Kovács 1994). Spectroscopic studies of absorption lines in the Blazhko stars offer support for the magnetic model, through indicating the existence of magnetic fields, for example in the case of RR Lyrae itself which is the brightest known Blazhko star as well (Chadid *et al* 1999), and through indicating the presence of non-linear pulsation. Chadid et al (1999) uses observations of the absorption line Fe II λ 4923.921 Å in the RR Lyrae to analyse the periodicity of pulsation because the star has a strong Blazhko cycle. In the paper the variations of several features of the absorption line profile are analysed for the frequencies they contain, analogously to Fourier decomposition of lightcurves. This is related to physical observables by matching the absorption line derived frequencies to quantities like the star's primary oscillation period or the Blazhko cycle. The Blazhko period is primarily detected through the presence of an appropriately spaced frequency multiplet, although for some data analysis parameters it also comes out as a separate frequency though with low signal to noise reliability. The presence of the Blazhko frequency in a frequency multiplet structure is said to imply that the radial mode interacts with some other mechanism (either a magnetic field, or another non-radial pulsation mode, or the later caused by the former, etc). However the magnetic models are not developed conclusively and admit a lot of changes, the

presence of a strong magnetic field in the RR Lyrae being dismissed by a later paper (Chadid *et al* 2004). On the other hand in support of the two pulsation modes resonance models Van Hoolst et al. (1998) found that, at the pulsation amplitudes typical for RR Lyrae stars, the instability of a radial pulsation and the concomitant resonant excitation of some non-radial oscillation modes is likely. Chadid (2000) further suggests that the Blazhko effect may be modified by shocks between colliding photosphere and the outer atmospheric layers above it, which are normally excluded from modelling RR Lyrae stars as they contribute relatively little to the total light output. Furthermore, in these layers velocity shifts may occur from one pulsation cycle to another, affecting the lightcurve, and making it difficult to obtain a representational period from the summation of data samples taken over many periods. The detection of non-radial pulsation modes proposed by the dominant model for the Blazhko effect requires high-resolution spectroscopic line profiles from these stars to check for additional velocity dispersion caused by the non-radial modes (for example Kolenberg *et al* 2007). Ultimately where high quality lightcurves are required they may have to be obtained from observations over a whole relevant cycles, both the primary radial oscillation and the Blazhko modulation, at least for test stars in each category of interest. The photometric part of the data can be obtained through combining observations from several sources and surveys. Thus currently the Blazhko effect does not have a full explanation, and the currently dominant proposed solutions are in need of development.

2 The things RR Lyrae stars teach

2.1 Local distance indicators

Starting with Bailey observations of RR Lyrae stars showed that within a particular globular cluster the dispersion in their magnitudes was small and they were on average about 1.5 or 2 magnitudes fainter than the brightest cluster members. The initial assumption was made that all RR Lyrae stars, in globular clusters and outside, had essentially the same magnitude. However, even if all else is equal, there is a few tenths of a magnitude difference in the luminosity of a RR Lyrae star between the beginning and end of its existence. These stars become brighter as they evolve through their RR Lyrae stage (Smith 1995).

2.1.1 Parallax

The method of statistical parallax finds an average absolute magnitude for a set of RR Lyrae stars. The stars can be sub-grouped by metallicity, or other quantities. A sample of RR Lyrae stars is made up from stars at different locations. The stars do not have to be part of a cluster or be directly associated, they can be located at the opposite ends of the Milky Way. In this method the RR Lyrae stars are viewed as a homogenous group with similar average properties that can be modelled statistically. For example the RR Lyrae stars are treated as having a small range of absolute magnitudes, and an average absolute magnitude is derived for all. The data necessary for the statistical analysis are the velocity and position of each star in the sample. The velocity is found from the radial velocity and the proper motion across the sky. The position is determined from the celestial coordinates, apparent magnitude, and reddening. The motion of the stars due to Earth's motion is subtracted out, and the remainder of the stars' velocities are modelled by for example an "ellipsoidal distribution of peculiar motions". The velocity distribution or its model is the informed

assumption of the method. The velocities are estimated from proper motions and an absolute magnitude estimate. These parameters are "moved" around and adjusted in a systematic way looking for the most likely average absolute magnitude of a given RR Lyrae sample that best fits the model of velocity distribution. Other properties of the RR Lyrae stars can be added into the mix. The criteria for searching the parameter space and assessing the likelihood of a given combination of parameters vary according to the parallax method used (Strugnell et al 1986, Hawley et al 1986). Or as summarised: "*This method works by balancing two measurements of the velocity ellipsoid of a given stellar sample, obtained from the stellar radial velocities and from the proper motions plus distances, via simultaneous solutions for a distance scale parameter. The underlying assumption is that the stellar sample can be adequately described by a model of stellar motions in the Galaxy"* (Cacciari and Clementini 2003). Since the 1960s results for the various statistical parallax solutions range in mean absolute magnitudes from about 0.5 to 1.0 for RR Lyrae stars. Though, recent statistical parallax results are in good agreement – they suggest a relatively small dispersion in absolute magnitude among the RR Lyrae stars (Table 2.1 in Smith 1995). However, the errors associated with statistical parallax magnitudes for subgroups based on metallicity are too large to exclude a modest correlation of luminosity and metallicity (Smith 1995 p 29).

The trigonometric Parallax method measures distances to stars geometrically, using the apparent shift of a star as the observer's perspective varies with Earth's orbital motion. However, currently even with a space based telescope this technique provides distances to sufficiently bright and relatively nearby stars only, within around 1 kpc. Provided a sample of RR Lyraes close enough to the Sun is identified in data from space missions, for example FAME (Full-Sky Astrometric Mapping Explorer) (Horner *et al* 2000), it can be used to calibrate their magnitudes. FAME had planned to obtain the parallaxes of 40 million stars to an accuracy of between 50 and 500 microarcseconds, with the accuracy depending on the particular star's brightness. These expected calibrations would settle the absolute magnitude question for at least some RR Lyrae stars provided

these projects proceed to completion, get fully funded and start gathering data. As of 2002 funding for the project had been withdrawn due to NASA budget cutbacks, and project cost increases. JASMINE (Japan Astrometry Satellite Mission for INfrared Exploration) is intended to target 10 million stars in the Bulge for parallax measurements to within 10 microarcseconds but is scheduled to launch only in 2015 (Gouda *et al* 2007). European Space Agency's GAIA mission is expected to launch in 2013 and last for about 5 years while conducting astrometric measurements of around 1 billion stars and other objects. GAIA's accuracy will depend on the magnitudes of the observed objects and vary between 6 microarcseconds for V = 6 mag and 200 microarcseconds for V = 20 mag (Sozzetti 2009). Accordingly the trigonometric parallax is so far not yet fully useful for RR Lyrae stars, as none have been found close enough for existing methods and instruments to provide highly accurate result (Sandage and Saha 2002).

2.1.2 Cepheids

Classical Cepheids are Population I stars, younger than RR Lyraes, and as such do not occur in older systems and some areas of the Galaxy, such as the Bulge or the globular clusters. The periods of these stars range from a few days to a few hundred days, and their luminosities vary over a range of several hundred. Globular cluster Cepheids however are Population II stars, type II Cepheids (BL Her, W Vir, and RV Tau stars). The BL Her, W Vir, and RV Tau stars have periods between, 1 and 10, 10 and 20, and longer than 20 days, respectively. Population II Cepheids make up only ~ 10% of globular cluster variables, and only in metal-poor globular clusters. Thus RR Lyrae stars complement Cepheids as distance indicators, as each group occurs where the other does not, or is scarce. Additionally RR Lyrae stars are more numerous than classical Cepheids, providing a more densely spaced distance indicator. For classical and type II their periods fit linearly with their magnitudes, but the two groupings follow different period-luminosity relations (Smith 1995). There is also a third group known as anomalous Cepheids, with periods in the range between 0.4

and 2 days, overlapping with the period range of RR Lyrae stars. The luminosities of anomalous Cepheids are 0.5 – 2 magnitudes brighter in V than those of the RR Lyrae stars (Santolamazza 1998). Cepheid stars are bright, easy to recognise, follow well-defined period-luminosity relations, and therefore are excellent distance indicators, but limited through their numbers and spatial distribution. Out to ~ 2 Mpc distances derived from observations of different Cepheids agree to within ~ 10% (summarised in Smith 1995, Storm 2006, Feast 2003, Feast 1999).

2.1.3 Accuracy

At the present time Cepheids are overall the most reliable and accurate local distance indicator because of their well-calibrated period-luminosity relation, and relatively frequent occurrence. The trigonometric parallax is a more accurate and more universally applicable method, but only at small distances (Storm 2006). Supernovae are too infrequent and transient, and effectively more useful at greater distances. RR Lyraes occur frequently and are well distributed in galaxies, but their absolute magnitudes have not been narrowed down sufficiently to make them an accurate distance indicator.

2.2 RR Lyrae stars as distance indicators

2.2.1 Advantages

The RR Lyrae variables are numerous and easily identifiable making them a very attractive choice for a distance indicator. They occur in all areas of our own Galaxy, and in all types of galaxies. Accordingly they are a widespread, numerous, and effectively always available standard candle. They are relatively bright at a few tens of times of Sun’s luminosity. These properties make them optimal for mapping our own Galaxy and its immediate neighbours.

2.2.2 Problems

Our knowledge about RR Lyrae stars is sufficient only to work out their luminosities with limited accuracy. Even within this constraint RR Lyraes are already used as approximate distance indicators. Their usefulness can only improve as they are studied more. However, the process is made more difficult by the variety of RR Lyrae types and the different ways these stars could have evolved.

2.2.3 Current approaches

2.2.3.1 Much ado about mass

Short of a fully direct measurement of a variable's luminosity, the mass of the star is involved at some level in determining the luminosity. Mass is the first order parameter determining the evolution of a star. Thus mass together with the star's age, or in particular the stage in its evolution, is the first order parameter that determines its luminosity. The determination of RR Lyrae masses is part of theoretical determination of their luminosities through stellar evolution theories. There is no single mass specific to RR Lyrae stars. Depending on the metallicity of the star, the evolution and mass required for a RR Lyrae type pulsation varies. Furthermore, the progenitors of these stars can lose mass, or gain it in binary systems. Thus the initial mass of a star does not automatically determine whether it will become a RR Lyrae, or pulsate in a RR Lyrae like fashion. Hence it is expected that the properties of stars with RR Lyrae pulsation are a function of location and epoch. In practice RR Lyrae stars are studied in the Milky Way and surrounding galaxies reducing these differences.

2.2.3.2 The controversy over absolute magnitudes

The task of determining the absolute magnitudes of RR Lyrae stars, or how they vary with a star's age and composition, remains unfinished. Only the approximate absolute magnitude of RR Lyraes is known. In order for these stars to become good distance indicators their absolute magnitudes need to be known within ± 0.1 mag (Smith 1995). Current calibrations for RR Lyrae observable properties to their absolute magnitude are reaching this level of accuracy as judged by internal errors. A period-luminosity relation has been established for RR Lyraes applicable to K band luminosities, and calibrated by the trigonometric parallax of the RR Lyrae star itself (see the equation below for one version, from Feast *et al* 2008). A period-luminosity relation for other wavelength bands has not been established, and may not exist in such a relatively simple form. Additional systematic differences in these magnitudes occur at about the same level as internal errors, depending on the derivation and calibration of the RR Lyrae magnitudes.

M_{K_S} = - 2.38(±0.04) log P + 0.08(±0.11)[Fe/H] – 1.05(±0.13)

M_{K_S} is the K_S magnitude in the 2MASS system

P is the period in days

In comparison the accuracy of parallax derived magnitudes for RR Lyrae stars depends on the accuracy the instrument used to obtain the parallaxes. Hipparcos parallaxes are available for a set of 142 RR Lyrae stars (Feast *et al* 2008), but all have relatively large errors. The most accurate parallax available to date for these stars is that of RR Lyrae itself as measured with the Hubble telescope, at π = 3.82 ± 0.20 (Benedict *et al*), which leads to M_V = -0.61 ± 0.1 and M_K = -0.56 ± 0.1 for an assumed absorption of A_V = 0.07 (Storm 2006). The parallax methods need to provide more accurate measurements for RR Lyrae stars and this should be possible with the planned instruments. When the results from the more accurate instruments suitable for measuring RR Lyrae parallaxes

become available, the magnitudes and relations derived from them will improve as well. However, the results will still depend on the uncertainties introduced by the absorption corrections used.

For variable stars it is important to note how the mean absolute magnitude was averaged from the light cycle variations because at the 0.1 mag accuracy level differences arising from the methods used become significant. Most recent investigations of RR Lyraes have defined the mean magnitude by integrating the lightcurves in intensity units to derive the intensity mean magnitude. Energy production in a star is not affected by the pulsation mechanism, and thus intensity mean magnitude is the same the star would have if it did not pulsate. In the end, currently the spread of RR Lyrae absolute magnitudes resulting from available methods is several times greater than the required 0.1 mag (among others Smith 1995).

2.2.3.3 The Baade-Wesselink method

The Baade-Wesselink method is based on the proposition that at points of equal colour on the ascending and descending branches of the lightcurve a variable star should have the same temperature and the same surface brightness. Thus any differences in luminosity between the two phases must be attributable to differences in the radius of the star. The changes in the radius of a star can be measured by observing the radial velocities of the photosphere during its light cycle. The two sources of information combined together give the radius of the star, and its absolute luminosity (originally Wesselink 1969).

In the case of RR Lyrae stars this approach becomes complicated, and needs to be adjusted. The assumption that equal colour corresponds to equal surface brightness is not true. The effective surface gravity of these stars is different between expansion and contraction. The colours and radial velocities are also distorted by shocks. The colours are further altered by flux redistribution,

unevenly with wavelength. Accordingly Baade-Wesselink solutions for RR Lyrae stars need to involve models of stellar atmospheres to derive temperatures and gravities. This moves the away from direct observations and makes the results model dependent and uncertain. To reduce these complicating effects the Baade-Wesselink method for RR Lyrae stars has been adapted to cover longer wavelengths, moved towards observations in the infrared, and the corresponding colours (Jones et al 1992; Carney et al 1992; Cacciari et al 1992).

2.2.3.4 The advantage of double mode RR Lyrae stars

Pulsation theory allows the determination of masses for double mode RR Lyraes, though with an uncertainty of at least 0.1 $M_\odot$ due to unknowns in chemical composition and opacities (Smith 1995). This step is independent of, or eliminates, much of the usual stellar evolution theory. The pulsational mass of an RR Lyrae can be calculated from

$$M/M_\odot = (Q_i/P_i)^2 (R/R_\odot)^3 = (Q_i/P_i)^2 (L/L_\odot)^{1.5} (T_e/T_\odot)^{-6}$$

Where Q is the pulsation constant, and the subscript indicates the pulsation mode. With two pulsation periods, and the same luminosity and effective temperature applying to both modes, masses can be read off a Petersen diagram (originally Petersen 1973).

2.2.3.5 Detached eclipsing binaries

Binary stars are detached if the components are well separated – their radii are typically less than about one-quarter of the mean distance between them. Or that the stellar surfaces of both components are fully within the equal potential surface (taking into account gravity and orbital rotation), also called the “common Roche surface”. In other words, the surfaces of the two

components are not meeting or joining at the inner Lagrangian point, “they are not touching” in anyway. For a spectroscopic binary, the two stars orbit each other close enough that their binary nature is only detectable spectroscopically, through the periodic shift of their spectral lines as they move towards and away from the observer along their orbits. When spectral lines of both stars can be observed, the system is called a double-lined spectroscopic binary. The following equation applies to such systems, where a_1 and a_2 are the semi-major axes of the actual orbits, while i is the acute angle between the plane of the orbit and a plane perpendicular to the observer’s line of sight (known as the inclination angle of the orbit).

$$M_1 a_1 \sin i = M_2 a_2 \sin i$$

Both $a_1 \sin i$ and $a_2 \sin i$ can be directly obtained from the spectroscopic velocity curves. In case of eclipsing binaries the orientation of the orbit with respect to the observer is known (the system is seen edge on), and thus the masses of the two stars are directly measurable. As usual, an accurate and direct determination of mass like this allows much more independent modelling of a star’s luminosity. In the case of the RR Lyraes orbital spectroscopic shifts will need to be untangled from the pulsation. However, the joint requirements of eclipsing binary and an RR Lyrae star make such systems rare. It is even more difficult to identify them, as an RR Lyrae type lightcurve will be mixed with an eclipsing binary lightcurve. There is no published identification for even one such star. The OGLE group has identified a single RR Lyrae star in an eclipsing binary system (Soszyński 2011).

3 The PLANET database

3.1 Introduction

The PLANET group (Probing Lensing Anomalies NETwork) is a multinational and evolving microlensing survey group with scientists from different countries co-operating to gather data and analyse the results. Optical telescopes around the Southern Hemisphere are observing mainly towards the Baades's window in the Galactic Bulge. The gravitational lenses are in all cases within our own Galaxy. The observing takes place continuously for several months during the winter of every year since 1995. Observations in 1995 were a test run, while all the following years were full observing campaigns towards multiple microlensing targets (Albrow et al 1997).

The primary scientific goal of PLANET is densely sampled in time observations of selected microlensing events around the time of maximum magnification that is the highest luminosity. Ongoing events are pre-selected for PLANET observing on the basis of estimated strength of the magnification and the likelihood of detecting planets around the lens. The initial detection and observations of a microlensing event are made by other surveys. The microlensing lightcurves are the basis for the theoretical modelling component of the project, and are interpreted through these models. PLANET was involved in the discovery of the first cool rocky terrestrial type "Earth – like" planet, or relatively close so at 5.5 Earth masses (Beaulieu et al 2006). The secondary aims of PLANET arise naturally from the way its data is collected. Extended microlensing sources and lenses produce signature distortions in the lightcurve as well. For example the limb darkening in a K3 giant star was measured for the first time in a distant star (Albrow *et al* 1997, Fields *et al* 2003). Repeated observations of the same fields of stars allow the detection and characterisation of luminosity changes, in mainly variable stars, but also transient phenomena like gamma ray bursts

and others. This makes the PLANET database, a valuable source for identifying and describing variable stars, among other uses.

The PLANET group is a follow up microlensing survey (Albrow et al 2000), complementary to the detection surveys like the OGLE, MACHO, EROS, and MOA groups. Detection surveys look for an indication of a microlensing event happening, and optimise the identification of as great a number of them as is possible. Detection surveys tend to involve a single telescope observing a high number of wide angle fields, thus maximising the number of stars monitored. Observations of around once per day per field enable the preliminary detection of a microlensing event, and this frequency allows the coverage of a greater number of fields than in a densely sampled survey. The microlensing effect has a constant probability per star on average, all other quantities remaining equal. The probability of finding an event depends on the number of stars observed. Thus observing the same fields of stars for many years is more practical than changing them from one observing season to another, as the same number of detections would be produced on average with both approaches.

A follow up survey aims to measure the details of a microlensing event. PLANET relies on microlensing alerts issued by the detection surveys, selected on scientific objectives, and measures the event at a much higher frequency (Albrow et al 2000). The sampling intervals for PLANET observations are continuously variable, adjusted on the basis of observing priorities and the progression of the event. The densest sampling occurs around the time of the maximum in the lightcurve and reaches down to intervals of approximately between 0.5 to 1 hour per event, and occasionally more in places when observations of two PLANET telescopes overlap, and less when adverse observing conditions interfere. The event observing frequency is decreased as time passes from the maximum magnification, and only relatively few points are needed to establish a baseline. By design PLANET is sensitive to microlensing events which occur over a time scale of a few

months, and this is the typical timespan interval of observations per field. Finally PLANET observing fields are a few arc minutes across, while for example OGLE fields are much larger, covering many more stars. In OGLE II the images or observing fields are up to 14.2 by 57 arcmin in the drift observing mode (Szymański 2005). This is again a direct result of the differing aims of detection and follow up surveys, maximisation of the number of stars monitored, versus the need to carefully monitor just a single star and real time data processing, respectively.

When used for variable star research, the origin of the data in microlensing surveys determines what can be learnt from it. In this regard, apart from features not related to microlensing, data arising from PLANET is mainly limited by the average timespan of just a few months, reducing the frequency resolution of any regular signals present, but providing short durations of high density sampling. In contrast, data from a detection survey, for example from OGLE II (the most directly relevant survey to the research presented here), has an average timespan of a few years and comparatively high frequency resolution, but its sampling rate is sparse at around one per day for the duration of a few months every year.

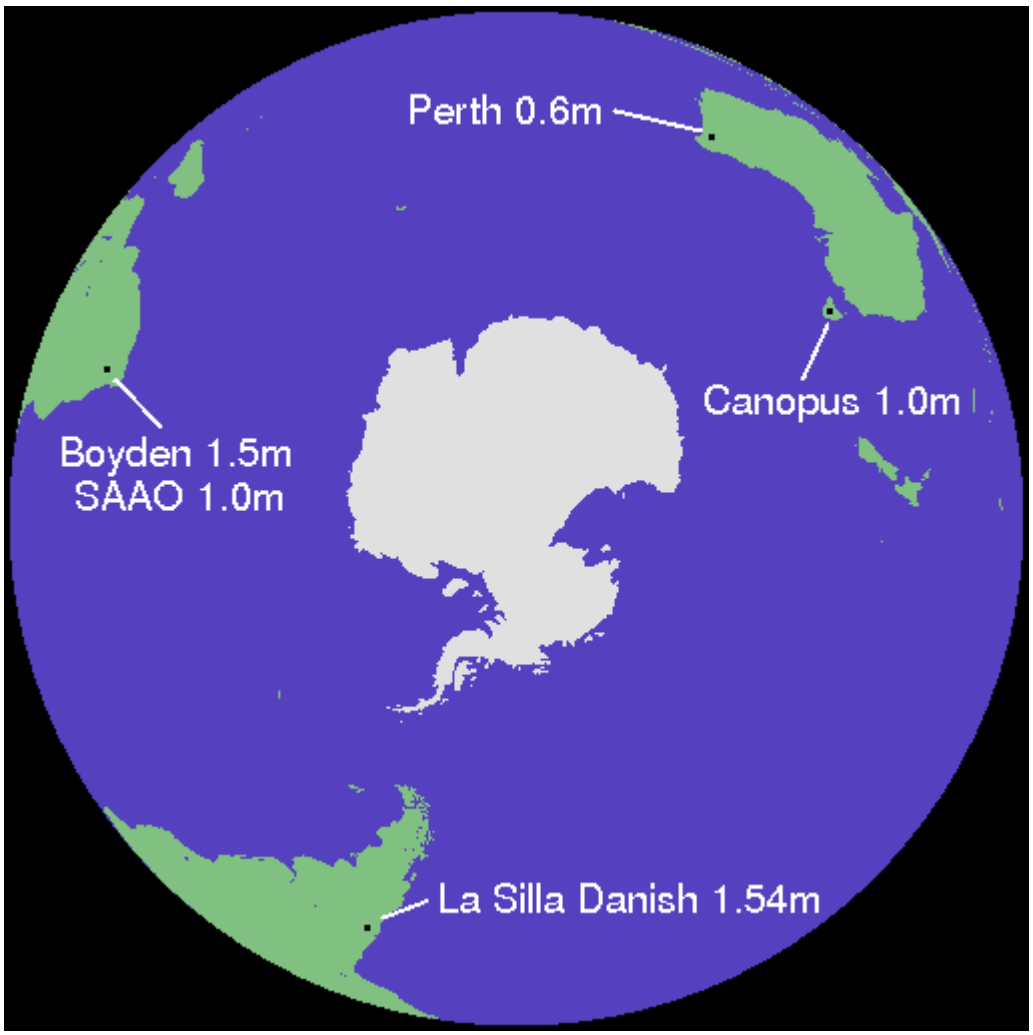

Figure 3.1: The network of PLANET telescopes as of April 2007. This may change in the future but is closest to the configuration used to gather the PLANET data analysed in this thesis. The four main telescopes involved in PLANET are:

- 1.0 m at the Canopus Observatory of the University of Tasmania, Australia
    - Longitude 147º32' , latitude -43º
    - 512 x 512 CCD with 0.434" per pixel, 3.7' by 3.7' field

- 0.6 m at the Perth Observatory, Australia
    - Longitude 116º8' , latitude -32º
    - 576 x 384 CCD with 0.58" per pixel for 1995-2000, 5.57' by 3.71' field

    - 512 x 512 CCD with 0.6” per pixel for year 2000 onwards, 5.12’ by 5.12’ field

- 1.0 m SAAO telescope at Sutherland, South Africa
    - Longitude 20º49’ , latitude -32º
    - 512 x 512 CCD with 0.35” per pixel, 2.99’ by 2.99’ field

- 1.54 m Danish telescope at ESO, Chile
    - Longitude 289º15’55.457” , latitude -29º15’15.433”
    - 2048 x 4096 CCD

The ability to continuously observe the same patch of sky becomes clear from the longitude coverage of the PLANET telescopes. For example, starting with the Hobart based Canopus observatory, the Perth telescope is 2.1 hours behind in the “same” night, followed by South Africa a further 6.4 hours behind, and Chile with 6.1 hours more. Finally, Hobart itself follows Chile by 9.4 hours, completing the cycle. Considering that the observing season takes place during the Southern winter, these time differences are sufficient to provide overlap in observing during Earth’s rotation.

In addition a number of different telescopes have been used through the years at the Chile site. Collaboration with other observing groups and surveys is evolving for PLANET. Co-operation with the RoboNet telescope network started in 2005. However, so far, these exchanges evolve around the microlensing aims, and data is collected for the source only. Accordingly the variable star results presented here are based on observations from the four main PLANET sites, with some changes to the telescopes and their equipment over the years.

The telescopes used for the majority of PLANET observing are of similar class, around 1 meter. Similarly all the instruments use equivalent I band filters, so that their bandwidth and

response is the same at all sites. The filters used by PLANET are the I and V filters from the standard Johnson-Cousins UBVRI set (Johnson and Morgan 1953, Cousins 1976, Moro and Munari 2000). On the relative magnitude scale the magnitude value for a non-variable star will usually be offset by a constant between different telescopes. This constant relative magnitude offset between telescopes can arise from various causes, instrumental and data analysis, differences in filters and or combination of these with the whole instrument response and will vary with wavelength. The important point for this work and for combining data from different telescopes is that all of these influences reduce to a constant relative magnitude offset for a star, but a different offset for different stars.

PLANET is a long term project. In its full form it has completed 16 years of observing as of 2011. It is intended to continue into the foreseeable future. By design the scientific returns will remain the same per observing effort invested as far as microlensing goals are concerned – the number of objects will not be "mined out". Over time, as the different areas of the observing regions are covered, the number of new regularly variable stars will decrease, including RR Lyrae stars.

The number of microlensing alerts, as expected, varies from year to year, and so does the number of fields followed up by PLANET. Table 1 in Dominik et al (2002) for the number of microlensing alerts issued versus the numbers observed by PLANET between 1994 and 2000. Clearly PLANET does not follow up all the potential alerts but manages to currently cover about 20% of these (as of the year 2007). For the years quoted the number of fields observed by PLANET is on the order of 30 per year. The number of the observed fields does not indicate the amount of data collected. Some fields are observed heavily, with several hundreds useful measurements from all the telescopes, while others have a few dozen measurements. This is due to PLANET adjusting its observing priorities as a microlensing event progresses.

The observing season for PLANET begins around the same time each year, between the end of April and in the first half of May, and finishes in September. The usual pattern of operation involves looking at microlensing alerts of detection surveys, and preselecting the events to follow. The initial selection is based on broad criteria of initial estimated peak magnification, the source star brightness, and the quality of measured lightcurve since noise in the data can reduce the probability of the detection of planets. After initial observing the priority and observing frequency of the observed events is adjusted based on the same criteria as initially, and increased to maximum around the magnification peak. For especially interesting events, a smaller number of baseline measurements is taken the following season. At the start of a microlensing event the time when the maximum magnification will occur is poorly known. In effect PLANET dynamically adjusts the observing frequency for all the monitored events, and this process is enabled by real time data processing and almost real time data sharing. During an observing night the accumulated data is processed and initially uploaded in several chunks, or later immediately (as of the year 2007) to a central site where it is available to everyone within the collaboration, and can be viewed online as a continuously updating lightcurves.

In such a scheme for gathering densely sampled data, weather and observing seeing consideration affect the average result more than in the case of a microlensing detection survey. Data is gathered at all times, even at less than optimal conditions. There is less room to manoeuvre in picking the best time for observing than in a case when one per day observation is required. In a similar way the average uncertainty in magnitudes measured by PLANET will be increased simply by the fact that some PLANET measurements will be taken at source positions closer to the horizon and thus through a greater depth of the atmosphere, worsening the seeing conditions.

3.2 Applicability to variable star searches

The more interesting variable stars discovered in microlensing surveys can be followed up with more observations. However, in practice the microlensing data at the start is what remains by the end of the process. Variable star searches in microlensing are a “target of opportunity” research, doable, but more of an afterthought than the primary goal in terms of how the data is collected. Observations and data collection for the microlensing surveys is designed around the expected results for microlensing events - none of the surveys optimise these for details that would improve variable star searches. It is natural to look for variable stars in microlensing data simply because of the large volume of observations available, and in case of the RR Lyrae stars typical survey data is well suited to their detection and basic characterisation, a lightcurve and thus period and amplitude.

The appearance of large scale microlensing surveys has changed variable stars research. It is no longer sufficient to just detect and catalogue a limited sample of for example RR Lyrae stars in a variable star survey with a few tens of observations per star. Variable star catalogues from microlensing surveys overwhelm in numbers what can be achieved from a specific variable star survey. An early microlensing survey EROS, conducted with the use of Photographic plates, produced a catalogue of 10,000 variable stars concentrated near the LMC bar, mostly of RR Lyrae type, with around 60 plates each in the B_J and R bands (Alard 1997). OGLE II has around 2700 clearly identified RR Lyrae stars with around 200 to 500 observations per lightcurve (Mizerski 2003). These are just a couple of examples. The data from microlensing surveys has become the primary source of detection of these stars. Current specific variable star projects have to have clear and specific aims beyond what is available from the surveys. It can be a survey of an area not covered or not likely to be covered in the near future by microlensing or other large scale surveys, providing RR Lyrae stars in a new location and environment. Or it can be theoretical modelling of some aspect of these stars. Alternatively it can be observations of a specific subset of RR Lyrae

stars looking for a detailed feature of behaviour beyond a simple detection and lightcurve composition, like colour behaviour throughout a pulsation cycle, stability of the Blazhko effect, spectral line profiles during pulsation, and so on.

The microlensing surveys enable the detection of a large number of RR Lyrae stars, among other objects. However, the specific details of the information that can be derived from the detections vary greatly, depending on the survey data. Detections based on high accuracy magnitude measurements taken over long duration, containing many samples that lead to precise lightcurves are superior to a simple catalogue entry. Interestingly the sheer amount of data available from microlensing surveys has led to the production of large catalogues first, with statistical analysis of some features derived from this information.

The considerations driving the gathering of microlensing survey data are different for the detection and follow up stages, and thus the two types of resulting surveys. Both have to be remembered to understand the variable star searches results. Depending on the geometric arrangement of the objects involved, the source and the lens, a microlensing event has different probabilities. In practice, when the Galactic Bulge or the Magellanic Clouds provide the background, or source stars, the probability is on the order of 1 in 1×10^6 per source star (Sackett et al 2004). Thus, in order to detect these events, large numbers of stars have to be monitored simultaneously, and this also results in the identification of greater numbers of variable stars. Therefore extended dense star fields are the best targets for maximising microlensing event detection. This has resulted in microlensing surveys targeting the Galactic Bulge and the Magellanic Clouds, as these areas are dense and relatively close. Nearby galaxies are similarly good targets, but the luminosity reduction with increasing distance becomes a disadvantage both for microlensing and variable star searches. PLANET almost exclusively targets source stars in the Bulge, to improve luminosity sensitivity and to describe Galactic planets. Furthermore, if such a galaxy is farther

away, there may not be enough potential lens objects at a correct location between it and the observer, if the correct location falls in the intergalactic space. Timescales and remaining characteristics of the events would change as well for more distant microlensing sources. In terms of variable star searches this puts a very heavy selection bias on where these stars are found, and as a result the range of properties of these stars as they depend on location is similarly affected. The number of, for example, RR Lyrae stars found from microlensing survey data is great, but they are almost exclusively concentrated in the Galactic Bulge and the Magellanic Clouds.

Best ground based photometry may in reach down to around 0.001 mag in the relative magnitude sense, and this level is sensitive to planets about 1/3 radii of Jupiter, more than sufficient for the detection of RR Lyrae stars, but useful for characterising any fainter secondary periods in these stars. In practice the best image subtraction based measurements (Woźniak 2000) from OGLE III have formal errors of 0.004 mag (from inspection of OGLE III data as used later in this thesis). Deviations in microlensing lightcurves caused by Jupiter mass planets last about 1 day – about 10 to 15 observed points are required to confirm its true nature(Dominik et al 2002). This requirement results in sampling duration of a little over an hour based on this requirement. In effect the sampling rate for PLANET of under an hour in the best sampled parts of lightcurves as mentioned above is the result of this, and the duration of the densest sampling is set by the width of the point source and point lens microlensing peak which for a Jupiter sized planet lasts typically for a few days. Photometric precision required is in the range of 1% – 2% of measured magnitudes in order to see a 5% deviation in the lightcurve, giving a significant chance of detecting a Jupiter sized planet.

The requirement for PLANET to measure and respond to microlensing lightcurves on up to hourly time scales requires immediate onsite photometry processing. The DAOPHOT program was used at some sites during the first trial run in 1995, and DoPHOT at the SAAO observatory. In the end DoPHOT was chosen for all the sites, and for all the following years, due to its higher speed in

light of real-time analysis required (Albrow et al 1998). As of 2006 image subtraction photometry was being added to the processing routine and tested in order to replace DoPHOT for all PLANET processing, and was added as of the year 2007 observing season. For well sampled stars image subtraction produces more accurate magnitudes as judged both by formal errors given by the method and subjective dispersion around test lightcurves Image subtraction can reach magnitude formal errors on the order of 0.001 magnitudes, but real errors will be somewhat greater.

PLANET photometry based on magnitudes relative to selected field stars rather than calibrating the data to absolute magnitudes. This approach was chosen as absolute photometry takes too long and is practically impossible in partly cloudy conditions.

The photometry processed observations from all the telescopes in the PLANET group are stored in the same electronic format. This format is a computer database which ends up as single data file which is called an archive. A separate archive is created for each observing field for each telescope. Usually a microlensing event is observed by four telescopes in the PLANET collaboration – this creates four observing fields for the same set of stars at the corresponding location. The observing fields differ between telescopes in size, resolution, the positioning of the microlensing event with respect to the field centre, and other differences arising naturally from the use of instruments with different specifications. Thus the observations by PLANET of each microlensing event produce four unequal sets of stars, with a lot of overlapping members between the sets. In practice all the archives corresponding to a single microlensing event are used to form a pool of observations for those stars that do overlap between the fields from different telescopes. Clearly the reason is to get the maximum possible number of observations per object. An archive stores the extracted and processed magnitudes from all observations for all the stars in its field and an array of associated information in a systematic and easy to access format. The additional information for all the observations and for all the stars detected in the observing field is composed

of: magnitude error from the dophot photometry; Modified Julian date as well as telescope date; the seeing; background/sky exposure; type of dophot photometry fit to the particular exposure for the star; FWHM of the photometry fit; air mass if recorded. In addition for each star detected in an observing field an archive stores its CCD pixel co-ordinates as per a field reference image. All the archives store a set of reference stars chosen from among the stars in the archive that are used to calibrate the magnitudes for all the stars in the archive. The archive also stores assorted information about the telescope used to obtain the data, the position of the microlensing event and some other information.

The number of reference stars is different for different events, and between telescopes. The reference stars for the same event can be different at different telescopes. It is inbuilt into the structure of the PLANET archives that the reference stars can be changed and the relative magnitudes quickly recalculated in a process that only affects the magnitudes for a star by a constant offset. The relative magnitudes thus depend on the reference stars and errors in measurements, spurious points, bad measurements, missing data, variability, etc, present in reference stars will affect magnitudes of all the stars in an archive at the dates when they occur in these reference stars. Thus this ability to optimise the reference stars is important for PLANET data, at least as far as the DoPHOT processed measurements. In practice, within the goals of this project, reference star optimisation is an important step in data analysis, as is described in more detail in section 4 (*Data Analysis*).

In the case of the PLANET data the errors in measured magnitudes calculated by DoPHOT are supposed to be a combination of uncertainties due to photon noise and blending, but the actual scatter in measured magnitudes of constant stars is ~ 1.5 times the mean DoPHOT derived error. This suggests that the DoPHOT derived errors are an underestimate, or other systematic effects are involved (Albrow et al 1998).

Another interesting effect of combining data from different telescopes and using relative magnitudes is a varying offset for the same stars but in fields from different telescopes. An offset in this context is the constant term required to change a star's relative magnitude in one telescope's field to the same star's magnitude in a field from a different telescope. When the offsets were calculated Albrow et al 1998 found: *"Relative photometry of stars in the monitored fields differed by up to a few percent among PLANET sites, even though the same set of reference stars was used. The offsets differed for different stars in the same field. The size of the scatter in the offsets within a given field prevented the assignment of a fixed offset per field or per site"*. This is as expected, since there is no such thing as a fixed offset per field or telescope, this offset being a function of a star's colour, and thus differing from star to star. Different amounts of blending due to differing resolutions of the telescopes and observing conditions at the sites will contribute to this effect for the more crowded stars, but can not explain this occurring in all cases, even for all well resolved and clearly unblended stars.

Observing fields for the different PLANET telescopes have different sizes (see Figure 3.1 for the details of PLANET observing sites), and the position of the lens is only approximately at the centre of these fields. More importantly the lens position differs between PLANET telescopes. This is not a design fault in data gathering, or a mistake, but simply the result of the project being organised around observing the source for a microlensing event. As long as the source is in the field of view, and approximately around the centre to enable a good magnitude calibration with reference stars while avoiding possible distortions around the field edges, the experimental aims are met. This has a couple of suboptimal consequences for finding variable stars in these fields. Variable stars identified close to the edges of the PLANET fields have an increased likelihood of not being found in data from all telescopes. Similarly, different sized fields will mean an increase in the number of variable stars found when data from one or more telescopes is not present. In addition the number of

detections will be dominated by the telescope with the largest field of view, simply because it will cover the largest number of stars. Some sources will be lost due to overcrowding and blending where the resolution is insufficient.

Since, for a single star, lightcurves from different telescopes can not be combined by calculating a standard offset for all stars between the two telescopes (for example by looking at the offset between non-variable stars matched between the telescopes), the lightcurves have to be combined on a case by case basis, star by star. This requires a reasonably well defined lightcurve, and thus if the number of available observations for a star from one or more telescopes in the set is below what is required to produce such a lightcurve, the whole of the data from that telescope has to remain unused for this particular star. Thus if a telescope is dominant in observing a particular event and one or more of the remaining telescopes observe it below the lightcurve creation threshold, the number of observations available to describe a variable star can be significantly less than what PLANET has observed.

4 Data analysis

4.1 Frequency analysis introduction

According to Scargle 1982 the Fourier periodogram analysis is the "standard workhorse technique" for the detection of periodic signals. The standard Fourier periodogram for evenly spaced data is redefined in a way that makes it applicable to unevenly spaced data, and preserves the statistical properties of the original. For folded data one objective way of determining the period is least-squares fitting of sine waves of various periods to the data. The same paper establishes that with the modifications proposed in it, the periodogram analysis and least square fitting of sine waves are exactly equivalent. The two methods end up with the same equation for determining where a best fit frequency occurs, and thus the same statistical considerations. In addition sine wave fitting to data is very clear conceptually.

The standard procedure well suited for non-uniformly distributed observations is folding data with a trial period and grouping them into phase bins. The maxAoV procedure in the PLANET pipeline is the analysis of variance method (AoV) applied as a test statistic to folded data (Schwarzenberg-Czerny 1989).

The performance of Fourier methods in detecting non-sinusoidal signals is poor. The power of a non-sinusoidal signal is spread among many harmonics in its Fourier decomposition. This is not a big concern in the case of RR Lyrae stars as their lightcurves vary from close to sinusoidal to a somewhat distorted sinusoidal form. *"Resolution of the AoV test statistics and of the Fourier spectrum for a sinusoidal signal is comparable. However, for narrow pulses the gain in resolution achieved by binning observations is substantial."* There is always some information loss in binning (Schwarzenberg-Czerny 1989).

In general the test statistics are functions of the trial period and of all the observations, and are designed to produce a response in some way proportional to the strength of the signal frequencies present in the data tested. For each test period, and for all available observations, the test statistic yields a single number. The plot of values of the statistic for a single range of periods is called a periodogram. Any detectable periodic signal in the observations produces a feature in the periodogram at its corresponding period. This general approach has been used to design a statistic specific to the AoV method. Oscillations in the observations, or component frequencies, correspond to features in the periodogram called lines by analogy to spectroscopy. However, since similar features may arise due to noise in the data, the essential ingredient of each period search method is a criterion for statistical significance of the lines. *"The intrinsic or natural profiles of the spectral lines are rarely observed in practice, in close analogy to spectroscopy. Profiles of lines in the periodogram are in most cases artefacts produced by observation and data analysis procedures."* (Schwarzenberg-Czerny 1989).

It is interesting to note that with the Analysis of Variance method (searchAoV procedure in the PLANET pipeline) we do not require good coverage of each cycle. On the contrary, the number of observations per cycle may tend to zero, as long as sufficient coverage of all phases is ensured by the whole sample. Large gaps in observations are permitted as long as all the phases are covered. This is precisely the kind of data PLANET accumulates.

With the various methods of period search relying on binning of observations, the differences between them seem to arise in the statistic chosen to describe the significance of a periodogram feature. In particular it is important how well the statistic is known for the case of interest, for example for small sample sizes. The answer to this becomes the probability distribution of the chosen statistic for a pure noise signal. This is needed to help to decide if a periodogram

feature is statistically significant, whether it is "real" or an "artefact". *"Hence it is important to critically analyse the statistical significance of a suspected spectral feature, by answering the question: 'What is the probability that this feature could have arisen from chance (noise) fluctuations?' "* (Schwarzenberg-Czerny 1998)

"In particular the well-known phenomenon of aliasing is a leakage of power from high frequencies to much lower frequencies. The way in which it arises makes it sensitive to a very precisely maintained evenness to the sampling. Hence anything from a slight to a major unevenness in the spacing substantially reduces aliasing." In this way the unevenly sampled PLANET data presents an advantage by reducing aliasing.

Error-free recovery of a band-limited signal (i.e. reproduction of the entire function X(t) from the samples $X(t_i)$) can be achieved with irregular sampling as long as the mean sampling rate exceeds the Nyquist rate (i.e. the average number of samples per unit time must exceed twice the highest frequency component in the signal). This is a simple statement for what signal can be recovered from PLANET data. In practice this is complicated by the fact that the data is highly irregularly sampled. Thus the average sampling is not an accurate description of the actual sampling intervals. In cases like this, an irregular sampling varying from object to object, simulations with artificial signals at the observed sampling times are the best way to test the possibility of a recovery of a real signal (Stellingwerf 1978).

4.2 Scripted analysis

The PLANET database is composed of a large amount of information. The existing data analysis pipeline is composed of single programs or procedures performing specific tasks necessary for the analysis of the observations for the microlensing aims of the project. A variable star search

in the PLANET database can be conducted by using the existing pipeline and doing some steps manually, but this approach is suitable for a small number of objects, or just to develop the steps to extract the information needed. For a larger number of stars to be inspected, as is the case with this study, the manual command input needed to run the pipeline programs becomes the most time consuming task and the bottleneck in the analysis. Additionally with a larger number of repetitive manual tasks the chance of a mistake grows introducing errors into the analysis. In order to speed up data analysis, allow the repetition of steps with varying input parameters to optimise them, avoid mistakes and subjective decisions, and introduce consistent and rule based data processing and result assessment, I have used the Perl programming language to write scripts that run the existing PLANET pipeline programs and sort the results. The approach is to reuse as far as possible the existing PLANET pipeline functionality. Where required I wrote Perl functions that perform analysis specific to this variable stars search, but not provided by the PLANET pipeline. In essence I have automated the majority of the data analysis for this project, even as far as parameters input and the running of the existing PLANET programs.

The structure of the Perl language is such that the most natural form for a program is a long script composed of a number of one purpose reusable functions. Hence, not all the parts of these programs have specific names or even boundaries, as data processing can jump from one section of the script to another dynamically as required. For book-keeping and descriptive purposes the sections performing a task are given names, with the understanding that they are not separate programs but rather functional sections of usually a larger script unless otherwise specified. Accordingly the data analysis for this project has been arranged in three individual scripts that perform all of the automatic analysis steps, *orient* for finding co-ordinate transformation between different observing fields for the same microlensing event, *template* for the bulk of the data processing, and *graph* for assembling combined lightcurves with data from different telescopes.

This approach required a large investment of time into writing computer programs. The great majority of time spent on data analysis was taken up by software development. By comparison the running of the resulting scripts required very little effort – they can be left to themselves until the processing is complete. This feature was used to rerun the analysis on certain sections as information was extracted from the data or programs within the PLANET pipeline were rewritten and previous analysis parameters were no longer optimal, all of which would have been impractical with manual data analysis due to the time required for the repeat. This also means that as each year's worth of PLANET observing becomes available, it can be processed in exactly the same way as for this project, extracting additional RR Lyrae stars and other types of variables if required.

4.2.1 Magnitude recalibration

An archive usually contains data from one observing season. In a few cases of the more interesting events or microlensing source baseline follow ups it can stretch to over one year. The systematic naming of the archive and its location in the data storage arrangement and analysis is conducted according to the year of the first observations. Sometimes observations may have been added to the archive after a set of magnitude reference stars was chosen. The new data can alter the best choice for the reference star set for the archive. Sometimes the reference stars chosen as a first guess are left in the archive with the understanding that they will be adjusted as needed. For these reasons, among some, it becomes important to check and optimise the magnitude calibration of the archive through picking some good set of reference stars. Thus the reference stars of all archives to be analysed for this project are checked in the way described below.

A Perl routine written specifically for this project called *reref* was used for magnitude recalibration. Two existing PLANET pipeline programs are used by *reref* to do some of the work, *findref* and *writepl*, for finding possible magnitude reference stars from among the stars in an

archive, and for recalculating and writing into the archive the magnitudes for all its stars with respect to the input reference stars, respectively. The *searchAoV* procedure from the PLANET pipeline is used on the archives to see if it works or fails – so they can be analysed with it later as described in the Period Search section below. The processing described in this section from "Archive testing and repair" to "Optimisation of magnitude reference stars" is conducted by the *reref* routine, with the steps and selection criteria described in detail.

4.2.1.1 Archive testing and repair

The first step in analysing a PLANET archive is to test that it can be searched for periods. This is necessary because some archives are damaged in that they cause the *searchAoV* period analysis to fail. Failures at this level disrupt the automatic data processing script, and must be eliminated. The test simply involves running *searchAoV* with a coarse frequency resolution (to save processing time) on the first 30 stars of an archive and checking that all the expected *searchAoV* output files were produced without the program crashing. If the archive passes the test, it is added to the processing queue for the observing year. Otherwise a repair is attempted on the archive. The repair consists of reducing the number of magnitude reference stars from among the existing ones to the minimum 3 required for a magnitude calibration, and retesting the archive with *searchAoV*. This fixes most failing archives, and the rest are discarded. After processing the data, it turned out that the problem occurs for only a handful of times in a year's worth of data, and usually for the smaller archives containing fewer observations, and unlikely to contribute to the final result because of this (as becomes clearer in later analysis steps). In hindsight the correction is done for completeness and to insure against problems with the stability of the data processing script, rather than simply discarding the small problematic archives. The problem with the magnitude reference stars turned out to account for the majority of this type of failure.

4.2.1.2 Extraction of potential magnitude reference stars

The next *reref* processing step is to pick candidates for the magnitude reference stars, improve on the default set all archives have to have for determining the relative magnitudes for their stars. *findref* does the candidate selection but the calls to it and the sorting of results are all done by *reref*. The most stable or constant stars are chosen. In the default setting *findref* pick stars within a radius of 30" of the microlensing source, and with rms in magnitude of less than 0.015 mag. The script attempts to select at least 6 candidates for reference stars and if it does not do so with the default *findref* settings, it proceeds in the following sequence, moving on to the next setting if the previous one did not work:

- it increases the search radius by 30"
- it increases the search radius by an additional 30" and increases the allowed rms for magnitude to 0.05 mag
- it increases the search radius by an additional 30" and the rms to 0.08
- it applies only the first 3 original reference stars to the archive (if the archive had a larger than this set of reference stars), and the whole sequence is repeated at the beginning at the default *findref* settings.

This sequence of steps has been determined manually by testing several archives, and was found to produce the desired result for all the archives processed here.

The result of the above steps is a sufficiently large set of reference star candidates as suggested by *findref*. However, *findref* does not pick the best reference stars from those chosen – it finds all the stars within its search radius that are constant in magnitude to within its input rms value. The selection of the best set of reference stars from these candidates is done by *reref* as the process continues below.

4.2.1.3 Data cleaning for reference star candidates

The *searchAoV* routine used in the later sections to find periodicities in the stars is very sensitive to incorrect magnitude measurements. In the extreme that the magnitudes are very inaccurate a small number of bad points in the lightcurve can destroy the variability detection. As a test a little over a dozen measurement points in the lightcurve of a very well detected RR Lyrae star were changed to be off by more than 1 magnitude, and at that point the periodicity in the lightcurve became undetectable. Thus correctly judging and removing incorrect measurements from observations is crucial to finding variable stars. The competing requirement is that as few as possible magnitude observations should be removed from a lightcurve in order to preserve the maximum amount of information.

All the stars in an archive have magnitude measurements taken at the same times, when their observing field was exposed. This, of course, includes the reference stars. Equally there are normal variations in the number of quality or usable magnitude measurements per star that can be extracted from a sequence of images of the same field of stars. Seeing conditions, cosmic ray strikes on the CCD, unstable CCD pixels, some stars close to the edge going off edge in some observing frames (though not a large contribution to the reference star candidates as those are chosen around the microlensing event which tends to be close to the observing field centre), even photometry processing artefacts, are some reasons for why even within the same archive stars will have different numbers of usable observations. A reference star can only be used to calibrate observations on the dates where it has usable observations. If an observation is missing or bad at a particular date for a magnitude reference star, observations on that date will be unusable for all the stars in an archive as their magnitudes can not be calibrated. This type of missing observations will add up across a set of reference stars. Hence in terms of extracting the maximum amount of information from an archive it is desirable to have magnitude reference stars that have as many as

possible usable observations. The cleaning process for the reference stars described below is a set of criteria against which a magnitude observation is tested to determine if it is of sufficient quality to be used for further analysis.

The *findref* chosen stars are further processed by *reref* to determine cleaned sample count of acceptable magnitude measurements (the number of useable luminosity observations for the stars), and the dispersion of these observations. Samples are discarded unless they fit all of the following criteria: belong to DoPHOT type 11, 13 or 17; have a non-zero magnitude; seeing is below 4.0"; background is below 50000. Next, the remaining observations are selected on the basis of their magnitude error. All observations with errors greater than the average error plus 3 times its standard deviation are discarded. The cleaning process continues on the selected observations by finding an acceptable range of magnitude values for a particular star undergoing the cleaning process. It makes an average by ignoring for the calculation 5% of the highest magnitude values, and 5% of the lowest (or at least 2 samples from each end, whichever number of samples is higher). The distance from this average to the remaining outermost magnitude values is multiplied by 1.5 for each, producing a lower and an upper limit of acceptable magnitudes. The values outside of these range limits are discarded, and the remaining data is considered cleaned. This is equivalent to throwing away points which are too far away from what is supposed to be a constant value (the points assumed to be faulty, or incorrect for some reason), but adapting this process to somewhat account for how the data is dispersed.

The end result of the cleaning process is the count of usable magnitude observations for all the reference stars suggested by *findref*, also called cleaned sample count, or cleaned data.

4.2.1.4 Optimisation of magnitude reference stars

In the final stage of magnitude recalibration of an archive the *reref* routine uses the information obtained in the above described steps to pick the best reference stars from among those suggested by *findref*.

For each potential reference star, the cleaned data is used to calculate the standard deviation in the set of observed magnitudes as the star is supposed to have a constant luminosity value. In this way standard deviation is used as a measure of dispersion and the stars with the smallest dispersion are assessed as being the closest to having a constant luminosity value. These stars are then scored for being in the top half of their number in the following quantities based on cleaned data, given one selection point for each:

- the greatest sample count of the observations
- the smallest dispersion
- the greatest magnitude (favouring the fainter constant stars).

The stars end up with a selection score between 0 and 3, and any stars with the same score are sorted among their group by placing the ones with the most samples at the top. These subgroups are then arranged into a sorted list of potential reference stars, higher scores at the top. Provided enough of these stars are available, the top 5 stars are picked as the chosen reference stars, up to the top 10 if their selection score is 3. After each round a check is performed if the same set of reference stars was chosen in a previous iteration. If the same set is chosen as in the very last round, the loop exits having selected a stable magnitude calibration. If the same set occurred in one of the other iterations, all the stars in the cycle are combined to form a larger set of reference stars, and the lower bound of the preferred number of stars is changed from 5 to the size of this set, up to the maximum number of reference stars which was set at 10 for this analysis. Otherwise the set remains unchanged, and the process continues. The set of reference stars constructed in a round is applied to

the archive being calibrated with the PLANET pipeline procedure *writepl* which recalculates and updates magnitudes for all the archive stars based on the new references. Finally a simple check is performed that the newly calibrated archive produces a minimum of 2 reference stars, enabling the continuation of the iterations. Then a new iteration restarts at the point of choosing stars with *findref*. The whole re-referencing process continues up to 20 iterations.

At the conclusion of recalibration the archive is tested again with *searchAoV* in the same manner as at the beginning of the iterations to make sure the process did not "break" it. If the test fails, the maximum number of reference stars allowed is reduced by 1 from the initial 10, and the whole sequence of iterations above is repeated. This is iterated until the archive is either fixed, or the maximum number of reference stars drops to 4. The reason for gradually reducing the number of reference stars is that for some archives too many reference stars creates problems. If the result continues to be a failure, the working set of reference stars prior to recalibration is reapplied, or if there was none, the archive is discarded from processing. This multilayered approach ensured that almost all of the larger archives were calibrated with the maximum number of reference stars that ensured stable processing with *searchAoV* for the later analysis. In the end the number of archives that totally failed the calibration and were not repairable was small, occurring just in cases where the number of observations for its field was small. However, many archives could be "broken" to the point of crashing the PLANET pipeline data processing software by the incorrect application of reference stars, usually by applying too many.

The end product of the *reref* routine is an archive calibrated with a good set of magnitude reference stars, optimised as described.

4.2.2 Period search

The stars with the well calibrated magnitudes are tested for the presence of variability in their lightcurves. Observations for all stars in an archive are analysed for the presence of periodic signals using the standard PLANET pipeline program *searchAoV* written in C, an implementation of the analysis of variance method (Schwarzenberg-Czerny 1989). Instead of producing an entirely new Perl script, the *searchAoV* program was modified by myself, and wrapped in a Perl script called *find_periods*. *Find_periods* determines the archives to be processed, the parameters to be issued to *searchAoV*, runs *searchAoV*, handles and sorts the output, and deals with error handling and any unusual situations. *Find_periods* is pointed to the directory where the archives to be analysed are stored and it does the rest. The modification to the *searchAoV* program was in the area of data cleaning to improve its methods and bring them into agreement with those used by the *reref* routine. The cleaning criteria for magnitude observations were rewritten to be the same as for the *reref* routine described above.

The data are searched for periods in the range between 0.15 and 100 days, and therefore variability with periods outside this range is not detected. The range covers the typical periods of RR Lyrae stars, but was chosen to due to data processing practicalities. Searching towards the shorter periods increases the computation time very steeply. The 0.15 days limit is chosen based on a maximum reasonable processing time per archive. The longer period limit is chosen from an inspection of periodograms, it is an estimate of beyond which period peaks in the periodogram stop being clearly resolvable based on the PLANET data. The period search step is 0.0005 days, and the default over-sampling factor of 50 is used around any detected periods to measure them with greater accuracy. *maxAoV* is the statistical significance metric in *searchAoV*, the PLANET pipeline implementation of analysis of variance as per Schwarzenberg-Czerny (1989). The cut off value for the statistical estimator *maxAoV* is set at 15, and any detection below this value is regarded as not

truly variable. The cut off value has been empirically determined by users of the PLANET pipeline and confirmed through this work as a good significance level for finding variable stars. All RR Lyrae stars detected in this thesis have signals with significance levels well above 15.

The result of *find_periods* processing an archive is a set of stars which show significant variability as judged by the statistical criteria used by *searchAoV*. However, this does not mean that the job of finding variable stars has been accomplished. Most of these detections of variability will not correspond to a variable star, but result from data sampling artefacts, and errors of all kinds. The complicated part is identifying the RR Lyrae stars among these detections – the follow on analysis addresses this.

4.2.3 Alias prediction and checking

The two terms, frequency and period, are used here interchangeably to describe the presence of variability. Every signal has both a period and frequency – the two are easily converted. When discussing the presence of variability in general, both terms can be used to describe it equally well. Of course, frequency and period are not the same, and are used appropriately in their specific usage.

Periods in narrow bands around 1 d and multiples of thereof are counted as spurious and ignored, they are assumed to be aliases. The approach is based on the determination that a very large number of this kind of periods arises from PLANET data when it is analysed with *searchAoV*, but from the significant fraction of them inspected none produced a recognisable lightcurve. In addition exactly this kind of artefact is expected to be produced by long periods beyond the interval searched for this project (the longest period *searchAoV* looks for is 100 days as explained above) as per Equation 4.1 and the description in this section.

The available observations were processed one year's worth of data at a time, one single archive at a time, star by star. It is expected that not all of the archives processed will have a sufficient number of good observations to pass the criteria for the minimum number required for further analysis. However, because the number of usable samples varies slightly for stars even in the same archive, as already mentioned, all the archives are initially analysed. Thus the selection criteria for the minimum number of observations required is applied at when the individual stars are processed. The variations in magnitude observations sample count between stars in the same archive arise for example from the slight misalignment of the observing field between exposures, making stars close to the edge missing in some observations. Differences in exposure can make some stars over or under exposed some of the time. Worsening seeing conditions will make some observations unusable or too uncertain for the analysis required.

Those stars that contain variability with a significance factor $maxAoV \geq 15$ are analysed further. The artefacts of all sorts are rejected, and the RR Lyrae stars are picked out. Some archives have relatively few artefacts and produce just a few variability detections from *searchAoV* with most of these corresponding to actual variable stars. Thus the variability candidates have to undergo several sorting steps.

One very strong artefact in PLANET data is a very predictable pattern of frequencies created by the presence of a real signal. These frequencies only appear when a real signal is present. Thus they are definitely artefacts without an independent existence. I have determined the pattern by inspection of real lightcurves and confirmed it by simulation. I added various sinusoidal signals into the magnitudes of the above mentioned magnitude reference stars, in order to use the real time sampling of the data. This has been done for multiple stars across all the telescopes in the PLANET group. The following pattern is obtained:

Equation: 4.1

$p_i = | n/(1.0029 + k \pm f) |$ *for* $n \geq 1$ *and* $k \geq 0$ *where* $f = 1/P$

plus multiples of the main period have to be distinguished from the fundamental period, given by: $p_j = nP$

– p_i is the period of one of the artefacts

– *n* and k are integers

– *i* and *j* are integer indexes

– *P* is the period of the real signal, and *f* is the corresponding frequency

The quantity 1.0029 has been determined from experiment, looking at the patterns from around real signals and creating artificial ones, as described above. The periods in PLANET data can be measured to within the precision implied in this number, and furthermore the artefact periods could be predicted to the precision contained in the number. No other corrections or adjustments were necessary to the predicted periods; they followed the formula above exactly for all archives. The absolute value above means that some negative predicted periods may match a positive predicted period, but will only be measured once in the data. Of course both such predictions correspond to a single feature. The *i* an *j* subscripts are just indexes for a sequence of periods. The artefacts have decreasing strength with increasing *n*, and usually for $2 \leq n \leq 4$ they reach the noise level or close to it. The fraction of SI Solar day to Sideral day, 86400 seconds, and 86164 seconds respectively, is 1.0027, very close to the number 1.0029 described above. However, the ratio is not exactly the same. This suggests that the Earth's rotation and/or orbital motion and the time standard are tied into creating these artefacts.

4.2.3.1 Sorting variabilities

The main routine for processing and identifying the variability type of a star is *process_star*, a part of the main *template* Perl script for data analysis. The *Process_star* co-ordinates other Perl routines written for data analysis as explained in more detail below.

The sorting and identification of real variability begins with associating the stars with their full range of parameters such as period, amplitude (calculated by the same PLANET pipeline *Fourcalc* program described in section 4.3.2 (*Creating combined lightcurves*) – this is an example of the automated Perl script jumping dynamically between its sections and procedures as required), and so on, and then loading these into the *process_star* script. This information is used to help identify the variability in the lightcurve. Frequently the strongest period picked by analysis with *searchAoV* is very close to 1 day, as already mentioned above. Similarly, but less frequently periods occur around 2 and 3 days. These periods are one-day aliases associated with sampling times. Some of them could also be part of a pattern created by long period outside of the *searchAoV* period search interval of 0.15 to 100 days. According to equation 4.1 a period just longer than 100 days would produce artefact peaks in the periodogram within ~ 0.013 days of the 1 day mark, and similarly for the higher multiples of *n*. For higher *k* the artefact pattern for periods longer than 100 days appears as signals with periods very close to 0.5, 0.333, 0.25 days, and so on.

In order to reduce the amount of analysis, and later visual sorting of the variable stars, the obvious artefacts ascribed above as due to long periods outside of the interval of the interest for the project were discarded from the analysis. These stars were marked within *process_star* and not followed up on the basis of the period corresponding to the artefacts – potentially some of them could still be brought back in for other reasons as will become clear with the description of other sorting steps. The choices made in these selection criteria were influenced by inspecting the results

and familiarisation with the data. They are not absolute but based on experience with the PLANET data; a different set of selection criteria producing similar selection results could be chosen. I have tried several sets of selection criteria, and fine tuned the best. Accordingly, after *searchAoV* identifies the possible variables, those stars with periods in the intervals of $1/(1.0029 \pm 0.0299)$, $1/(2.0029 \pm 0.0299)$, and $1/(3.0029 \pm 0.0299)$ days were judged to correspond to sampling artefacts and not analysed further by *process_star*. The intervals correspond to the parts of the pattern given by the equation above that produced the most false positives at this stage. The number 0.0299 is the frequency corresponding to period of 101 days (noting this is not the same number as the 1.0029 factor from the equation above), a period just outside the interval being analysed, plus a frequency tolerance factor *ftol* = 0.02. The frequency tolerance was chosen specific to the data, by inspection, and is meant to account for a typical interval occupied by a periodogram feature from a real signal.

The similar expected artefacts around the periods 0.5, 0.333, 0.25 days were retained for further processing at this stage. The main reason for this is that there is a smaller if still a significant number of them in the PLANET data. As such they can be dealt with effectively by follow up sorting.

After the above sorting step *process_star* reduces the number of the most likely artefacts among the variability detections, but does not remove all artefacts. The more detailed analysis that follows is continued by *process_star* on stars remaining after this “pre-sorting”. Some of the remaining stars that are analysed in detail are expected to be variability detections not corresponding to correctly identified variable stars, processing them is part of sorting this out.

4.2.3.2 Simulating strength of artefacts

The artefacts or aliases described by the above equation are the dominant recognisable interference in selecting the actual variable stars. Their distribution and strength in the pattern was simulated in order to better predict them when they are caused by an actual variability. A separate simulation was done by *get_alias_levels* Perl script for each data archive, called as part of the processing done by *process_star*. The magnitude reference stars were used to provide the actual sampling times, thus simulating artefact patterns specific to each archive. The algorithm in *get_alias_levels* is designed to find the highest levels at which the artefacts occur for a set of test signals at a real set of sampling times representing the specific dataset. The operation of this simulation is described in this section.

The current reference stars are read in from the archive header. The observations for these stars are extracted, and then cleaned following exactly the same procedure as during magnitude recalibration. The cleaning of the magnitude observations for these stars has to be done again, as after the optimised magnitude reference stars were used to recalibrate an archive their cleaned data is discarded. Thus the data has to be read from the archive again and cleaned. Otherwise the cleaned data would have had to be stored, compared against the little extra processing time required to clean it again. It is easier and faster to repeat the process in the cases of archives for which it is needed. The simulation in *get_alias_levels* added sinusoidal signals with all the periods in the test range (as described below), one at a time, with amplitude of 0.2 mag to the magnitudes of all the reference stars. The value of 0.2 relative magnitudes (0.4 mag peak to trough) is chosen because it represents the amplitude in the lower range of typical RR Lyrae stars. Thus rather than setting the magnitude to a constant value at the sampling times given for a reference star, the sinusoidal signal was added to whatever real magnitude values the star had. This retained the noise and whatever systematic variations in magnitude were present in the actual data, but kept at a level amounting to a constant

magnitude or non-variable reference star as per the criteria used above. This is meant to preserve all the variations present at the telescopes instead of conducting simulations based solely on the sampling dates. The period of the sinusoidal signals covered the range between 5.4 and 9 days inclusive, in ten 0.4 days steps. Each reference star for an archive was tested with all the periods in range to account for any variations in the result caused by varying period. However, to simplify the tracking of the resulting pattern, the period range chosen was outside the usual range for RR Lyrae stars. The working assumption based on experience with these data is that the strength of the pattern is not affected by this change, or affected only weakly at the level being checked.

Following the creation of an artificial lightcurve as described above, the periodogram of it is inspected for the presence of the expected alias pattern as described below.

4.2.3.2 Assessing the strength of artefacts

The follow up analysis is conducted in the same way for each period for all the stars used for the simulation. Using the equation 4.1 the periods for artefacts are calculated for $k = 0$ to 4 and $n = 1$ up to 16. For each value of k the sequence for n is processed up to the 16 times, though it is expected to exit well before the maximum is reached. The whole set is repeated for all the test periods and the results are combined.

For a pair of test period and k, starting with $k = 0$, the position of the artefact is calculated running this sequence in n. Then using the simulated data a narrow band around the predicted position is searched with *searchAoV* for the presence of a peak in the periodogram. The width of the band is equal to *ftol*, or 0.02 in frequency space (where periods are in days in period space). The band is centred on the predicted position. The test conditions for the presence of a significant peak were fine tuned to take account of the response of PLANET data:

– The *maxAoV* significance indicator for showing a real variability has to be greater than 13, slightly lower than the usual 15 because these tests are meant to create an exclusion conditions for the artefacts and the strength of these statistical indicator is significantly changeable depending on the exact test parameters used to run *searchAoV*.

– In addition any peak present has to be at least 5 units in *maxAoV* lower than the previous peak in the current sequence for *n*. The reason for requiring a minimum decrease in the statistical parameter is the possibility that an unrelated signal at or around the predicted position is strengthening the artefact peak, and thus a peak that is too strong for its position in the sequence becomes an unreliable prediction.

– Similarly the peak has to be farther than 1.5 *ftol* from all the positions predicted by the p_j sequence, as otherwise it is unclear whether it belongs to the p_i or p_j pattern. This distance is chosen on the basis of comparing the position of an exactly known frequency to an unknown one, on the working assumption that any value in a bound of width *ftol* centred on a frequency is the same because of frequency resolution, and thus the maximum possible distance from the exactly known frequency to the measured one while there is any overlap is 1.5 *ftol*. Rather than guessing whether the peak is part of p_i or p_j, the pattern strength at this position can be estimated for another test period where this overlap will not apply.

If a significant peak is found at the predicted position, the same process is repeated for the next value of *n*. Otherwise the previous value of *n* becomes the score for how far in the sequence the artefact pattern is detectable for this particular *k*. In exactly the same way this whole process is repeated for all the magnitude reference stars, for all the chosen test periods. As the results are obtained from the simulation runs, the highest score for each *k* is chosen as its final result. The

highest value being the most meaningful from the point of trying to exclude the artefacts from real signal – the strongest effect is the limiting case.

The result of this simulation and the output of *get_alias_levels* routine is a set of scores for $k = 0$ to 4 for a given archive. In combination with the equation these scores determine the position and the presence of these artefacts caused by the presence of a real variability. The score corresponds to the maximum n for which an alias feature is detectable. Thus for an actually detected period, k value, and n values up to its score give a prediction through the equation above at what frequencies these artefacts will appear. As such this information is used in trying to find periods in the lightcurves additional to the main one as described in the next section. Knowing where the artefacts are allows distinguishing them from additional periods.

4.2.4 Secondary and residual period detection

Stars can pulsate with more than a single period at a time, and they do so in a plethora of ways. Different pulsation modes would simply overlay together to produce the observable lightcurve, and disentangling or resolving them may not always be possible. Initially the search for periods other than the main one is done on lightcurves from one telescope at a time. The assembly and analysis of lightcurves from multiple telescope observations is done for selected stars in later analysis.

4.2.4.1 Data preselection

The analysis is continued by *process_star* routine. Before the star's lightcurve is inspected for additional periods it has to be cleaned for the same reasons as described in sections 4.2.3.1 to 4.2.3.3. Though, this time the cleaning is applied to variable stars, as before the stars were

functionally assumed to have a constant magnitude with variability produced by noise and systematic errors. The data cleaning rules used for the magnitude reference stars are adapted to better respond to a lightcurve with a true, non-noise and non-error based dispersion in the data. The updated cleaning rules are applied to a variable star at a time by the *process_star* routine as described below.

Data for all the observations for the star being analysed by *process_star* is extracted from the archive. As the first step the same observation selection criteria are used to preselect the observations as during the cleaning of constant star candidates for the magnitude reference stars as already described, minus the second part dealing with the acceptable range of values.

The second part calculating the acceptable range of magnitude values for a given lightcurve is modified to better follow a variable lightcurve. The data cleaned by the first step is folded by the period of variability obtained with *searchAoV* to produce a lightcurve of magnitude against phase, the shape of light variation for one cycle of the strongest period identified. The data arranged by phase is binned. Each bin contains 40 magnitude observations samples consecutive by phase, and starting with the first observation. Thus the bin width is variable in phase. This scheme was chosen because of the uneven sampling of data. Using this arrangement of the observations by phase reduced this unevenness. Within each bin the data was cleaned by exactly the same criteria as in the second part dealing with the creation of acceptable range of magnitude values for the cleaning of magnitude reference stars. As compared to the treatment of a constant star, clearly this method would make the most difference for the best sampled stars. Thus the number of phase bins is variable, depending on the number of observations for the lightcurve, but the number of observation samples in each bin is constant at 40.

If there are less than 80 measurements for a given star left in the cleaned data, analysis for it is discontinued. The star is marked as unavailable from the telescope corresponding to its archive. This requirement is necessary to ensure that sufficient data is present to describe the lightcurve at the level of detail required, and to combine data between telescopes where possible.

After the data cleaning process the *process_star* routine has a potential variable star lightcurve with a reduced number of suspect magnitude observations, and it continues the analysis based on it.

4.2.4.2 Secondary period detection

Additional pulsation periods were searched for in the variable stars in two main ways. The first, described in this section, is to account for artefacts and to look for the additional periods in the periodogram of the original data, and this task is done with a *get_secondary_period* Perl routine called by *process_star*. The periodogram is produced by *searchAoV* based on analysis of variance as described above. The simulated extent of the artefact pattern as derived above by *get_alias_levels* routine is used by *get_secondary_period* to predict periods which are excluded from being identified as a secondary detection. To these the p_j sequence periods are added for n = 1 to 4 inclusive, that is simply the multiples of the main period. The intervals in period between the exclusion values are searched for the secondary periods. These intervals start and finish *ftol* = 0.02 away in frequency from the exclusion values, same value for the parameter as used before. In addition, within a frequency distance of 2 × *ftol* from the edges of the interval (3 × *ftol* from the exclusion positions) the *maxAoV* parameter is raised to 25 for the threshold of detection of significant frequencies, as a real variability would have to come out at least this strong in the periodogram this close to an artefact. Otherwise, a weaker signal in the periodogram so close to an artefact peak could be part of the artefact. The strongest detection among the secondary periods as

judged by its *maxAoV* value is the result of this search, as in the presence of a secondary real signal a corresponding set of artefacts will be created just like for the primary period.

If a secondary frequency is found, its artefact pattern and the exclusion frequencies are calculated in the same way as initially and combined with the existing exclusion values. The secondary frequency is noted, and the steps for detection of secondary periods repeated exactly as done in the first round above. This process is iterated until no new periods are found, or 20 loops are completed. In practice the maximum 20 loops are highly unlikely to be ever needed as the expected number of periods distinguishable is on the order of a few of them. Double beat RR Lyraes would have two main periods, Blazhko stars would have up to around 3 distinguishable periods, depending on period resolution. Thus in up to 20 loops there is a lot of room left to accommodate any unexpected results.

The routine *get_secondary_period* exits when all the secondary periods in the lightcurve of the star being analysed above detection thresholds are identified. It transfers the details of these periods to the *process_star* routine which continues the analysis of the star.

4.2.4.3 Residual period detection

The second way of looking for additional periodicities in the lightcurves is the residual approach. A best fit model to the data for the lightcurve is constructed in some way, and then the model value at the date of an actual observation is subtracted from the observation value. This produces a lightcurve of magnitude residuals with values at exactly the same dates as the original observations. The residual lightcurve is checked for any remaining periodicities by the *get_residual_period* Perl routine I wrote wrapped in the *process_star* script. The *get_residual_period* routine uses two existing PLANET pipeline functions, the already mentioned

searchAoV and *Fourcalc*. *Fourcalc* finds a best fit model to a lightcurve data and outputs the model values at the observation dates as well as a set of Fourier coefficients as per the equation below. The fitting process uses sinusoidal functions chosen in a best least square manner for the period being fitted and the number of harmonics used. The number of harmonics chosen for the fitting was set to a constant 5 for all uses of *Fourcalc*, and the period for the model is exactly the detected main period for the lightcurve as derived from *searchAoV*. Fourier parameters are derived from this. These Fourier parameters provide the model values here.

The model magnitude values are calculated from the Fourier parameters and subtracted from the observations. An average and a standard deviation are calculated for these residuals. The same lightcurve as cleaned by the end of section 4.2.4.1 (*Data preselection*), prior to analysis by *get_secondary_period*, is cleaned more according to the Fourier model. Observations which are farther from the model than the average difference plus 2 standard deviations are discarded from the lightcurve. It is assumed they differ too much from what is predicted, and the measurements must be faulty, without identifying a specific cause. Using the remaining observations an improved Fourier model is fitted with *Fourcalc*. These final calculated Fourier parameters are saved for the star.

The improved model is then subtracted from the data by *get_residual_period* to produce the final magnitude residuals. The residuals are then processed with *searchAoV* to detect the strongest remaining significant period (as before for secondary periods with *maxAoV* $\geq$ 13). First, in order to save processing time for the script, the *searchAoV* is run with fast period step setting of 0.005 day, and if this detection is positive, it is rerun with the finer step of 0.0005 day. As used in the previous data analysis sections. This provides the final residual period to the same level of accuracy in this regard. In the same way as described in the "Alias checking and prediction" section, residual periods in the intervals 1/(1.0029 ± 0.0299), 1/(2.0029 ± 0.0299), and 1/(3.0029 ± 0.0299) days are

judged to correspond to sampling artefacts and treated as a non-detection. Finally the residual period is checked for the distance in frequency space from the previous main period, and if the distance is less than *ftol* = 0.02 d^{-1}, it is judged as a non-detection on the basis that most likely the Fourier model did not entirely remove the previous main period.

If a significant residual period is present, the result is stored, and the analysis by *get_residual_period* loops back to the point where the first Fourier model is fitted. The found residual period is set as the input for the modelling, and the remaining steps are unchanged. The process is limited up to 20 iterations, but no star is expected to contain this many residual periods (same reasons as for finding secondary periods in the sections above). In effect the condition is set for the extraction of all detectable residual periods.

Similarly to secondary period searching, the routine *get_residual_period* exits when all the residual periods in the lightcurve of the star being are identified. It transfers the details of these periods to the *process_star* routine which continues the analysis of the star. This concludes the analysis by the *process_star* routine. The results of the residual and secondary period analysis, the Fourier parameters, and associated information is written to output files, and the data analysis is transferred back to the control of the main *template* Perl script.

The results of this analysis are a main component of this project and together with a discussion are presented in section 5 (*Result*s). A summary of the number of stars analysed and numbers of primary variability detections as per the criteria described in the previous subsections of this section 4 are given in Table 4.1. The remainder of the results in this table are described in the following subsections of this section 4.

Table 4.1: Data Analysis Summary. RR Lyraes: is the number of these stars identified in the year's data. Events: are the single telescope archives from observing fields that contained sufficient data for detailed analysis. Fields: are the PLANET observing fields. Useful Fields: is the number of observing fields where RR Lyrae stars were detected. Variables: are the number of combined lightcurves that were inspected for RR Lyrae variability. Preselected Variables: are the numbers of single telescope lightcurves that passed the selection criteria for constructing combined multi telescope lightcurves.

Year	1995	1996	1997	1998	1999	2000	2001	2002	2003	2004	2005	**Total**
RR Lyraes	3	1	2	1	12	32	2	2	12	0	20	**87**
Events	7	8	11	32	33	22	23	27	37	39	9	**248**
Fields	7	13	21	75	79	77	60	57	65	74	18	**546**
Useful Fields	2	1	2	1	5	12	2	2	6	0	10	**43**
Variables	57	40	3170	6665	5279	4925	1917	1405	2487	5178	817	**31940**
Preselected Variables	57	40	3246	6686	5560	5993	1922	1434	2487	5216	820	**33461**

4.2.5 Star matching

The same microlensing event is observed by four telescopes as mentioned in the description of PLANET. Each telescope stores the observations in its own archive. Thus to extract all available data for a variable star, the information has to be extracted and combined from up to four separate sources. A coordinate transformation between the different fields is needed. This is a very complicated pattern matching problem. It turned out that a Perl procedure had to be written and customised to work effectively with the specific information available in PLANET data. The

procedure for doing the pattern matching and calculating a set of coordinate transformations is called *orient*, as mentioned in the introduction describing the Perl script based data analysis. Adapting a program already written for another environment would have been a programming task in itself, and *orient* produces a high quality and very reliable result taking advantage of the specific features of the PLANET data.

The *orient* routine is a standalone Perl script, and it writes the transformation it calculates to a coordinate file which is then read by *template*. If *template* needs a transformation it first checks the file, and if it does not find it, *orient* is invoked and the new transformation is appended to the file so it can be reused later. The transformation between two observing fields or archives consists of an angle of rotation plus a scaling factor.

The *orient* script has been highly optimised for reducing the calculation time of the transformation. The algorithm proofing version of the script took around 50 minutes of processing time to find one transformation for a typical pair of PLANET archives, for some archive pairs the time increased to hours. After optimisation the processing time for a typical transformation reduced to 10 to 20 seconds. The algorithm is dynamically adapting to reduce processing time, as it follows different processing paths as it recognises the pattern it deals with. This script is perhaps the most interesting programming outcome of this project, and it took many months of code development time.

The stars in PLANET archives are identified by a unique catalogue number. Unfortunately these catalogue numbers are specific to the archive. The same star has different catalogue numbers in different archives. In effect the same star has different identification numbers in data from different telescopes. Moreover the archives do not have a common co-ordinate system, and positions are given by pixel co-ordinates specific to it and unrelated to any frame reference common

across the archives and telescopes. The result is that given a catalogue star number for one archive there is no available transformation that can be used to find this star's catalogue numbers in the other archives corresponding to the same microlensing event. It is possible to load the fits file for the archive's observing field, identify the star from its pixel coordinates, and visually identify the same star in fits files for other archives, but this is very time consuming when thousands of stars are to be considered as can be seen in the table above. In some cases it is impossible, for example when the fits files have gone missing from the PLANET data repository.

The *orient* script addresses the above problem. The potential magnitude reference stars as found by *findref* are used by *orient* as the sets with likely some common members across different archives, a reasonable assumption based on my experience with PLANET archives. It is crucial that such two sets exist with common members between them, as trying to match large numbers of stars takes up a large amount of computer processing time. The processing time grows much faster than the number of stars involved (the exact rate depends on the algorithm and its path), but a large number of stars is not necessary to obtain a highly reliable coordinate transformation. The rotation of the different observing fields with respect to each other is conducted around the lens star which is known across all archives for an event, simplifying finding the transformation. The procedure can cope with any degree of rotation, small or large, equally well, simply by the design of its algorithm. It is not limited into finding a transformation between fields that can only be rotated by a small amount, failing for those that exceed such rotation. An initial scale ratio between the two fields also comes from information provided by *findref*, but is fine tuned by *orient* from matched reference stars before being output as part of the coordinate transformation. As long as *findref* provides the correct scaling between the images, and some common potential magnitude reference stars as suggested by *findref* exist between the fields being matched, *orient* always manages to find a correct transformation. Given a coordinate transformation calculated by *orient* the main data processing script *template* uses a star's pixel co-ordinates in one field to predict its pixel position in the related

field, and the closest star to that location identified by its archive number using the PLANET function *searchXY* (this function simply queries and archive for any stars located within a specified radius of a set of pixel coordinates). Thus the stars are matched by their archive catalogue numbers.

In short the *orient* script in combination with star matching in *template* script always finds a very accurate transformation, and matches the stars exactly. It has no problems with scaling, and it does not crash. The code has been highly optimised, and even though it is just a PERL script, not a compiled program, it finds a solution quickly. It fails to find a transformation only in a very small number of cases when the PLANET archives do not have the correct information about field scales (this can be resolved by manual intervention), or there is a problem with finding suitable reference stars for an archive (in itself an indication of unsuitability of the archive for analysis for this project).

During the star matching process and as part of it, the data processing script calculates a range of detailed information on all the processed stars: cleaned number of samples; residual periods; lightcurves and model lightcurves; fourier coefficients for the best model lightcurve; average magnitude error and the standard deviation; a range of numbers and statistics on the processing steps described in the preceding part of section 4.

The *template* script finishes its work by writing out the star matches between observing fields for the same events and the other information calculated above. The follow on analysis is conducted with other Perl scripts as described in the remainder of section 4.

4.3 Identifying RR Lyrae stars among the variables

The potentially variable stars are now matched between the databases for different telescopes, where the data of satisfactory quality is available in sufficient quantity. They are still just “potential” variable stars because the variability detected by *searchAoV*, the strongest signal in the period range of interest, can still be the result of a range of artefacts other than the ones already discarded in previous analysis steps up to this point. The most common of these new artefacts is a discontinuity in the folded lightcurves for a clearly variable star; judging the presence variability by the amplitude range over which the observations are spread. This suggests that the period used to fold it with is not correct. Thus in some cases the periods determined by *searchAoV* are not correct, but this is unlikely to be a fault with the procedure, and more likely is a data dependent result, artefact of the sampling. This analysis steps picks out the actually variable stars. Since this is a search for RR Lyrae stars the selection concentrates on this type of star alone – other types are ignored. The combined data and the results of the processing steps up to this point are also available for other types of variables, some of which like eclipsing binaries can be easily recognised at the same time as looking for RR Lyrae lightcurves.

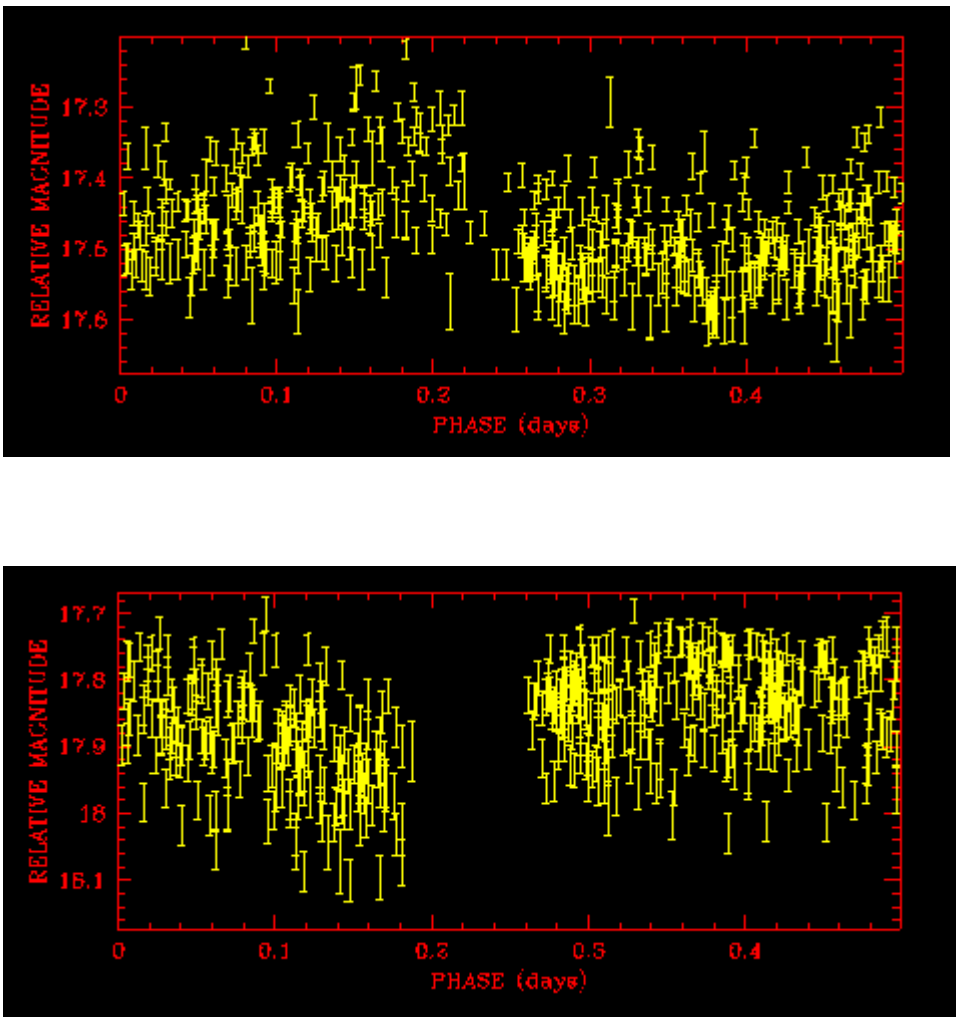

Figure 4.1: Two examples in folded lightcurves of the discontinuity artefact. The lightcurves for the two stars were folded by the period found by *searchAoV* in their data, and plotted by Phase versus relative magnitude. Upon inspection it becomes clear that the lightcurves are folded by an incorrect period. *searchAoV* failed to determine the correct period. Discontinuities like this are not a feature of lightcurves for real variable stars.

4.3.1 Visual inspection of lightcurves

The matched stars were arranged in columns by telescope with all the data specific to individual stars by the *template* Perl script and printed to a file. Their database numbers, periods derived from each telescope, numbers and type of secondary and residual periods, amplitudes and

the other Fourier parameters, number of cleaned or useful observations, and so on, were all lined up in order to be easily compared and used for assessing the type of variability these stars have.

The *searchAoV* routine in display mode was used to inspect lightcurves folded by the strongest period found by it. Manually, star by star, the lightcurves were judged in combination with their parameters. This amount of independent information, the different parameters of the lightcurves, makes identifying RR Lyrae stars much easier. For example when quality data from multiple telescopes is available for a matched variable star, the periods in days derived across the telescopes will be very close to each other, within at least 3 decimal places. Amplitudes will be similar. If the detected variability is a misdetection or an artefact, it is extremely unlikely that there will be agreement in these quantities for different telescopes. False detection matches from other telescopes may be non-variable, or correspond to different artefacts. The different telescopes will tend to have different sampling and instrumental causes behind the artefacts. Thus this kind of false frequency detection match in PLANET data is quickly spotted and another level of artefacts discarded, and unless there is some additional reason, this kind of set of lightcurves is not visually inspected saving time.

Some archives tended to have much larger numbers of potential variable stars with no clearly identifiable variability type. The great majority of these are clearly period misidentifications, as judged by the discontinuity in the folded lightcurve described above. This increased the number of lightcurves that had to be visually inspected. A very long time was wasted on such archives. Certain periods were found to repeat many times within these archive, and upon inspection always corresponded to some kind of fault or artefact in period detection. None were due to an RR Lyrae star. With practice the set of these repeatable periods would become quickly apparent for an archive, and once identified was used to skip the manual check for the stars with the dominant period in a narrow band around one of them. This was the approach that most reduced the time

required for this analysis step. It was most useful for stars with data from usually just one telescope per archive, as the rest of artefacts were dealt with as described above.

Type c RR Lyrae stars and type EW eclipsing binaries have very similar appearing closely symmetrical sinusoidal lightcurves. These could be distinguished by the asymmetry of the lightcurves. The ratio of the length of the rising to falling part was used for the asymmetry measurement. If a lightcurve had a noticeable asymmetry (in the 0.8 range or more), it was classified as a type c RR Lyrae. In addition bumps on the rising edge of the lightcurve were also used as an identifying feature of these stars. This approach allowed the identification of at least some type c RR Lyrae stars.

The RR Lyrae stars identified in this way were named in the following regular fashion:

- the PLANET name of the microlensing event
- underscore followed by the capital letter indicating the telescope which produced one of the archives for the star, joined with the catalogue number of the star in the same archive
- the same designation as above repeated for all archives from which data for the particular star is used
- a dot followed by the indication of the type of variability, ab for type ab RR Lyraes, c for type c RR Lyraes, and w for unusual lightcurves

For example: EB2K005I_d774_P753_U625_Y1200.ab

4.3.2 Creating combined lightcurves

A separate data processing Perl script *graph* was written for the creation of lightcurves combined from data from different telescopes. The approach chosen was to use Fourier coefficients and the lightcurves models described by these for reasons as described in more detail in section 4.4

(*Colour correction*). At each stage a best fit model lightcurve is used to produce the Fourier coefficients without adjusting for or modelling the varying distortions in data from different telescopes, using the *Fourcalc* PLANET pipeline procedure as described in section 4.2.4.3 (*Residual period detection*). All these functions are performed automatically by the *graph* script. A lightcurve for the same stars but made with data from different telescopes can appear significantly different in shape, although the period seems to be preserved with very little change. The shape of these lightcurves is distorted due to observing conditions at the various sites, the varying resolutions of the telescopes, different seeing conditions, and any and all the reasons combined. All these distortions or changes are treated as unrecoverable or lost information. For the purposes of this experiment trying to find accurate measurement of periods and frequency structure, any modelling of the distortions and stretching the lightcurves to compensate and better agree across the telescopes, would be applicable only to the stars for which observations from more than one telescope are available. In addition a way to actually recover the information while actually improving the measured quantities such as periods and amplitudes is not apparent. Equally cosmetic changes to the lightcurves are not worth the effort and the risk of introducing artefacts into these measurements. Thus the lightcurves are used as best as they can be extracted from the observations of a telescope, but without any alteration to make it more similar to a lightcurve for the same star from a different PLANET site, or an average of these.

The Fourier coefficients as used for this work are specified in the following format:

Equation 4.2:

$$\text{Mag}(t) = r_0 + r_1 \times \cos\left(\frac{t \times 2\pi}{p} + p_1\right) + r_1 \times \sum_{n=2}^{n} r_{n1} \times \cos\left(\frac{n \times t \times 2\pi}{p} + p_{n1}\ n \times p_1\right)$$

- r_0, r_1, p_1, r_{n1}, and p_{n1} are the Fourier coefficients as fitted by PLANET's *Fourcalc*
- Mag (t) is the best fit to data magnitude at time t (it is a date in units of days)
- p is the period in days

– n is the number of "harmonics" fitted

Thus the "model" lightcurve can be calculated at any date given the set of coefficients. In fact the model is a least square best fit of sinusoidal curves and their harmonics as shown above.

The periods derived from single telescope data are nearly the same for different telescopes for the same star, but not exactly the same. The first step in constructing a star's lightcurve is to combine the available data from different telescopes, and obtain a first period based on it. The data from the telescopes is extracted and cleaned in the same way as used for variable stars in the Data Preselection section, through all the steps under Secondary and Residual Period Detection. Fourier coefficients as per above equation are computed for one telescope data at a time by *Fourcalc*. Next, the constant term r_0 based on data from one of the telescopes is set as reference and thus unchanged, and the r_0 terms from the remaining telescopes are used to calculate the magnitude shifts required to make them equal to the first one. The relevant magnitude shifts are then applied to adjust the observed magnitudes for all the telescopes. In effect the magnitudes are so adjusted as to make the r_0 term the same for lightcurves from all the telescopes. In short, once the relevant Fourier coefficients are calculated the magnitude adjustment required to combine the data is a simple addition of the same telescope specific constant to all the magnitudes from that telescope. Nothing else is changed in the data. After this is done the combined data from all the available telescopes is used to calculate a single period for all of it, with *searchAoV* at the same settings as used so far.

This first combined period is used in the first iteration of bringing together data from all the telescopes. The data is combined in exactly the same fashion as above, with one exception. The period used for fitting the Fourier parameters, and thus deriving the magnitude shifts, is the above derived combined period, this time around the same for fitting data from all sources. The result is a

second round combined lightcurve with improved accuracy in terms of the magnitude shifts used. Iterating the procedure more than the two rounds did not change the result measurably.

The final lightcurve is used to produce a set of Fourier coefficients describing the star from all available data. At this point *Fourcalc* calculates the amplitude of the lightcurve as quoted for the stars found. The period quoted for stars is found from this final combined data.

A model lightcurve is calculated at the same times as the observations were taken and the model is subtracted from data to produce a residual lightcurve. The script calculates the first and second derivatives of the model lightcurve at each point where the original data was taken. The derivates are calculated from definition in a straightforward manner by using a 0.0001 day intervals around the date of interest, and calculating the predicted model magnitudes using the equation above. The first derivative is the slope of the line between predicted magnitudes at ± 0.0001 day around a given date. Similarly first derivatives are calculated at ± 0.0001 day around the date, and used to get the second derivate for the date. Thus first and second derivates have a resolution of 0.0002 and 0.0004 day. The derivatives are normalised by the highest value for easier plotting, they are meant to be used for locating features in the model lightcurve and for this their actual values are not required.

The Fourier coefficients, the folded combined lightcurve, the residual lightcurve, are all output to file format for easier graph plotting in Microsoft Excel. The script then searches for periods which are flagged at various significance levels, the following are checked: single telescope residual lightcurve within ± 10% of the original period; the whole combined residual lightcurve; the combined residual lightcurve within ± 10% of the original period.

In cases where data from only one telescope was available for a star, the data is processed and assessed for exactly the same results, minus of course the magnitude shifting and data combination.

The *graph* script results in combined lightcurves as plotted for example in Figures 4.2 and 4.3 below.

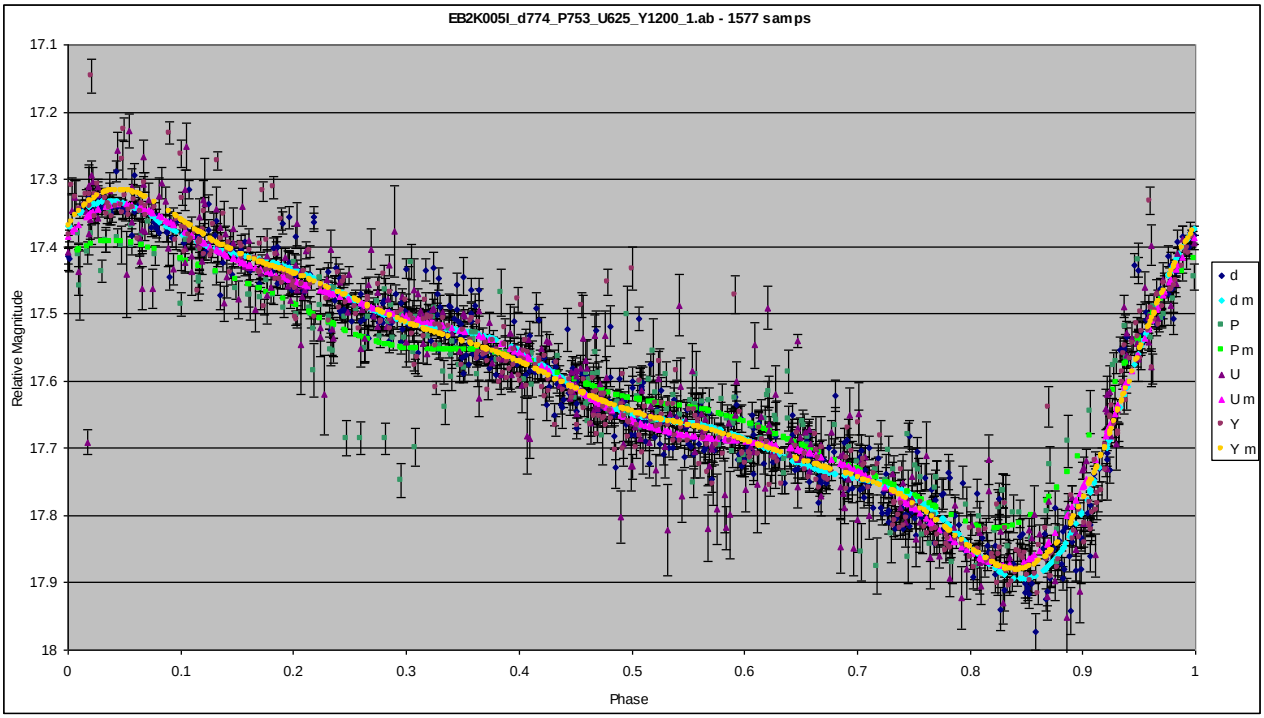

Figure 4.2: An example of a very well sampled combined lightcurve produced from data from four PLANET telescopes, produced in the way described above. The coloured curves correspond to best fit Fourier based model based on data from single telescopes as indicated by the legend. It is shown how they align through combining the data.

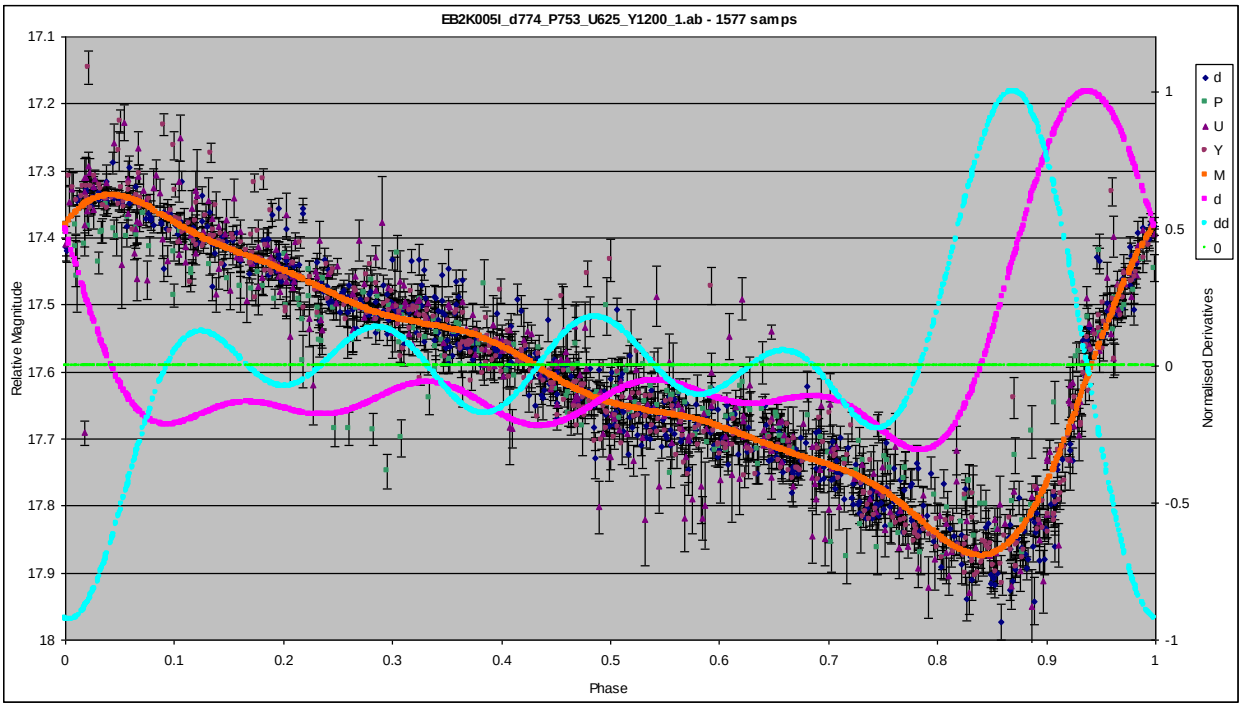

Figure 4.3: The same combined lightcurve as in the previous Figure. This time the orange line represents the best fit model to all combined data. The pink curve is the first derivative of the model. The light blue curve is the second derivative.

4.4 Colour correction

Taking the following equation directly from Da Costa (1992):

$$V_{std} = v_{inst} + a_0 + a_1(B\text{-}V)_{std} + a_2 X + a_3 X(B\text{-}V)_{std} + a_4 UT + \ldots$$

V_{std} - is the *standard magnitude* of the star,

v_{inst} - is the *instrumental magnitude* (corrected for exposure time),

$(B\text{-}V)_{std}$ - *colour of the star*, (using V as an example, similar equations apply to other bandwidths)

a_0 - the *zeropoint*, a measure of the sensitivity of the CCD/telescope system in this bandpass

a_1 - the *colour-term,* a measure of how well the instrumental system approximates the standard system. In most circumstances a_1 should be less than 0.1

a_2 - the *first order extinction coefficient,* this depends on the atmospheric transmission and therefore varies from site to site and often from night to night

a_3 - the *second order extinction coefficient,* this terms is necessary, particularly for B, because extinction varies rapidly across the bandpass so that combined with the change in effective wavelength with spectral type, a variation in effective extinction with spectral type results.

The magnitudes in PLANET database are relative to a set of reference stars. The same statistical method used to find variable stars, the searchAoV procedure, is used to find stars which are least variable, effectively constant in their light output. Preferably a set of at least three constant stars is chosen in this way per observing field. Within the same observing archive these stars have been sampled at exactly the same times, accordingly the instrumental magnitudes for each set of constants are summed and averaged at each observing time, and the result set to a magnitude of 15.0. This process reduces any variability still present in the constants, either due to measurement errors or due to changes in the stars. The same variability is unlikely to be present at the same time in different stars. Thus the PLANET magnitudes have no relation to actual effective or absolute magnitudes. The reason behind this is that the scientific goals of PLANET depend on the measurement of relative changes in brightness, and not their absolute values. The relative magnitudes of all the stars within an archive depend on which from among them are chosen to be the constants. If the constants are changed, all the magnitudes change as well.

Looking at the equation above in the context of PLANET's relative magnitudes, taking a difference in magnitude between two stars, or a star and the set of constants, removes the common terms.

$$1/i \sum_i v_{inst_i} = 15.0$$

$$= 1/i \sum_i V_{std_i} - a_0 - a_1 \times 1/i \sum_i (B\text{-}V)_{std_i} - a_2 X - a_3 X \times 1/i \sum_i (B\text{-}V)_{std_i}$$

$$\Delta V_{std} \quad \Delta v_{inst} \quad \Delta(B\text{-}V)_{std}$$

$$v_{inst} = V_{std} - a_0 - a_1 (B\text{-}V)_{std} - a_2 X - a_3 X (B\text{-}V)_{std}$$

$$v_{inst} - 1/i \sum_i v_{inst_i} = (V_{std} - 1/i \sum_i V_{std_i})$$

$$- a_1 \times [(B\text{-}V)_{std} - 1/i \sum_i (B\text{-}V)_{std_i}]$$

$$- a_3 X \times [(B\text{-}V)_{std} - 1/i \sum_i (B\text{-}V)_{std_i}]$$

$$\Delta v_{inst} = \Delta V_{std} - a_1 \times \Delta(B\text{-}V)_{std} - a_3 X \times \Delta(B\text{-}V)_{std}$$

so,

$$v_{inst} = 15.0 + \Delta v_{inst}$$

For the same star observed with two different telescopes, the difference in the instrumental magnitudes becomes:

$$v_{inst_I} - v_{inst_{II}} = \Delta v_{inst_I} - \Delta v_{inst_{II}}$$

$$= - (a_{1_I} - a_{1_{II}}) \times \Delta(B\text{-}V)_{std} - (a_{3_I} \overline{X}_I - a_{3_{II}} \overline{X}_{II}) \times \Delta(B\text{-}V)_{std}$$

$$= - \Delta a_1 \times \Delta(B\text{-}V)_{std} - (a_{3_I} \Delta \overline{X} + \Delta a_3 \overline{X}_I) \times \Delta(B\text{-}V)_{std}$$

Note:

$$a_{3_I}\,\overline{X}_I - a_{3_{II}}\,\overline{X}_{II} = a_{3_I}\,\overline{X}_I - (a_{3_I} - \Delta a_3) \times (\overline{X}_I - \Delta\overline{X})$$

$$\cong a_{3_I}\,\Delta\overline{X} + \Delta a_3\,\overline{X}_I$$

assuming that Δa_3 and $\Delta\overline{X}$ are small and thus: $\Delta a_3 \times \Delta\overline{X} \cong 0$

Furthermore:

$\Delta V_{std_I} \equiv \Delta V_{std_{II}}$ $\Rightarrow$ cancels out

$\Delta(B\text{-}V)_{std_I} \equiv \Delta(B\text{-}V)_{std_{II}}$ $\Rightarrow$ use $\Delta(B\text{-}V)_{std}$ in place of both

$\overline{X}$ is the average air-mass in the dataset for an observing site. Subtraction of magnitudes in observations from the same site is simplified by the type of data stored in PLANET archives. Effectively all the measurements are taken at the same time and thus air-mass, making it possible to keep the air-mass a constant per sample pair or sample set. This removes the pure air-mass term for relative magnitudes. The combined air-mass and colour term remains, and it will distort and broaden the lightcurve proportionally to the product of variation in the air-mass and average colour difference from the constant stars over the data collection period, and not proportionally to the air-mass. The average or constant part of the air-mass term is removed, while the variations around it make the difference. In effect, for the same star observed at different sites, the lightcurve will be more broadened, and less accurate, at the site with the larger variations in air-mass.

The comparison of magnitudes for the same stars from different telescopes introduces even more differences. The a_3 is different for each telescope and the samples between telescopes are not taken at the same time and thus some kind of average air-mass for a telescope has to be used

(irrespective of whether the average is over entire sample run, or phase bin, etc). The pure air-mass term remains subtracted out by the use or relative magnitudes.

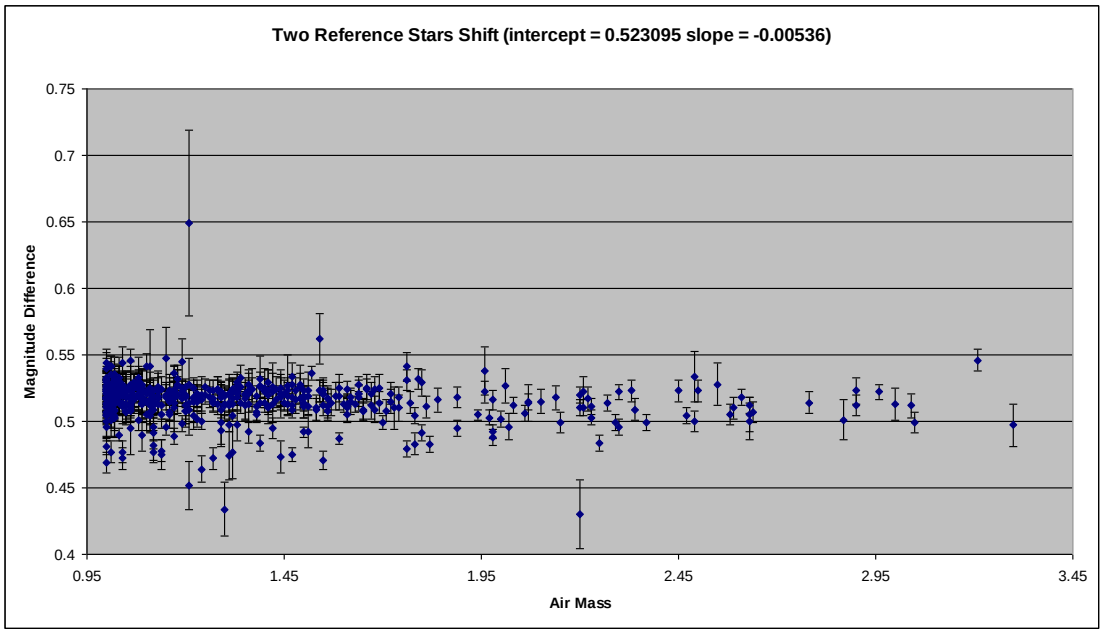

Figure 4.4: The magnitudes of two constant reference stars in the same archive were subtracted at each measurement time and the difference plotted against the air-mass at that time. The stars were chosen to have the greatest colour difference among the constants as judged by their magnitude shifts when compared to data from a different telescope. Since the stars are measured by the same telescope, this subtraction isolates the term containing the a_3 constant as the only one variable with air-mass. The slope of this plot then becomes the product of the a_3 constant and the colour difference between the two stars. This is a demonstration that the terms associated with a_3 make only a very small contribution to the instrumental magnitude.

The motivation for this process is to combine lightcurves, instrumental magnitude data, from different telescopes in order to maximise their sampling and thus detail. Due to the colour dependence of instrumental magnitudes, the change in relative magnitudes is different for different stars. Hence it is not possible to calculate an average shift for a set of stars and apply this to the

objects of interest. For a constant star the solution is trivial: the average magnitudes for data from different telescopes are equated, and this determines the relative magnitude shifts between them.

The case for a variable star is more complicated. The question reduces to: what is a valid way of finding an average magnitude for an unevenly and irregularly sampled variable star? Especially in the absence of information about the telescope response parameters and object colours apart from the relative magnitude data itself. Using the same constant stars for calibrating magnitudes in observations from different telescopes simplifies the above equations by making the term $\Delta(\text{B-V})_{std}$ the same across all telescopes and cancelling out the ΔV_{std} terms, but by itself this does not fully remove the colour related magnitude shifts between telescopes. For a case of different telescopes, with the same constant stars chosen as references in all of them, the magnitude shift necessary for a single star simplifies to a constant shift (using average air-masses). While it is possible to construct arguments by which the relative colours are worked out by comparing the size of the magnitude shifts for the same stars in different telescopes, for the variable stars case this needs the use of an average magnitude.

The reason behind finding the magnitude shifts between different telescopes is to combine the data in a way that recreates as nearly as possible the effect of taking the same data with a single telescope, for the purposes of the experiment. The purposes at this point are the production of well sampled light-curves, and finding the frequency components of the lightcurves.

A first order improvement on combining light-curves from different telescopes is to use the same constant stars for archives from different telescopes. The telescope magnitude terms tied in with the colour difference are relatively small. Provided the constant reference stars are chosen with colours likely to be close to the stars of interest, this method will remove most of the magnitude shift between different telescopes as the term giving the standard magnitude difference between

different sets of constant stars disappears. In case of the PLANET data this works reasonably well because the stars observed are located in Baade's Window, and tend to be red in colour.

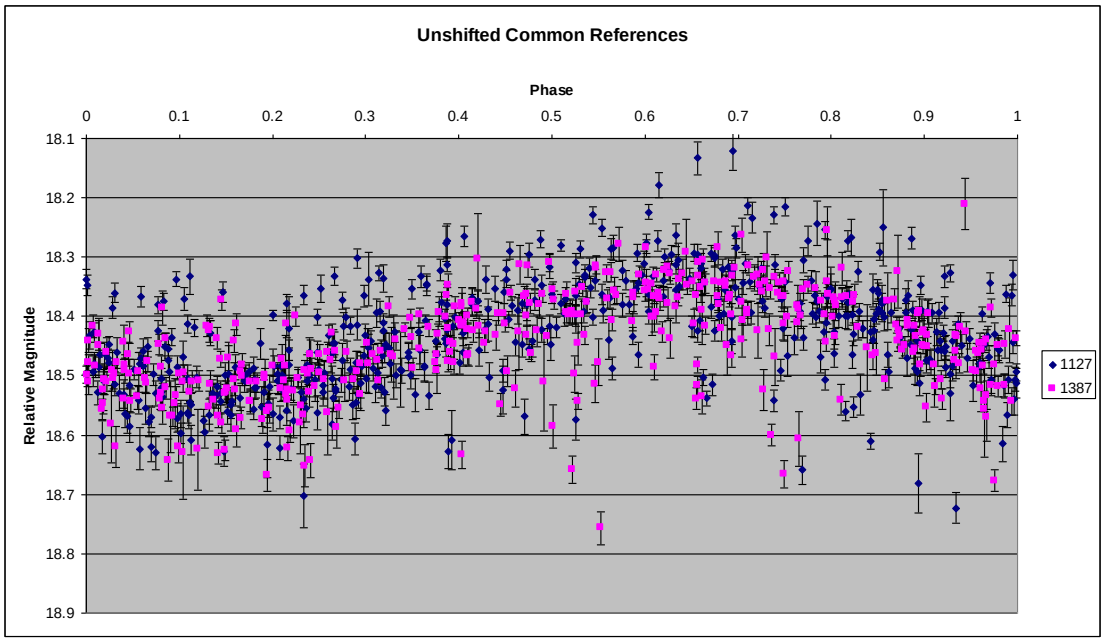

Figure 4.5: An example of two well sampled lightcurves of the same star taken by different telescopes. The star is type c RR Lyrae. The data for this was combined by simply choosing the same constant references stars for the fields from both telescopes, no other changes were applied. This is an example of how well the approach works for some stars.

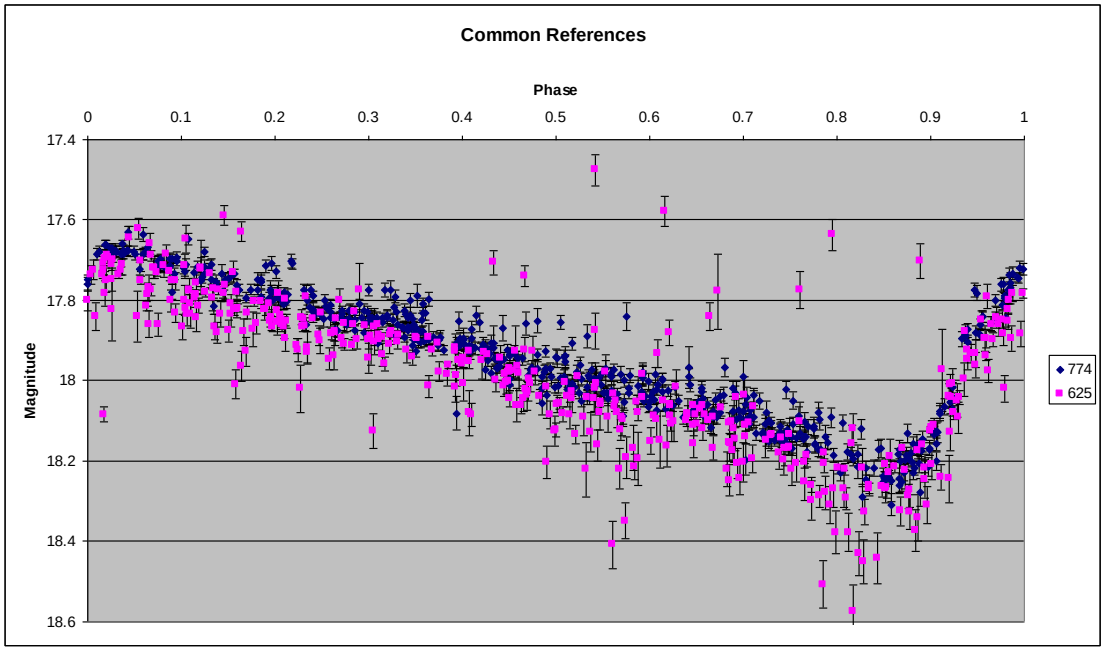

Figure 4.6: An example of type ab RR Lyrae star. The fields, telescope archives, and constant reference stars are exactly the same as for the type c above. Thus again two lightcurves are combined by the method of choosing the same reference stars for two telescopes. This time however, the points designated as 625 appear to tend to lie below the others. This case demonstrates that the overlap for lightcurves varies from star to star, most likely due to colour dependence of one kind or another.

The next step in increasing accuracy for finding the magnitude shift is to determine the average magnitude of the variable star. The first approach used is to fit a Fourier harmonic model at the dominant period, and use the zeroth Fourier component as the average magnitude. This comes from the definition that the zeroth component is equal to the average of all the harmonics. The model is fitted separately to data from each telescope, and the magnitude shift is determined by making the average equal for all models. The advantage of this approach is that it is a consistent way of treating data from different sources, but for smaller number of samples the model fitting becomes inaccurate. Additionally the model is likely to be sensitive to the telescope or site specific distortions of the lightcurve. For example if the data from one telescope contains a larger spread

around the lightcurve, the model fitted is different (see the figure below). This way will produce a visually balanced overlap of lightcurves, but at the risk of removing real differences between sites.

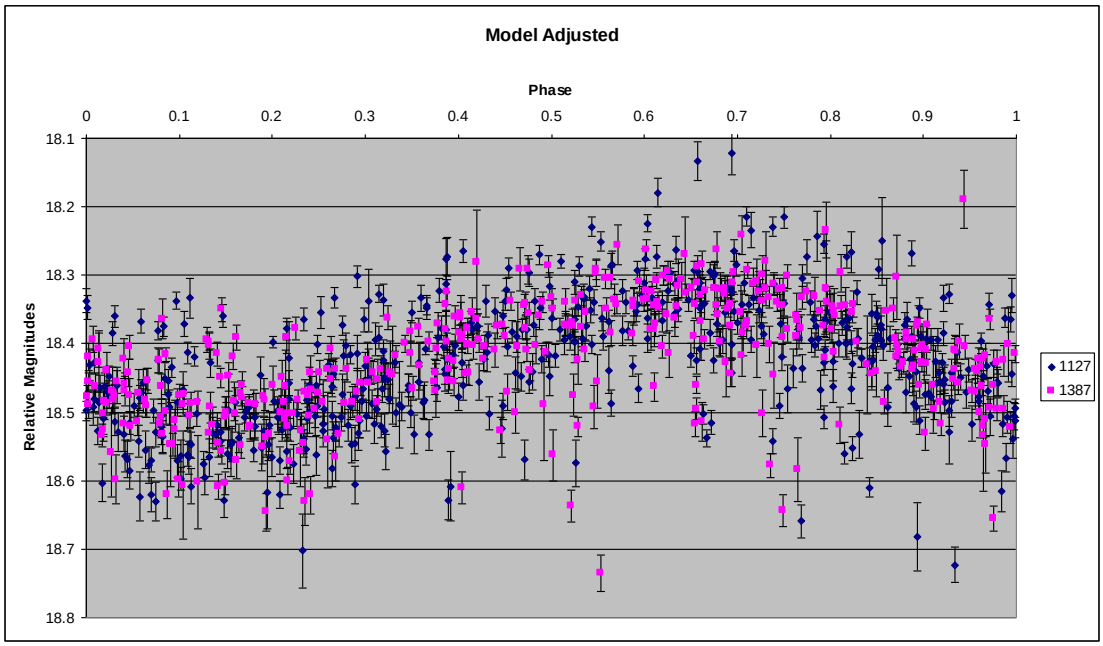

Figure 4.7: The same type c RR Lyrae star and the same data as in Figure 4.5. This time a Fourier components model has been fitted to each lightcurve, and the data slightly shifted to make the zeroth Fourier component the same for both models. This produces a satisfactory overlap of the lightcurves, but the 1387 data seems to be shifted a little too high.

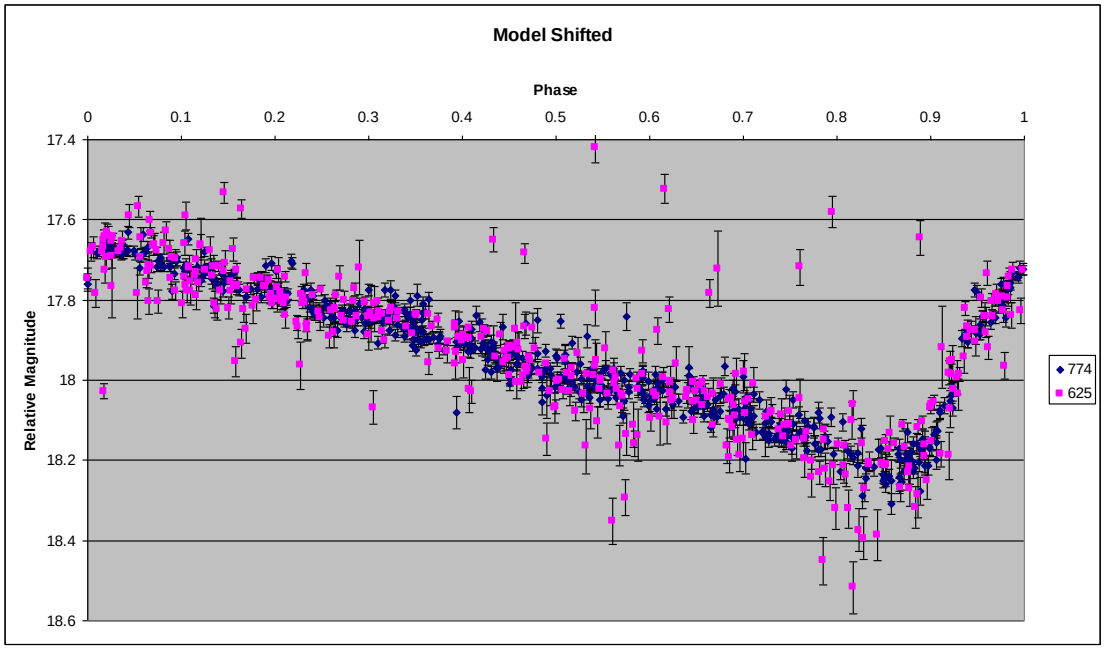

Figure 4.8: The same type ab RR Lyrae star and the same data as in Figure 4.6 with observations plotted after adjustment for Fourier model derived magnitude shift. This time the overlap is very balanced, as expected from a model fit. This also demonstrates the varying result of a method for different stars.

The second way to approach this part of the problem is to find a phase-weighted average. This takes into account the uneven sampling present in the PLANET data. The advantage of this method is that it is cleaner and model independent. However, like any approach it starts to fail when the number of samples per telescope grows small, because it relies on averaging samples in unevenly sized phase bins. When the number of samples gets small, some phase bins get large, and the average becomes inaccurate.

To obtain the phase-weighted magnitude of the average intensity-luminosity of a variable star's lightcurve the following formula is used from Silberman et al (1998):

$$\langle m \rangle_{Intensity} = -2.5 \log \left[\sum_{i}^{N} 0.5 \, (\phi_{i+1} - \phi_{i-1}) \, 10^{-0.4 m_i} \right]$$

This is the same as saying:

$$\langle m \rangle_{Intensity} = -2.5 \log \left[\sum_{i}^{N} \text{phase-bin}_i \times \text{Intensity}_i \right]$$

The phase-bin is the phase-width around the intensity measurement. In particular it is the distance between the two mid-points a phase has with its closest neighbours.

Similarly to above, in terms of average magnitudes rather than intensity, this becomes:

$$\langle m \rangle = \sum_{i}^{N} \text{phase-bin}_i \times \text{Magnitude}_i$$

The above principle has been used to get the phase weighted average magnitude:

$$\langle m \rangle = \sum_{i}^{N} 0.5 \, (\phi_{i+1} - \phi_{i-1}) \, m_i$$

Ultimately, whichever method is used to combine data, the process runs into the natural limitations of data accuracy. For example in a very well sampled archive, on the order of several hundred measurements each, the same set of four constant reference stars has an average magnitude over entire sample run of 15.021 for one telescope, and 15.027 for another. As explained above, at each measurement time for a telescope the average magnitude of all the constants is set to 15.0. The standard error for the constants is usually around 0.01 magnitudes, and has to be below 0.015 by constant star selection criteria. Thus for a perfect situation, these averages for both telescopes should have been at 15.0. The difference from 15.0 is one indication of to within what error data from two telescopes can be combined. The distribution of values around a mean lightcurve tends to have a width on the same order as these differences. Combining lightcurves by the use of the same constant reference stars for all telescopes moves them to within the same order of distance. While using any of the average magnitude methods will shift the lightcurves so that they overlap more so

than just agree to within their error ranges, using the same reference stars maybe sufficient in terms of finding the main frequency component.

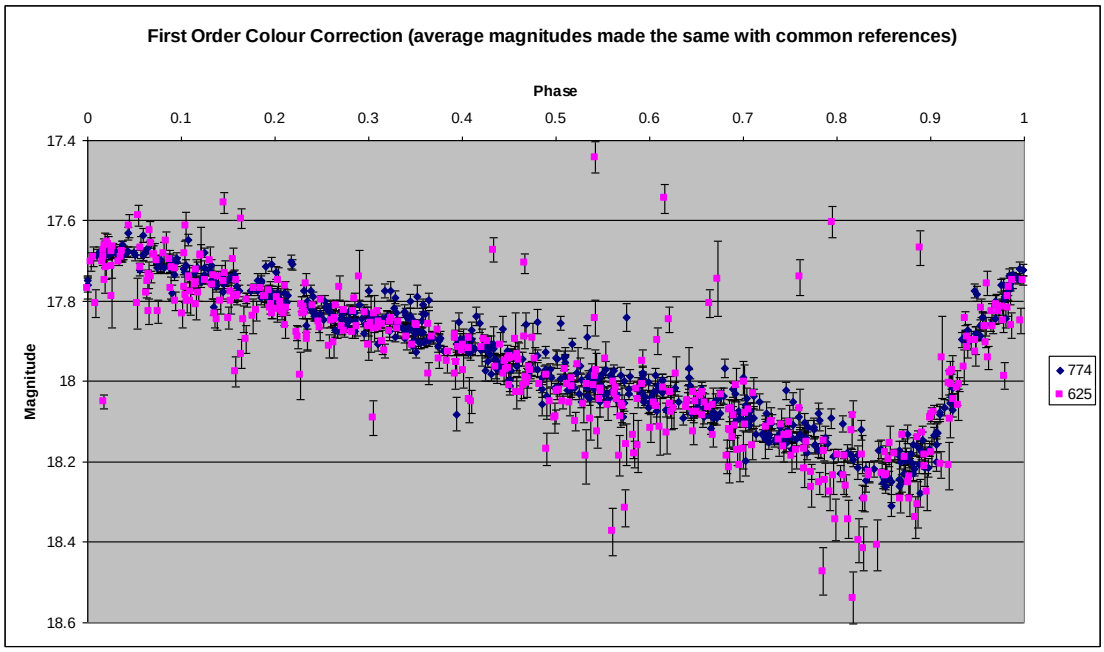

Figure 4.9: The same type ab RR Lyrae star and the same data as in Figure 4.6. In this example the data is shifted so that the average magnitude is equal. The result is almost exactly the same as for the Fourier model approach, as expected in this very well sampled case.

There also secondary considerations arising from the colour dependence of translating magnitudes between telescopes. The RR Lyrae stars undergo changes in their outer atmospheres as the light output varies. The changes in the photosphere of an RR Lyrae cause changes in its colour. Thus different parts of an RR Lyrae lightcurve are shifted by different amounts. For example, the star SU Dra is a type ab RR Lyrae with a V band peak to peak variation of around 1 magnitude, and depending on the band, its peak to peak colour variation is between 0.2 and 0.45 (Smith 1995 p 86). The smallest variation occurring for the (V-R) colour, and the highest for (V-I). The changes in colour over the main period are similar in size to the value of the colour, and thus significant in terms of the translation of magnitudes between telescopes, at least for some variable stars. In such cases using a method based on an average magnitude for the variable star to translate magnitudes

between telescopes will erase the real difference of the shift being phase dependant. Furthermore the additional correction accounted for in this way is on the same order as a new difference being introduced by it, possibly making this step unnecessary.

Figures 4.10 and 4.11 show the Fourier models overlaid on the observed magnitudes for the two stars used as examples for magnitude shifts derived with different methods. The phases are shifted when compared to Figures 4.5 – 4.9 because they are relative and in these two examples data from a single telescope is plotted. The starting point for a phase is picked from the earliest available data point as precisely defining a phase starting point is not necessary for this work. The shapes of the lightcurves remain the same.

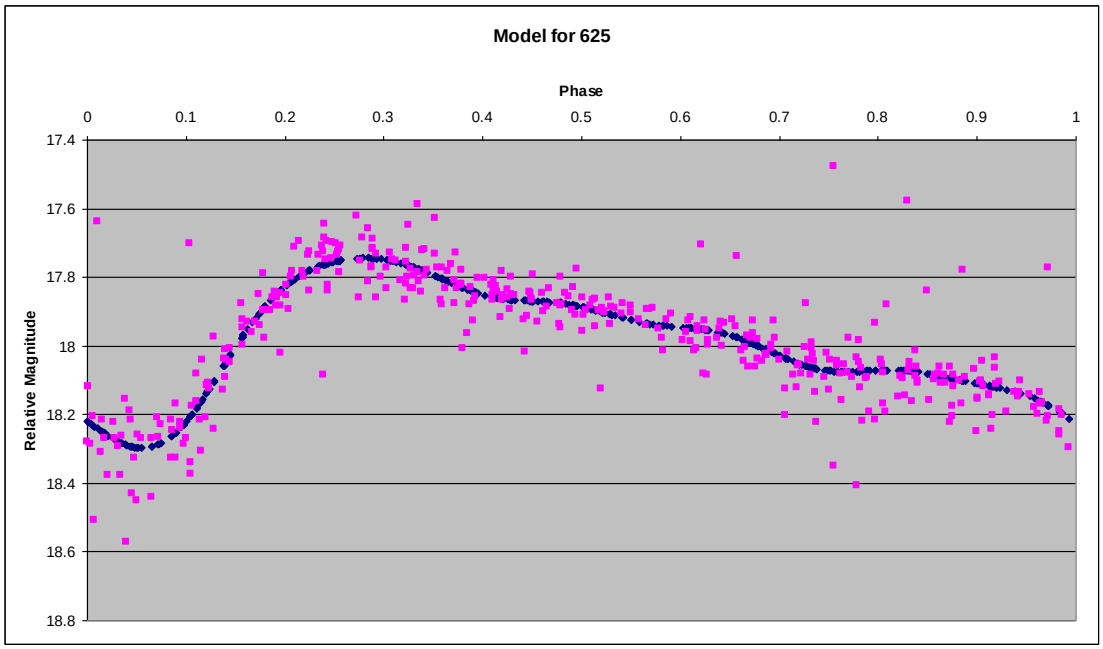

Figure 4.10: Part of the data for the type ab RR Lyrae star from a single telescope with the Fourier model included in it.

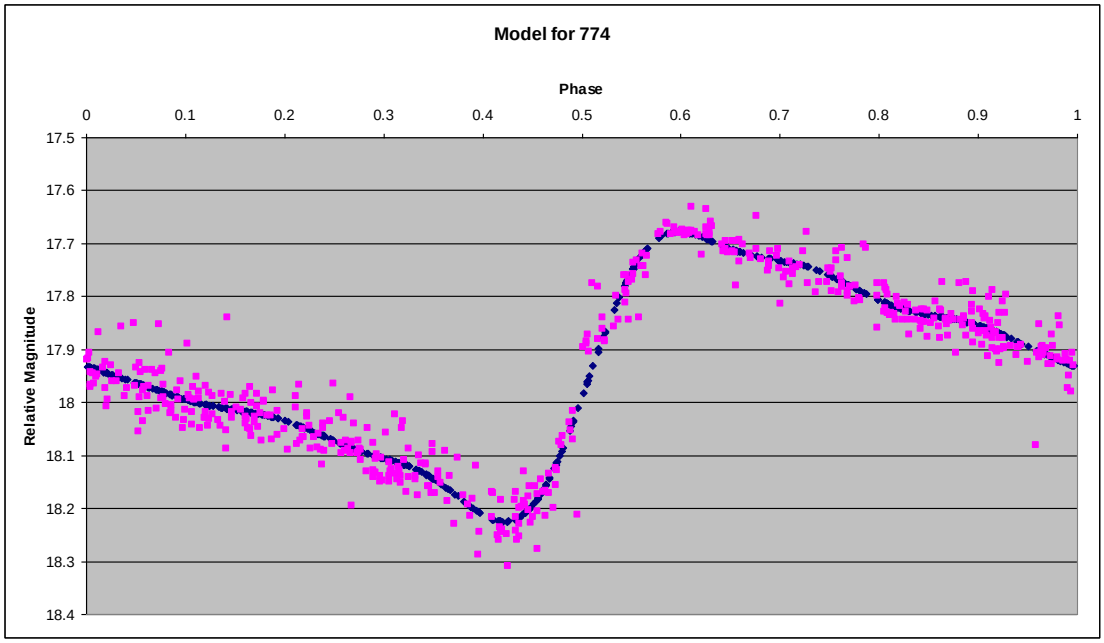

Figure 4.11: Similar to above, the second part of the type ab RR Lyrae data with Fourier model fitted. This demonstrates how the model changes due to telescope specific differences in the data.

5 Results of the identification of RR Lyrae stars in PLANET observations

5.1 Summary of results

I have identified 87 RR Lyrae stars from data in the PLANET database for years 1995 to 2005 inclusive. See Figure 5.1 for the period distribution of the identified stars, and Table 5.1, Table 5.2, Table 5.3, and Table 5.4 for details about them, such as period, absolute magnitude, colour, cleaned sample counts, time span and combined time span of data, OGLE II matches, and others, with sources as explained in table descriptions. The stars 48 and 63 (as numbered in the tables) are atypical from and possibly not part of the RR Lyrae type. The majority of known RR Lyrae stars are of the ab type and the result from PLANET data follows this. Among the RR Lyrae stars found in the specified PLANET data there are 69 type ab, and 16 type c RR Lyraes. Due to the difficulties in distinguishing the type c star lightcurves from some eclipsing binary star lightcurves, the fraction of type c among the RR Lyrae stars found is likely to be an underestimate of the true number among the variables in the PLANET database, as per selection criteria used for these results. The two mentioned atypical stars are given the custom type suffix *w* to indicate that they are similar to RR Lyrae stars but I am not certain that they belong to their group.

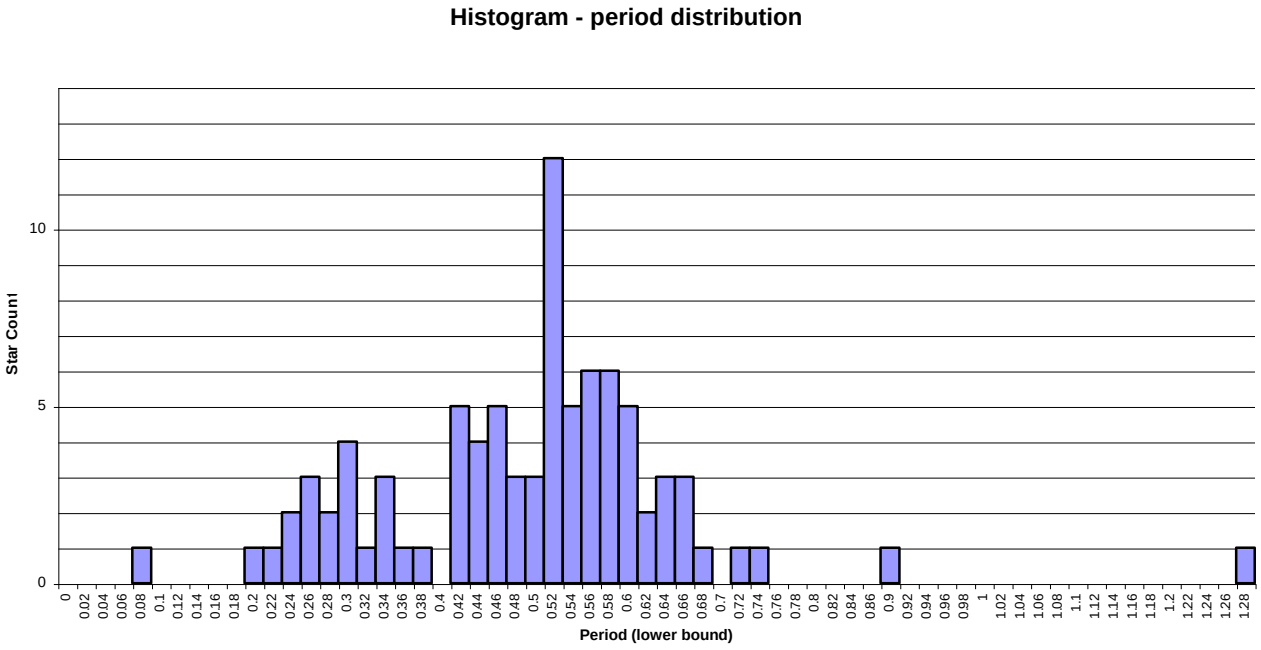

Figure 5.1: The period distribution of all the RR Lyrae stars identified in the PLANET database (including the two atypical stars). Note the two groupings, with the one around lower periods corresponding to RRc stars. Although due to the relatively small number of RRc stars the lower periods grouping is somewhat indistinct. The period values are in units of days.

For 30 out of the 87 stars identified sufficient data from more than one telescope was available, as described in the data selection criteria in section 4, and the lightcurves were produced from the data combined between the telescopes. The remaining majority, 57 stars, had usable data available from a single telescope only.

Only 2 RR Lyrae stars have lightcurves from data combined from the four PLANET telescopes observing together a microlensing event and producing sufficient observations per telescope for analysis, as described in Data Analysis section. A further 7 stars have lightcurves based on data from three telescopes. Thus even for the multiple telescope data the majority of lightcurves are based on observations from two telescopes. This result points to a very strong selection effect against the availability of multiple telescope data from the observing strategy used and for the type of analysis conducted in this thesis. Two reasons for this exist. First the size of

PLANET observing fields varies between telescopes and their positioning varies between exposures reducing the chances for the stars lying closer to edge of observing fields being covered every time at all telescopes. Usually the telescope with the largest field of view dominates in terms of the number of variable stars detected. When the stars closer to edge are out of the observing field in some exposures, the number of available magnitude observation samples from a telescope may drop to below the minimum required to produce a lightcurve that can be combined with others, the minimum 80 such samples as per the data analysis criteria used in this analysis, and all of the data for the star from this field and event is ignored. Second and the greater contribution is the event observing coverage between the telescopes. Comparing the Fields and Events entries in the Data Analysis Table 4.1, it is clear that not all events were covered by all four PLANET telescopes in sufficient detail to produce an archive for each telescope's field. The average number of telescopes producing archives for events is closer to two. In addition a significant number of the existing archives contain less than the minimum number of observations required for processing, for most or all of the stars in them.

The main numerical results for the group of PLANET RR Lyrae stars are given below in Tables 5.1 and 5.2.

Table 5.1: PLANET RR Lyrae identifications

	Star - Name	OGLE II ID	Mag I	V-I	Samp Ex	Samp	Ndetect	Co-ordinates OGLEII	PLANET Co-ordinates
1	EB2K005I_d774_P753_U625_Y1200.ab	none				1577			17:53:13.904 -30:56:52.01
2	EB2K005I_d901_P634_Y992.c	none				1093			17:53:08.534 -30:57:35.58
3	EB2K005I_P1258_Y2248.ab	none				707			17:53:12.844 -30:53:32.46
4	EB2K005I_P3115_Y1556.ab	none				657			17:53:04.678 -30:53:43.59
5	MB99008I_C1012.c	none				92			17:56:28.192 -29:38:39.36
6	MB99008I_C1559.ab	none				95			17:56:18.539 -29:40:15.44
7	MB99008I_C2285.ab	none				94			17:56:33.577 -29:40:47.58
8	MB99008I_C3607.c	none				93			17:56:33.534 -29:41:39.24
9	OB2K025I_Y3107.ab	bul_sc37_i_645268	16.597	2.212/13	403	91	341	175257.84-293333.9	17:52:57.831 -29:33:34.23
10	OB2K025I_Y3746.c **+**	bul_sc3_i_203622	16.894	2.216/10	514	79	325	175308.74-293211.6	17:53:08.764 -29:32:11.51
11	OB2K031I_Y608.ab	bul_sc12_i_430188	16.229	1.907/6	282	123	225	181622.27-241528.8	18:16:22.295 -24:15:29.20
12	OB2K046I_Y2807.ab	bul_sc4_i_732074	16.138	1.727/14	504	145	447	175500.57-292653.8	17:55:00.565 -29:26:53.96
13	OB2K046I_Y3981.ab	bul_sc4_i_755313	16.486	2.132/14	498	117	474	175452.73-292222.0	17:54:52.715 -29:22:21.91
14	OB2K046I_Y4537.c **+**	bul_sc4_i_744012	16.139	1.953/9	500	116	417	175505.11-292520.3	17:55:05.104 -29:25:20.42
15	OB2K048I_P1804_Y1581.c **OGLE BL2**	bul_sc30_i_636915	16.145	1.221/9	317	217	289	180144.39-285827.7	18:01:44.357 -28:58:27.95
16	OB2K048I_P1901_Y1323.c	bul_sc30_i_455213	16.154	1.308/8	278	216	237	180136.94-285738.7	18:01:36.914 -28:57:38.94
17	OB2K048I_Y1865.ab	bul_sc30_i_636934 bul_sc31_i_24053	16.405 16.399	1.511/8 1.507/6	280 276	130	263 227	180153.34-285818.6 180153.33-285818.6	18:01:53.312 -28:58:18.78
18	OB2K048I_Y457.c **+**	bul_sc30_i_636615 bul_sc31_i_23369	14.8814 14.878	1.124/5 1.126/6	212 320	74	172 221	180156.37-285710.3 180156.36-285710.3	18:01:56.353 -28:57:10.39
19	OB2K012I_Y1114.ab	bul_sc43_i_123530	17.271	2.337/10	364	185	228	173506.20-273343.2	17:35:06.198 -27:33:43.49
20	OB2K026I_d698_P1940_Y933.ab	bul_sc3_i_490084	15.726	1.637/10	511	434	474	175340.72-300450.7	17:53:40.774 -30:04:50.85
21	OB2K026I_d722_P1909_U1395_Y2184.ab	bul_sc3_i_479471	16.215	1.797/11	425	582	349	175343.84-300459.4	17:53:43.894 -30:04:59.61
22	OB2K026I_d1087_P1608_Y2485.ab	bul_sc3_i_479099	16.276	1.723/12	491	430	516	175349.59-300647.3	17:53:49.654 -30:06:47.51
23	OB2K026I_d1749_Y2201.ab	bul_sc3_i_479962	16.739	1.753/11	395	267	324	175344.22-300625.9	17:53:44.252 -30:06:26.12
24	OB2K026I_P2054_U1156_Y2531.ab	bul_sc3_i_490215	16.334	1.777/12	501	373	500	175350.58-300417.5	17:53:50.630 -30:04:17.62
25	OB2K026I_Y1865.ab **+**	bul_sc3_i_490223	16.359	1.824/12	502	124	517	175338.18-300412.9	17:53:38.219 -30:04:13.05
26	OB2K029I_Y1752.ab	bul_sc37_i_463456	16.620	2.121/14	403	127	337	175234.60-293934.3	17:52:34.603 -29:39:34.52
27	OB2K029I_Y4341.ab **OGLE BL1**	bul_sc37_i_464953	17.067	NA	377	125	253	175245.03-293820.1	17:52:45.041 -29:38:20.28
28	OB2K029I_Y4880.ab	bul_sc37_i_623081	16.924	2.542/11	404	127	308	175254.56-294127.7	17:52:54.561 -29:41:27.87
29	OB2K034I_d596.ab	bul_sc43_i_265124	16.762	2.297/10	369	87	260	173529.32-272325.0	17:35:29.296 -27:23:25.24
30	OB2K038I_d549_Y1703.ab	bul_sc3_i_104269	16.150	1.908/12	521	239	504	175314.93-295637.7	17:53:14.971 -29:56:37.82
31	OB2K038I_d1716_Y3199.ab	bul_sc3_i_91895	16.753	2.090/12	509	260	465	175313.71-295902.6	17:53:13.761 -29:59:02.59

32	OB2K038I_Y1988.ab **OGLE BL1**	bul_sc3_i_315349	16.309	1.953/12	518	95	479	175319.71-295517.2	17:53:19.745 -29:55:17.34
33	OB2K038I_Y3098.ab	bul_sc3_i_105206	17.131	1.963/10	507	97	406	175311.47-295628.2	17:53:11.440 -29:56:29.61
34	OB2K038I_Y3334.ab	bul_sc3_i_104529	16.338	1.897/12	513	99	514	175316.60-295532.3	17:53:16.642 -29:55:32.40
35	OB2K038I_Y352.ab **+**	bul_sc3_i_90110	14.501	1.882/11	535	100	542	175314.17-295851.3	17:53:14.220 -29:58:51.43
36	OB2K038I_Y3547.ab +	bul_sc3_i_316298	16.669	1.997/12	498	96	461	175320.83-295512.5	17:53:20.879 -29:55:12.64
37	MB95013I_L1072.ab	none				118			18:08:38.978 -27:42:18.93
38	MB95017I_L469.ab – **not OGLEII RR**	bul_sc32_i_154959	15.666	1.301/7	310	92	274	180305.75-282059.0	18:03:05.731 -28:20:58.87
39	MB95017I_L784.ab	bul_sc32_i_154418	15.700	1.289/7	309	90	282	180307.93-282200.4	18:03:07.906 -28:22:00.30
40	MB96020I_T106.c	bul_sc20_i_715713	13.954	0.935/7	317	83	313	175938.30-284547.8	17:59:38.286 -28:45:47.95
41	MS98001I_S91.ab	smc_sc4_i_38956	17.203	0.639/28	325	173	255	004539.77-725253.2	00:45:39.771 -72:52:53.75
42	MB99008I_A2199_U739_Y1278.ab	none				807			17:56:18.540 -29:40:15.42
43	MB99008I_A2324_U1242_Y1737.ab	none				762			17:56:33.576 -29:40:47.52
44	MB99018I_Y2018.ab **OGLE BL1**	bul_sc30_i_365051	15.931	1.577/9	318	95	271	180115.66-282937.3	18:01:15.602 -28:29:37.24
45	MB99018I_Y2544.ab	bul_sc30_i_165806	16.146	1.446/9	316	102	286	180100.05-283043.7	18:01:00.000 -28:30:43.52
46	OB99035I_A2778.ab	bul_sc44_i_14663	18.431	NA	331	89	41	174902.72-301821.3	17:49:02.746 -30:18:22.64
47	OB99036I_A424_Y220.c **OGLE BL1**	bul_sc11_i_101274	15.729	na	211	304	183	182036.95-215830.9	18:20:37.021 -21:58:32.42
48	OB99005I_A831.w	bul_sc26_i_314049	15.442	1.093/8	343	109	305	174711.40-344609.3	17:47:11.437 -34:46:09.15
49	OB99005I_A2239.ab **OGLE BL1**	bul_sc26_i_687150	16.415	1.238/7	330	123	302	174735.96-344416.1	17:47:36.013 -34:44:15.95
50	MB97018I_L1036.ab	none				84			18:03:20.426 -28:01:27.89
51	MB97028I_L516_S248.ab	none				376			18:00:29.936 -28:02:05.83
52	KB01002I_Y585.ab	none				220			17:55:06.710 -28:44:46.10
53	KB01012I_d487_Y340.ab	bul_sc21_i_557615	15.583	1.261/7	312	242	295	180027.49-285458.8	18:00:27.479 -28:54:58.77
54	KB03035I_A403.ab	none				112			18:07:16.901 -28:39:48.93
55	KB03035I_A724.ab	none				108			18:07:05.382 -28:38:05.15
56	OB03167I_A551_W878.ab	none				192			17:44:51.197 -34:02:33.69 **B**
57	OB03167I_A1317_W1551.ab	none				243			17:44:54.209 -034:02:34.41 **B**
58	OB03167I_A2056.ab	none				175			17:45:00.359 -34:07:13.52
59	OB03167I_A2799.ab	none				176			17:45:04.413 -34:05:14.57 **B**
60	OB03177I_A589.c	Can't calibrate fits				105			17:39:02 -22:18:32
61	OB03200I_A573.ab **OGLE BL1**	bul_sc6_128105	15.722	0.956/8	303	101	287	180746.23-314241.3	18:07:46.289 -31:42:41.99
62	OB03200I_A710.c **+**	bul_sc6_i_251848	16.232	1.302/7	297	100	251	180748.05-314507.1	18:07:48.053 -31:45:08.76
63	OB03208I_A844_W681.w	none				240			17:58:12.411 -33:31:13.10
64	OB03208I_A1106.ab	none				152			17:58:10.016 -33:34:08.13
65	OB03262I_W1001.ab	none				90			17:57:09.3 10 -30:18:17.83
66	KB02033I_d1250.ab **OGLE BL2**	bul_sc34_i_607633	16.420	1.496/9	328	93	303	175819.17-290547.4	17:58:19.154 -29:05:47.37
67	OB02181I_d1091.ab	none				82			17:56:08.567 -30:22:23.06
68	OB05153I_W1401_Z734.c	bul_sc2_i_359204	15.793	1.127/6	262	402	233	180427.61-284016.4	18:04:27.586 -28:40:16.47

69	OB05099I_W345.ab **OGLE BL1**	bul_sc39_i_575408	15.008	1.627/13	382	97	372	175546.37-292557.1	17:55:46.352 -29:25:57.36
70	OB05099I_W1162.ab	bul_sc39_i_744680	16.573	2.204/16	410	91	335	175558.01-292734.6	17:55:58.034 -29:27:34.87
71	OB05099I_W2434.ab	bul_sc39_i_576545	16.554	1.964/14	377	105	336	175547.03-292540.1	17:55:47.023 -29:25:40.29
72	OB05099I_W2828.ab	bul_sc39_i_764911	16.779	2.147/15	411	81	374	175602.19-292332.7	17:56:02.189 -29:23:33.29 **B**
73	OB05099I_W2540.c **+**	bul_sc39_i_576668	16.612	1.785/14	359	90	238	175551.49-292502.4	17:55:51.492 -29:25:02.54
74	OB05099I_W1548.c **+**	bul_sc39_i_754030	16.342	1.850/16	410	106	345	175557.43-292505.9	17:55:57.443 -29:25:05.93
75	OB05304I_W1187_Z569.ab	bul_sc33_i_703300	15.944	1.343/7	269	474	256	180552.90-283416.2	18:05:52.891 -28:34:16.29
76	OB05304I_W765_Z176.ab **OGLE BL2**	bul_sc33_i_702993	15.499	0.910/5	157	492	145	180602.99-283341.1	18:06:02.969 -28:33:41.13
77	OB05304I_Z527.c	bul_sc33_i_702904	15.500	1.146/6	272	357	254	180555.91-283435.4	18:05:55.896 -28:34:35.46
78	OB05018I_W2479_Z1970.ab	none				362			17:51:17.724 -29:38:07.01
79	OB05018I_W3343_Z2705.ab	none				472			17:51:20.672 -29:39:30.44
80	OB05216I_Z486.ab	none				85			17:45:37.794 -24:03:46.52
81	OB05226I_A1346_W1119_Z516.ab	none				673			17:44:50.550 -34 :09:57.37
82	OB05226I_A2234_W1032.ab	none				181			17:44:32.556 -34:10:37.06 **B**
83	OB05259I_Z487.ab	none				148			17:58:53.071 -29:38:44.45
84	OB05327I_A947_Z345.ab	none				532			17:58:59.987 -31:47:50.89
85	OB05331I_Z1035.ab	bul_sc5_i_182170	17.290	3.440/12	363	124	253	175011.05-293614.7	17:50:11.052 -29:36:14.67 **B**
86	OB05331I_Z1604.ab	bul_sc5_i_183604	17.629	na	352	124	97	175020.18-293636.8	17:50:20.187 -29:36:36.63 **B**
87	OB05390I_W1068_Z538.ab	none				225			17:54:17.486 -30:22:55.93

Explanation for column headings in Tables 5.1 and 5.2:

Star – Name: A star ID constructed from the details of PLANET data. The Star - Name is made up of the PLANET observing field (also called the microlensing event) followed by underscore and a single letter telescope ID combined with an internal star number for that telescope (this combination is repeated for each telescope from contributing data to this lightcurve). This sequence is closed with a period followed by the type of variability.

Period: is the period in days derived with searchAoV in data combined from all the indicated telescopes.

Amplitude: is the amplitude of the model fitted to the combined data.

Time Span: is the length of time from the earliest samples to the latest samples in the combined data

Mag I: average I magnitude for the star taken from the DIA section of OGLE II online database (derived from image subtraction photometry).

V-I: colour index from OGLE II

Ndetect: the number of detections of the star in OGLE II data through image subtraction. This is a good indication of variability and a test for correctness of the match to the PLANET RR Lyrae. For a RR Lyrae star this number has to be a high fraction of the number of observed samples.

Samp ex: extra samples, the number of samples from OGLE II data.

Samp/les: the number of samples from combined PLANET data.

The additional notes in the fields are as follows:

B – following the co-ordinates stands for "blended". These are cases where the star in PLANET observations is close enough to another star to appear to visually overlap and share light. Thus this is a semi-qualitative indication that blending may be shifting the balance of flux and affecting the accuracy of position determination.

NA – the value is not available from the OGLE II database, presumably it is not measured

none – this PLANET star has not been matched to an observed OGLE II star.

OGLE BL1/2 – this star has been identified in OGLE II data as a Blazhko star of type BL1/2 as per Mizerski 2003.

+ - after a Star – Name indicates that this star was not classified as a RR Lyrae from PLANET data alone. In some cases PLANET data did not allow a star to be clearly classified as a RR Lyrae but the classification became possible when their OGLE II observations were checked. These cases are marked in this way.

Co-ordinates are given in the J2000 epoch.

In a couple of cases where the OGLE II observing fields overlapped the same star was matched to multiple OGLE II IDs. For these stars data and lightcurves from both OGLE II fields are used.

Table 5.2: Summary of RR Lyrae identification – additional information

	Star - Name	Period (d)	Amplitude (mag)	Time Span (d)	Samples	PLANET Co-ordinates
1	EB2K005I_d774_P753_U625_Y1200.ab	0.687600	0.537757	464.415	1577	17:53:13.904 -30:56:52.01
2	EB2K005I_d901_P634_Y992.c	0.255222	0.099331	490.281	1093	17:53:08.534 -30:57:35.58
3	EB2K005I_P1258_Y2248.ab	0.536711	0.361673	491.445	707	17:53:12.844 -30:53:32.46
4	EB2K005I_P3115_Y1556.ab	0.559366	0.529498	490.540	657	17:53:04.678 -30:53:43.59
5	MB99008I_C1012.c	0.359648	0.139747	160.512	92	17:56:28.192 -29:38:39.36
6	MB99008I_C1559.ab	0.660181	0.312045	160.705	95	17:56:18.539 -29:38:39.36
7	MB99008I_C2285.ab	0.526169	0.821798	160.907	94	17:56:33.577 -29:40:47.58
8	MB99008I_C3607.c	0.216707	0.239592	160.907	93	17:56:33.534 -29:41:39.24
9	OB2K025I_Y3107.ab	0.299918	0.240748	113.080	79	17:53:08.764 -29:32:11.51
10	OB2K025I_Y3746.c **+**	0.551175	0.586767	114.078	91	17:52:57.831 -29:33:34.23
11	OB2K031I_Y608.ab	0.584220	0.389396	82.370	123	18:16:22.295 -24:15:29.20
12	OB2K046I_Y2807.ab	0.623306	0.441639	40.063	145	17:55:00.565 -29:26:53.96
13	OB2K046I_Y3981.ab	0.596099	0.633073	35.697	117	17:54:52.715 -29:22:21.91
14	OB2K046I_Y4537.c **+**	0.281149	0.240990	39.612	116	17:55:05.104 -29:25:20.42
15	OB2K048I_P1804_Y1581.c	0.352159	0.296080	380.991	217	18:01:44.357 -28:58:27.95
16	OB2K048I_P1901_Y1323.c	0.308668	0.233212	380.976	216	18:01:36.914 -28:57:38.94
17	OB2K048I_Y1865.ab	0.426143	0.880400	67.039	130	18:01:53.312 -28:58:18.78
18	OB2K048I_Y457.c **+**	0.233875	0.065641	57.399	74	18:01:56.353 -28:57:10.39
19	OB2K012I_Y1114.ab	0.450527	0.745344	138.304	185	17:35:06.198 -27:33:43.49
20	OB2K026I_d698_P1940_Y933.ab	0.316262	0.228283	474.865	434	17:53:40.774 -30:04:50.85
21	OB2K026I_d722_P1909_U1395_Y2184.ab	0.313555	0.272185	484.783	582	17:53:43.894 -30:04:59.61
22	OB2K026I_d1087_P1608_Y2485.ab	0.476499	0.810553	471.861	430	17:53:49.654 -30:06:47.51
23	OB2K026I_d1749_Y2201.ab	0.544585	0.651255	442.294	267	17:53:44.252 -30:06:26.12
24	OB2K026I_P2054_U1156_Y2531.ab	0.456654	0.772482	484.170	373	17:53:50.630 -30:04:17.62
25	OB2K026I_Y1865.ab **+**	0.499151	0.604980	145.835	124	17:53:38.219 -30:04:13.05
26	OB2K029I_Y1752.ab	0.525613	0.593390	95.960	127	17:52:34.603 -29:39:34.52
27	OB2K029I_Y4341.ab	0.436789	0.639361	95.580	125	17:52:45.041 -29:38:20.28
28	OB2K029I_Y4880.ab	0.528058	0.627065	93.918	127	17:52:54.561 -29:41:27.87
29	OB2K034I_d596.ab	0.641979	0.526384	32.198	87	17:35:29.296 -27:23:25.24
30	OB2K038I_d549_Y1703.ab	0.543720	0.764476	377.694	239	17:53:14.971 -29:56:37.82
31	OB2K038I_d1716_Y3199.ab	0.431787	0.808449	377.694	260	17:53:13.761 -29:59:02.59
32	OB2K038I_Y1988.ab	0.533447	0.409751	71.063	95	17:53:19.745 -29:55:17.34
33	OB2K038I_Y3098.ab	0.537956	0.611420	71.467	97	17:53:11.440 -29:56:29.61
34	OB2K038I_Y3334.ab	0.515280	0.912479	71.467	99	17:53:16.642 -29:55:32.40
35	OB2K038I_Y352.ab **+**	0.740064	0.449963	71.467	100	17:53:14.220 -29:58:51.43

36	OB2K038I_Y3547.ab +	0.481282	0.634061	71.063	96	17:53:20.879 -29:55:12.64
37	MB95013I_L1072.ab	0.399129	0.254913	25.327	118	18:08:38.978 -27:42:18.93
38	MB95017I_L469.ab	0.604113	0.307023	35.359	92	18:03:05.731 -28:20:58.87
39	MB95017I_L784.ab	0.613703	0.599217	35.359	90	18:03:07.906 -28:22:00.30
40	MB96020I_T106.c	0.366986	0.480725	39.589	83	17:59:38.286 -28:45:47.95
41	MS98001I_S91.ab	1.264039	0.380850	49.576	173	00:45:39.771 -72:52:53.75
42	MB99008I_A2199_U739_Y1278.ab	0.659971	0.260093	410.228	807	17:56:18.540 -29:40:15.42
43	MB99008I_A2324_U1242_Y1737.ab	0.526144	0.800482	390.380	762	17:56:33.576 -29:40:47.52
44	MB99018I_Y2018.ab	0.548877	0.407300	49.076	95	18:01:15.602 -28:29:37.24
45	MB99018I_Y2544.ab	0.562815	0.817946	53.045	102	18:01:00.000 -28:30:43.52
46	OB99035I_A2778.ab	0.731242	0.576960	49.909	89	17:49:08.200 -30:18:00.6
47	OB99036I_A424_Y220.c	0.328725	0.251437	78.450	304	18:20:37.021 -21:58:32.42
48	OB99005I_A831.w	0.086362	0.203790	107.078	109	17:47:11.437 -34:46:09.15
49	OB99005I_A2239.ab	0.584561	0.615284	138.396	123	17:47:36.013 -34:44:15.95
50	MB97018I_L1036.ab	0.572860	0.487833	39.933	84	18:03:20.426 -28:01:27.89
51	MB97028I_L516_S248.ab	0.537506	0.487934	76.473	376	18:00:29.936 -28:02:05.83
52	KB01002I_Y585.ab	0.531361	0.684041	144.868	220	17:55:06.710 -28:44:46.10
53	KB01012I_d487_Y340.ab	0.616356	0.479360	115.435	242	18:00:27.479 -28:54:58.77
54	KB03035I_A403.ab	0.582095	0.252121	32.904	112	18:07:16.901 -28:39:48.93
55	KB03035I_A724.ab	0.587329	0.373851	32.904	108	18:00:05.382 -28:38:05.15
56	OB03167I_A551_W878.ab	0.667436	0.640620	115.825	192	17:44:51.197 -34:02:33.69
57	OB03167I_A1317_W1551.ab	0.675648	0.260648	117.611	243	17:44:54.209 -34:02:34.41
58	OB03167I_A2056.ab	0.527087	0.603790	37.772	175	17:45:00.359 -34:07:13.52
59	OB03167I_A2799.ab	0.458888	0.591811	37.772	176	17:45:04.413 -34:05:14.57
60	OB03177I_A589.c Can't calibrate fits	0.274168	0.235366	33.224	105	17:39:02 -22:18:32
61	OB03200I_A573.ab	0.510964	0.429370	19.362	101	18:07:46.289 -31:42:41.99
62	OB03200I_A710.c **+**	0.318083	0.249410	19.362	100	18:07:48.053 -31:45:08.76
63	OB03208I_A844_W681.w	0.896772	0.355609	108.320	240	17:58:12.411 -33:31:13.10
64	OB03208I_A1106.ab	0.476098	0.551619	37.070	152	17:58:10.016 -33:34:08.13
65	OB03262I_W1001.ab	0.464268	0.730618	95.430	90	17:57:09.3 10 -30:18:17.83
66	KB02033I_d1250.ab	0.438502	0.612526	33.908	93	17:58:19.154 -29:05:47.37
67	OB02181I_d1091.ab	0.568814	0.574926	74.198	82	17:56:08.567 -30:22:23.06
68	OB05153I_W1401_Z734.c	0.272851	0.410753	56.026	402	18:04:27.586 -28:40:16.47
69	OB05099I_W345.ab	0.566667	0.490624	82.290	97	17:55:46.352 -29:25:57.36
70	OB05099I_W1162.ab	0.610209	0.484405	80.161	91	17:55:58.034 -29:27:34.87
71	OB05099I_W2434.ab	0.462626	0.723988	80.669	105	17:55:47.023 -29:54:40.29
72	OB05099I_W2828.ab	0.444733	0.321351	82.214	81	17:56:02.189 -29:23:33.29
73	OB05099I_W2540.c **+**	0.249134	0.249257	80.183	90	17:55:51.492 -29:25:02.54
74	OB05099I_W1548.c **+**	0.356017	0.224078	82.290	106	17:55:57.443 -29:25:05.93
75	OB05304I_W1187_Z569.ab	0.523558	0.831972	71.196	474	18:05:52.891 -28:34:16.29

76	OB05304I_W765_Z176.ab	0.568890	0.621395	65.087	492	18:06:02.969 -28:33:41.13
77	OB05304I_Z527.c	0.274299	0.266606	68.637	357	18:05:55.896 -28:34:35.46
78	OB05018I_W2479_Z1970.ab	0.584684	0.346354	135.711	362	17:51:17.724 -29:38:07.01
79	OB05018I_W3343_Z2705.ab	0.438086	0.630129	141.241	472	17:51:20.672 -29:39:30.44
80	OB05216I_Z486.ab	0.486250	0.694103	21.292	85	17:45:37.794 -24:03:46.52
81	OB05226I_A1346_W1119_Z516.ab	0.654227	0.319654	48.745	673	17:44:50.550 -34 :09:57.37
82	OB05226I_A2234_W1032.ab	0.474887	0.584022	48.152	181	17:44:32.556 -34:10:37.06
83	OB05259I_Z487.ab	0.618299	0.543619	77.871	148	17:58:53.071 -29:38:44.45
84	OB05327I_A947_Z345.ab	0.633051	0.389828	55.019	532	17:58:59.987 -31:47:50.89
85	OB05331I_Z1035.ab	0.538667	0.651674	50.195	124	17:50:11.052 -29:36:14.67
86	OB05331I_Z1604.ab	0.510591	0.457866	50.195	124	17:50:20.187 -29:36:36.63
87	OB05390I_W1068_Z538.ab	0.569794	0.678334	35.202	225	17:54:17.486 -30:22:55.93

5.2 Secondary and residual period detection

The RR Lyrae stars identified in PLANET data were analysed for the presence of variability at periods additional to the strongest period. The main aim of this step was the detection of Blazhko stars through the identification of multiplets composed of the main and one or more additional close frequencies producing long term modulation of the amplitude of the main lightcurve through the beating between them. This is the currently accepted feature for identifying Blazhko stars (Alcock *et al* 2002, Moskalik and Poretti 2002, Moskalik and Poretti 2003).

The extensive analysis as described in section 4, both through looking for secondary periods, and through looking for additional periods in lightcurve model residuals analysis, identified an additional variability in only a single star in the PLANET data. The star number 3 named EB2K005I_P1258_Y2248.ab has a main period of 0.536711 days and an additional period at 0.528070 days. The two periods for this star appear clearly in the normal periodogram, and in the residuals lightcurve. The two periods are also present in single telescope data from both telescopes, and in the combined lightcurve. Thus this is a strong and consistent detection of a Blazhko star. A very strong modulation can be clearly seen in the combined and folded lightcurve for this star – see this star in section 8.2 (*The lightcurves*).

This result is against expectation for the number of Blazhko stars in a sample of RR Lyrae stars. Depending on location, the fraction of Blazhko stars among RR Lyrae stars is on the order of 20 to 25% based on RR Lyrae surveys. Mizerski 2003 finds ~ 25% of Galactic Bulge RR Lyrae stars are also Blazhko stars. Alcock *et al* 2002 finds ~ 20% of fundamental mode RR Lyraes to be Blazhko stars. These numbers are indicative for other locations as well. Thus in the PLANET RR Lyrae sample the expected number of Blahko stars is on the order of 17 to 22. This disagrees with finding only a single such star. No other survey identified such small fraction of Blazhko stars, and

in fact this result is contradicted by other surveys from the Bulge. The main conclusion becomes that for some reasons Blazhko stars have been missed, and likely there are Blazhko stars in the PLANET data that have not been identified as such.

The above result is based on *searchAoV* periodograms, or the Analysis of Variance signal determination. The lightcurves contain other residual periods but well below the minimum *maxAoV* factor of 15 that has been accepted as the level of significance corresponding to a real variability, and without the consistency of results described above (repeatability in data from different telescopes and secondary or residual period determination), and thus can not be taken as a clear result for the presence of a real additional signal.

5.3 Period analysis with the Lomb-Scargle method

In order to investigate the reason for the much lower than expected number of Blazhko stars found in the PLANET data, the residuals of the model lightcurves were reanalysed for the presence of additional periods with the Lomb-Scargle method. This was done to check if a method of period analysis different to Analysis of Variance and independent from it produced the same results. The software used for this purpose is the Peranso version 1.37 program distributed by the CBA Belgium Observatory (http://www.peranso.com). A further motivation for this was that when periodograms produced by *searchAoV* were compared to Lomb-Scargle periodograms for the same data, the Lomb-Scargle method produced signal peaks higher above the surrounding noise. Based on the inspection of a set of lightcurves, the working assumption was used that the Lomb-Scargle method is more sensitive to weaker signals than *searchAoV* in the PLANET data being analysed. The Lomb-Scargle analysis was run at a coarser period resolution or period stepping for the same period range as checked with *searchAoV* (0.15 to 100 days), and then the period ranges showing possible

signals were highly over resolved to the point where the resulting period and the strength of its peak in the periodogram became stable (stopped changing with further increase in the period resolution).

The Peranso software contains an option to conduct a Monte Carlo simulation of a section of the lightcurve to determine the statistical significance of periodogram signals. The method used is the Fisher Randomisation test for significance (Linel Nemec and Nemec 1985). The magnitude values of a lightcurve are shuffled between the sampling dates, while the dates are kept unchanged. The periodogram is recomputed for each shuffled lightcurve. The number of iterations is at least 100 in order to provide a reliable statistical significance. Thus calculated significance level is the proportion of runs that contained a period anywhere in the test interval with a peak higher than the peak of the period being tested for significance. In this case it is a measure of the probability that the period being tested is likely to be part of the noise.

All peaks identified with the Lomb-Scargle method were tested with the Monte Carlo simulation as described above. The periods found all had very high significance, with at worst only a few percent chance of being not real. However, this significance test does not distinguish real periods from periods corresponding to peaks that are artefacts of different types or even real periods that are not part of the Blazhko modulation. This significance test does not identify the nature of the period. Periodicities produced by sampling and data combination artefacts, and other distortions that produce real and measurable periods, may pass the significance test in a Monte Carlo simulation even though they are for example the result of systematic bias in the data. In addition significance analysis is an inexact procedure highly dependant on the underlying assumptions. For example, the significance calculated above varies somewhat with the period interval over which the simulation is conducted: the significance of exactly the same peak will change with the interval over which the simulation is run. A narrow test interval will tend to produce a higher significance because the potential period space is smaller, but a larger test interval providing statistically significant period

space will take much longer to compute. In turn picking the test interval which is too large will confuse the analysis through the increased likelihood for the presence of other periods. At 100 plus iterations and high frequency resolution of the periodogram the length of the test interval becomes also limited by the time required for the simulation. In addition too large an interval may not be meaningful if it extends into a period range beyond what can be measured by the sampling of the data. The track record of significance analysis seems poor, the traditional, and much faster to compute false alarm probabilities used in Lomb-Scargle analysis have been shown to be incorrect (Cumming et al 1999). This leaves the Monte Carlo simulation as the method of choice, albeit with the described caveats in regards to the period interval and the meaning of a real or significant period in the context of instrumental errors, data sampling, analysis artefacts and real periods not related to those being searched for.

Most of the RR Lyrae stars had residual periods with peaks clearly above the surrounding features in the periodograms, confirmed by the Monte Carlo based significance analysis described above. The single Blazhko star detected directly from PLANET data, star number 3, originally identified through *searchAoV* analysis of residual periods, has a secondary period very clearly visible in the Lomb-Scargle periodogram (see the figure 5.2 below). This secondary period in Star 3 is much stronger than the surrounding noise level and with a value of 0.528070 days is very close to the star's strongest period at 0.536711 days. The two periods in Star 3 form a Blazhko star signature doublet.

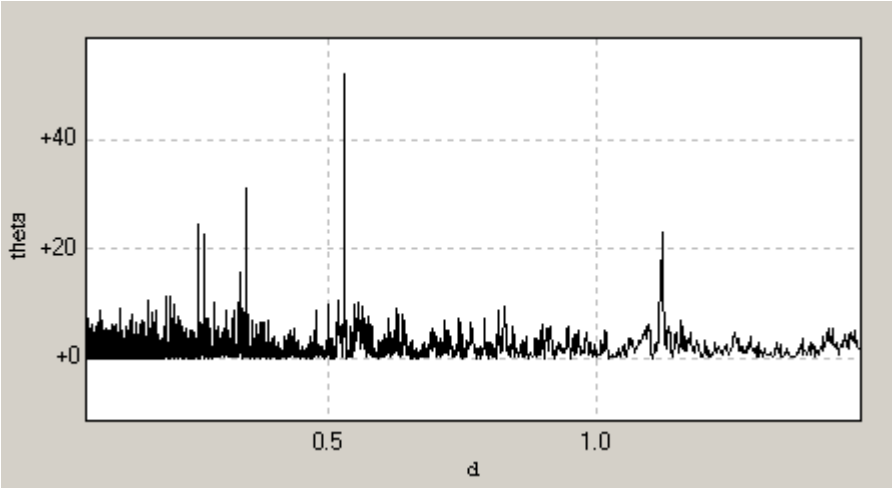

Figure 5.2: Star 3, EB2K005I_P1258_Y2248.ab Lomb-Scargle periodogram of residuals, bottom scale is in days. Theta is a signal significance metric implemented in Peranso.

Many more residual periods than the single Blazhko detection in PLANET data can be identified through the Lomb-Scargle analysis, unfortunately the results are not conclusive on the identity of these periods. Most of the other residual periods detected correspond to periodogram peaks much closer to the surrounding features, or noise (see Figure 5.3). They are detections of weaker periodogram peaks than in the case of the single Blazhko star identification in PLANET data.

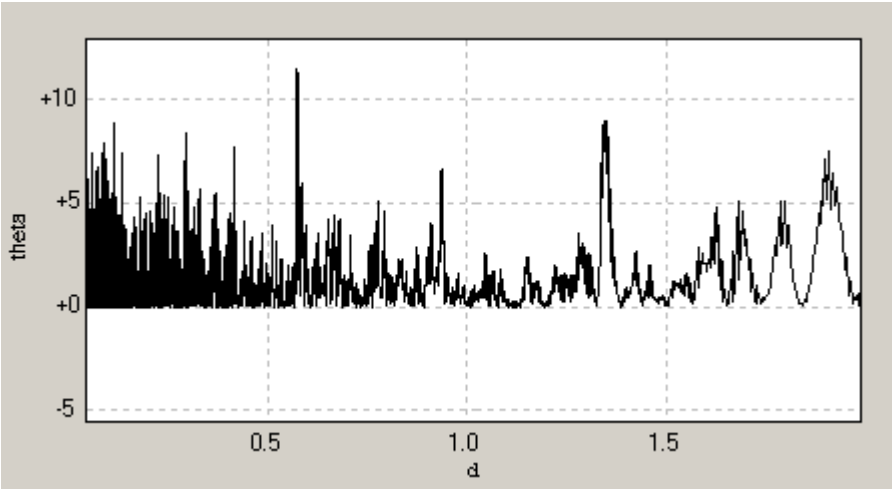

Figure 5.3: Star 30, OB2K038I_d549_Y1703.ab Lomb-Scargle periodogram of residuals, bottom scale is in days. Theta is a signal significance metric implemented in Peranso.

For star observed by a single telescope this kind of residual periods can be interpreted as the signature of Blazhko modulation, for example in the OGLE and OGLE II RR Lyrae surveys (Moskalik and Poretti 2003, Mizerski 2003). However, the residual period results here lack consistency that would allow accepting them as detections of the Blazhko modulation. Most of the residual periods identified are too far away from the main period to correspond to a Blazhko period multiplet. Peaks corresponding to periods close to the main RR Lyrae period are relatively weak, and not the strongest over the full period range analysed in the residuals. Peaks that appear in combined data do not appear in single telescope data, an effect due to either the increased resolution of combined data, or an artefact of the combination, and there is no way to determine which case occurs. Furthermore, a lot of the stars have very strong short residual periods on the order of 0.1 days. These very short periods have clear periodograms peaks and are often stronger than the ones in the area which correspond to Blazhko star identifications. This is the reason why the table 5.3 below has two columns for residual periods, rather than adding additional constraints, and choosing either the strongest peaks, or peaks closer to the main period of the variable star, the strongest very short period is given in addition to the strongest period in the remainder of the period range. These short periods could be created by combining data from different telescopes, or be data analysis artefacts, or they could correspond to high order non-radial pulsation modes in the stars.

Thus the Lomb-Scargle analysis has confirmed the identification based on PLANET data of the strongly modulated Blazhko star. However, the residual period results for the other stars need an independent confirmation of their nature. If the PLANET data is reprocessed with image subtraction photometry (see the reasoning in section 5.5), and the resulting residual lightcurves reanalysed for additional periods, noise and errors in magnitude can be reduced as the source of these periods.

Table 5.3 contains the residual periods obtained in the way described above, with Monte Carlo confirmed significance levels close to 100%. In cases where multiple telescope data is

available to make up a combined lightcurve for a star, the residual periods given refer to the combined lightcurves. The accuracy of the residual periods is to within one significant figure in the last digit, as derived with Peranso, but this should not imply how real or what the periods are. Some of the identified stars do not appear in this table because they are the extra stars added as the result of the comparison with OGLE II data (see below), and because these residual period analysis results are inconclusive, redoing the same Lomb-Scargle analysis for the handful of extra stars is not likely to add any useful conclusions.

Table 5.3: Residual periods in PLANET RR Lyrae stars

	Star – Name	**Period (d)**	**Short Residual Period (d)**	**Close Residual Period (d)**
1	EB2K005I_d774_P753_U625_Y1200.ab	0.687600	0.322387/17.16	0.814045/12.13
2	EB2K005I_d901_P634_Y992.c	0.255222	0.065581/11.81	1.012658/16.86
3	EB2K005I_P1258_Y2248.ab	0.536711	0.177920/11.49	0.528070/52.06
4	EB2K005I_P3115_Y1556.ab	0.559366	0.032831/9.92	0.479985/20.81
5	MB99008I_C1012.c	0.359648	–	–
6	MB99008I_C1559.ab	0.660181	0.051181/8.97	0.768994/6.27
7	MB99008I_C2285.ab	0.526169	0.087705/14.16	–
8	MB99008I_C3607.c	0.216707	–	–
9	OB2K025I_Y3107.ab	0.551175	0.047971/6.61	0.421230/4.28
11	OB2K031I_Y608.ab	0.584220	0.052201/8.28	–
12	OB2K046I_Y2807.ab	0.623306	–	–
13	OB2K046I_Y3981.ab	0.596099	0.050409/7.07	0.563857/3.89
15	OB2K048I_P1804_Y1581.c	0.352159	0.066741/8.04	0.267408/7.88
16	OB2K048I_P1901_Y1323.c	0.308668	0.058672/9.13	0.638570/6.32
17	OB2K048I_Y1865.ab	0.426143	0.066323/15.90	–
19	OB2K012I_Y1114.ab	0.450527	–	–
20	OB2K026I_d698_P1940_Y933.ab	0.316262	0.166586/9.83	0.265929/7.45
21	OB2K026I_d722_P1909_U1395_Y2184.ab	0.313555	0.069658/10.17	0.980563/10.46
22	OB2K026I_d1087_P1608_Y2485.ab	0.476499	0.079412/20.59	–
23	OB2K026I_d1749_Y2201.ab	0.544585	–	–
24	OB2K026I_P2054_U1156_Y2531.ab	0.456654	–	–
26	OB2K029I_Y1752.ab	0.525613	0.256463/9.82 0.075347/8.75	0.829585/11.47
27	OB2K029I_Y4341.ab	0.436789	0.059717/8.74	–
28	OB2K029I_Y4880.ab	0.528058	–	–
29	OB2K034I_d596.ab	0.641979	0.066648/12.97 0.151204/8.69	
30	OB2K038I_d549_Y1703.ab	0.543720	0.117036/8.85	0.575076/11.45
31	OB2K038I_d1716_Y3199.ab	0.431787	0.051674/10.89	0.315433/9.93
32	OB2K038I_Y1988.ab	0.533447	0.065805/8.60	–
33	OB2K038I_Y3098.ab	0.537956	0.064242/6.95	0.645884/6.95
34	OB2K038I_Y3334.ab	0.515280	0.120247/7.54 0.085899/7.07	1.999631/8.04
37	MB95013I_L1072.ab	0.399129	0.056876/8.99	0.799467/9.64
38	MB95017I_L469.ab	0.604113	–	–
39	MB95017I_L784.ab	0.613703	–	1.868810/9.80
40	MB96020I_T106.c	0.366986	0.265887/9.48	1.074691/10.32
41	MS98001I_S91.ab	1.264039	–	0.198266/16.92

42	MB99008I_A2199_U739_Y1278.ab	0.659971	-	0.850521/15.32
43	MB99008I_A2324_U1242_Y1737.ab	0.526144	0.184405/14.09	0.496070/14.14
44	MB99018I_Y2018.ab	0.548877	-	0.306391/12.66
45	MB99018I_Y2544.ab	0.562815	-	-
46	OB99035I_A2778.ab	0.731242	-	-
47	OB99036I_A424_Y220.c	0.328725	-	-
48	OB99005I_A831.w	0.086362	0.067434/19.65	0.246815/13.08
49	OB99005I_A2239.ab	0.584561	0.081683/7.95	0.679348/13.51
50	MB97018I_L1036.ab	0.572860	-	-
51	MB97028I_L516_S248.ab	0.537506		0.221028/12.25 0.335255/11.49
52	KB01002I_Y585.ab	0.531361	0.111551/23.20	-
53	KB01012I_d487_Y340.ab	0.616356	0.079688/9.48	-
54	KB03035I_A403.ab	0.582095	-	0.575076/14.10
55	KB03035I_A724.ab	0.587329	0.070284/7.58	0.360868/6.93
56	OB03167I_A551_W878.ab	0.667436	0.111247/8.13	-
57	OB03167I_A1317_W1551.ab	0.675648	-	0.397820/15.58
58	OB03167I_A2056.ab	0.527087	0.087866/11.49	0.562873/10.09
59	OB03167I_A2799.ab	0.458888	0.076437/7.15	-
60	OB03177I_A589.c	0.274168	0.052895/7.82	0.269092/17.55
61	OB03200I_A573.ab	0.510964	-	-
63	OB03208I_A844_W681.w	0.896772	0.112057/10.39	0.566187/6.44
64	OB03208I_A1106.ab	0.476098	0.157803/7.83	0.471165/11.13
65	OB03262I_W1001.ab	0.464268	0.077445/10.32	-
66	KB02033I_d1250.ab	0.438502	-	0.926097/13.89
67	OB02181I_d1091.ab	0.568814	-	-
68	OB05153I_W1401_Z734.c	0.272851	-	0.214055/9.70
69	OB05099I_W345.ab	0.566667	-	-
70	OB05099I_W1162.ab	0.610209	-	0.456350/13.22
71	OB05099I_W2434.ab	0.462626	-	-
72	OB05099I_W2828.ab	0.444733	0.140509/9.15	0.311478/9.15
75	OB05304I_W1187_Z569.ab	0.523558	-	-
76	OB05304I_W765_Z176.ab	0.568890	0.094831/25.78	-
77	OB05304I_Z527.c	0.274299	-	0.207966/10.49
78	OB05018I_W2479_Z1970.ab	0.584684	0.056455/14.02	0.459348/10.58
79	OB05018I_W3343_Z2705.ab	0.438086	-	-
80	OB05216I_Z486.ab	0.486250	-	0.315826/9.95
81	OB05226I_A1346_W1119_Z516.ab	0.654227	-	0.451019/8.92
82	OB05226I_A2234_W1032.ab	0.474887	-	-
83	OB05259I_Z487.ab	0.618299	-	0.350238/10.95
84	OB05327I_A947_Z345.ab	0.633051	-	-
85	OB05331I_Z1035.ab	0.538667	0.089537/9.31	0.303279/9.82
86	OB05331I_Z1604.ab	0.510591	-	0.765723/9.27
87	OB05390I_W1068_Z538.ab	0.569794	0.110581/10.03	0.360658/9.01

5.4 Comparison to OGLE II

In order to get an independent confirmation of the efficiency of RR Lyrae star detection in PLANET data these results were compared against the catalogue of RR Lyrae stars from the OGLE II microlensing survey by Mizerski 2003. The OGLE II survey covers many of the same areas of they sky as the PLANET survey (Udalski *et al* 1997, Szymański 2005). The OGLE group is one of

the sources of microlensing event alerts that PLANET uses, and thus the expectation is that there will be a significant overlap in the observing areas between the two. Equally important to a comparison is that the two groups use the same standard light filters allowing a direct comparison of the magnitudes. Mizerski 2003 describes the RR Lyrae stars from OGLE II and searches for Blazhko stars among them by the close period multiplet criteria, but does not publish the catalogue. In order to compare the two sets of RR Lyrae stars, the actual OGLE II catalogue of these stars, as used for the paper Mizerski 2003, was obtained by private communication with the author. The data for stars identified in PLANET observations that also appeared in OGLE II fields was downloaded from the publicly available OGLE II Photometry database at http://ogledb.astrouw.edu.pl/~ogle/photdb. This version of OGLE II data derived magnitudes through image subtraction photometry. The physical quantities from OGLE II in Table 5.1 come from the online database, while the Blazhko status of the stars is based on the Mizerski (2003) catalogue.

In order to assess the efficiency of the methods used to find RR Lyrae stars in the PLANET database and confirm the identifications a comparison with the OGLE II fields in areas of overlap was done. Co-ordinate limits were estimated from the calibrated fits images of PLANET fields searched for RR Lyrae stars and the OGLE II RR Lyrae stars in between these co-ordinates selected. It should be remembered that the coverage of the fields varied a little between exposures with the variation in the pointing of the telescope but the difference introduced by this factor should have a relatively small influence on this comparison. Nine additional stars were added to the group of PLANET RR Lyrae stars, three of which were stars missed in the original selection, and the remaining six were RRc stars with borderline lightcurves in PLANET data that were excluded in the original RR Lyrae search in the PLANET data because the lightcurves are noisy and could not be distinguished from eclipsing binaries. There were seven stars with lightcurves identified in the OGLE II catalogue as RR Lyrae, but with PLANET data lightcurves too noisy to classify and agree

with their OGLE II classification. The seven stars with the very noisy lightcurves identified in this comparison were not added to the group of PLANET RR Lyrae stars because their PLANET observations were judged to be unusable. Finally there is one RRab star identified from PLANET data but missed in the OGLE II catalogue. The remainder of the PLANET RR Lyrae detections were the same as the OGLE II detections in the areas of the PLANET observing fields. Thus apart for the differences in the precision of the magnitudes of these observations the detection rate for RR Lyrae stars in the two surveys is nearly the same.

Some PLANET fields did not overlap with the OGLE II fields and could not be compared. These can be seen in Table 5.1 as the stars with missing entries corresponding to the OGLE II data. The extra stars identified in PLANET data from comparison to the OGLE II catalogue are marked with a "+" after their name string.

Adding the single Blazhko star clearly identified in PLANET data, as it happens in a field not overlapping with OGLE II, together with the stars identified a Blazhko in the OGLE II data, the analysed PLANET fields contain at least 11 Blazhko stars. In addition a small number of additional Blazhko stars may be hiding among the PLANET RR Lyrae in fields not overlapping OGLE II. It is also possible that combining the PLANET and OGLE II data may reveal additional Blazhko stars in combined data that has a longer time span of sufficient data sampling allowing the resolution of even more closely spaced periods, and thus even longer Blazhko cycles. Therefore the 11 Blazhko stars are a lower limit to the true number in the PLANET fields with enough observations to be searched for RR Lyrae stars.

Overall the two catalogues agree very well in the areas that they overlap, even though the PLANET data is noisier. The greater amount of noise in PLANET data is primarily due to its origin in dophot photometry, while the OGLE II catalogue is based on Image Subtraction photometry, and

secondarily to a better location and size of the OGLE II telescope. The median seeing for the OGLE II data is estimated at ~ 1.1 arc seconds (Udalski *et al* 1997). The much larger number of OGLE II RR Lyrae stars, more than 2700 in Mizerski 2003 catalogue, arises mostly from the much bigger size of its observing fields, and secondarily from the better magnitude precision providing better lightcurves. The size of the composite OGLE II observing fields is 2048x8192 pixels corresponding to an area covering 14.2 by 57 arc minutes on the sky per field, for a total of 49 observing fields in the Galactic Bulge covering together 11 square degree of arc (Szymański 2005). This is supported by the good agreement between the two in the numbers of identified RR Lyrae stars in areas where the two do overlap.

Furthermore while the OGLE II data is much less dense per unit of time, it has much greater time span than PLANET data, in addition to usually having more observations per star (see Figures 5.5 and 5.6 for histograms of OGLE II and PLANET magnitude observation samples). The OGLE II time span is around 1300 days for all stars, with the data collected over typically four observing seasons. By comparison the PLANET time span is variable, typically on the order of a few months of the duration of a microlensing event (see the histogram in Figure 5.4). Since in order to separate or resolve two different close frequencies, the time span of the data has to be at least as long as the inverse of their difference in frequency, the shorter overall time span of data from PLANET will lower detection of Blazhko stars. The close frequencies will not be resolved, and the Blazhko stars will not be identified. It is a feature of PLANET data that most observations are made over relatively short periods of time, across the peak magnification of the microlensing event, with some follow up observations later. As a result even though the time span for a star may be relatively long, most of its observations can cluster over a much shorter duration.

Overall I have shown that the methods used to identify RR Lyrae stars in the PLANET data yield very good results, even allowing the identification of some type c RR Lyrae which are

difficult to distinguish from eclipsing binaries. Close to the same number of RR Lyrae stars is identified in the less photometrically accurate PLANET data as in the OGLE II data in the areas where the two overlap. Thus the methods used for this work do not miss RR Lyrae stars. However, the PLANET data is sufficient for the detection of only very highly modulated Blazhko stars, as shown by the single example found from it. The less modulated Blazhko stars are not detectable in the PLANET observations, the caveat being that if PLANET data is reprocessed with Image Subtraction photometry and the accuracy of magnitude improves as expected, at least some Blazhko stars should become visible in these observations as well.

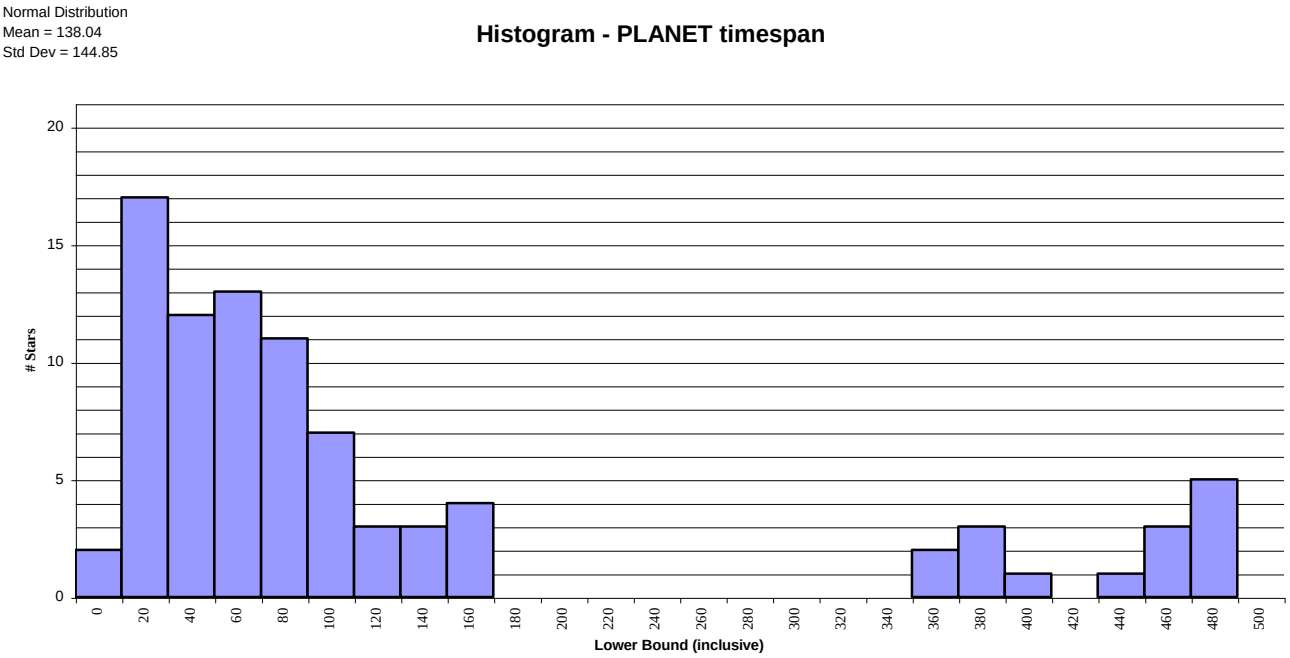

Figure 5.4: Histogram of timespans for the set of PLANET RR Lyrae stars. The bottom scale is in days

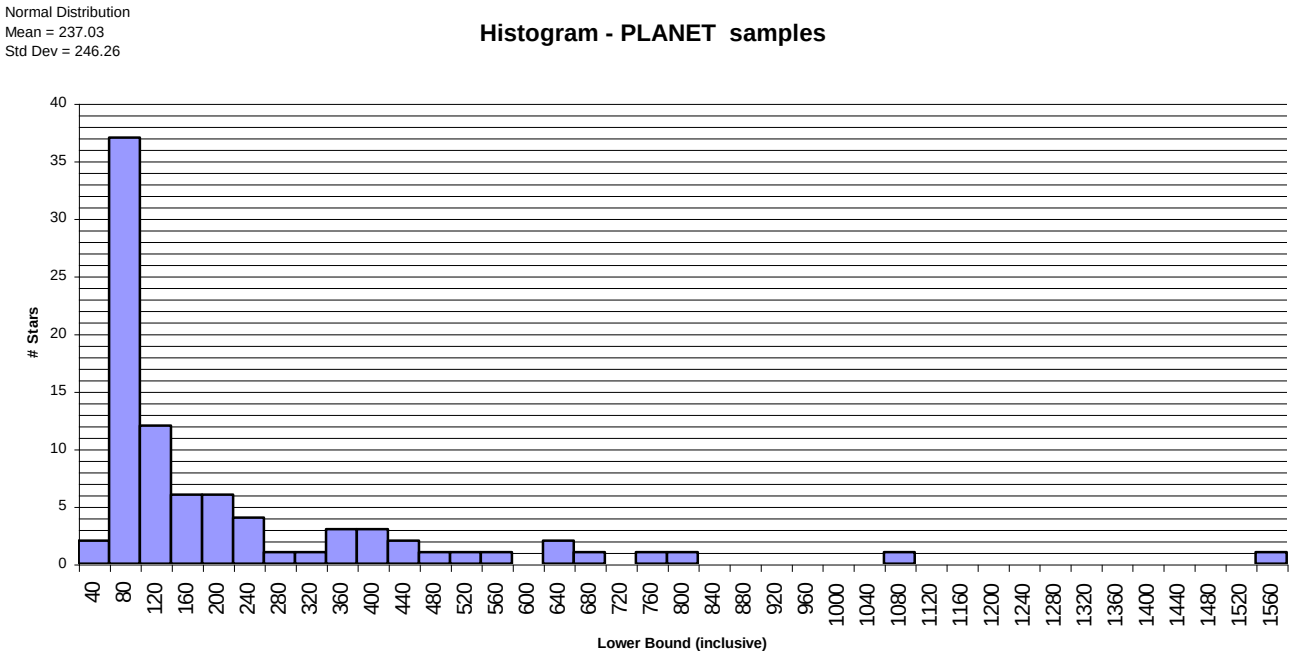

Figure 5.5: Histogram of samples in the combined lightcurves for the set of PLANET RR Lyrae stars. The bottom scale is the number of samples or usable observations per star

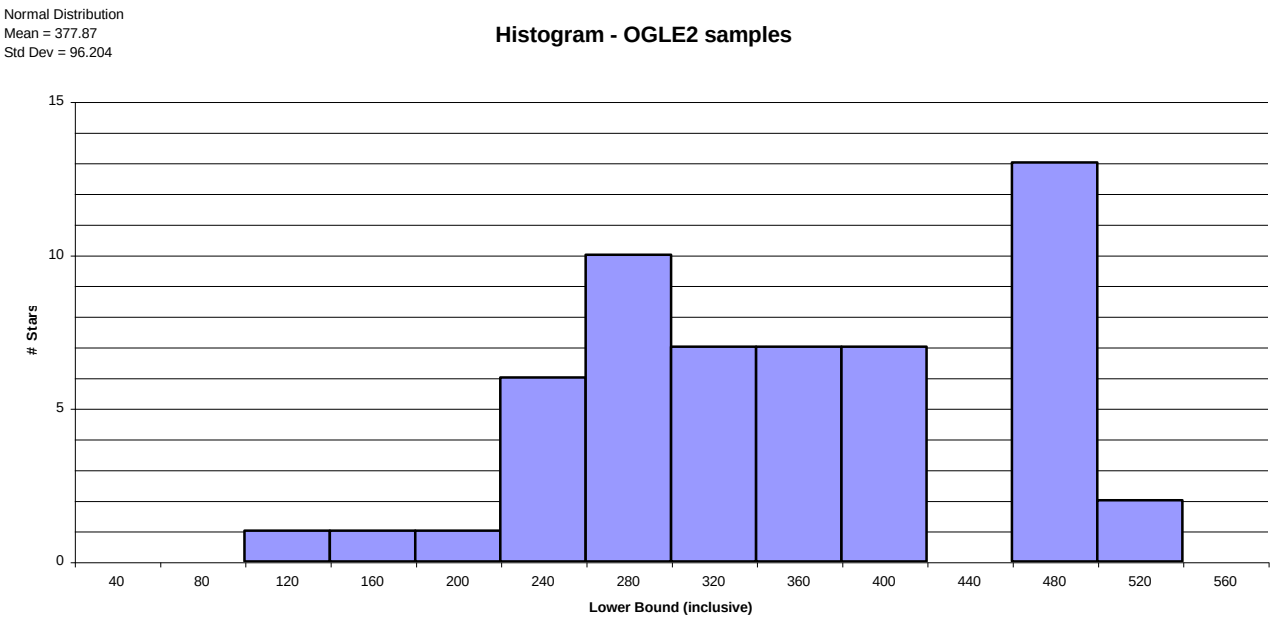

Figure 5.6: Histogram of samples for the OGLEII RR Lyrae lightcurves. The bottom scale is the number of samples or usable observations per star

5.5 Magnitude accuracy and frequency resolution

The PLANET data with dophot based photometry is sufficient for the identification of RR Lyrae type variable stars. However, the two requirements for the detection of Blazhko stars among the RR Lyrae stars are accuracy of the magnitudes, so the modulation of the main light variability can be resolved, and frequency resolution, needed to distinguish close frequency/period multiplets characteristic of Blazhko stars. The magnitude accuracy of the PLANET data can be improved through careful reprocessing of the observations to obtain Image Subtraction photometry for selected stars.

The second connected source of magnitude based inaccuracies in period analysis is the combination of lightcurves where data is available from more than one telescope. If the lightcurves are based on magnitudes with more inaccuracies, this translates into a less accurate magnitude shift while aligning them between telescopes. Loss of accuracy in the shift will translate into a loss of sensitivity in detecting signals in periodograms, some signals will become undetectable. This could be a significant pathway to the demonstrated loss of Blazhko star detectability in PLANET data based on dophot photometry. The solution to this is the same as above, Image Subtraction data reprocessing for more accurate photometry. More accurate photometry will automatically translate into more accurate lightcurve combination, and conversely there is no simulation or modelling that will improve the process, if accuracy of the photometry is not improved first. Modelling can not create information in the data that has been lost to magnitude inaccuracies.

The frequency resolution depends on the time span of the data, and on how the data is distributed. For example, a long time span with most of the data accumulated over short period of time, and just a few points at the long end of the range, will not produce much different results to a short time span. There is no way to improve the time span of the PLANET or OGLE data by

themselves. However, combining data for RR Lyrae stars common to the two surveys can improve the time span of the resulting lightcurve and thus the frequency resolution and the ability to identify Blazhko stars. The collection of OGLE II data began in 1997, and as mentioned above most stars have four observing seasons worth of it. Therefore, depending on the year when the PLANET data was collected, a star's combined lightcurve can have a time span of up to around 8 years, or about double the frequency resolution of existing OGLE II data.

Table 5.4: Properties of combined PLANET and OGLE II data.

	Star – Name	**OGLE II ID**	**OGLE II time span**	**Combined time span**	**Samp Ex**	**Samp**
1	EB2K005I_d774_P753_U625_Y1200.ab					1577
2	EB2K005I_d901_P634_Y992.c					1093
3	EB2K005I_P1258_Y2248.ab					707
4	EB2K005I_P3115_Y1556.ab					657
5	MB99008I_C1012.c					92
6	MB99008I_C1559.ab					95
7	MB99008I_C2285.ab					94
8	MB99008I_C3607.c					93
9	OB2K025I_Y3107.ab	bul_sc37_i_645268	1295.73	1295.73	403	91
10	OB2K025I_Y3746.c **+**	bul_sc3_i_203622	1307.60	1307.60	514	79
11	OB2K031I_Y608.ab	bul_sc12_i_430188	1282.70	1282.70	282	123
12	OB2K046I_Y2807.ab	bul_sc4_i_732074	1293.70	1293.70	504	145
13	OB2K046I_Y3981.ab	bul_sc4_i_755313	1292.61	1292.61	498	117
14	OB2K046I_Y4537.c **+**	bul_sc4_i_744012	1292.61	1292.61	500	116
15	OB2K048I_P1804_Y1581.c **OGLE BL2**	bul_sc30_i_636915	1302.70	**1634.73**	317	217
16	OB2K048I_P1901_Y1323.c	bul_sc30_i_455213	1302.70	**1634.73**	278	216
17	OB2K048I_Y1865.ab	bul_sc30_i_636934 bul_sc31_i_24053	1297.69	1297.69	280 276	130
18	OB2K048I_Y457.c **+**	bul_sc30_i_636615 bul_sc31_i_23369	1297.69	1297.69	212 320	74
19	OB2K012I_Y1114.ab	bul_sc43_i_123530	1276.71	1276.71	364	185
20	OB2K026I_d698_P1940_Y933.ab	bul_sc3_i_490084	1308.71	**1597.70**	511	434
21	OB2K026I_d722_P1909_U1395_Y2184.ab	bul_sc3_i_479471	1318.73	**1621.74**	425	582
22	OB2K026I_d1087_P1608_Y2485.ab	bul_sc3_i_479099	1318.73	**1607.72**	491	430
23	OB2K026I_d1749_Y2201.ab	bul_sc3_i_479962	1308.71	**1582.12**	395	267
24	OB2K026I_P2054_U1156_Y2531.ab	bul_sc3_i_490215	1308.71	**1611.72**	501	373
25	OB2K026I_Y1865.ab **+**	bul_sc3_i_490223	1308.71	**1611.72**	502	124
26	OB2K029I_Y1752.ab	bul_sc37_i_463456	1295.73	1295.73	403	127
27	OB2K029I_Y4341.ab **OGLE BL1**	bul_sc37_i_464953	1295.73	1295.73	377	125
28	OB2K029I_Y4880.ab	bul_sc37_i_623081	1295.73	1295.73	404	127
29	OB2K034I_d596.ab	bul_sc43_i_265124	1276.71	1276.71	369	87
30	OB2K038I_d549_Y1703.ab	bul_sc3_i_104269	1318.73	**1552.15**	521	239
31	OB2K038I_d1716_Y3199.ab	bul_sc3_i_91895	1318.73	**1552.15**	509	260
32	OB2K038I_Y1988.ab **OGLE BL1**	bul_sc3_i_315349	1318.73	1318.73	518	95
33	OB2K038I_Y3098.ab	bul_sc3_i_105206	1308.71	1308.71	507	97
34	OB2K038I_Y3334.ab	bul_sc3_i_104529	1308.71	1308.71	513	99
35	OB2K038I_Y352.ab **+**	bul_sc3_i_90110	1308.71	1308.71	535	100
36	OB2K038I_Y3547.ab +	bul_sc3_i_316298	1308.71	1308.71	498	96
37	MB95013I_L1072.ab	none				118
38	MB95017I_L469.ab – **not OGLEII RR**	bul_sc32_i_154959	1278.69	**1945.42**	310	92

39	MB95017I_L784.ab	bul_sc32_i_154418	1278.69	**1945.42**	309	90
40	MB96020I_T106.c	bul_sc20_i_715713	1274.59	**1536.10**	317	83
41	MS98001I_S91.ab	smc_sc4_i_38956	1243.89	1243.89	325	173
42	MB99008I_A2199_U739_Y1278.ab	none				807
43	MB99008I_A2324_U1242_Y1737.ab	none				762
44	MB99018I_Y2018.ab **OGLE BL1**	bul_sc30_i_365051	1307.70	1307.70	318	95
45	MB99018I_Y2544.ab	bul_sc30_i_165806	1307.70	1307.70	316	102
46	OB99035I_A2778.ab	bul_sc44_i_14663	1272.68	1272.68	331	89
47	OB99036I_A424_Y220.c **OGLE BL1**	bul_sc11_i_101274	1282.70	1282.70	211	304
48	OB99005I_A831.w	bul_sc26_i_314049	1273.71	1273.71	343	109
49	OB99005I_A2239.ab **OGLE BL1**	bul_sc26_i_687150	1273.71	1273.71	330	123
50	MB97018I_L1036.ab	none				84
51	MB97028I_L516_S248.ab	none				376
52	KB01002I_Y585.ab	none				220
53	KB01012I_d487_Y340.ab	bul_sc21_i_557615	1273.76	**1621.31**	312	242
54	KB03035I_A403.ab	none				112
55	KB03035I_A724.ab	none				108
56	OB03167I_A551_W878.ab	none				192
57	OB03167I_A1317_W1551.ab	none				243
58	OB03167I_A2056.ab	none				175
59	OB03167I_A2799.ab	none				176
60	OB03177I_A589.c	Can't calibrate fits				105
61	OB03200I_A573.ab **OGLE BL1**	bul_sc6_128105	1297.67	**2284.25**	303	101
62	OB03200I_A710.c **+**	bul_sc6_i_251848	1297.67	**2284.25**	297	100
63	OB03208I_A844_W681.w	none				240
64	OB03208I_A1106.ab	none				152
65	OB03262I_W1001.ab	none				90
66	KB02033I_d1250.ab **OGLE BL2**	bul_sc34_i_607633	1273.64	**1954.95**	328	93
67	OB02181I_d1091.ab	none				82
68	OB05153I_W1401_Z734.c	bul_sc2_i_359204	1292.76	**3071.31**	262	402
69	OB05099I_W345.ab **OGLE BL1**	bul_sc39_i_575408	1292.75	**3048.83**	382	97
70	OB05099I_W1162.ab	bul_sc39_i_744680	1293.64	**3049.72**	410	91
71	OB05099I_W2434.ab	bul_sc39_i_576545	1292.75	**3048.75**	377	105
72	OB05099I_W2828.ab	bul_sc39_i_764911	1292.75	**3048.83**	411	81
73	OB05099I_W2540.c **+**	bul_sc39_i_576668	1292.75	**3048.83**	359	90
74	OB05099I_W1548.c **+**	bul_sc39_i_754030	1292.75	**3048.83**	410	106
75	OB05304I_W1187_Z569.ab	bul_sc33_i_703300	1293.70	**3062.68**	269	474
76	OB05304I_W765_Z176.ab **OGLE BL2**	bul_sc33_i_702993	1281.68	**3062.16**	157	492
77	OB05304I_Z527.c	bul_sc33_i_702904	1299.68	**3055.23**	272	357
78	OB05018I_W2479_Z1970.ab	none				362
79	OB05018I_W3343_Z2705.ab	none				472
80	OB05216I_Z486.ab	none				85
81	OB05226I_A1346_W1119_Z516.ab	none				673
82	OB05226I_A2234_W1032.ab	none				181
83	OB05259I_Z487.ab	none				148
84	OB05327I_A947_Z345.ab	none				532
85	OB05331I_Z1035.ab	bul_sc5_i_182170	1272.61	**3055.18**	363	124
86	OB05331I_Z1604.ab	bul_sc5_i_183604	1272.61	**3055.18**	352	124
87	OB05390I_W1068_Z538.ab	none				225

The exact time spans that would result from combining OGLE II and PLANET data are shown in Table 5.4. The OGLE II and PLANET time spans were determined from Mean Julian Dates for the magnitude observations as available in the downloaded OGLE II star data files and the PLANET archives. The column headings follow the same terminology as for Tables 5.1 and 5.2.

The time span of OGLE II data is approximately the same at around 1300 days for all the stars matching to the PLANET set of RR Lyraes. The PLANET time spans vary more, but are much shorter than for the OGLE II observations. The dominant factor determining the time span of combined PLANET and OGLE II data is the dates at which the PLANET observations were made (OGLE II observations all being made during approximately the same period). Thus, for example, the longest combined time spans occur for stars that have PLANET data from the 2005 observing season. This also means that while the combined data will have longer time spans, it will also tend to have long periods without any observations, for the 2005 set of RR Lyraes between when the OGLE II data finishes and the PLANET observations begin. While the longer time spans mean an increased frequency resolution in periodograms using the combined data, the long empty sections may introduce variations in this. The final effect depends on the details of the sampling, and the data has to be analysed to determine it.

Overall 29 out of 87 stars from the PLANET set of RR Lyraes have their times spans increased by adding the OGLE II data, among those that are matched to OGLE II observations. Twelve stars have their time spans and frequency resolutions increased only slightly, to roughly a factor of 1.2 of the original OGLE II time span. Another twelve stars have their time spans increased significantly to a factor of about 2.3 of the original. The rest have improvements in between these two groups. Five of the stars with potentially improved frequency resolution are confirmed Blazhko stars, and of those two Blazhko stars fall in the group where time spans of combined data are more than double of the OGLE II observation, and far beyond the frequency resolution of the PLANET data.

Hence combining the data from the two microlensing surveys presents the chance to test the more detailed structure of frequency multiplets in Blazhko stars. The precise multiplet structure is a strong constraint for possible models of the Blazhko modulation. Depending on results this could be

a test case for and an argument for a more extensive study of the fine structure of frequency multiplets in Blazhko stars. Similarly, the longer time spans on non-RR Lyrae stars may allow the detection of additional longer term Blazhko modulation through the resolution of even more closely spaced frequency multiplets. Equally, depending on results, a further argument for a long term study of the PLANET RR Lyrae sample through follow up observations can be made, with the aim of identifying Blazhko stars with long duration modulations that would otherwise not be identified

6 RR Lyrae pulsation

6.1 Introduction

The search for RR Lyrae stars in the PLANET database did not produce data sufficient to describe Blazhko stars in such a way that allowed new constraints to be put on the theoretical models for the process. Section 6 contains a deeper reassessment of stellar pulsation in the context of RR Lyrae stars as a lead in to proposals for future work and to the separate analysis in section 9.

It is useful to view the RR Lyrae stars in the wider context of general stellar pulsation. At the precision of mmag in photometry and ms^{-1} in radial velocity we can say that most stars do not pulsate. However, in the Sun radial velocities for example are detectable to a level above a noise of $0.5\ \mathrm{ms}^{-1}$, and similarly luminosity resolution is much better. Similarly for more distant stars pulsation may exists at lower levels, but not be detectable with current techniques and instruments. In general all compressible objects have some possible pulsation modes depended on their structure and composition. Stars are compressible and no different in this regard from any other structures… they are just larger, more distant, and harder to observe than some. In addition a pulsating object needs a source of energy flowing into and driving the process. In similar ways to other objects that are capable of pulsation in some fashion, and this includes most things that exist, stars through their structure favour certain modes of pulsation, while others are suppressed. The details of temperature, chemical composition, and energy production define which way a star can pulsate.

The pulsation equations formalisms, terminology, concepts, and classification of modes used for describing RR Lyrae stars is the same as used in astroseismology, and pulsation theory in general. The description of pulsation in the two following sections 6.2 and 6.3 is a small summary

of material relevant to RR Lyrae stars from *Lecture Notes on Stellar Oscillations* (Christensen-Dalsgaard 2003).

6.2 Types of Pulsation

In stars two main types of pulsation modes are present, the p-modes and the g-modes. All the pulsation modes are based on the regular movement of the material inside the star. They differ in the types of forces involved in their propagation.

The p-modes are also known as “pressure” modes. They are essentially acoustic waves familiar from everyday life moving through a star’s plasma. The restoring force in this kind of pulsation is gas pressure. These waves propagate in mode and stellar structure dependant acoustic cavities. The acoustic cavity is simply the region of the star where the given pressure mode propagates. For modes that are not directed at the centre of a star, that is for the non-radial modes, the lower part of the mode is deeper and thus in a higher temperature environment. Sound waves travel faster with higher temperature in the same material. Thus together with the chemical composition of the plasma temperatures determine their speed.

Equation 6.1:

For a perfect gas, speed of sound:

$$\nu_s = \sqrt{\frac{\Gamma k T}{\mu}}$$

Γ is the adiabatic exponent, T is the temperature, and μ is the mean molecular weight.

As a consequence of the above arrangement a non-radial mode wave is refracted back to the surface, where it is then reflected back towards the interior, since the acoustic energy is trapped in the star. Thus the depth to which the sound or pressure wave can reach is the lower boundary of the

acoustic cavity, with the star's surface being the upper boundary. The depth of the acoustic cavity is different for different modes. Higher degree modes penetrate down to shallower depths.

The simplest oscillation mode is the fundamental radial mode – in this mode the star swells and contracts, heats and cools, in spherical symmetry with the core as a node and the surface as a displacement antinode. This is the mode in which most RR Lyrae stars pulsate. The next higher radial mode, the first overtone radial mode has one node that is a concentric shell within the star, and again an antinode at the surface. The first overtone occurs by itself in type c RR Lyrae stars and together with the fundamental in the RR d type, and to smaller extent perhaps by itself in others. Stars are not uniform in temperature, chemical composition, and density, all of which affect the speed of propagation of pressure waves. One interesting and useful result of this, combined with the presence of two radial modes is that the period ratios of fundamental and first overtone are not as expected for a uniform material. These period ratios vary in a small range around a value unique for a given type of star, different for Cepheids, δ Scuti stars, and RR Lyrae stars. The value of this period ratio is also slightly different and non-overlapping for double mode RR Lyraes in the Milky Way and the Magellanic Clouds, again pointing to differences in composition in this type of stars at the two locations

The g-modes are also known as "gravity" modes. These are not acoustic waves. They arise because gravity tends to smooth out inhomogeneities along equipotential level surfaces, disturbing density. The restoring force of this type of pulsation is buoyancy. These modes are motions in three dimensions with material displacement usually dominant tangentially to the equipotential level surfaces. The paths of the gravity waves are essentially loops around the core of the star, a kind of orbits. These modes do not propagate in the convective part of stars, for the most part, although they are potentially weakly observable at the surface from their effects on the convection zone. Thus they do interact with and affect at least the inner parts of the less dense levels of a star. Depending

on structure and density of some types of stars, they are observable on the surface, for example in white dwarf pulsators. In the case of RR Lyrae stars they are trapped in the interior, but may affect those p-modes whose acoustic cavities intersect their zones, those that reach down to the gravitational mode cavities.

6.3 Pulsation driving mechanisms

Pulsation modes in stars require a sustained input of energy. Otherwise, as the star loses the energy it produces, both in general and from the pulsation, the modes would decay over time, irrespective of whether the remainder of the stellar structure allows their existence or not. Of course unlike in the case of a string or an organ pipe, energy production, distribution and thus input into the pulsation is a function of the same structure. Energy supply to the pulsation is internal to the star. Just the same, understanding of the process requires the recognition of how it is driven and how it gains energy from the system. Furthermore as much energy has to be fed into the pulsation at the input points as is damped in the pulsation throughout the bulk of the star, the energy supply has to be sufficient to produce and maintain the pulsation.

For RR Lyrae stars and other numerous types the dominant pulsation driving mechanism is ionisation of gases, and it is known as the κ-mechanism. Since H and He are the most plentiful in the majority of stars, they are the main contributing materials, usually arranged in a shell or layer for this purpose. In the ionisation layers for H and He opacity blocks radiation, the gas heats up and pressure increases while the gases are being ionised, causing the star to swell up while its outer layers accelerate outwards. The majority of the energy is stored in the kinetic motion of the particles. At some point in the process the density, ionisation, and pressure change sufficiently to decrease opacity to the point where more energy flows out of the ionisation layers than is absorbed, the star’s expansion slows down and eventually reverses, as the gas begins to compress again, until

the conditions change back to those driving expansion and the pulsation cycle repeats. Some of the energy is stored through the ionisation process as electrostatic potential energy, and also contributes to driving the pulsation. It is also possible that other elements perform a similar function, even though this occurs less frequently. The pulsation in β Cep stars is based on the same opacity process just described, but with Fe being the material involved. Apparently in these stars diffusion manages to create a layer with sufficient concentration of Fe iron at a correct location to drive the pulsation.

Another driving mechanism is stochastic driving. In this case the convection zone accumulates acoustic energy, and the some of it occurs at the natural oscillation frequencies for a given star's structure causing it to resonate. Thus this pulsation is essentially convection driven. It may have an effect on pulsation of RR Lyrae stars, through perhaps interference in the convective layers, but it is not the dominant mechanism involved in it.

The third major driving mechanism is theoretical, the ε-mechanism. It is based on the idea that energy generation rate in the core varies, in turn driving global pulsation. Currently there is no known class of pulsating stars driven in this way. The RR Lyrae stars are treated with the assumption that the core provides a constant supply of energy, at least on the time scales of the oscillations found in these stars.

The position of the driving zone can determine which pulsation mode occurs. If a layer of material suitable for opacity driving is located at the position of an anti-node for one of the stars natural frequencies, pulsation at that frequency will be supported. If the layer is located at the position a node for a natural frequency, that pulsation will not occur. You cannot drive a mode by putting energy in a node where the mode does not oscillate. Though this is not an exact relation – a close match will be effective in driving the pulsation as is the case for example with RR Lyrae stars oscillating in the fundamental mode. The fundamental mode has a single anti-node at the surface,

but the driving layer is not at the surface. Thus the layer driving the fundamental mode in RR Lyrae stars, and equally in other stars, has to be relatively shallow inside the star. This is an indication of structure and composition in these stars. This is an example of the general principle that some physical property of the star either selects for or suppresses an oscillation mode. A strong dipolar magnetic field determines that dipole pulsation modes are favoured. Similarly, additional modes are created through any other physical process or quantity that forces a node at a given location, injects energy around the position of an anti-node, disturbs, deforms, or otherwise removes the degeneracy of existing modes.

For real 3-D stars there are three quantum numbers to specify oscillation modes: *n* is the number of radial nodes and is called the *overtone* of the mode; *l* is the *degree* of the mode, and specifies the total number of surface nodes present; *m* is the *azimuthal order* of the mode and specifies how many of the surface nodes are lines of longitude. Surface nodes are loops across the surface, straight lines with respect to the surface, and come only in the two mentioned kinds. Radial nodes are concentric shells. Rotation provides the possibility of distinguishing negative and positive values of *m*. In a rotating star, for each non-zero case of *m*, there are two values of it, the negative and positive, and two different non-degenerate pulsation modes. Clearly, from the definitions, for a value of *l* the number of surface nodes is between 0 and *l*. Thus if for example *l*=3, the possible values of *m* are: 0, -1, 1, -2, 2, -3, 3. In a spherically symmetric star, all the modes for a given order have the same frequencies. Deformations from sphericality remove this frequency degeneracy, with rotation as the most likely cause in a star. In a rotating star the Coriolis force adds a circular component to up-and-down motions, with the direction of the Coriolis force being against the direction of rotation. Thus pulsation modes or components travelling in the direction of the rotation will be slowed down, and those going opposite the direction of rotation will be speeded up, in the co-rotating frame of reference. The frequencies will be shifted accordingly. In addition, differential rotation, varying with depth, has been detected within the convection zone of the Sun, and this may

also happen in other stars. Thus the frequency splitting may be more complicated than derived by assuming even rotation through a star. Furthermore the coriolis effect will be different between the top and bottom hemispheres, and will depend on the pattern and phase of the mode. For example whether the hemispheres or smaller subsections are moving away from or towards the observer, and whether they are all moving the same way, or in anti-phase. Clearly the possible combinations are many and mode dependant. Finally taking note that for a given non-zero order there is more than one distinct pulsation mode. A mental picture of how the pulsation modes appear helps an intuitive understanding of how the modes may interact, and how they may be observed. Reading through arguments about various aspects of theory also makes much more sense when filtered through this understanding.

6.4 Theoretical models of the Blazhko effect in RR Lyrae stars

There are two main models being considered for the explanation of the Blazhko effect, the resonant frequency model, and the Oblique rotator model. Currently neither can fully account for the observed properties of Blazhko stars, but the majority opinion is moving in favour of the resonant frequency model. The consensus is along the lines of improving the details in the resonance model. The main outstanding question is which type or types of oscillation comprise the additional periods in Blazhko stars, specifically the *n*, *l*, and *m* parameters for the modes involved.

In the case of the resonant model, there is a secondary natural frequency close to the main radial pulsation frequency, and in a stellar case of forced oscillation, the pulsation at the dominant frequency becomes the driving force for the secondary one. The energy is transferred from the main process into oscillations at the above-mentioned natural frequency. In turn the beating of the two closely spaced frequencies produces the modulation of the RR Lyrae pulsation known as the Blazhko effect. The devil is in the detail.

Resonance between two radial modes has been discounted as a good description for the Blazhko effect in RR Lyrae stars. One possibility was the so-called 2:1 resonance between the fundamental and the third overtone modes. However, the Amplitude Equations (AEs) parameters required to obtain modulated solutions are outside the range of RR Lyrae models (Kovács 1993, and references therein). Moreover, in this scenario, there is no sign of modulation in hydrodynamic simulations (Kovács and Buchler 1988).

Currently better results involve the excitation of non-radial modes. For the resonance between two modes with nearly equal frequencies, the 1:1 resonance, both AEs and polytropic stellar models allow for the presence of a non-radial frequency close to that of the second radial overtone, and several different types of pulsation including ones with amplitude modulation analogous to the Blazhko effect, depending on the input parameters (Van Hoolst 1992).

Power spectra of RR Lyrae stars have been identified which revealed the presence of additional modes whose frequencies could not be attributed to radial modes (Dziembowski and Cassisi 1999 and references therein). The authors construct evolutionary models of RR Lyrae stars using the FRANEC code, with a range of starting parameters. The paper follows the approach of Van Hoolst et al (1998) given for a single RR Lyrae star, and expands it to the study of a set of models. Oscillation is studied at multiple points along evolutionary path with the method of Dziembowski 1997, (updated by Van Hoolst et al 1998). The results are assessed according to linear instability of the modes present in the model RR Lyrae stars as expressed through their growth rates. The same treatment applies to both radial $l = 0$, and non-radial modes. The idea being that the modes with higher growth rates will be more likely to occur. It is unclear what the authors mean by stating that at $l = 1$ for even the best trapped modes more than 80 percent of the kinetic energy is contributed by the g – mode propagation, as these are opacity driven pressure modes. This

maybe referring to the transition of modes in the interior to gravity supported modes, and the coupling between the two types of propagation. In particular, in the description used for this system and the equations employed as in Van Hoolst et al (1998): *"We focus on modes of low spherical degrees ($l \leq 12$) with frequencies in the range of the first three radial modes. When $l \neq 0$, all such modes in models of evolved stars have dual character. In the outer envelopes they have properties of low degree p-modes, whereas in the deep interior they become gravity modes of high radial order. In the interior we describe the oscillations by means of an asymptotic approximation."* The equations used are evaluated with an assortment of numerical methods, for different parts of the equations and sections of the star. There are two groups of unstable modes with significantly bigger growth rates as assessed with the given scenario, for values of l = 0, 1, 6 and 10. It should be remembered that for modes at l = 5 to 10 and higher the cancellation of contributions to luminosity from areas of the star moving in opposite radial directions would reduce the disc averaged amplitude variations to at most a few millimagnitudes. These would be the modes most likely to occur in RR Lyrae stars, and all have similar growth rates, and thus chances of occurring. However, it is a basic fact from observation that RR Lyrae stars pulsate in the radial modes, and the linear theory does not yield an answer why they are so highly preferred. There is no evidence for non-pulsating stars in the RR Lyr domain of the H-R diagram (to clarify, observationally non-pulsating, as mentioned before, a star can be pulsating in a non-radial mode where the surface averaged luminosity is relatively stable). However, Van Hoolst et al (1998) presents a different emphasis on the same facts, as the single model they analyse has moments of inertia for the most likely non-radial modes several times higher than the corresponding radial modes, suggesting that while the driving rates for these modes are lower this still is not sufficient to prove their absence. In the models presented, if the fundamental mode is unstable, there always exists an unstable l = 1 mode. This suggests that for type ab RR Lyrae stars, pulsating in the fundamental mode, the presence of the Blazhko effect is most likely due to the dipole mode (i.e. l = 1 mode). Additionally at least for some type c RR Lyrae stars, the three from Olech et al (1999) for example, the secondary

frequencies can not be explained in terms of modes with order higher than 1, i.e. leaving only $l = 1$ modes, even though this is still not free of difficulties in terms of the observed frequencies being lower than the radial one, and being relatively high in amplitude. This raises the possibility that Blazhko stars are a subset of RR Lyrae stars with non-radial mode pulsation. Furthermore, while so far not available, a simple test of this aspect of the theory would be to carry out a high resolution spectroscopy on a sample of RR Lyrae stars, including non-Blazhko versions, and see if the non-radial modes occur in Blazhko and perhaps some non-Blazhko stars. Thus an otherwise unidentifiable subset of RR Lyrae stars can be shown to exist. In short, the most likely candidates coming from modelling the stability of RR Lyrae stars for the secondary frequency causing the Blazhko effect are low order non-radial modes, most likely $l = 1$, although this explanation still needs refinement more in some observed stars than others.

Van Hoolst *et al*. (1998) confirmed the plausibility of the 1:1 resonant excitation of non-radial modes in a radially pulsating star as an explanation of the Blazhko type modulation. The authors point out that periodic modulation of the lightcurve is not the only possible result in case of instability of the radial mode towards the 1:1 resonance with a non-radial mode (but the other possibilities are not described in this paper beyond the statement). Thus the statistics for the likelihood of this type of resonance are only an upper limit for the occurrence of the Blazhko effect, given at about 20 – 30 percent. A complicating factor is that the probability of resonance depends on the amplitude of modulation of the primary period, in effect the strength of the driving mode. Dziembowski and Cassisi (1999) give a range for probability of excitation at a typical amplitude of type ab RR Lyrae star of between 0.25 and 0.5 with the $l = 1$ mode, and a joint probability of instability, involving all the likely non-radial modes, always greater than 0.5 and close to 1 in most cases. Thus specifying the fraction of Blazhko RR Lyrae stars from the probability of the resonance is far from simple, and not fully answered so far. Furthermore, the identification of the precise mode involved is important. As the paper points out there are many densely spaced possible non-

radial modes around the frequency of the fundamental one. Why is only one of the modes excited? Why not multiple non-radial modes? Why that particular one? From Dziembowski and Cassisi (1999), the criterion for instability of radial pulsation to excitation of a resonant non-radial mode:

Equation 6.2

$$(\frac{\delta R}{R})^2 > \sqrt{\frac{D^2 + \kappa^2}{C}}$$

Where:

- δR is the amplitude of radius variations in radial pulsation.
- D denotes the frequency distance between the radial and the non-radial mode.
- κ is the damping rate of the non-radial mode in the limit cycle of the radial mode.
- C is the coupling coefficient.

Looking at the plots of modes of inertia for various degrees of modes, three features of the $l = 1$ modes becomes apparent, they have the lowest moments of inertia, they are spread out over a wider or broader range of frequencies, and some of them are among the closest in frequency to the corresponding radial mode. All factors, as seen above, favour being picked in the resonance. This still would not explain why other modes are not excited, assuming the modes that do occur are observable with current methods… or the discrepancy is merely apparent. To further clarify, it should be noted that the non-radial modes, are combination gravity and pressure based, as mentioned, and the modes likely to be excited lie close to the fundamental mode in frequency. They are termed as STU modes, strongly trapped unstable modes. Essentially at close to fundamental radial frequency they start extracting energy from the H and He ionisation zones. The paper does not directly detail whether the energy is transferred from the radial mode because the outer pressure based parts of the non-radial mode start to match it, or whether the same driving mechanism applies to both more independently. In either case, through the evanescent zone, the border where both p

and g-modes exist, the opacity mechanism derived energy is transferred into the pure g-mode zone. Judging by the model, the efficiency of this transfer depends on the width of the evanescent zone, and is the source of the increased likelihood of resonant excitation at some degree *l* non-radial modes over others. However, all this was done for only one stellar model, and Dziembowski and Cassisi 1999 expanded upon it by looking at multiple RR Lyrae star models.

Dziembowski and Mizerski (2004) conduct an energy budget for the flow into the resonant non-radial modes. They describe energy transfer "*through parametric instability of the radial mode to excitation of non-radial modes at nearly resonant frequency (the 1:1 resonance)*". Thus they are talking about transfer of energy from the radial mode pulsation into the non-radial mode, instead of full or partial opacity driving. This is followed by assuming that the frequency differences between the two modes are negligible, easing transfer, and ignoring the saturation of the radial mode, in effect saying that the energy flowing into the non-radial mode is not replaced because the radial mode remains fully saturated even after losing energy. The observably testable prediction in the paper is that the consequence of energy transfer is radial mode amplitude reduction below the saturation level. A large sample of Galactic RR Lyrae stars containing Blazhko stars is used to test the prediction. The radial amplitudes of RR Lyrae stars with and without the Blazhko effect are compared. The amplitude reduction in the sample stars is less than expected from the models and assumptions used. A possibility remains that the predicted and observed quantities agree within their uncertainties, but a determination on this is not made. One notable point in the paper is that the energy cannot be fed into the non-radial mode in a steady state manner, because at least in some cases there is no frequency synchronisation.

Nowakowski and Dziembowski (2003) model at what surface amplitude strong linearity begins in stellar interiors. The RR Lyrae stars have the lowest so called surface critical amplitudes, when the effect begins in the interior. In their case the critical amplitudes are significantly lower

than the observed amplitudes of secondary frequencies. Thus the secondary frequencies in RR Lyrae stars cannot be interpreted in terms of linear non-radial modes. This is a problem with all models of Blazhko stars, as the weakness arises from the description and modelling of non-radial modes, and not how they are induced. The conclusion is that a correct treatment of non-radial modes in RR Lyrae stars is needed, so far nonexistent, to model the Blazhko effect among other features.

Nowakowski and Dziembowski (2001) present a detailed description of resonant excitation of non-radial modes in RR Lyrae stars through amplitude equations. Although a later paper Nowakowski and Dziembowski (2003) points out that in the interior the g-mode parts of non-radial modes are strongly nonlinear, and this contradicts the assumption used in this paper in the liner treatment of the same. Currently two approaches are available for the description of pulsation, full numerical simulations with nonlinear pulsation, and an approximate approach using the amplitude equations (AEs). The treatment of non-radial oscillations, and thus the cases involving the Blazhko effect, has only been developed through AEs. The solutions of AEs may be stationary (fixed-point), periodically modulated (periodic limit cycle), or even chaotic. The authors suggest that the Blazhko effect may be a manifestation of periodic limit cycle solution of the AEs, but it may also be caused by non-radial mode excitation with constant amplitude, that is a fixed-point solution of the AEs. Based on the results of their stability to small perturbations calculations, the authors argue that stationary solutions dominate the parameter space, and the paper deals with this type of resonance exclusively. However, the perturbation calculations are based on equation coefficients derived from stationary solutions. Furthermore, the later result on strong nonlinearity of interior modes makes a re-examination of the results necessary (for example Nowakowski and Dziembowski 2003). The overall treatment is based around the 1:1 resonance of radial and non-radial mode in the absence of rotation, and then is extended to include rotation of the star whereby the non-radial mode is split into distinct modes and the resonance has a frequency triplet signature. An emphasis is made on

describing the properties of pulsation in RR Lyrae stars. Radial modes are purely acoustic and propagate only in the envelope. *The outer layers determine the properties of radial modes and the interior plays no role. In the case of the non-radial modes one may calculate separately the integrals over the deep interior (gravity waves propagation zone) and over the envelope (acoustic waves propagation zone).*

Kovács and Buchler (1988) describe theoretically predicted resonances between the radial modes in RR Lyrae stars. The radial modes are treated with the inclusion of nonlinear pulsations, but as expected these contributions are small. The paper is interesting in that it describes resonances in a wide context, and presents the paradigm before radial and non-radial resonance became the favoured explanation for the Blazhko effect. The resonances are treated in terms of linear combinations of integer numbers of the fundamental and overtone frequencies, and some of these sums approximately equal another overtone frequency for a possible resonance. This is the result of density and temperature differences at different depths of the star changing the speed of sound inside the star, as mentioned before, and thus moving the frequency values of the overtones away from the exact fractional relations for a uniform media. It is the background from which the current theories of Blazhko stars grew, and it is an expanded treatment of resonance modelled with numerical hydrodynamical code. It describes useful properties of resonances: resonances destabilise the driving cycle, and this shows up in the reduction and instability of the driving amplitude. It clarifies the terms used in this area, a *"limit cycle"* is simply a singly periodic oscillation, and an *"attractor"* is a stable state to which models evolve if started away from it, provided it exists, and is reachable based on initial conditions. Resonances are described which evolve towards a constant limit cycle, i.e. constant amplitudes at the frequencies involved. No examples of periodic limit cycles occur in the models presented. This is a good reminder for keeping in mind all resonances, among other things, as probes of RR Lyrae structure.

Moskalik (1986) presents the now sidelined explanation for the Blazhko effect in terms of a 2:1 resonance between fundamental mode and the 3rd overtone. Currently this explanation has been discarded because the parameters of the models required to produce it disagree with likely physical properties (see Moskalik and Nowakowski 2001). It remains interesting in its historical context, and for its description of a periodic limit cycle, where the amplitudes of the two resonating modes are not constant but periodic. Periodic limit cycle of a resonating radial and non-radial mode is one possible description of the Blazhko effect. An interesting point made in the paper is that the multiplet frequency structures currently associated with the presence of closely neighbouring distinct frequencies, and the current definition of a Blazhko star signature, can be reproduced in Fourier spectrum by *"frequency splitting due to periodic modulation of amplitudes and phases of interacting modes"*. In this paper the statement applies to relatively widely spaced in frequency fundamental and third overtone modes and not two close modes. This presents an interesting point that the very defying frequency signature of Blazhko stars can occur in another way. However, the paper does not clarify how the multiplet signature arises in the 2:1 resonance, and so it is unclear if this is a real problem.

6.5 Summary

The Blazhko stars are no longer thought of as monomode pulsators. Recently it has been established that they are characterised by the presence of frequencies in addition to the main and strongest radial pulsation frequency. This had not been recognised immediately because the additional frequencies are close to the main one and depended on the frequency resolution and detectability inherent in the observational data. The beat between the two is an explanation for the Blazhko modulation. The "majority opinion" is that the second frequency is a non-radial mode, but its identity has not been demonstrated. The mechanism for the excitation of the non-radial

frequency is thought to be a resonance with the main radial mode, but details for the process have not been established in the theoretical models.

7 Summary and conclusions on the identification of RR Lyrae stars in PLANET observations

7.1 Summary of completed work

The work involved in analysing PLANET database to find RR Lyrae stars produced an extensive toolset of data analysis software. These programs or the algorithms developed for them can be used for an ongoing year to year variable star search as the PLANET group accumulates observations in the future. The programs can be equally well used to find other types of variable stars. During the search process for RR Lyrae stars large numbers of eclipsing binaries were identified in PLANET data but a further study of this type of stars was not carried out as it would not have fit with the primary goal of studying Blazhko starts. Every year the PLANET data can now provide new identifications of RR Lyrae stars, eclipsing binaries, or other types of variables as required.

Perhaps the most interesting algorithm developed is a star pattern matching procedure. This program has been optimised to be very efficient in computational time, and takes advantage of the information available about the star fields being matched, avoiding a brute force pattern matching approach. This resulted in a very high ability to match the PLANET observing fields with a high accuracy. The program has calculated the co-ordinate transformations between PLANET fields for the years of data analysed in this thesis (the results are in a file), and if required it can produce files matching the ID numbers of all the same stars in the PLANET archives for different telescopes. The algorithm is directly useful for PLANET data outside this project, and perhaps has general application in astronomical work where matching patterns of stars is a frequent requirement.

The analysis of the PLANET database for the years 1995 to 2005 inclusive has produced 87 detections of RR Lyrae stars. Out of these 87 stars 33 are newly identified stars not listed in the

OGLE II catalogue (Mizerski 2003, and private communication for the details of the catalogue used in the paper), one star is covered by OGLE II observations but not identified as RR Lyrae variables in the catalogue, and 53 are stars that have been identified as RR Lyrae variables both in the PLANET data and the OGLE II catalogue.

The group of the stars identified in the PLANET database is a mixture of the two most numerous subdivisions of RR Lyraes: type ab and type c. As expected the majority of these RR Lyrae variables are of type ab at 69 stars, and type c at 16 stars. The total is finished off by the two atypical stars as described in the Results section. The ratio of type ab to type c is 4.3 for the PLANET group, and 2.5 for the OGLE II group. The difference between the two surveys is likely caused by the type c RR Lyrae having on average lower amplitudes of variability and more noisy lightcurves in PLANET data, and thus being more likely to remain undetected. These results are based on PLANET observations for the years specified but very similar outcomes are likely to occur from the analysis of the PLANET database for other years.

The successful detections show that the selection methods used in this thesis for identifying RR Lyrae variables are effective, and that the PLANET database contains observations of sufficient quality to find these stars. The comparison made to the database of RR Lyrae stars derived from the OGLE II microlensing survey observations further showed that the numbers of detections are similar for these stars where the observing fields for the two surveys overlap. The only RR Lyrae stars found in OGLE II data and missing from PLANET are those for which magnitude observations were too inaccurate to clearly identify them: this happened for 9 RR Lyrae stars in the analysed PLANET fields overlapping OGLE II fields. Of the 9 stars 3 stars were added into the PLANET set upon comparison with OGLE II data – in the PLANET data these stars had noisy type c lightcurves that were initially not identified as RR Lyrae stars but could have been. Finally, one star was identified as RR Lyrae but not identified as such in the OGLE II catalogue.

Thus this sample of RR Lyrae stars in PLANET database is effectively complete within the limitations of the instrument for the well observed fields searched. The amplitude of variability in RR Lyrae stars is sufficiently large to be detected unless other factors interfere. The few stars that were missed in the PLANET detections had noisier lightcurves because their observed magnitudes were fainter which means they were simply farther away. The limit on the detection of RR Lyrae stars in PLANET data is primarily their distance and secondarily the accuracy of the observed magnitudes which are in turn affected by seeing conditions and the type of photometry extraction used. The analysis methods used for the PLANET observations did not miss RR Lyrae stars and did not create false detections to the same degree as for the independent OGLE II survey, but rather the absence of these differences between the two shows the accuracy of both in this regard. Since the PLANET observing fields were chosen for analysis simply on the basis of the presence of sufficient observations a data selection bias is unlikely and the same conclusions should apply to PLANET data in general. The distribution of observing times for the PLANET data is better than required to cleanly detect the primary variability in RR Lyrae stars and the alias and artefact cleaning routines implemented in this thesis worked successfully at choosing these stars without missing any observed with sufficient accuracy in magnitudes. PLANET data is problematic at describing Blazhko stars due to its relatively short time span, problems with combining data between telescopes and the accuracy of magnitudes obtainable is not always sufficient to detect the smaller amplitude Blazhko modulations.

Best fit models of the lightcurves were used to combine data from the different PLANET telescopes for the same stars, and to obtain their Fourier parameters for this purpose. Only 2 of the RR Lyrae stars found in the PLANET database had data available from all the four PLANET telescopes. The majority of these stars were found in data from a single telescope. The two main reasons for this are the large differences in observing field sizes between the PLANET telescopes,

and a lot of fields being observed less than the minimum 80 clean magnitude measurements chosen as the criterion for producing a lightcurve accurate enough for further analysis. This minimum number of good observations is forced by: the need to combine lightcurves from different telescopes; have enough observations to fit a good model of the average lightcurve to produce residuals to test for the presence of additional frequencies; the other requirements described in detail in section 5 “Results”. In terms of using PLANET data to find variable stars a simple improvement would be to make sure each field was observed at least 80 times or so by each telescope, and perhaps a few more times to compensate for losing some observations for the various reasons described in the Data Analysis and Results sections.

The PLANET data based lightcurves of all the RR Lyrae stars identified were analysed for the presence of variabilities in addition to the main one with the aim of identifying Blazhko stars through the signature of the additional variability having a frequency close to the first one, typically within a few percent of its value. Although Mizerski (2003) sample has type BL1 Blazhko stars with the long term modulation down to 5 days, corresponding to somewhat larger percentage differences in frequencies between Blazko multiplets components. The BL1 and BL2 designations are as per Mizerski (2003) and refer to Blazhko stars with a detectable frequency doublet and triplet respectively. To confirm all results two independent frequency analysis methods were used: Analysis of Variance and Lomb-Scargle. Monte Carlo simulations were conducted for all the residual period detections to determine their significance. However, it became clear that Monte Carlo simulations alone are not able to determine whether these residual frequencies contribute to the Blazhko modulation or are part of other variabilities. Only a single Blazhko star was found among the PLANET RR Lyrae stars in this way, the star EB2K005I_P1258_Y2248.ab as per PLANET RR Lyrae sample naming convention adopted in this thesis. Among Galactic type ab RR Lyraes the typical percentage of Blazhko stars is between 20% and 25%. 41 type ab RR Lyrae stars in the PLANET sample are matched to OGLE II RR Lyrae stars. Thus the expected number of

Blazhko stars among these matched type ab stars is in the range of 8 to 10, compared to none actually found. In addition among the 53 RR Lyrae stars that had OGLE II matches 10 are listed as Blazhko stars in Mizerski (2003) catalogue. Thus the same stars are detected as Blazhko stars in OGLE II data at a rate consistent with existing frequencies of occurrence but not in PLANET data. This discrepancy is caused by the specifics of PLANET data.

Two oscillations with frequencies close in value acting on the same space will overlay together and produce a beating, or periodic change, in their combined amplitude. The frequency of the beating is simply the difference and sum in frequency between the two. A period of the beating is simply the inverse of the frequency. In order to describe one beat period the time span of the data has to be at least equal to it. Thus in order to resolve two close frequencies and assuming a reasonably even distribution of observation times the time span of the data describing them has to be at least equal to their beat period. This is the same as saying in Fourier analysis that the frequency resolution is equal to the inverse of the time span of the data.

Table 7.1 it shows that out of the 10 Blazhko stars detected for the OGLE II catalogue but not detected as Blazhko from the PLANET data, only 3 have time spans in the PLANET data that could provide the frequency resolution required to identify the additional periodicities. The remaining 7 stars could not have been identified from PLANET data because the observations have not been made over a long enough duration of time to resolve the frequencies required. The 3 stars with the theoretically required time span in the PLANET data have most likely been missed due to the larger errors in observed dophot based magnitudes for PLANET as compared to OGLE II image subtraction processed observations and through uneven distribution of observations over their time span.

Table 7.1: The Blazhko stars detected in the OGLEII data that have matches to the RR Lyrae stars detected in PLANET data. *PLANET ID* is the star number in the PLANET sample of RR Lyrae stars, the same across all references; *OGLE II catalogue ID* is an internal identification number in the RR Lyrae and Blazhko stars catalogue obtained by private communication from Mizerski 2003; *Blazhko type* is the type of Blazhko star as per Mizerski 2003, BL1 type has one frequency close to the main one, BL2 type has two additional frequencies; *Periods* are the OGLE II periods starting with the strongest, i.e. the main period, and continuing in order of decreasing strength, given in units of days; Δ *frequency* the difference in frequency of the additional periods from the main one; *Beat periods* are the periods that would result from beating between the strongest the corresponding additional period, they are the inverses of the frequency differences, given to within the nearest full day; *PLANET timespan* is the same as given in the other tables, presented for comparison. All the OGLE II quantities in the table are from catalogue as used by Mizerski 2003.

PLANET ID	**OGLE II catalogue ID**	**Blazhko type**	**Periods (d)**	**Δ frequency (1/d)**	**Beat Periods (d)**	**PLANET timespan (d)**
15	2216	BL2	0.35215237 0.35233049 0.35200721	 -0.0014356 0.0011710	 697 854	380.991
27	6655	BL1	0.43700691 0.43219091	 0.02549898	 39	95.580
32	4156	BL1	0.53349539 0.53343576	 0.00020955	 4772 **?!**	71.063
44	5890	BL1	0.54941785 0.54115327	 0.02779699	 36	49.076
47	2097	BL1	0.32876752 0.32858278	 0.00171007	 585	78.450
49	3809	BL1	0.58449779 0.57270547	 0.03522775	 28	138.396
61	2914	BL1	0.51085697 0.51160990	 -0.00288084	 347	19.362
66	3989	BL2	0.43814928 0.43653684 0.43920231	 0.00843025 -0.00547206	 119 183	33.908
69	6138	BL1	0.56638119 0.56800549	 -0.00504898	 198	82.290
76	3903	BL2	0.56895719 0.56936941 0.56893228	 -0.00127251 0.00007694	 786 12997 **?!**	65.087

The curious thing to note is that stars PLANET ID 32 and 76 have beat periods much longer than the time span of OGLE II data. The time span for all the observing fields varies closely around 1300 days. Thus it should not have been possible to resolve these two beat periods from OGLE II data. The explanation is that the catalogue of OGLE II RR Lyrae stars provided here was in a version that later got cleaned of this type of misidentification.

Overall the reason for not identifying the same number of Blazhko stars in PLANET data as were detected in OGLE II data is a combination of less accurate magnitudes, distribution of observations in time and insufficient frequency resolution of the PLANET data. The lack of frequency resolution is due to the relatively short time spans PLANET data was collected over.

Hence the PLANET sample of RR Lyrae stars was analysed correctly for the presence of Blazhko stars, and the lightcurves of the stars were identified and assembled as presented in section 9 “Finder charts and lightcurves”. The discrepant result, just a single Blazhko star detection, is explained and accounted for in detail.

The single Blazhko star detection is an interesting example of the modulation, and a newly identified star without an OGLE II or other catalogue match. This means that the resolution of the component frequencies of its light variation cannot be improved, but it is a relatively well observed star with 707 good measurements over the time span of 491 days (most of the observations are concentrated over a shorter time period). This star has a very strong Blazhko modulation and this was the reason why it was possible to identify it in PLANET data. The ratio of the amplitudes for the secondary to primary periodicities is 0.69 as estimated from the star’s lightcurve. Mizerski (2003) gives the maximum values for this ratio as 0.537 and 0.595 for type BL1 and BL2 Blazhko stars, respectively. Keeping in mind that the OGLE II amplitudes are from Fourier analysis, star P3 shows amplitude modulation at least as strong as the strongest detected in OGLE II data. Thus this

star is an interesting object in terms of the strength of it modulation, and is a good candidate for frequent observations over a relatively short time that could be used to follow amplitude stability and energy flows between its pulsation modes, as proposed below.

7.2 Future Work

7.2.1 Introduction

The asymptotic stability of a disturbed system tends towards a constant amplitude or cyclic modulation of the amplitudes of the modes present in the Blazhko stars is based on assumptions and simplifications of the physics and equations involved. This is a regular result of theoretical descriptions of Blazhko stars. Thus it would be interesting to check these predictions against observational data.

The amount of theoretical predictions about RR Lyrae and Blazhko stars is extensive, but the comparisons to observational data are fewer. The various shapes, proportions, and structures of the frequency spectra for these stars have been described from observations, but theory is not yet able to predict them in detail. The amplitude reduction of the radial mode in a resonance with the non-radial mode has been shown statistically by Dziembowski and Mizerski (2004) in observational data, but with some potential difficulties in the details.

The stability of amplitudes of frequency components in stars that are identified as exhibiting the Blazhko effect should be explored. In cases where the amplitudes appear constant, constraints can be established on how stable they are. In cases where the amplitudes vary, the variability should be described. This type and similar research benefits from more accurate photometry produced by

image subtraction techniques and it is often advantageous to reprocess older data with image subtraction as it is combined with new observations.

7.2.2 Possibilities for future work

The PLANET data as it currently exists can only be used to identify Blazhko stars with very strong additional periods as is the case with the star 3 Blazhko identification. The only way to identify additional Blazhko stars within the PLANET database the accuracy of the observed magnitudes has to be improved and the frequency resolution improved either through additional observations or through adding data from other sources. For example the combination of the PLANET and OGLE II data is likely improve the quality of the Blazhko stars lightcurves beyond that provided by either survey alone, and may allow the detection of additional Blazhko stars among these thanks to the improved frequency resolution.

More accurate magnitudes can be extracted from existing PLANET observations by reprocessing the data with image subtraction photometry in place of the existing dophot derived magnitudes. Once this is done, at least a few new Blazhko stars unique to the PLANET database should be found, but the number of additional Blazhko stars is still likely to be below the 6 to 8 stars expected from the 20% to 25% frequency of this type applied over the 33 type ab RR Lyrae unique to PLANET due to the shorter time spans of PLANET data. The necessary software and procedure have been developed within the PLANET pipeline data processing software as of 2007. However, the PLANET data analysed in this thesis has been observed and processed before this time. Reprocessing lightcurves for the PLANET RR Lyrae stars with image subtraction should produce more accurate magnitudes but this effort may be limited by the availability of the archival observational data. Not all of the data is currently available or easily accessible as the microlensing nature of the PLANET survey did not result in regular storage of unprocessed photometric data. The

main reason that OGLE II magnitudes are more accurate than existing PLANET data, is that the OGLE group has reprocessed their observations with image subtraction photometry. The image subtraction method has become available and accepted in the last few years.

The frequency resolution of the lightcurves can be improved by combining PLANET and OGLE II data. The combination takes advantage of the different dates and time bases over which the data was collected for the two surveys, resulting in greater coverage at different times and often over longer time spans. For example if PLANET and OGLE II data for the same star was collected a few years apart, this results in a few year time span for the combined data and a greater frequency resolution provided the gaps in data are not too large. In addition PLANET data gives more frequent sampling over shorter periods. The existing software written for this thesis to combine lightcurves from different telescopes can be used to combine the PLANET and OGLE II data (see description of *graph* routine in section 4, *Data Analysis*). Table 5.4 shows that 29 out of the 87 PLANET RR Lyrae stars have their time spans increased by combining data. Thus doing this will provide a description of the frequency structure of these stars in a greater detail than either PLANET or OGLE II data can provide alone.

The increased frequency resolution of combined data will confirm the OGLE II Blazhko detections in PLANET data, and possibly provide additional Blazhko star detections among this set of RR Lyrae stars by resolving close frequencies previously not resolved in OGLE II data alone and providing some very long modulation period examples of these stars (a Blazhko modulation period not covered by time spans in OGLE II or PLANET alone). The additional Blazhko detections would be new Blazhko star identifications not previously resolved from the OGLE II or PLANET data alone, an extension of the Blazhko stars beyond the modulation period covered by OGLE II, or a limit on the likelihood of their occurrence in that period range.

The discussion in the RR Lyrae pulsation section describes how the exact structure of the period multiplets in a Blazhko stars indicates the type of processes causing the additional oscillation and the Blazhko modulation as the effect. Hence it is important to know this structure in as great a detail as possible for confirmed Blazhko stars, even if the additional resolution confirms the existing multiplet arrangements and discounts new features. The number of distinct frequencies in the frequency multiplet of Blazhko stars is one of the selection criteria for different models. The triplet structure of frequency peaks in a periodogram is an indication of a resonant excitation of non-radial modes (Dziembowski and Cassisi 1999, Dziembowski and Mizerski 2004), while the oblique pulsator model predicts a quintuplet structure among others (Shibahashi 2000). The detection of frequency triplets in Blazhko stars is a very strong argument for the excitation of non-radial modes in RR Lyrae stars as the explanation of the Blazhko effect. The counter argument is that suitable data has not been available to resolve the finer frequency structure expected for the multiplets with greater number of frequency components. Recently this counter argument has been supported by the detection of a frequency quintuplet in the Blazhko star RV UMa, found from corrected long term optical observations for the star (Hurta *et al* 2008). The combined PLANET and OGLE II data will provide exactly the higher frequency resolution required to look for this kind of structures, and one of the constraints for different models and explanations of the Blazhko effect will be as simple as the presence or absence of additional frequency components in the highly resolved Blazhko frequency multiplets. The above suggestion for combining data from the two surveys and analysing it again should provide this answer.

Data from OGLE III for the Galactic Bulge also exists, but is not publicly available as yet. Contact has been initiated with the OGLE group and most likely this additional data will be available for follow up work. The extra data will increase frequency resolution for the lightcurves in a similar way to using OGLE II data but beyond that already described, and provide more detail on amplitude changes through the extra observations.

The result of combing PLANET and OGLLE II data for the RR Lyrae stars identified here will be a set of lightcurves with a very large number of magnitude observations over very long time spans and thus providing high frequency resolution, for example see Table 5.2 and note the numbers that result when the two columns indicating the number of observations from both surveys are added up. These numbers will be even greater with the OGLE III data added in. Such well-described lightcurves are a good opportunity to study the stability of the amplitudes of the frequency components associated with the Blazhko effect. As described in more detail in section 6 "RR Lyrae Pulsation", the stability of these amplitudes relates to the interactions of the different postulated pulsation modes in a Blazhko star, and the energy flows between them. Thus these combined PLANET and OGLE II RR Lyrae lightcurves should be analysed for the stability of the amplitudes of the Blazhko frequency components. Wavelet based analysis of the amplitudes seems one general method of approaching it, but I have not found a theoretical method for separating variations from the multiple components based on data from lightcurves alone. The wavelet method has been used to look at variable stars (Foster 1996), but not at Blazhko stars. Thus to complete this step an adequate method of analysis to extract this information has to be found or developed. However, even if such a method does not already exist, a simple assumption of one of the components being constant and looking for variations in the amplitude of the remaining ones should provide some constraints on the stability of amplitudes. This last approach would be similar to the one used to find periods in residual lightcurves, and the existing software tools can be used to carry it out, but this time perhaps it would be carried out in reverse by subtracting out the additional periods from the lightcurve and looking at the stability of the remaining main oscillation.

The greater frequency resolution, improved magnitude accuracy, and more detailed lightcurve description with increased number of observations from combined data will all answer whether the short residual periods as presented in Table 5.3 and discussed in section 5.3 "Period

analysis with the Lomb-Scargle method" are real or artefacts. If these shorts periods survive the changes in different levels of noise and magnitude errors provided by image subtraction photometry and the additional observations added in from OGLE II, they are likely to be true. Once these factors are ruled out, comparing the results across different PLANET telescopes and stars from the same telescopes can test for sampling and instrumental artefacts. Thus an answer one-way or the other can be provided. In case these periods are real this would also present a significant new and important result on different types of oscillations in RR Lyrae stars. However, at this stage there is no sufficient information available in the data to answer this. The other expected results obtainable as described above are probable, while this one is only a possibility that needs checking. Once the data is combined to obtain the above results, checking this question will be very fast and easy to do by simply running an accurate period search around the frequency range in question for the PLANET RR Lyrae stars.

8 Finder charts

8.1 Astrometry of identified stars

Except for the microlensing object, PLANET data uses internal CCD pixel co-ordinates. Finder charts in the form of fits images are available for most observing fields, but they are not calibrated with any standard co-ordinate system. In order to give locations for the objects identified here, the PLANET finder charts were calibrated to have RA and Dec co-ordinate system overlaid on the pixel co-ordinates. This was done by using the Gaia data analysis package, part of the Starlink Software Collection at the Joint Astronomy Centre at the University of Hawaii. The calibrations were based on the positions of 10+ stars per field from the 2MASS catalogue, and usually many more. The rms of the calibration to the catalogue stars is 0.1’ or better for all fields and this indicates the accuracy of the positions from the calibration. The final positions of the stars found in the PLANET database were determined from the calibrated images using the star position fitting routine available in the Gaia package. The intensity scale in the finder charts is logarithmic, with the bounds adjusted manually for contrast to show the desired stars. All the fields shown here, except for telescope Z, are shown in the same orientation, North at the top, and East at the right side. In the fits files showing observing fields from telescope Z the orientation is altered by about 45º due to the CCD orientation at the telescope, as the fields are presented here, their top right hand corner corresponds to North, and the bottom right hand corner to East.

8.2 The lightcurves

The lightcurves are plotted with all the data included in the analysis. The data points are labelled with the first letter of the PLANET telescope which made the observations as per the legend on the figures. The magnitudes provided are relative as per the PLANET convention as the magnitude

variations are of interest. The model of best fit derived through Fourier components is labelled with *'M'* and plotted in orange. The *'Normalised Derivatives'* are: *'d'* the first derivative of the model lightcurve plotted in pink; *'dd'* the second derivative of the model lightcurve plotted in light blue; *'0'* is the zero reference line for the derivative, derivative values below it are negative and values above are positive. The derivative values are plotted to help with assessing the model lightcurve. For example, the intersections of the pink first derivative line with the green line indicate accurate positions for the model maxima and minima. The intersection of the second derivative with the zero reference line can be used to locate the position on the rising edge of RR Lyrae when the increase in luminosity starts to slow down.

The finder charts and lightcurves are presented in the same order as in Tables 5.1 and 5.2

UEB2K005I 3.24’ by 3.24’ for event EB2K005I

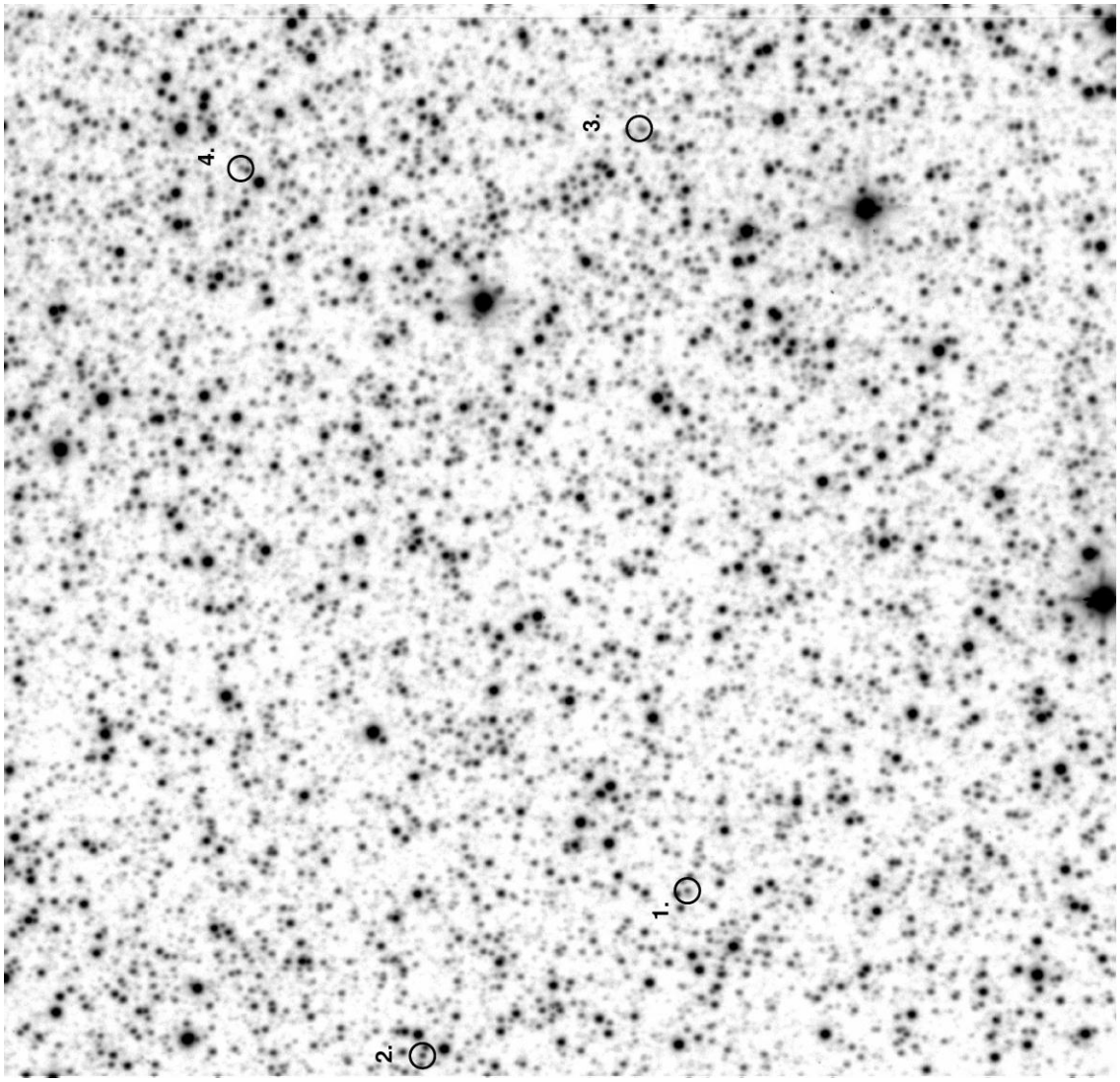

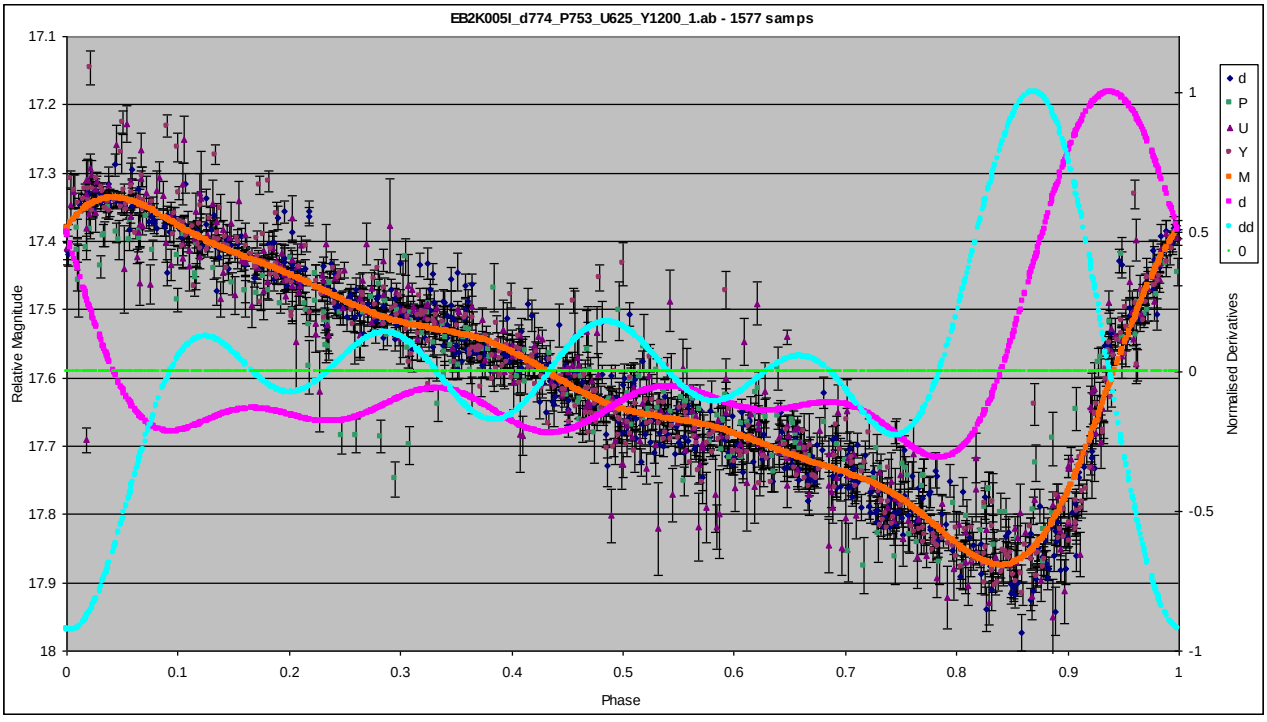

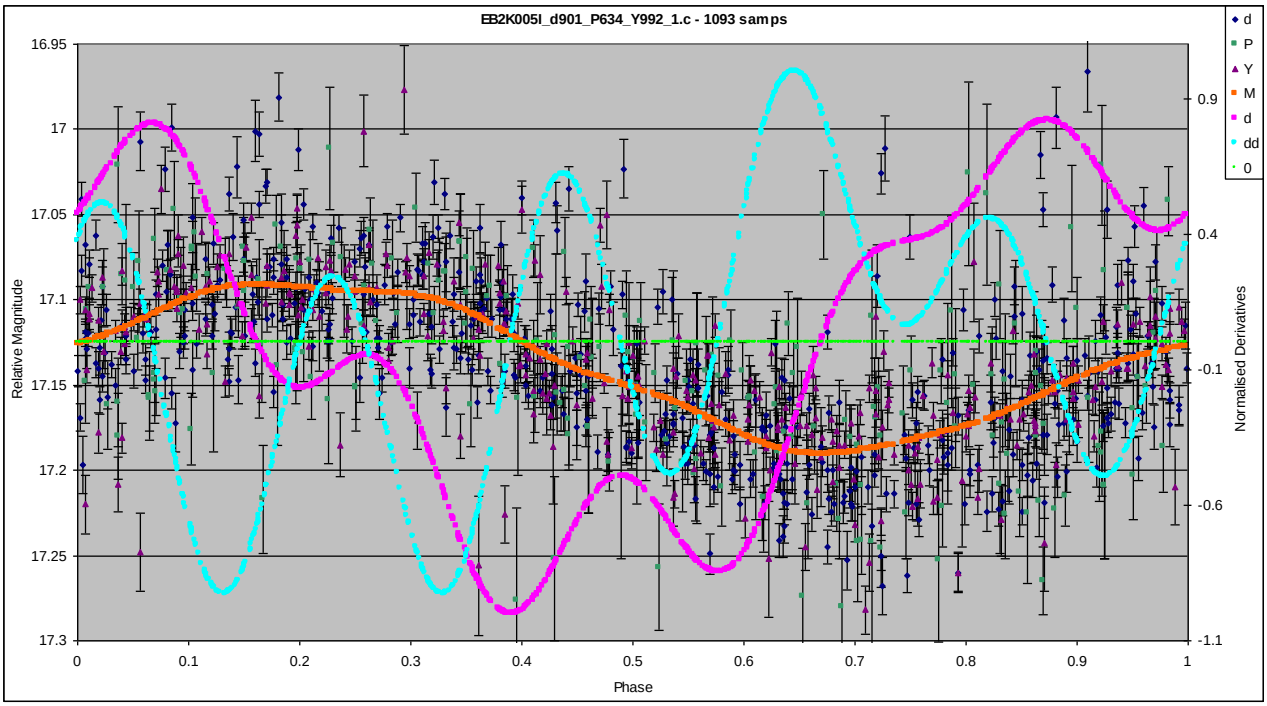
EB2K005I_d901_P634_Y992_1.c - 1093 samps
Relative Magnitude
Normalised Derivatives
Phase
d
P
Y
M
d
dd
0

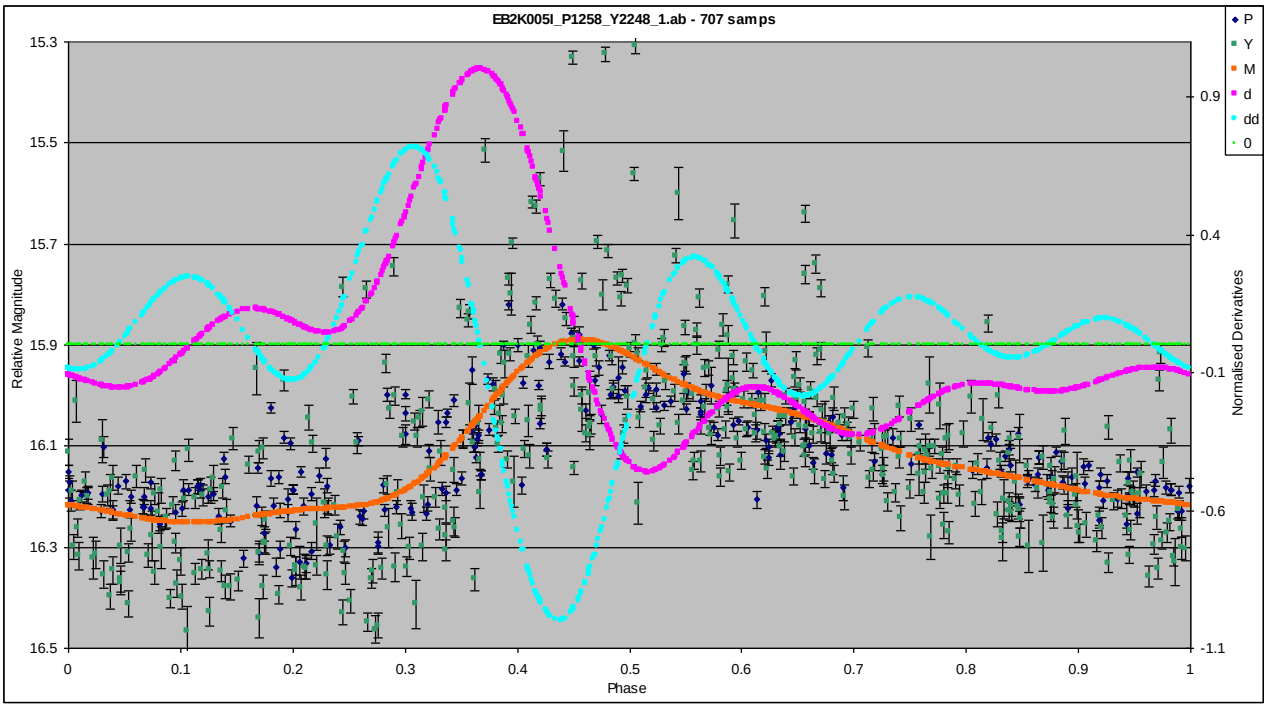
EB2K005I_P1258_Y2248_1.ab - 707 samps
Relative Magnitude
Normalised Derivatives
Phase
P
Y
M
d
dd
0

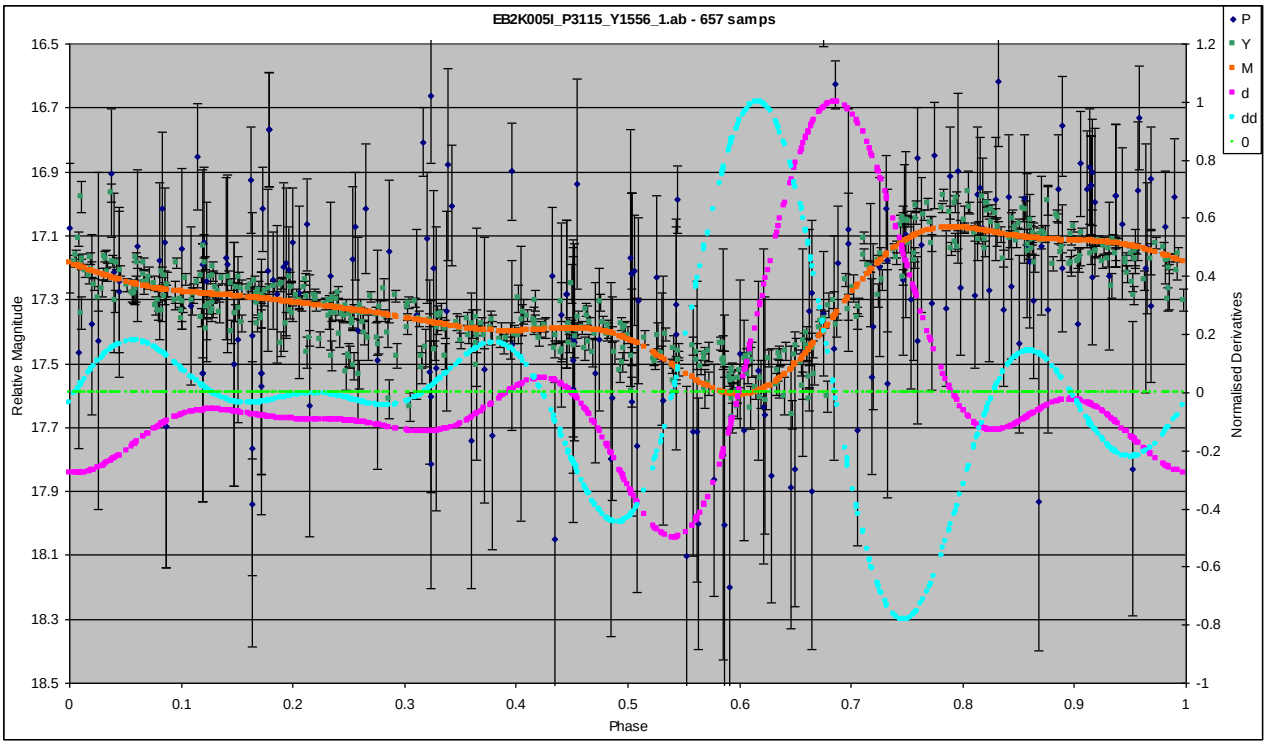

CMB99008I for event MB99008I ~ 5.13’ by 5.13’

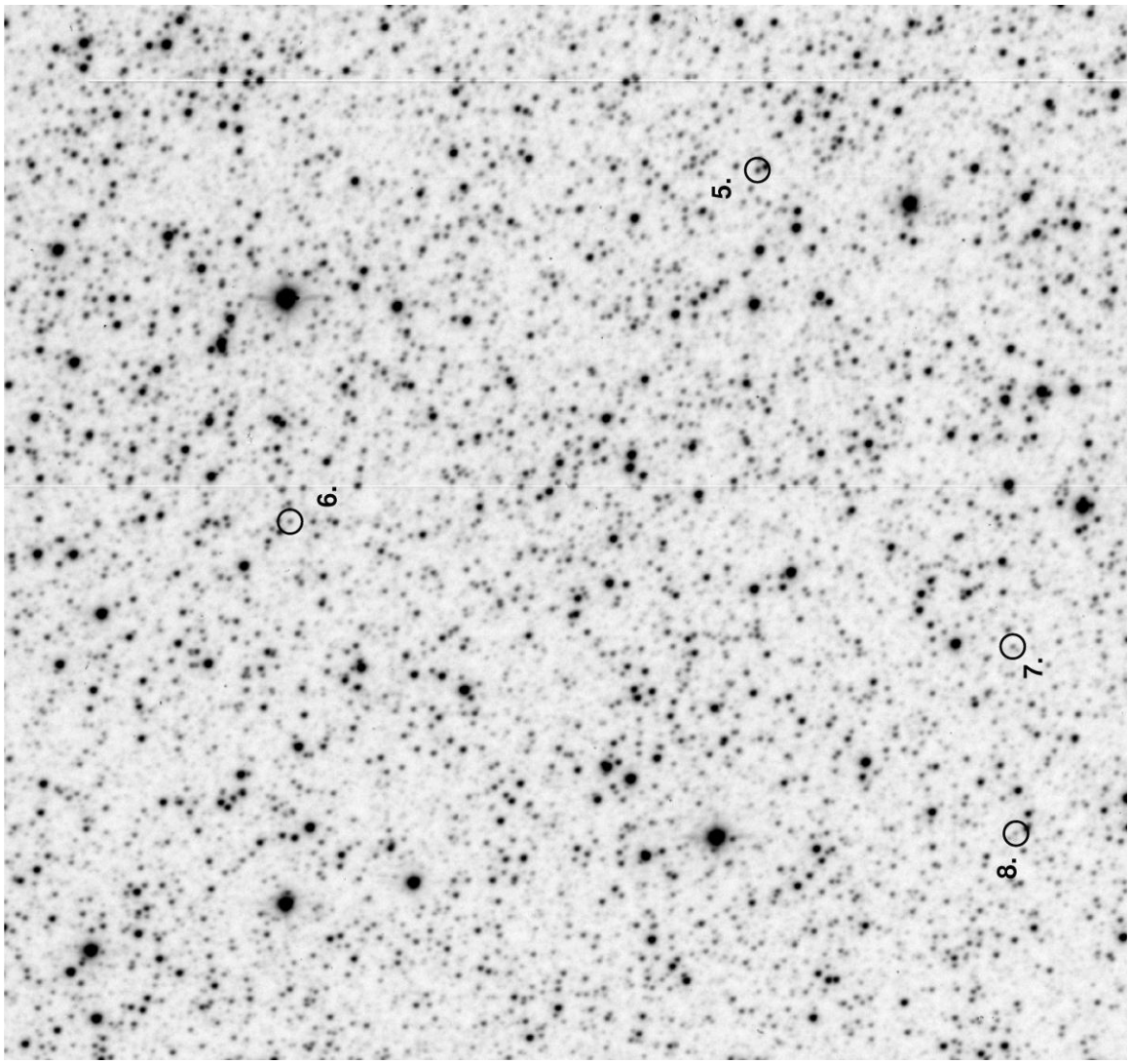

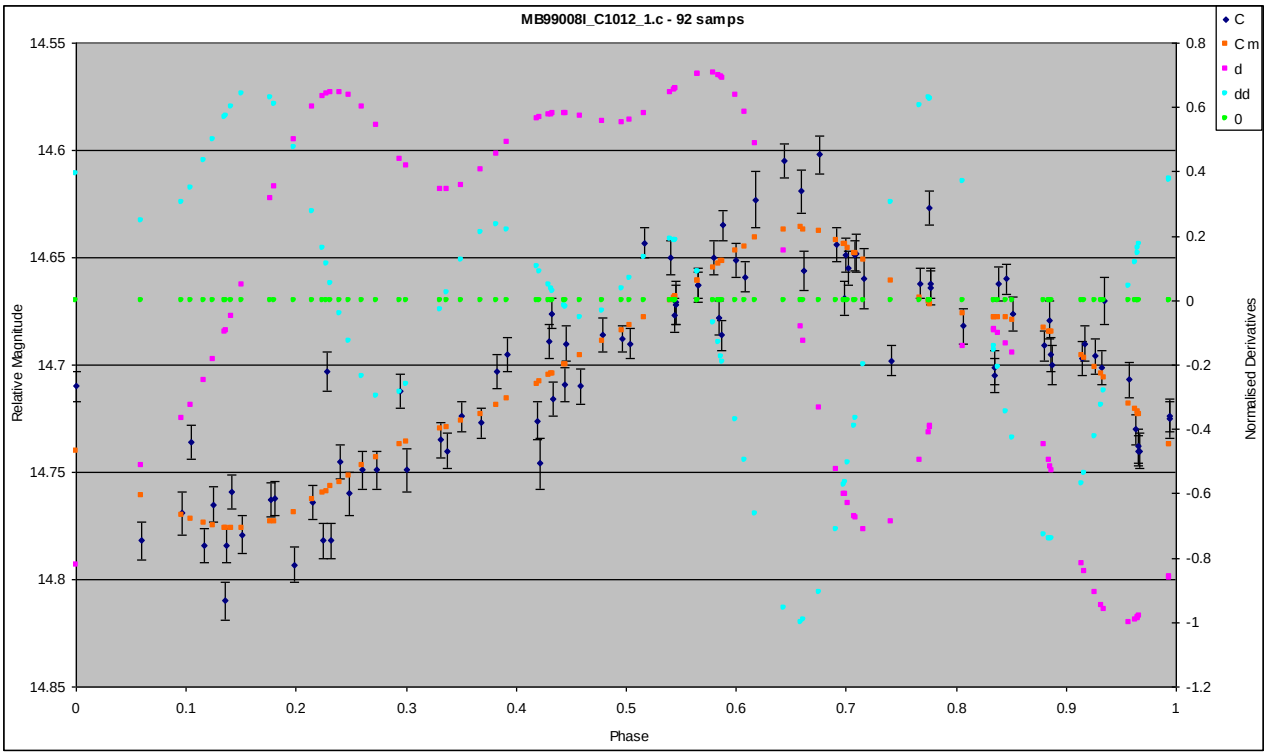
MB99008I_C1012_1.c - 92 samps
C
C m
d
dd
0
Relative Magnitude
Normalised Derivatives
Phase
14.55
14.6
14.65
14.7
14.75
14.8
14.85
0.8
0.6
0.4
0.2
0
-0.2
-0.4
-0.6
-0.8
-1
-1.2
0
0.1
0.2
0.3
0.4
0.5
0.6
0.7
0.8
0.9
1

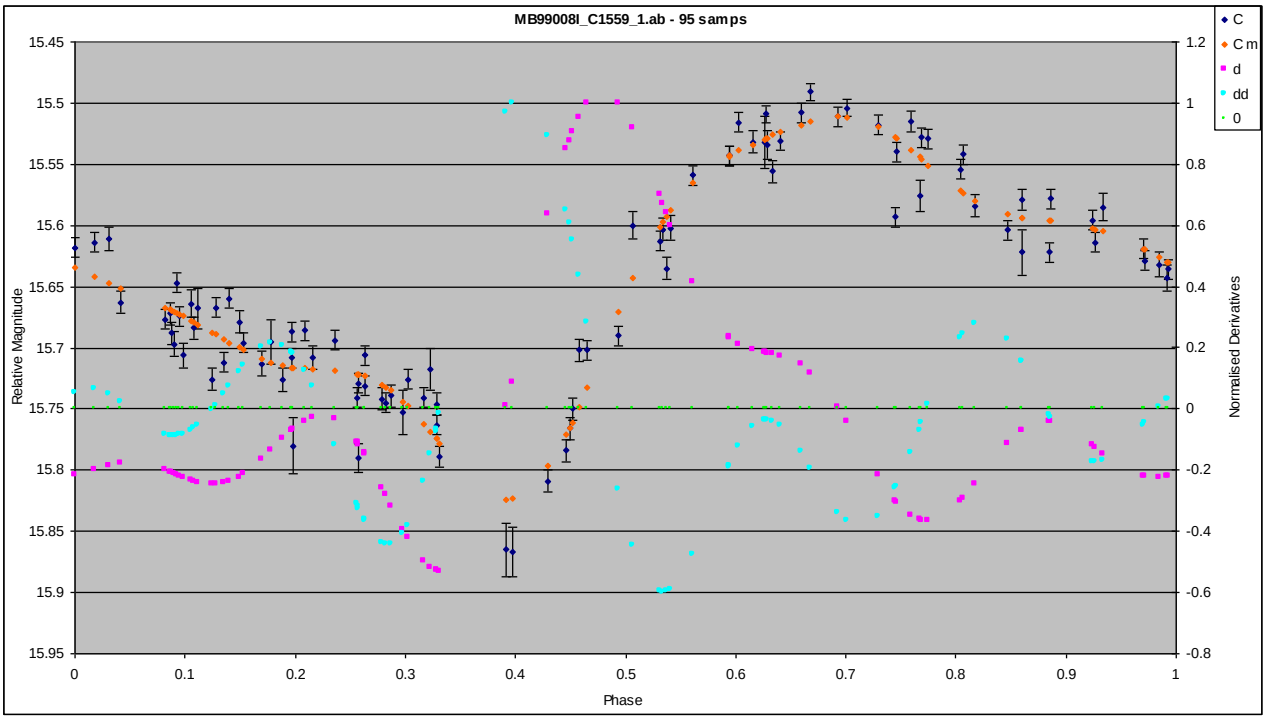
MB99008I_C1559_1.ab - 95 samps
C
C m
d
dd
0
Relative Magnitude
Normalised Derivatives
Phase
15.45
15.5
15.55
15.6
15.65
15.7
15.75
15.8
15.85
15.9
15.95
1.2
1
0.8
0.6
0.4
0.2
0
-0.2
-0.4
-0.6
-0.8
0
0.1
0.2
0.3
0.4
0.5
0.6
0.7
0.8
0.9
1

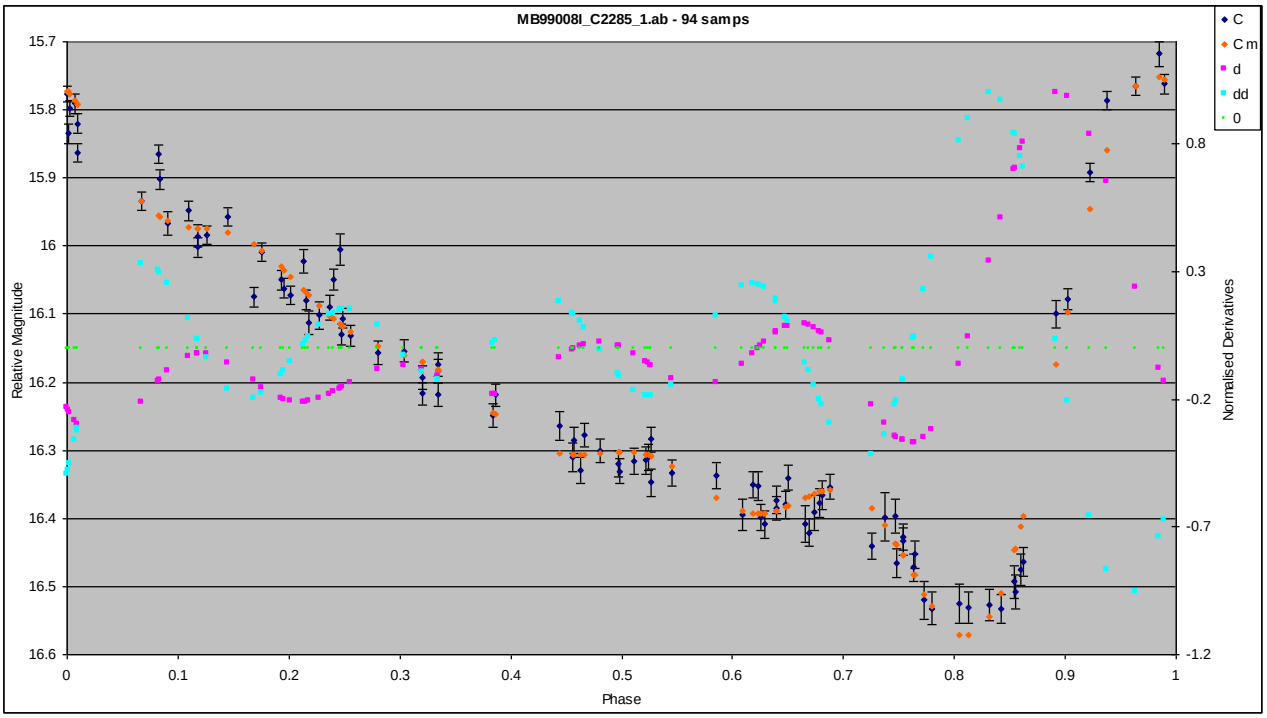
MB99008I_C2285_1.ab - 94 samps
C
C m
d
dd
0
Relative Magnitude
Normalised Derivatives
Phase
15.7
15.8
15.9
16
16.1
16.2
16.3
16.4
16.5
16.6
0.8
0.3
-0.2
-0.7
-1.2
0
0.1
0.2
0.3
0.4
0.5
0.6
0.7
0.8
0.9
1

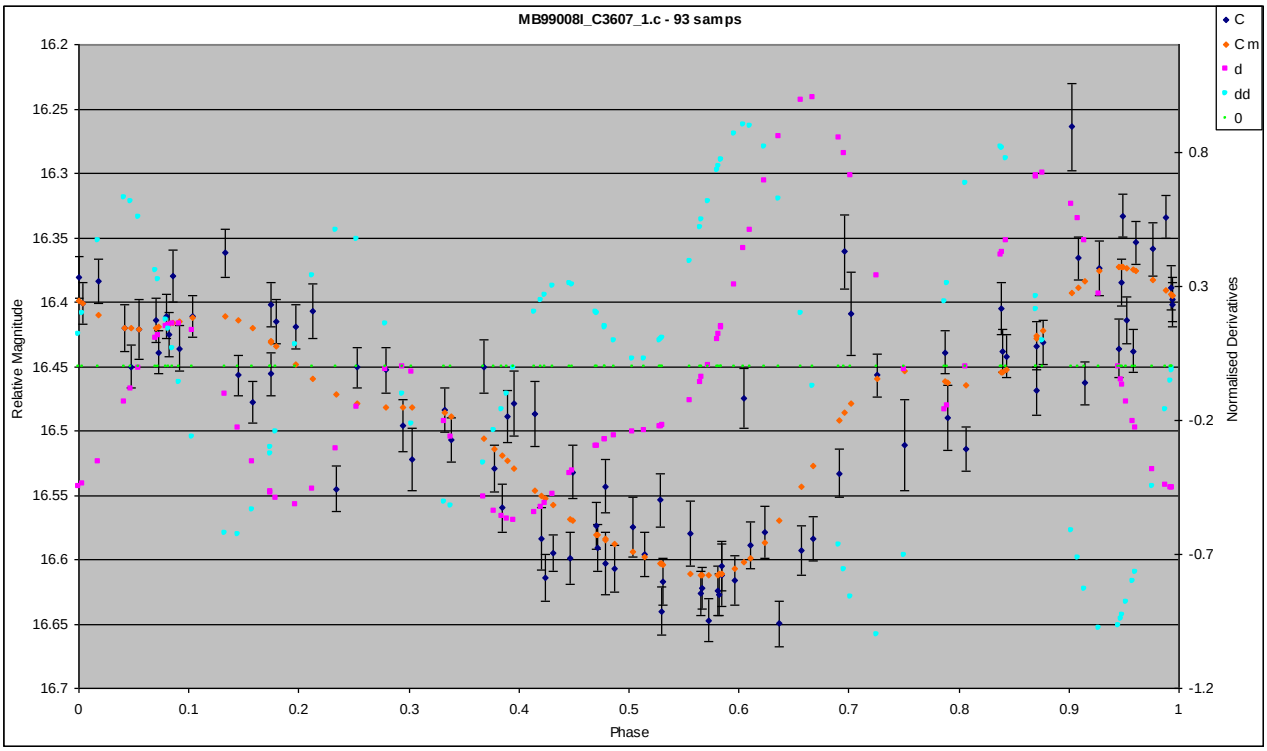
MB99008I_C3607_1.c - 93 samps
C
C m
d
dd
0
Relative Magnitude
Normalised Derivatives
Phase
16.2
16.25
16.3
16.35
16.4
16.45
16.5
16.55
16.6
16.65
16.7
0.8
0.3
-0.2
-0.7
-1.2
0
0.1
0.2
0.3
0.4
0.5
0.6
0.7
0.8
0.9
1

YOB2K05I for event OB2K025I ~ 5.13’ by 5.13’

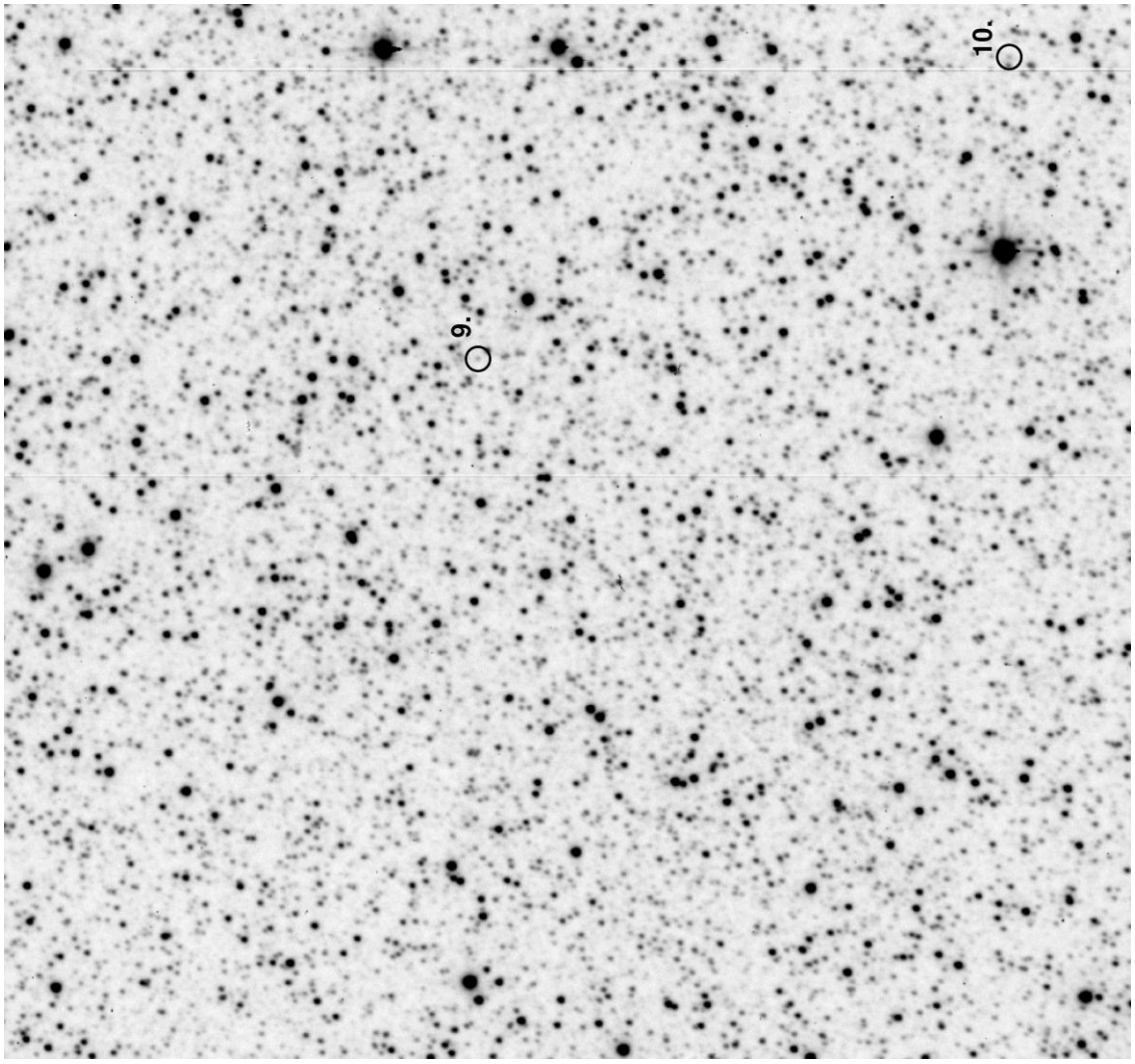

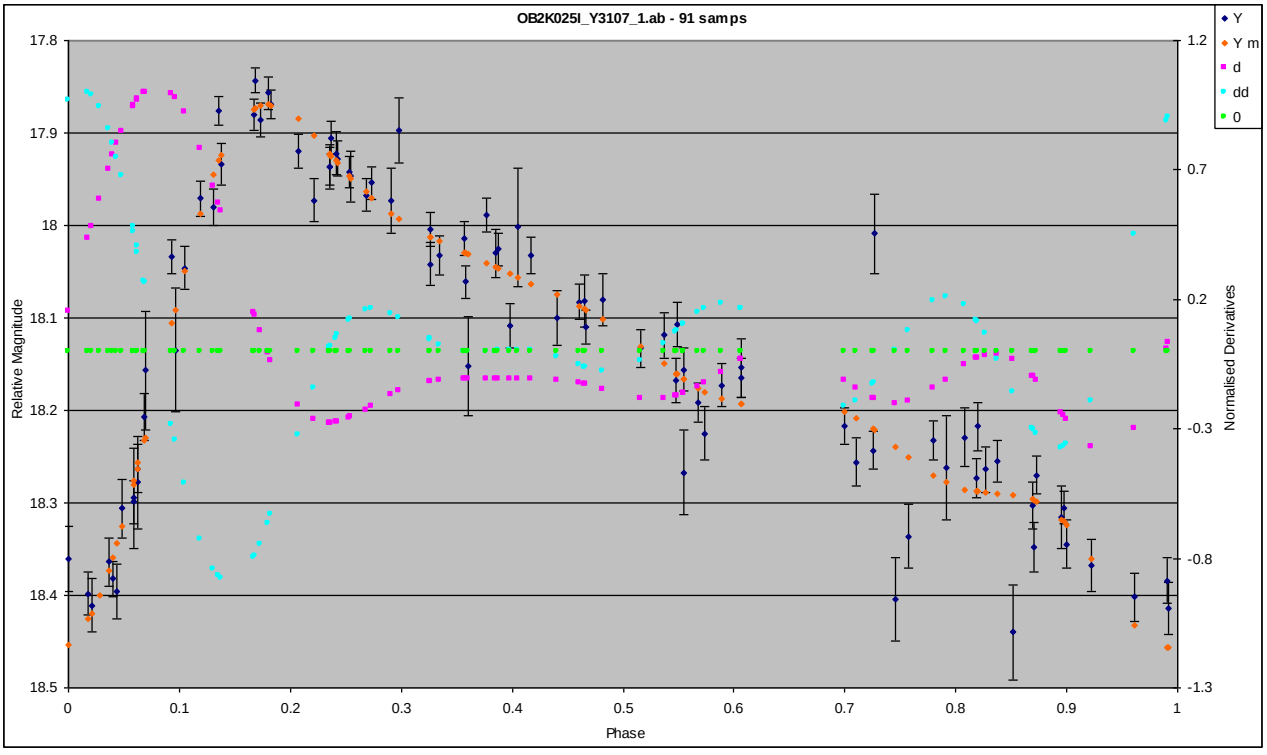

YOB2K031I for event OB2K031I ~ 5.13’ by 5.13’

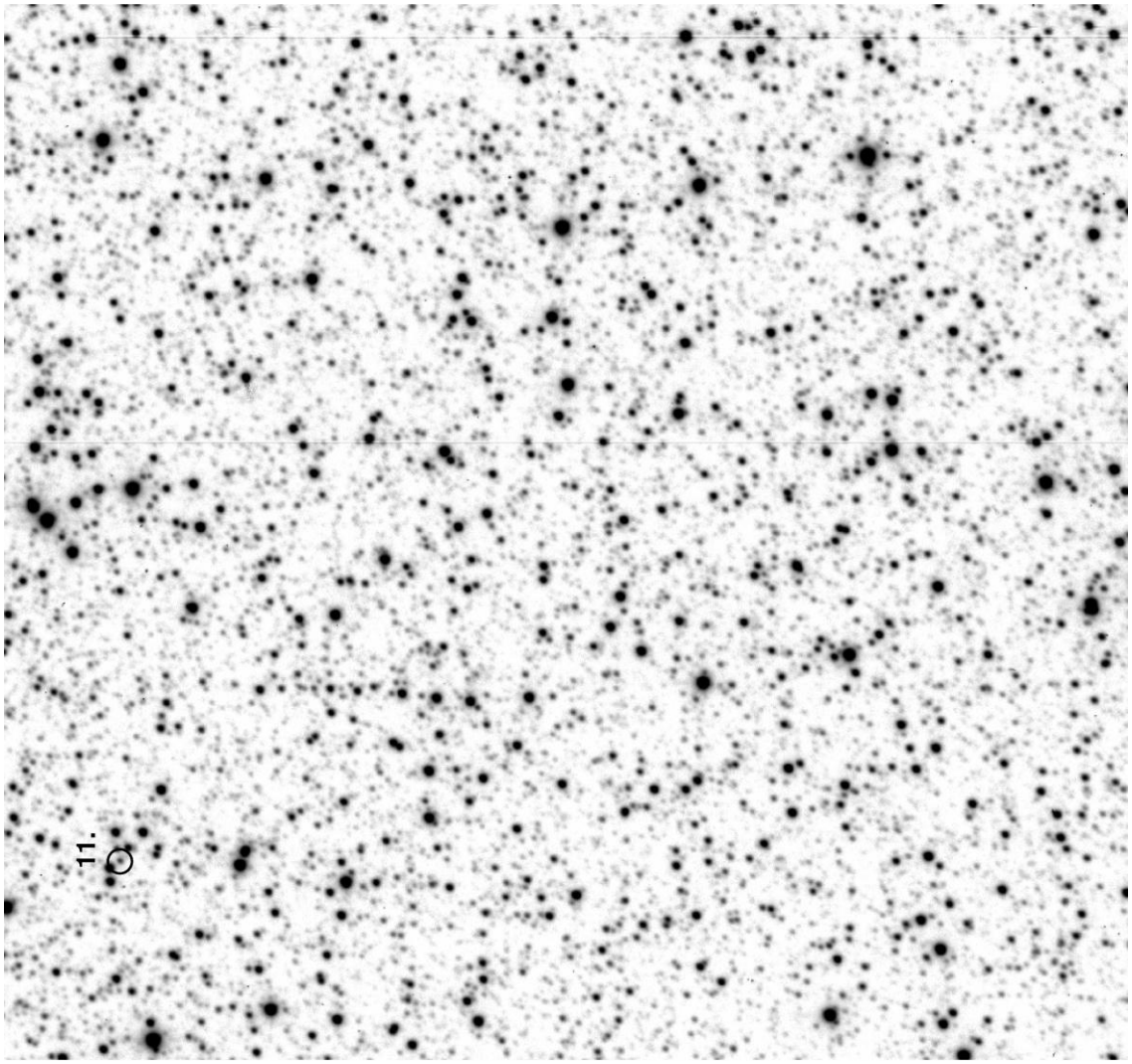

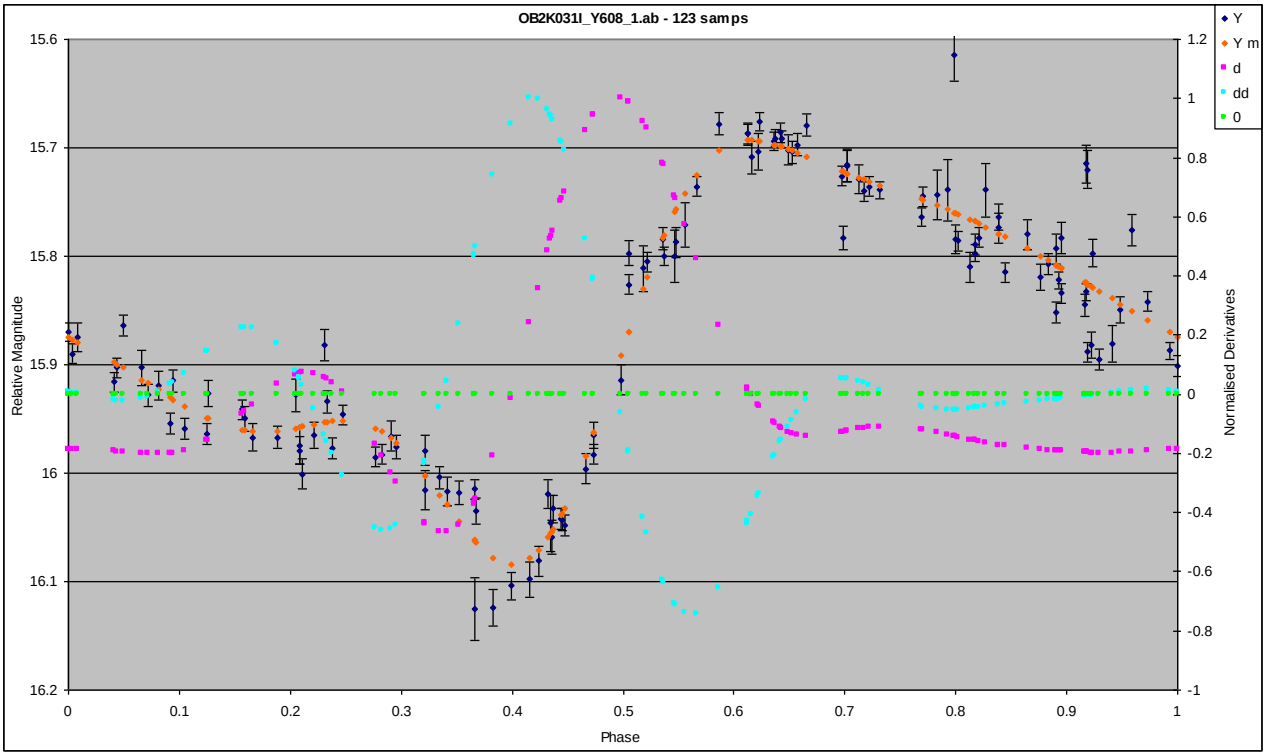

YOB2K046I for event OB2K046I ~ 5.13’ by 5.13’

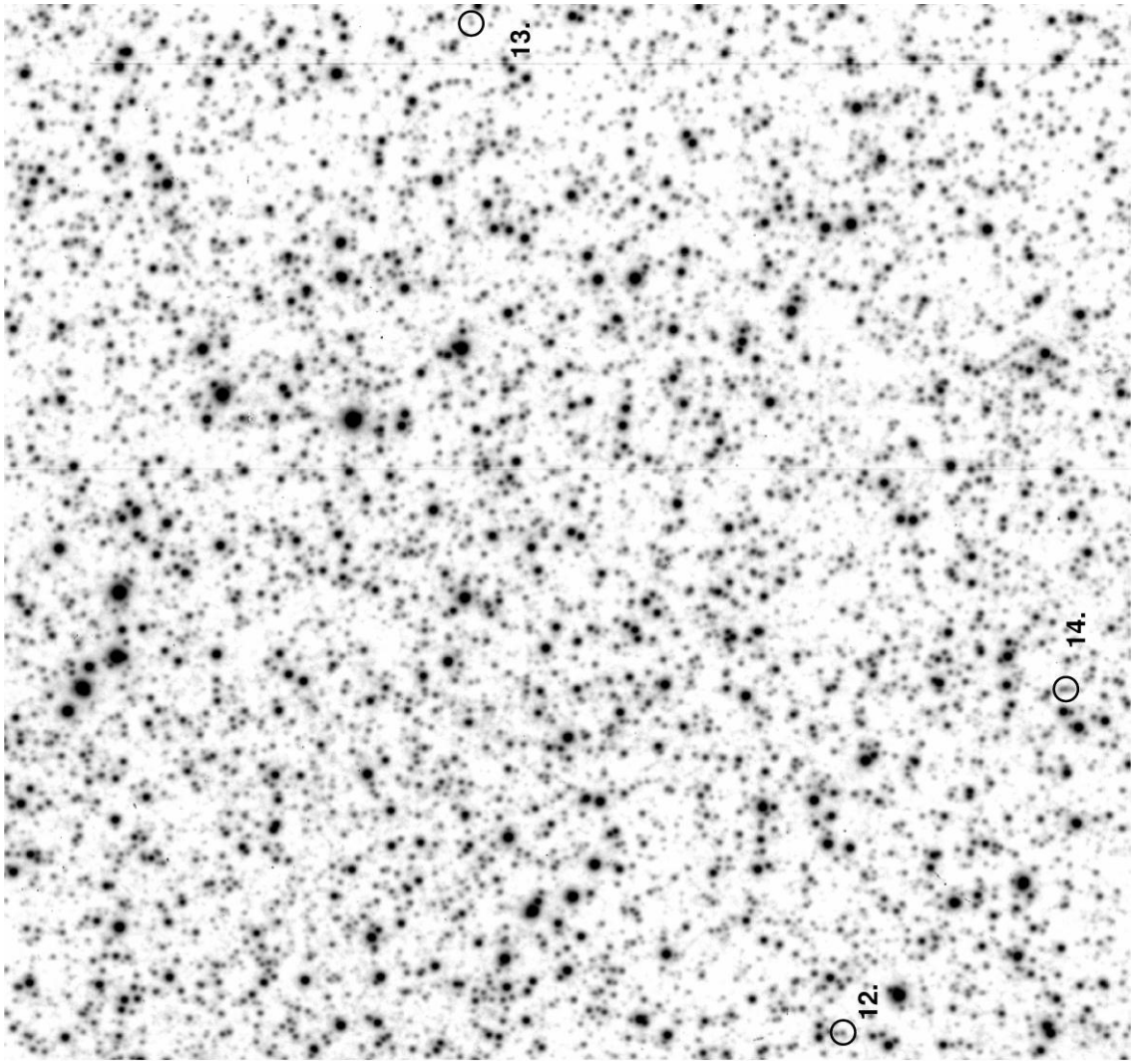

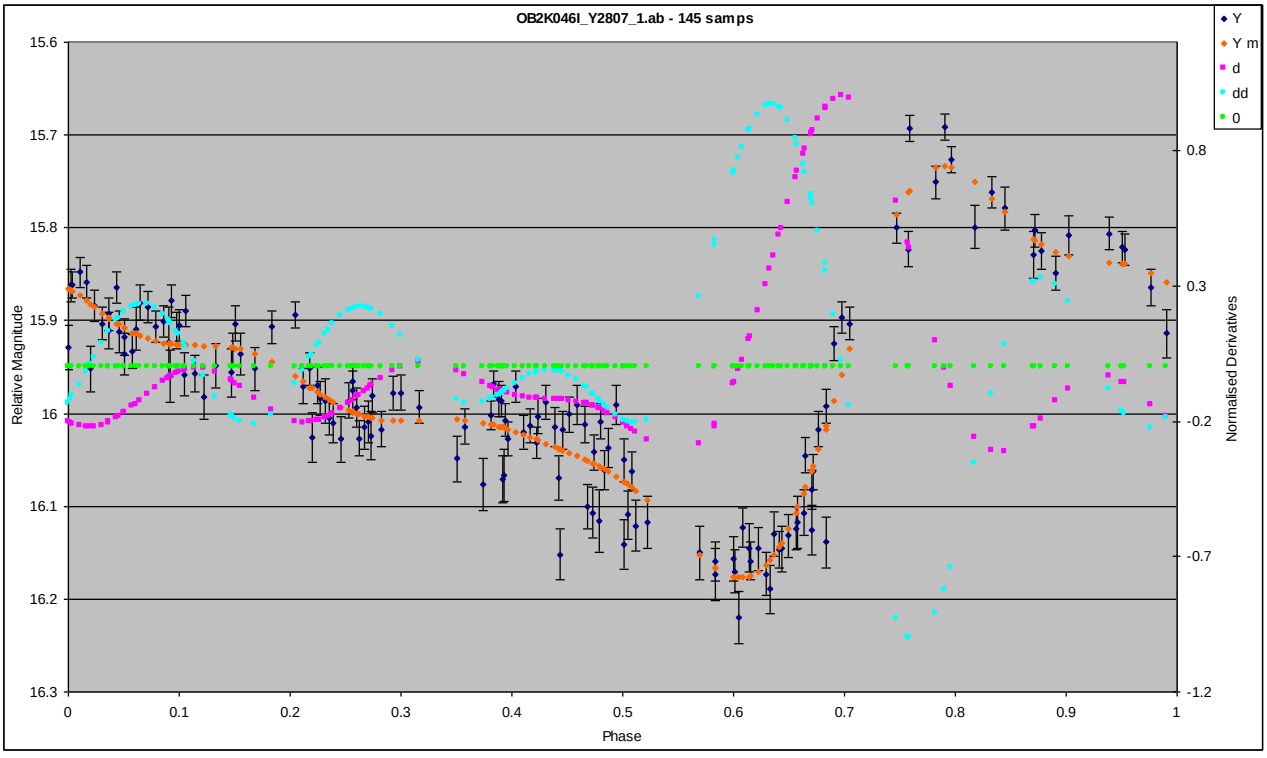

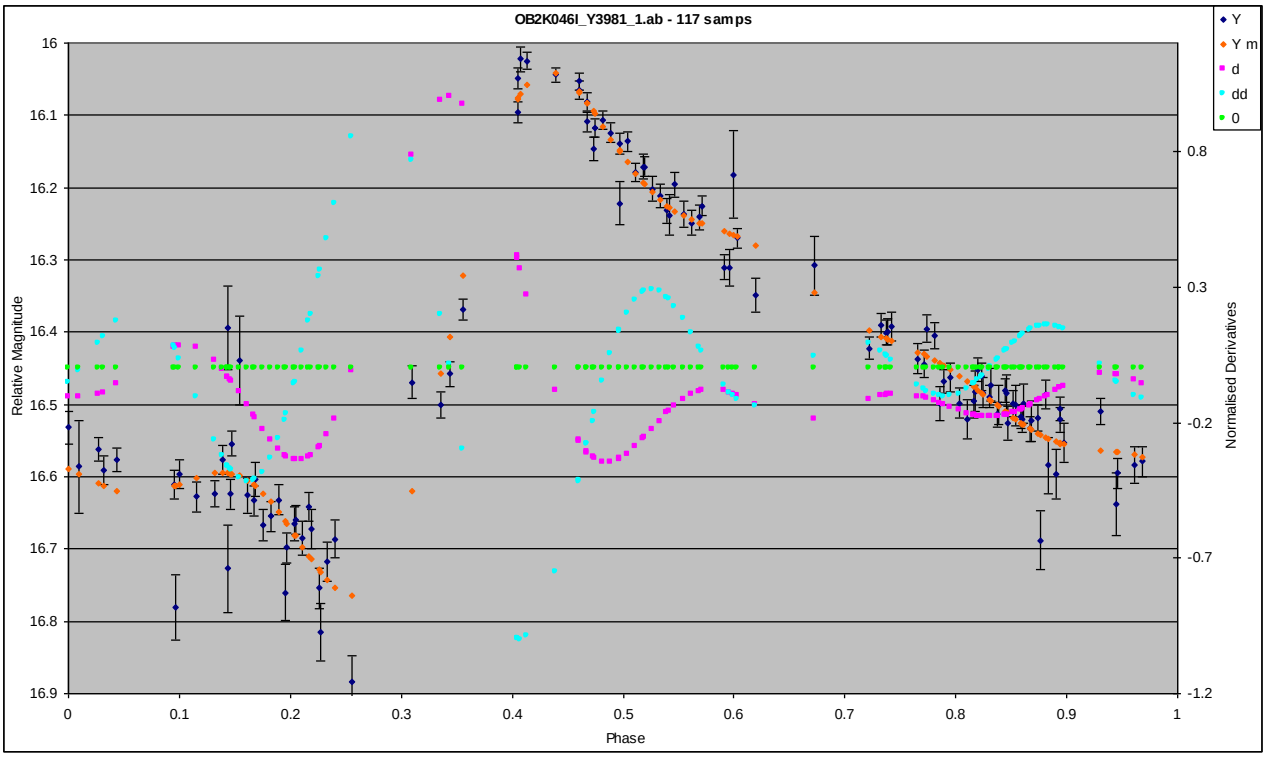

YOB2K048I for event OB2K048I ~ 5.13’ by 5.13’

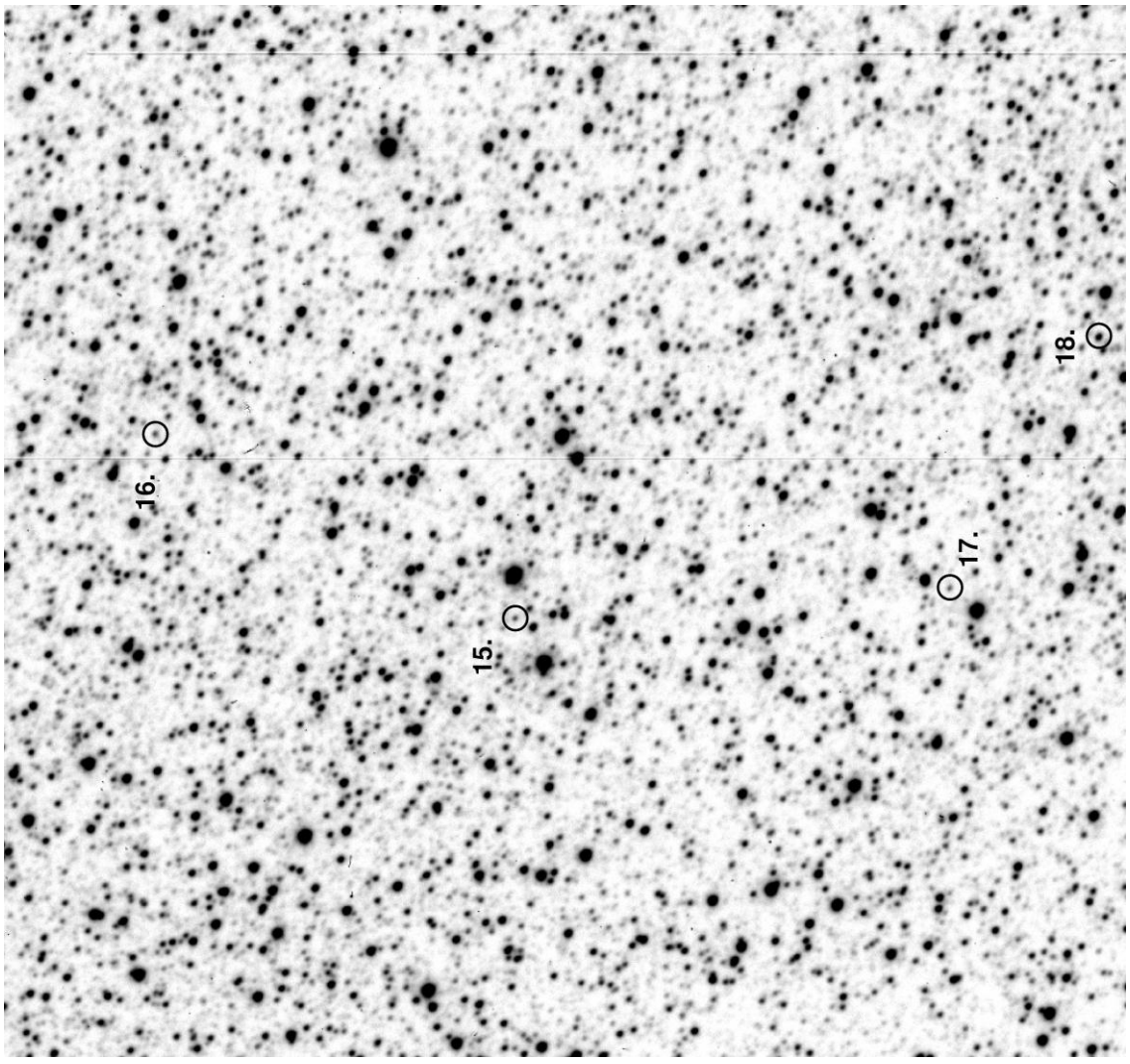

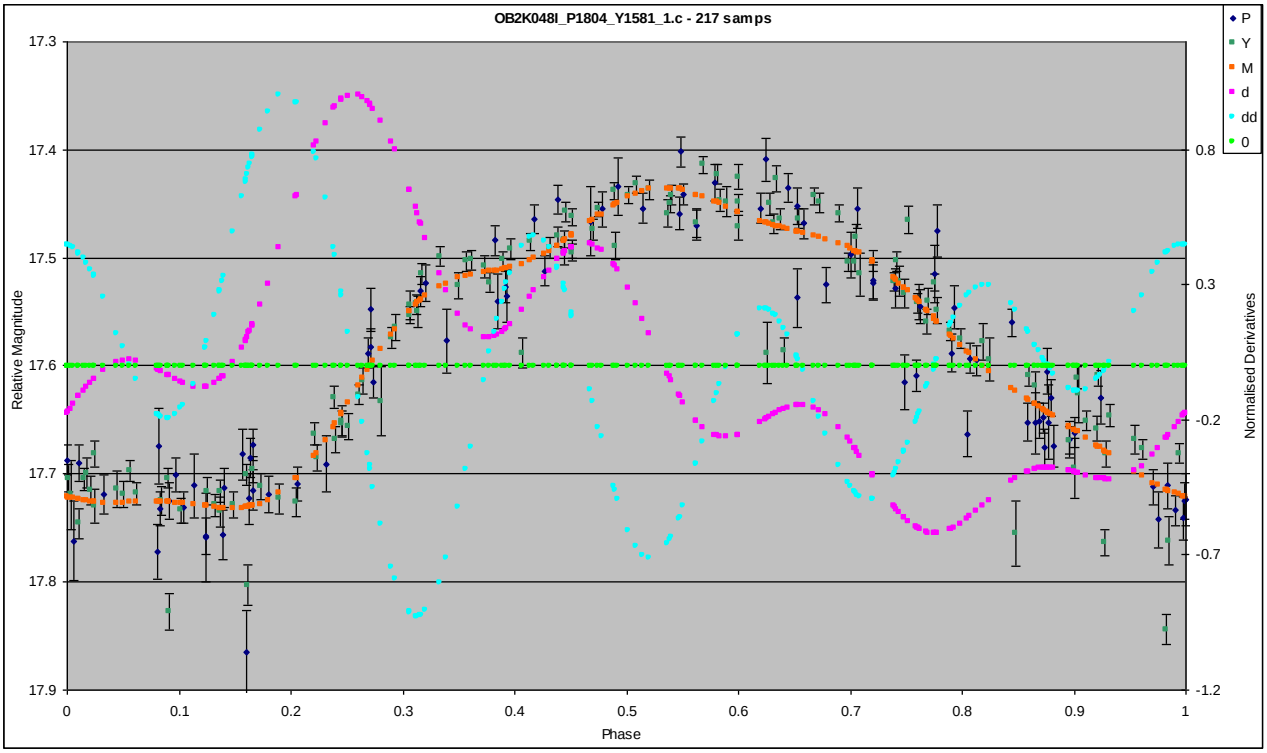
OB2K048I_P1804_Y1581_1.c - 217 samps
P
Y
M
d
dd
0
Relative Magnitude
Normalised Derivatives
Phase
17.3
17.4
17.5
17.6
17.7
17.8
17.9
0.8
0.3
-0.2
-0.7
-1.2
0
0.1
0.2
0.3
0.4
0.5
0.6
0.7
0.8
0.9
1

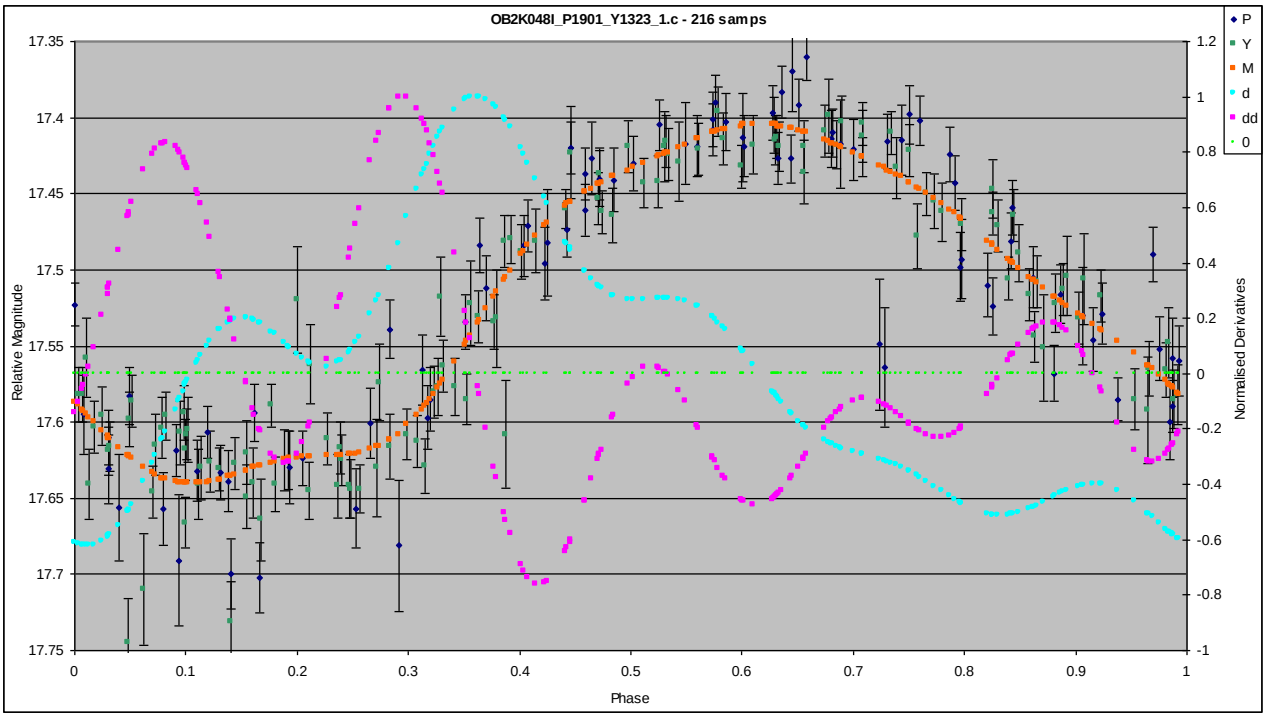
OB2K048I_P1901_Y1323_1.c - 216 samps
P
Y
M
d
dd
0
Relative Magnitude
Normalised Derivatives
Phase
17.35
17.4
17.45
17.5
17.55
17.6
17.65
17.7
17.75
1.2
1
0.8
0.6
0.4
0.2
0
-0.2
-0.4
-0.6
-0.8
-1
0
0.1
0.2
0.3
0.4
0.5
0.6
0.7
0.8
0.9
1

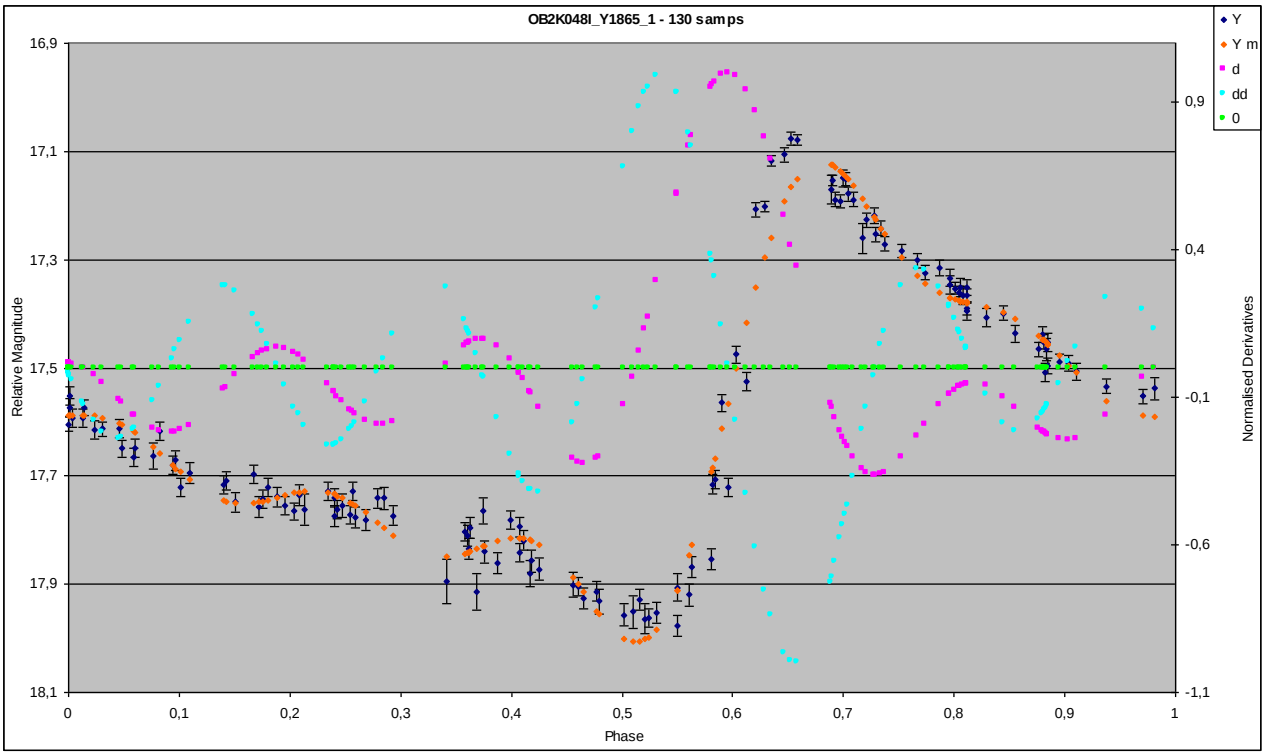

YOB2K012I for event OB2K012I ~ 5.13’ by 5.13’

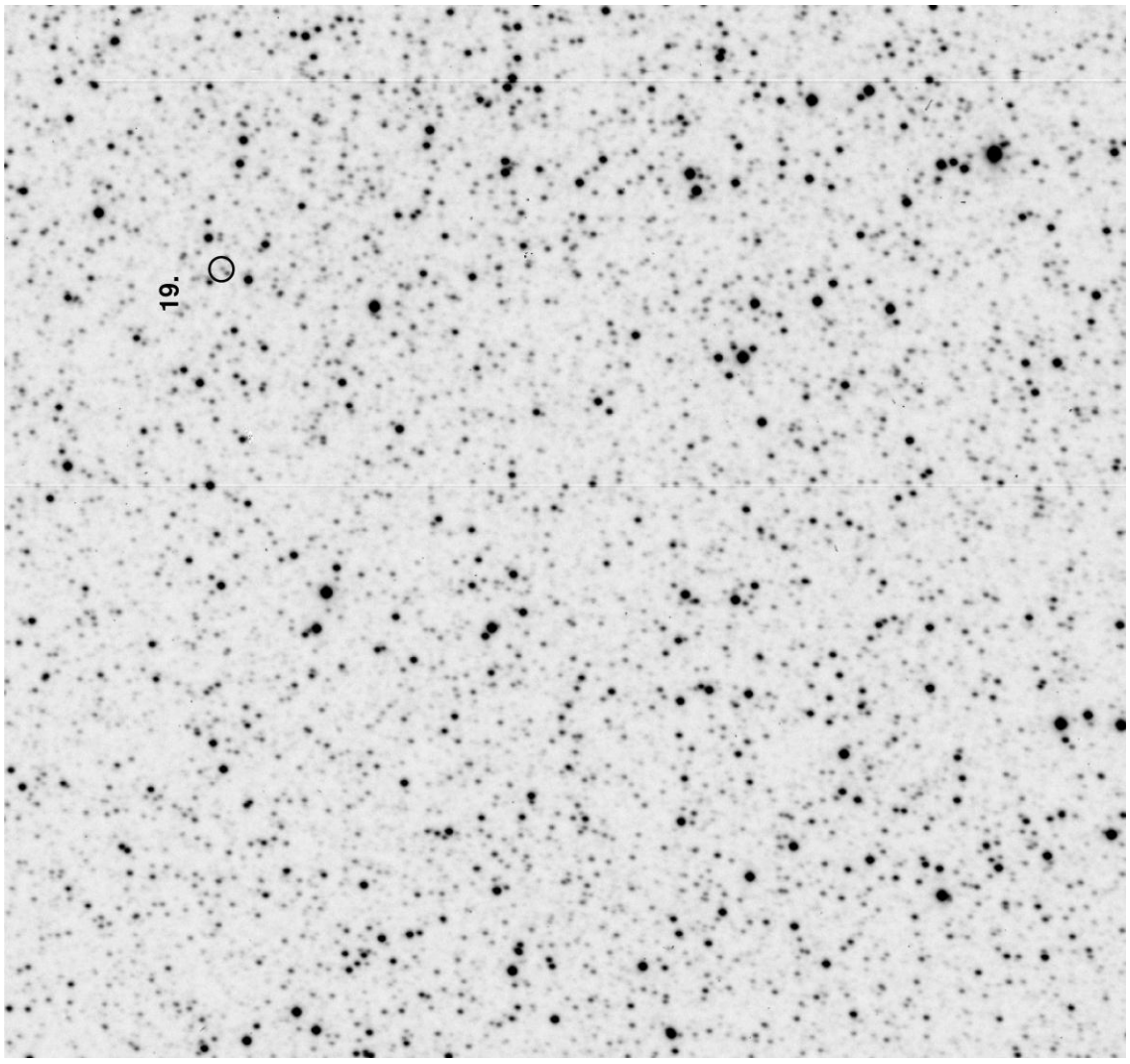

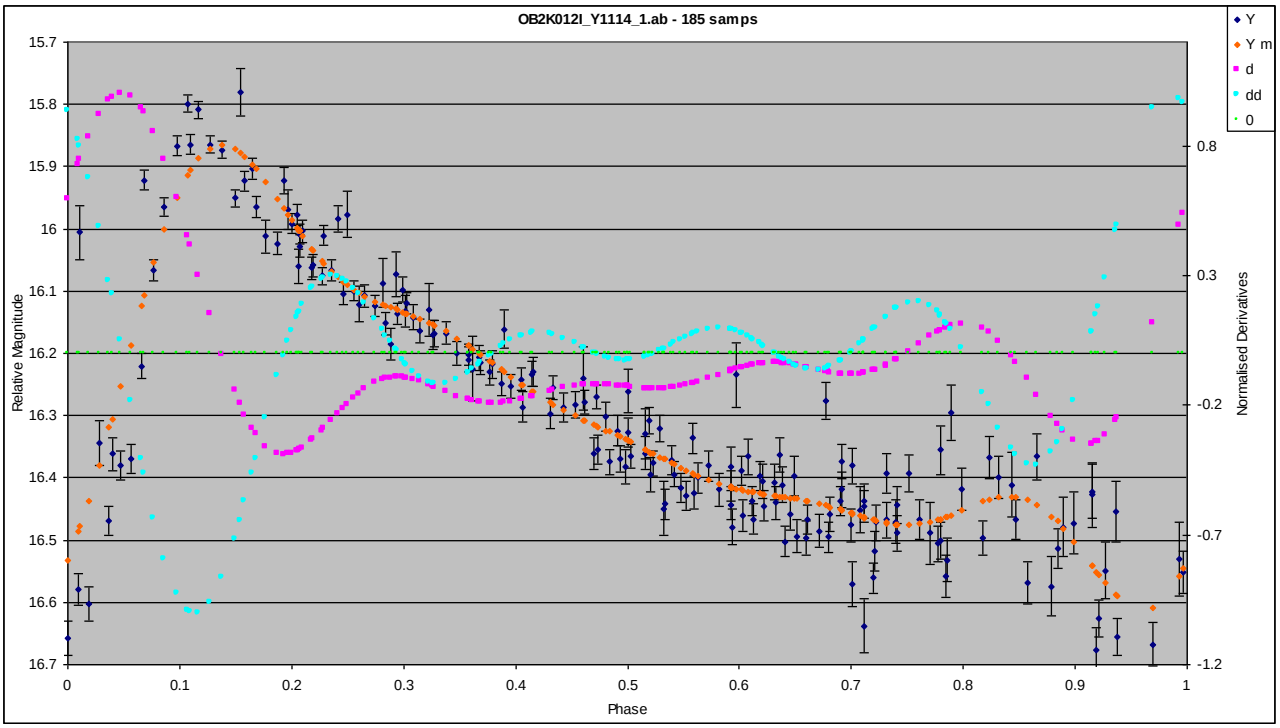

YOB2K026I for event OB2K026I ~ 5.13’ by 5.13’

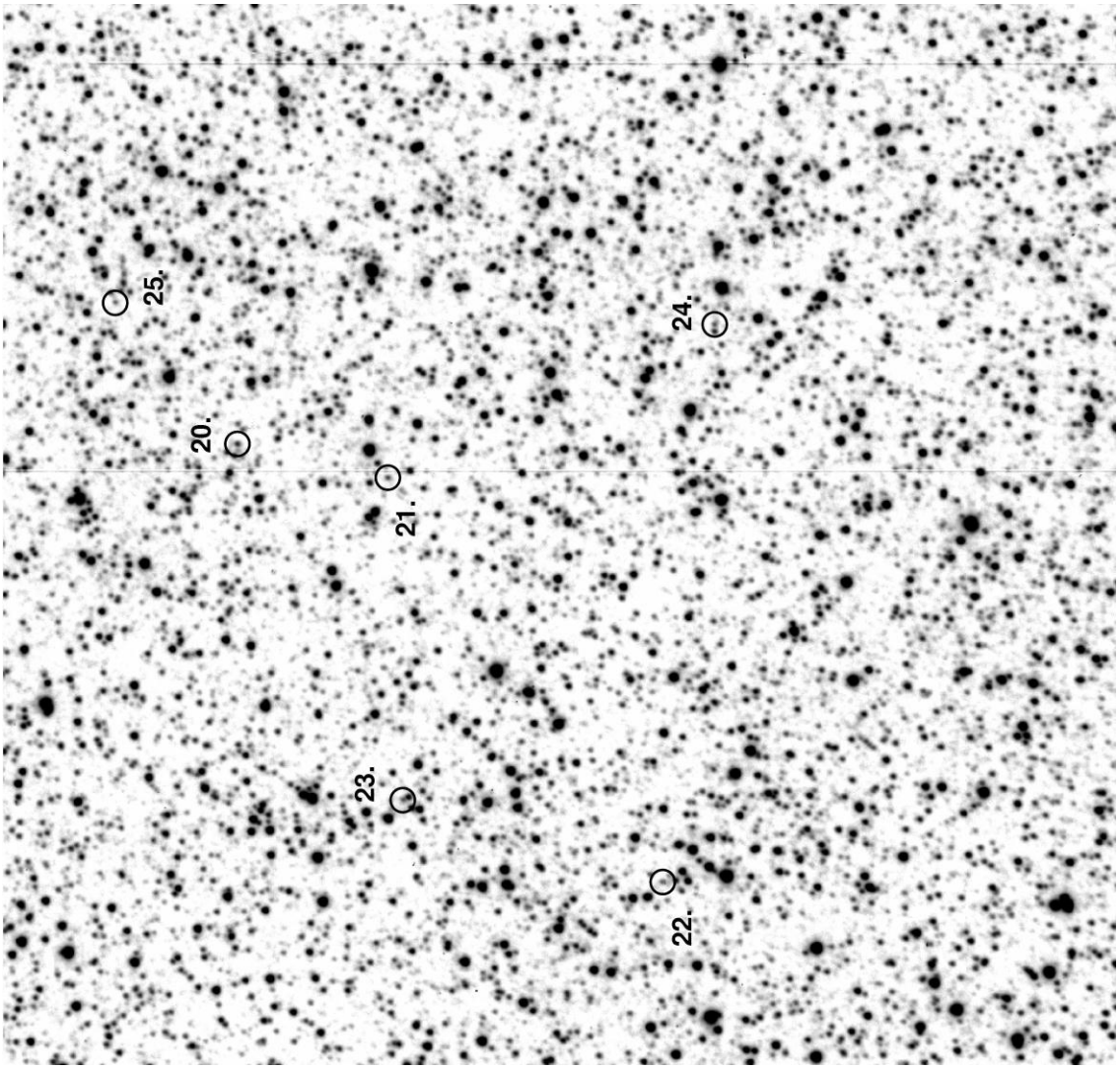

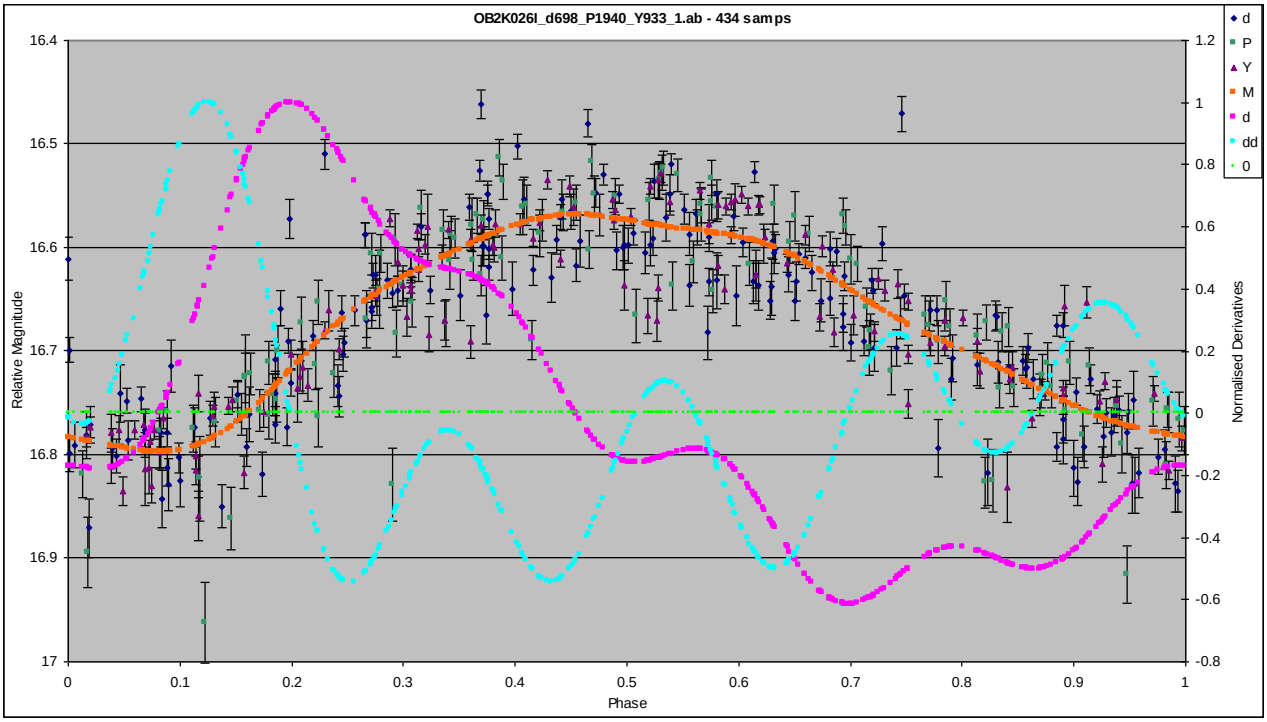
OB2K026I_d698_P1940_Y933_1.ab - 434 samps
Relative Magnitude
Normalised Derivatives
Phase
d
P
Y
M
d
dd
0

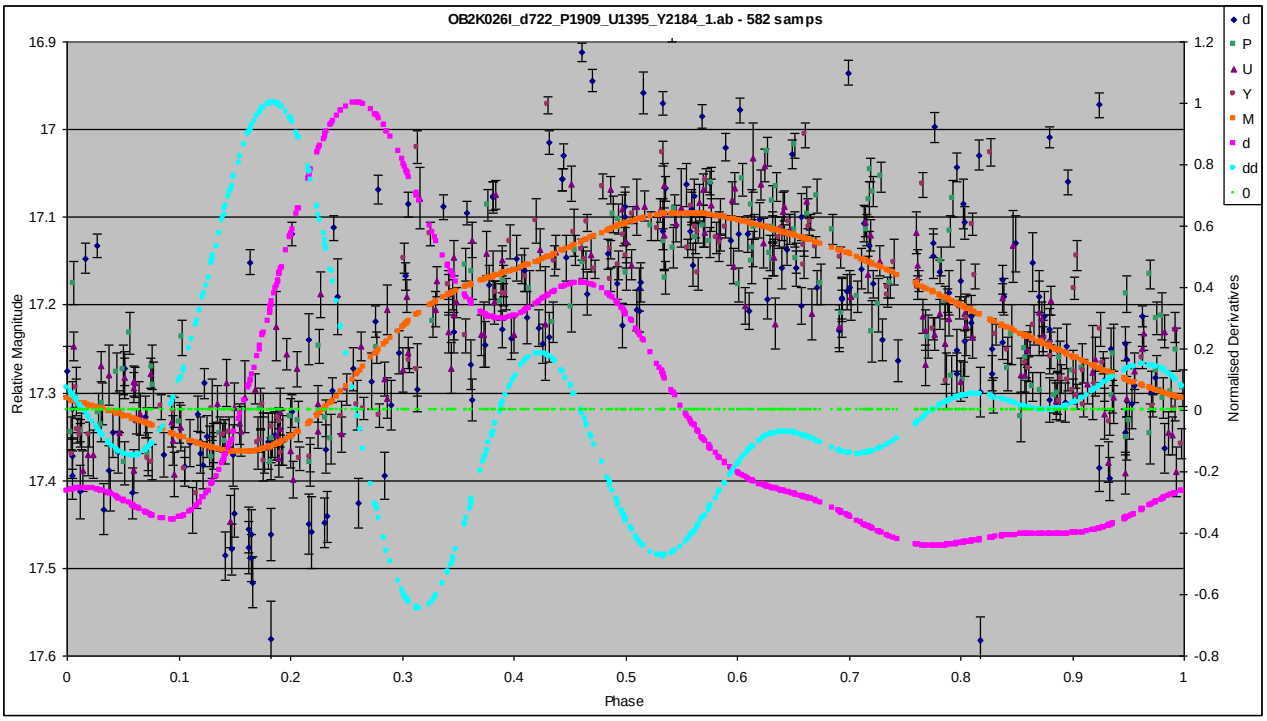
OB2K026I_d722_P1909_U1395_Y2184_1.ab - 582 samps
Relative Magnitude
Normalised Derivatives
Phase
d
P
U
Y
M
d
dd
0

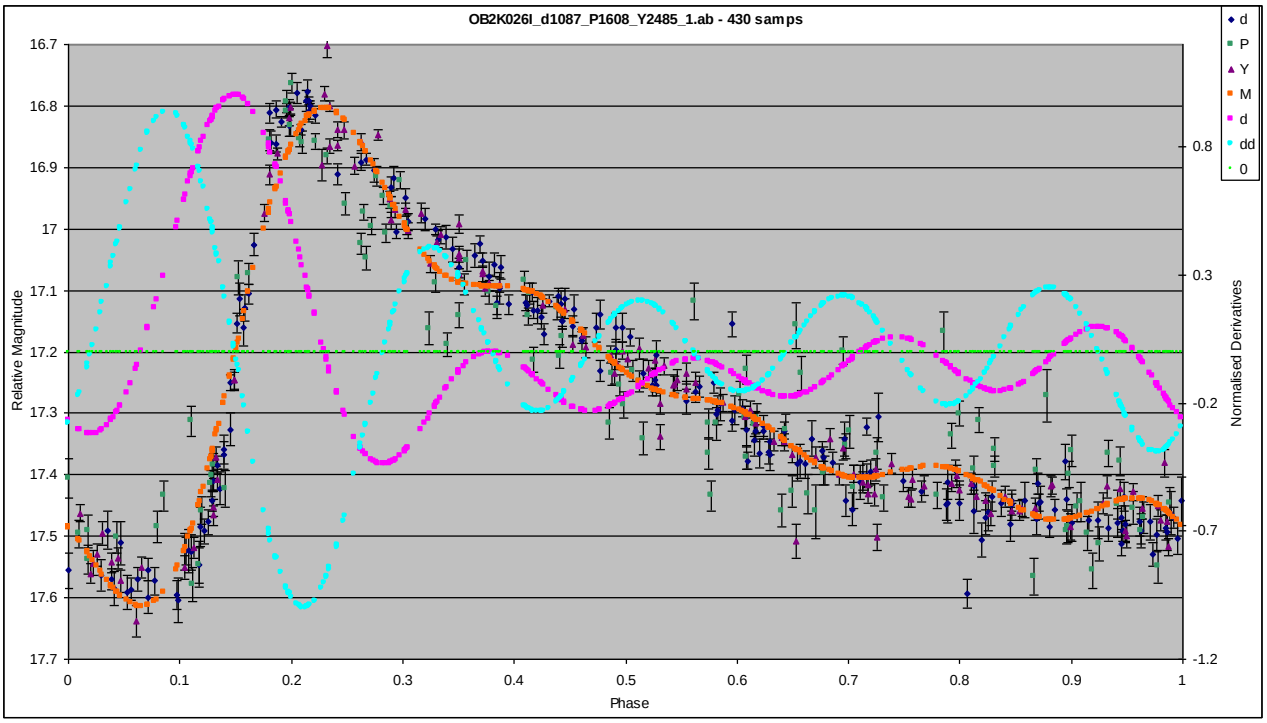
OB2K026I_d1087_P1608_Y2485_1.ab - 430 samps
d
P
Y
M
d
dd
0
Relative Magnitude
Normalised Derivatives
Phase

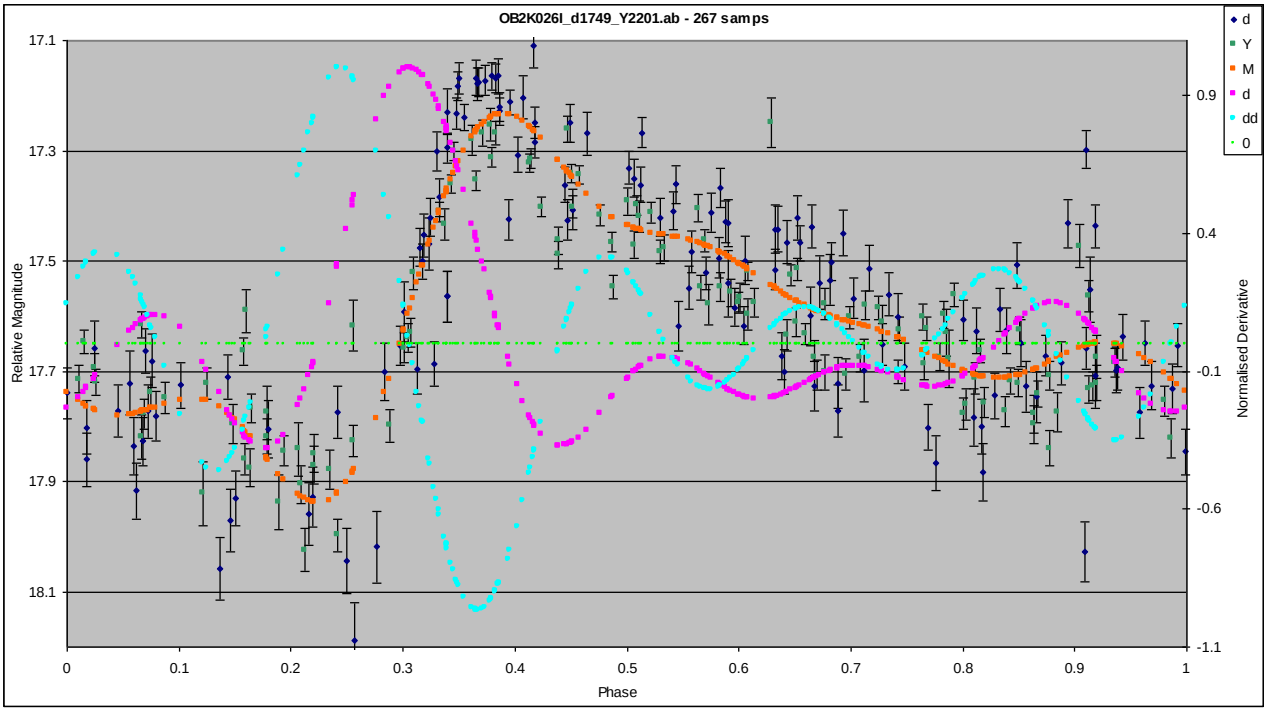
OB2K026I_d1749_Y2201.ab - 267 samps
d
Y
M
d
dd
0
Relative Magnitude
Normalised Derivative
Phase

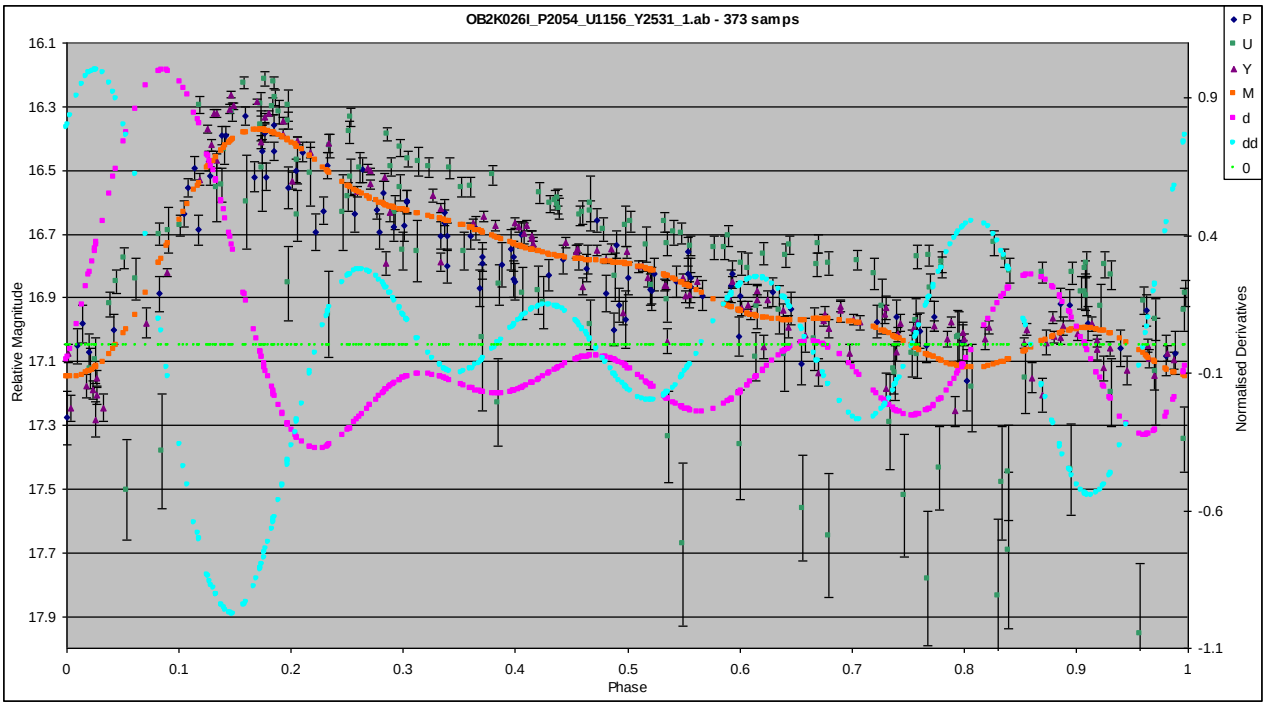

YOB2K029I for event OB2K029I ~ 5.13’ by 5.13’

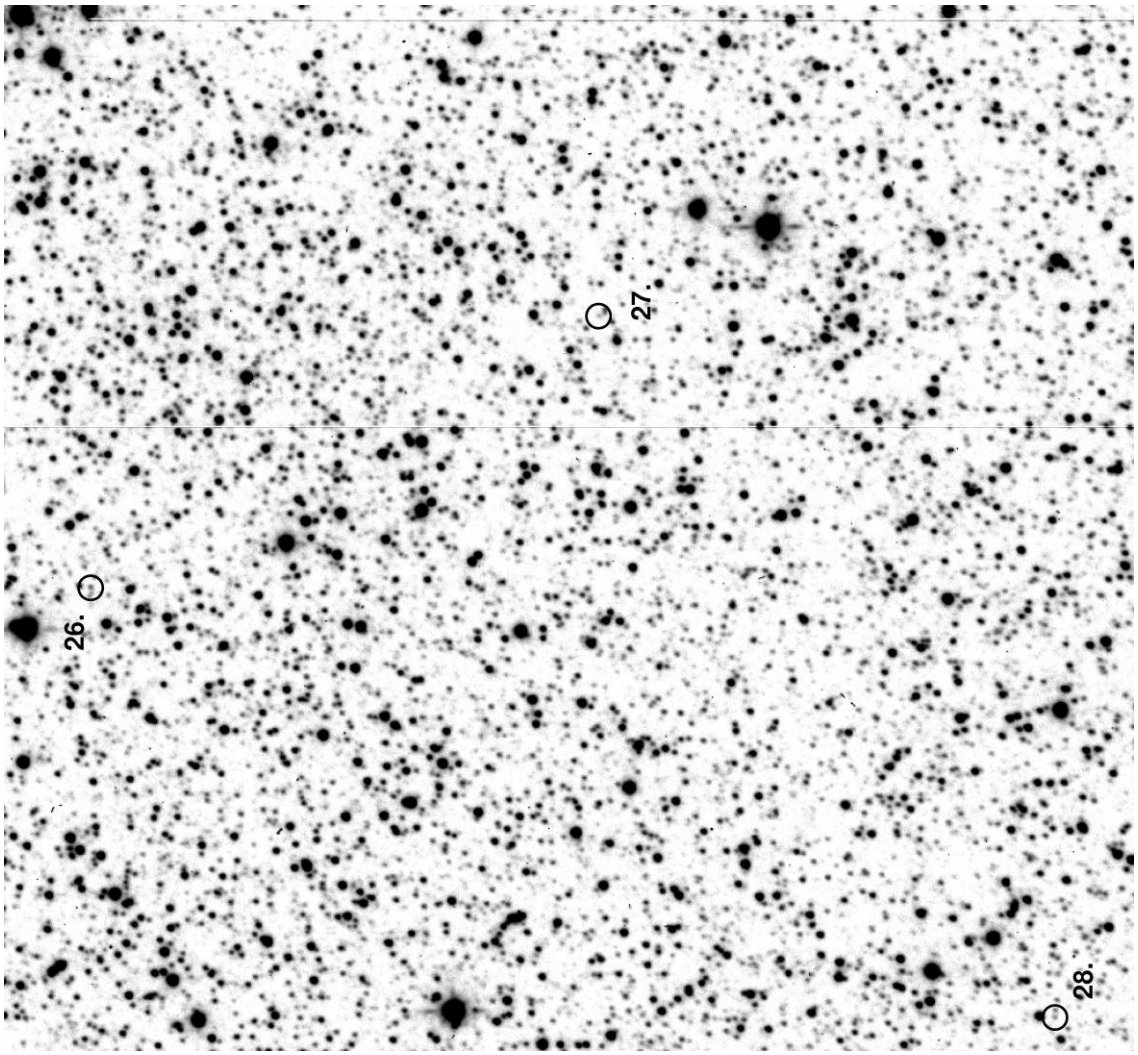

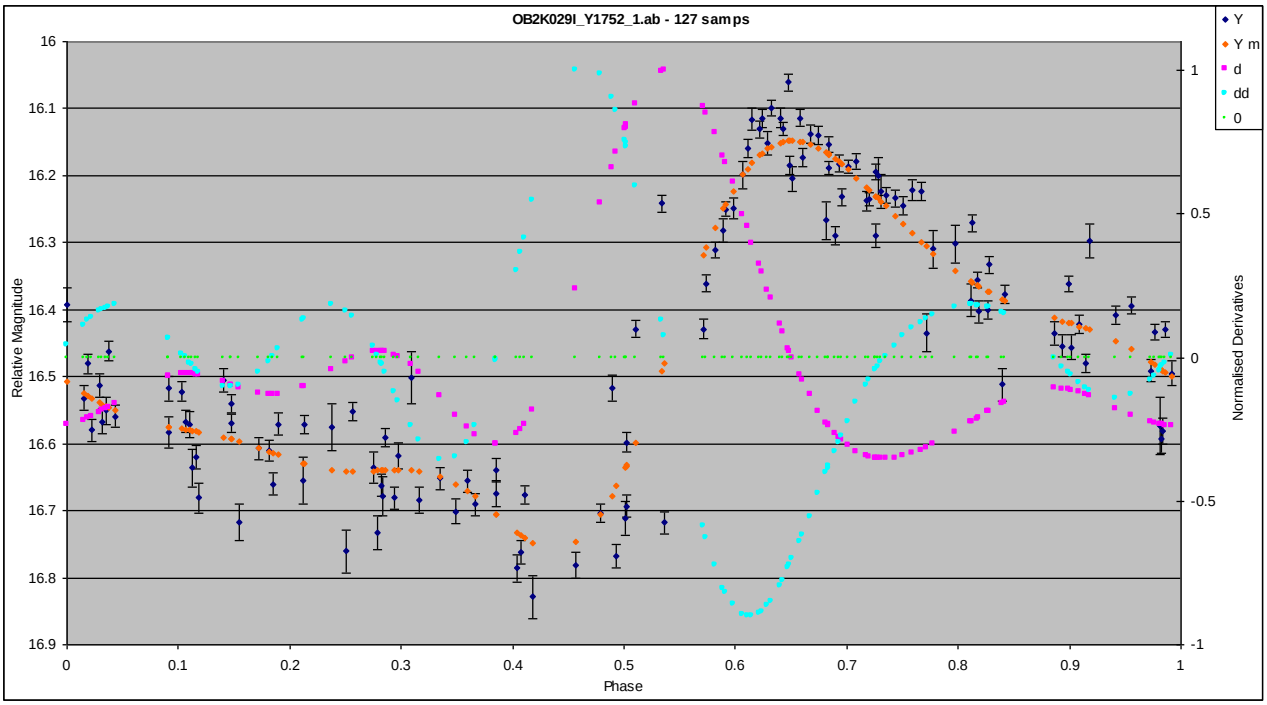
OB2K029I_Y1752_1.ab - 127 samps
Y
Y m
d
dd
0
Relative Magnitude
Normalised Derivatives
Phase
16
16.1
16.2
16.3
16.4
16.5
16.6
16.7
16.8
16.9
1
0.5
0
-0.5
-1
0
0.1
0.2
0.3
0.4
0.5
0.6
0.7
0.8
0.9
1

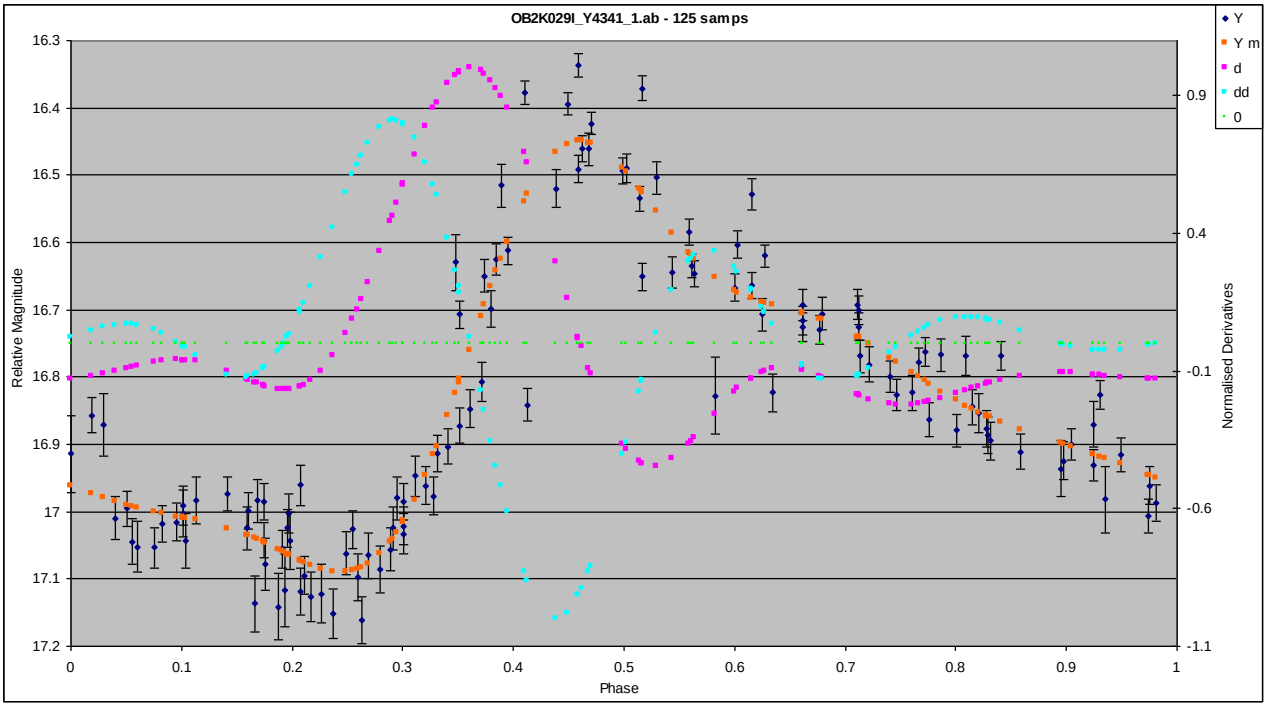
OB2K029I_Y4341_1.ab - 125 samps
Y
Y m
d
dd
0
Relative Magnitude
Normalised Derivatives
Phase
16.3
16.4
16.5
16.6
16.7
16.8
16.9
17
17.1
17.2
0.9
0.4
-0.1
-0.6
-1.1
0
0.1
0.2
0.3
0.4
0.5
0.6
0.7
0.8
0.9
1

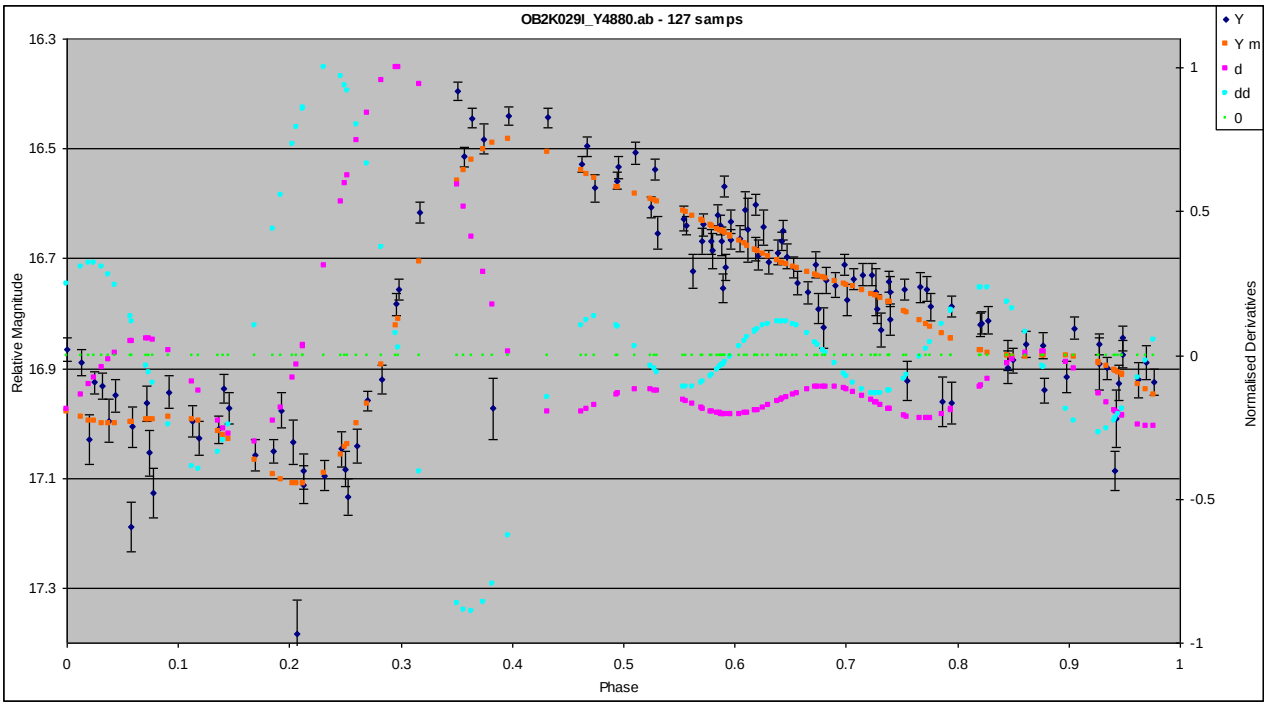

dOB2K034I for event OB2K034I ~ 3.73’ by 3.73’

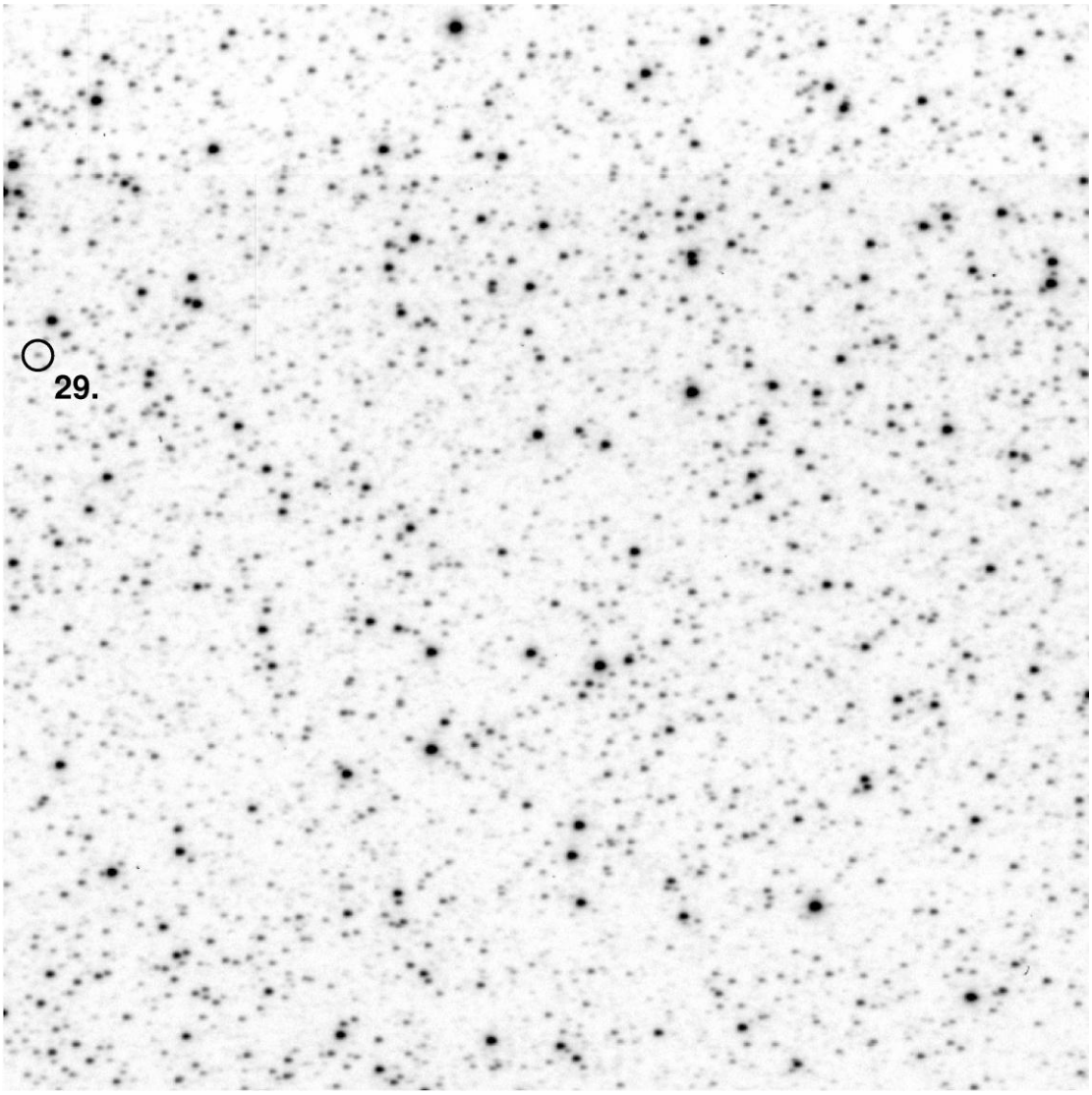

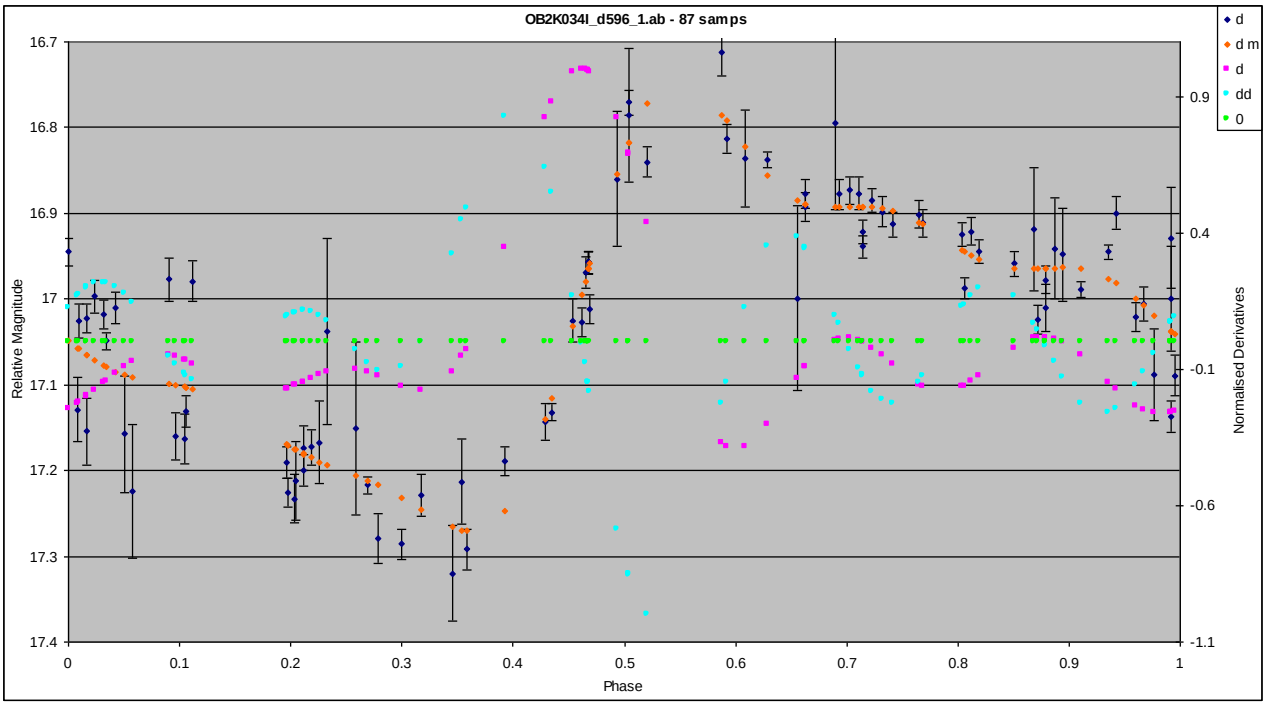

YOB2K038I for event OB2K038I ~ 5.13’ by 5.13’

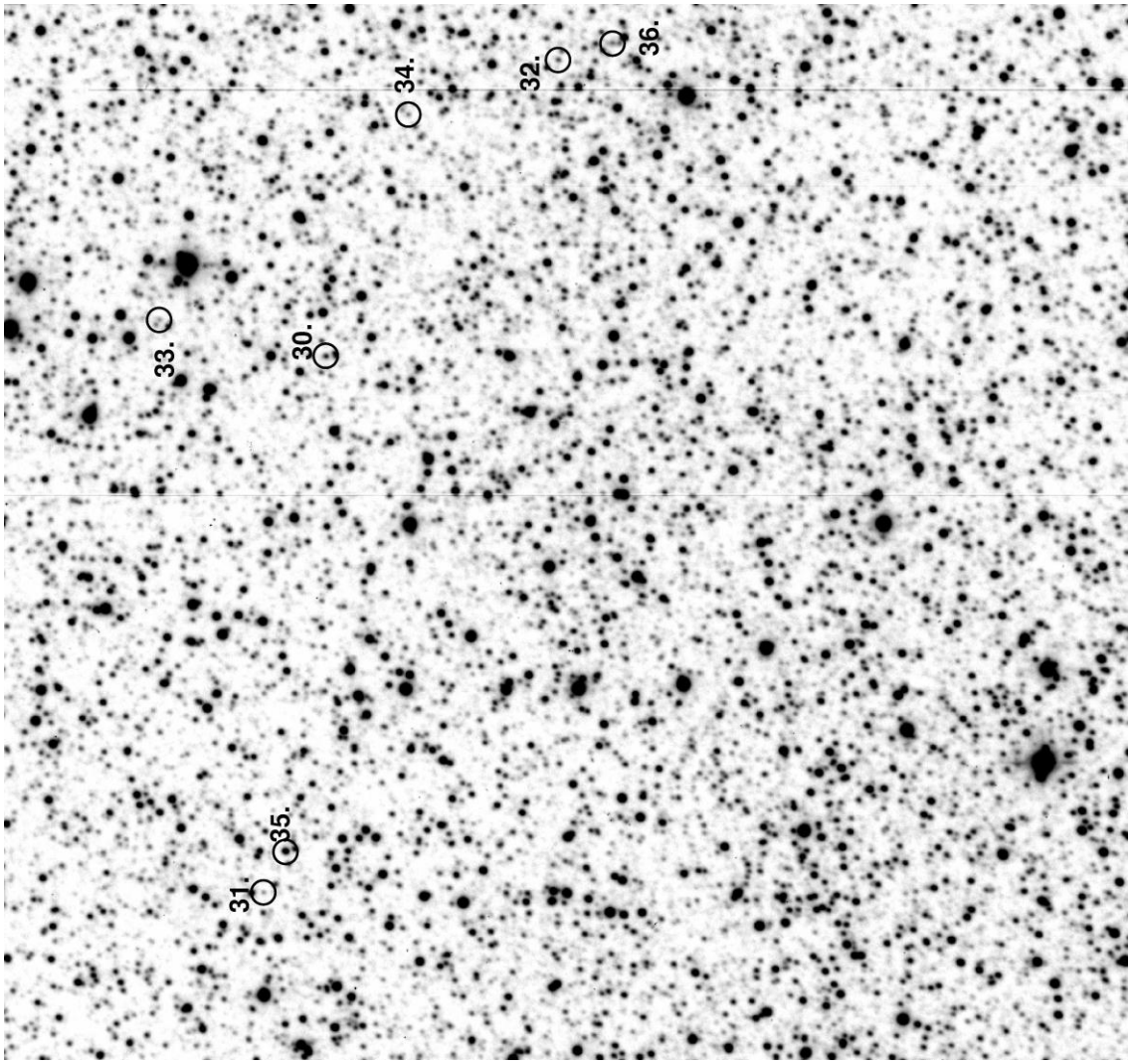

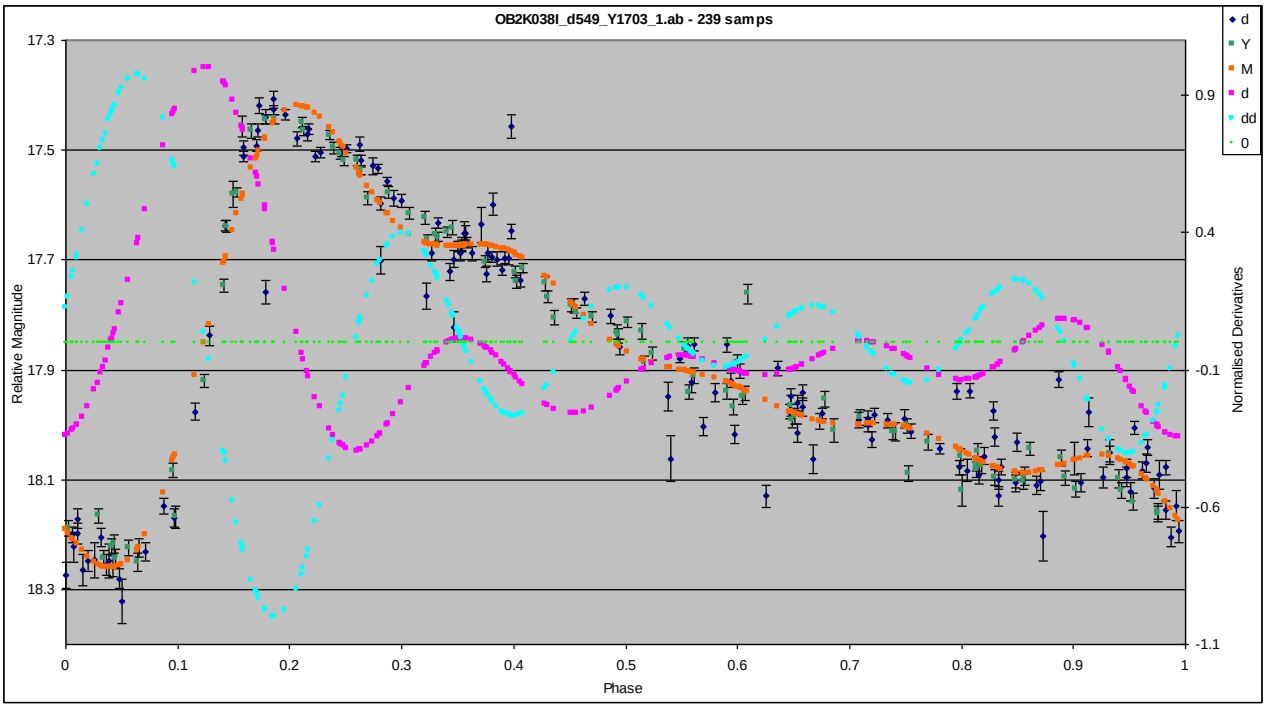
OB2K038I_d549_Y1703_1.ab - 239 samps
Relative Magnitude
Normalised Derivatives
Phase
d
Y
M
d
dd
0

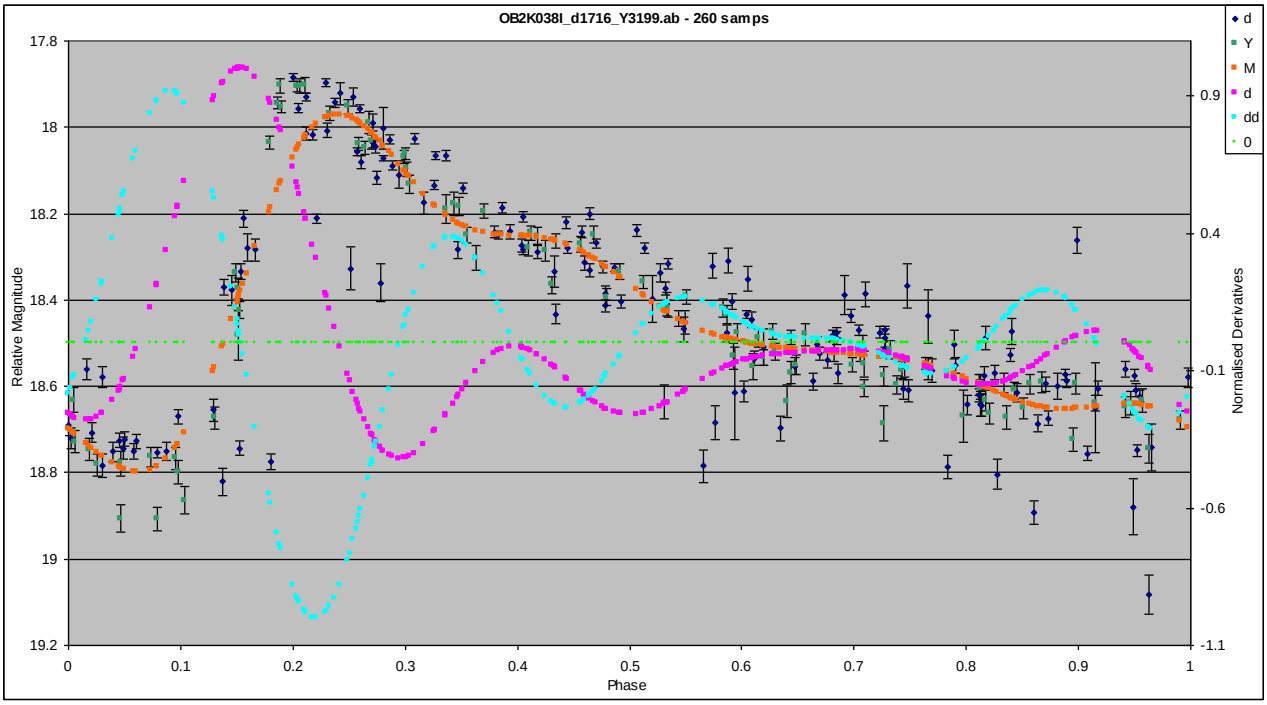
OB2K038I_d1716_Y3199.ab - 260 samps
Relative Magnitude
Normalised Derivatives
Phase
d
Y
M
d
dd
0

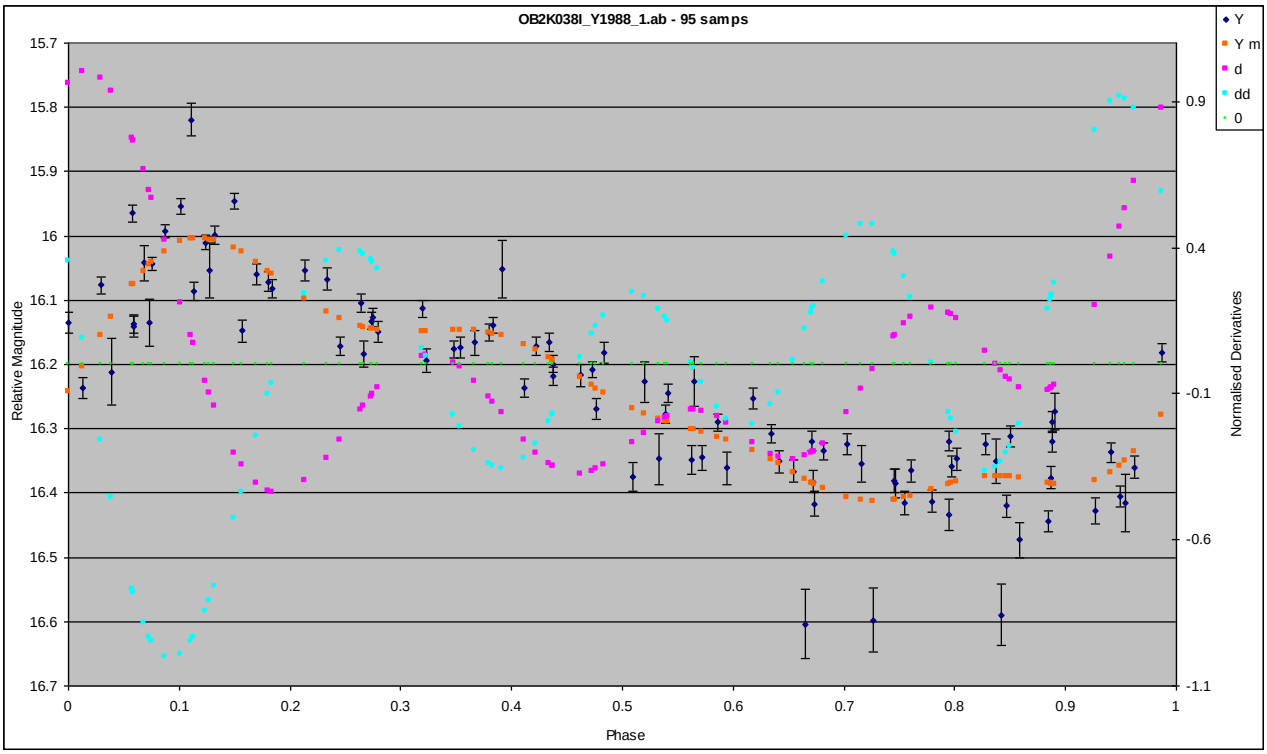
OB2K038I_Y1988_1.ab - 95 samps
Y
Y m
d
dd
0
Relative Magnitude
Normalised Derivatives
Phase
15.7
15.8
15.9
16
16.1
16.2
16.3
16.4
16.5
16.6
16.7
0.9
0.4
-0.1
-0.6
-1.1
0
0.1
0.2
0.3
0.4
0.5
0.6
0.7
0.8
0.9
1

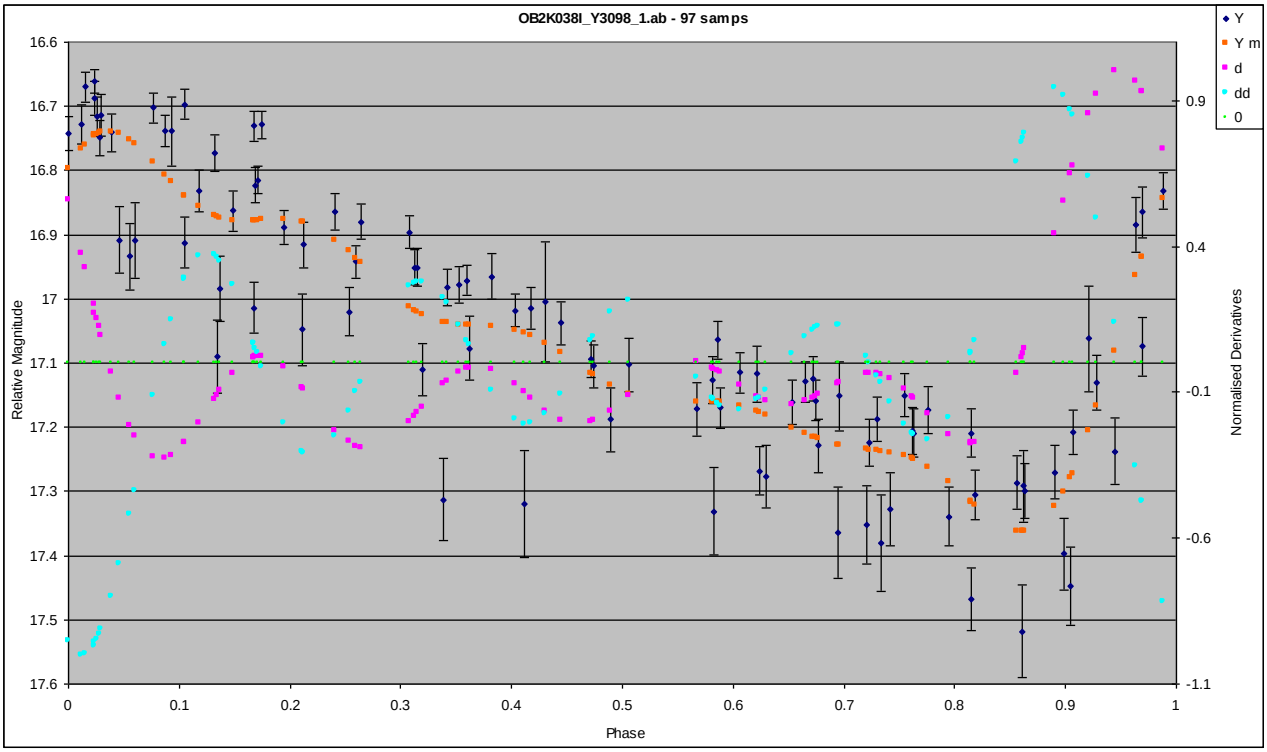
OB2K038I_Y3098_1.ab - 97 samps
Y
Y m
d
dd
0
Relative Magnitude
Normalised Derivatives
Phase
16.6
16.7
16.8
16.9
17
17.1
17.2
17.3
17.4
17.5
17.6
0.9
0.4
-0.1
-0.6
-1.1
0
0.1
0.2
0.3
0.4
0.5
0.6
0.7
0.8
0.9
1

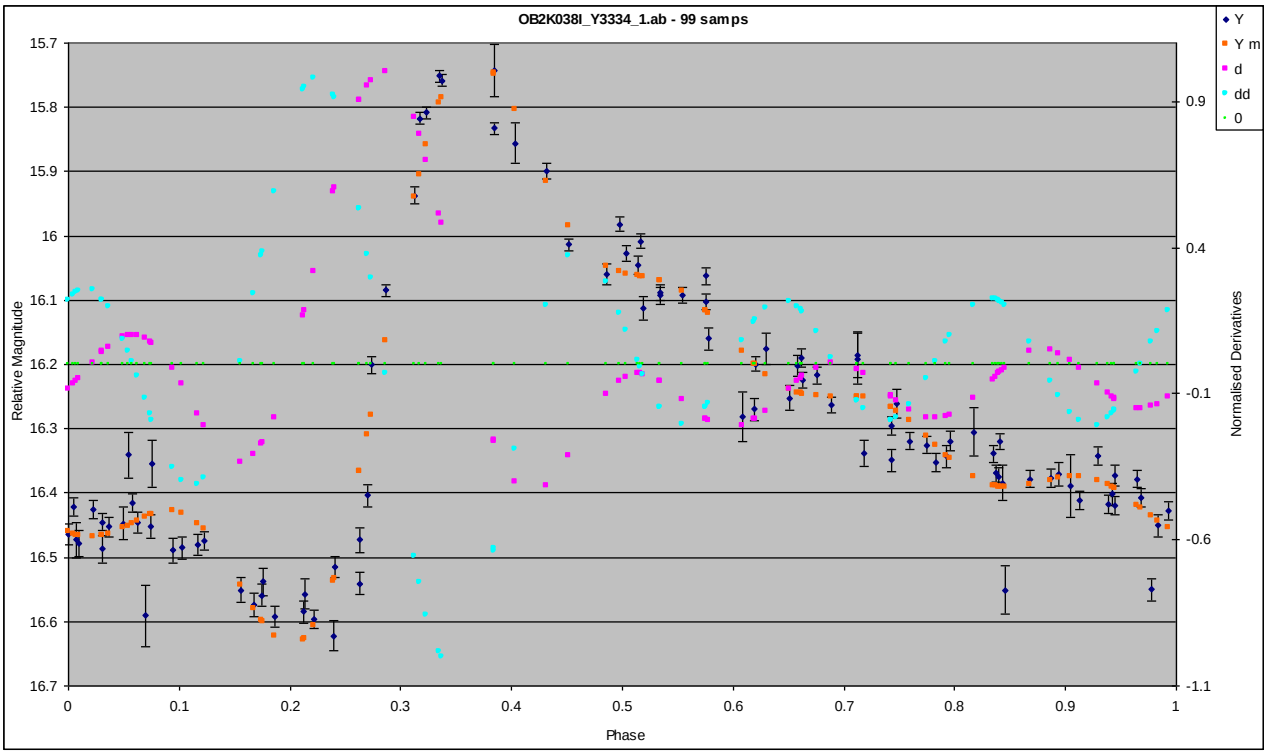

LMB9503I for event MB95013I ~ 3.77’ by 3.77’

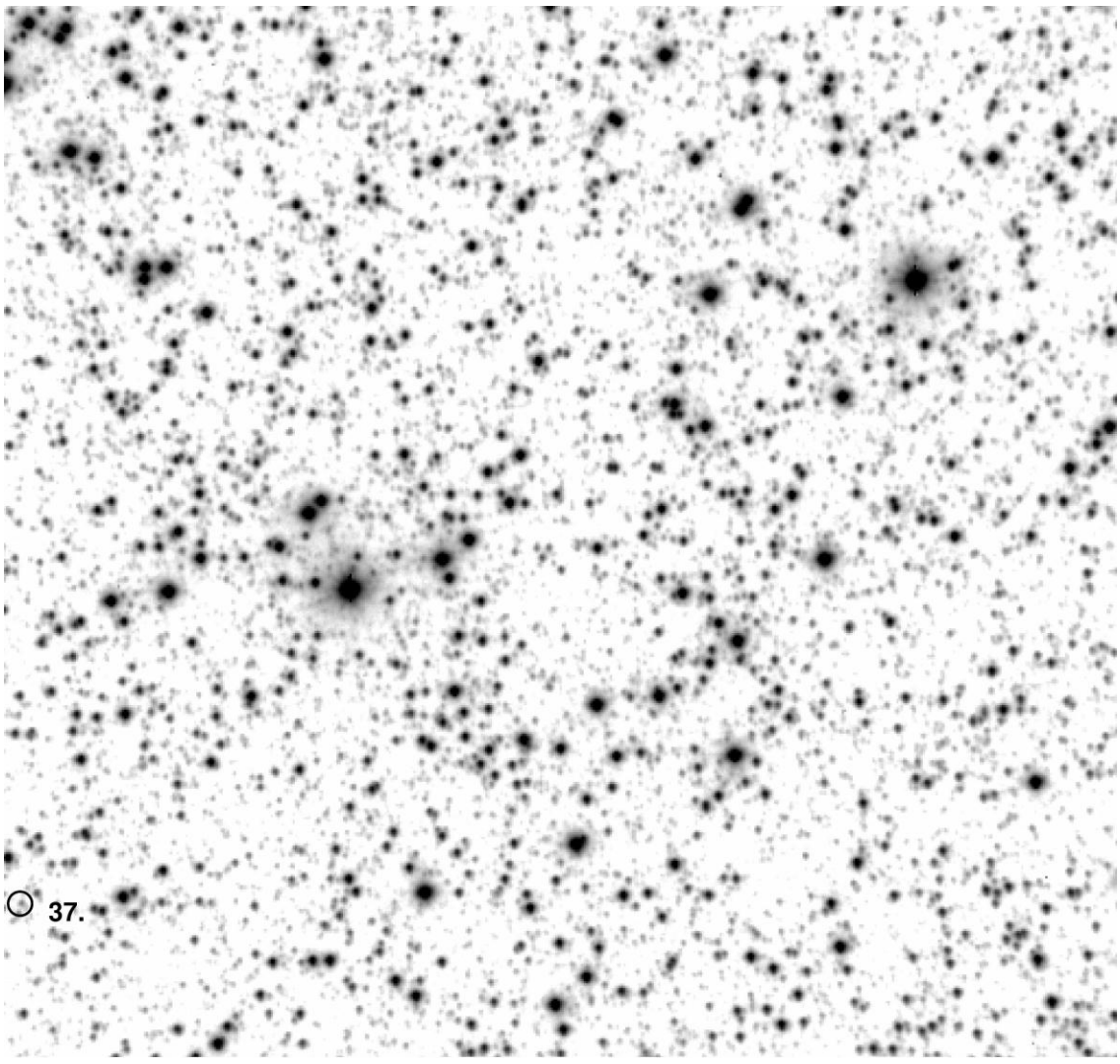

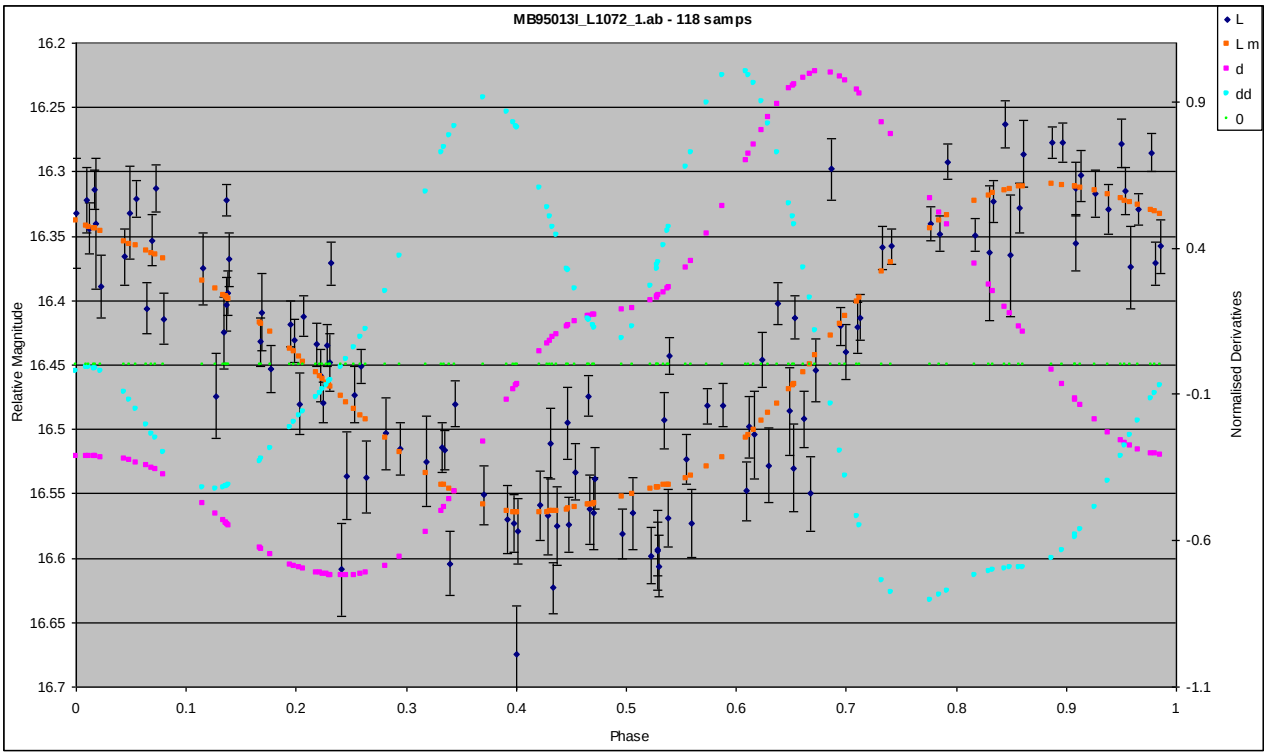

LMB95017I for event MB95017I ~ 3.77' by 3.77'

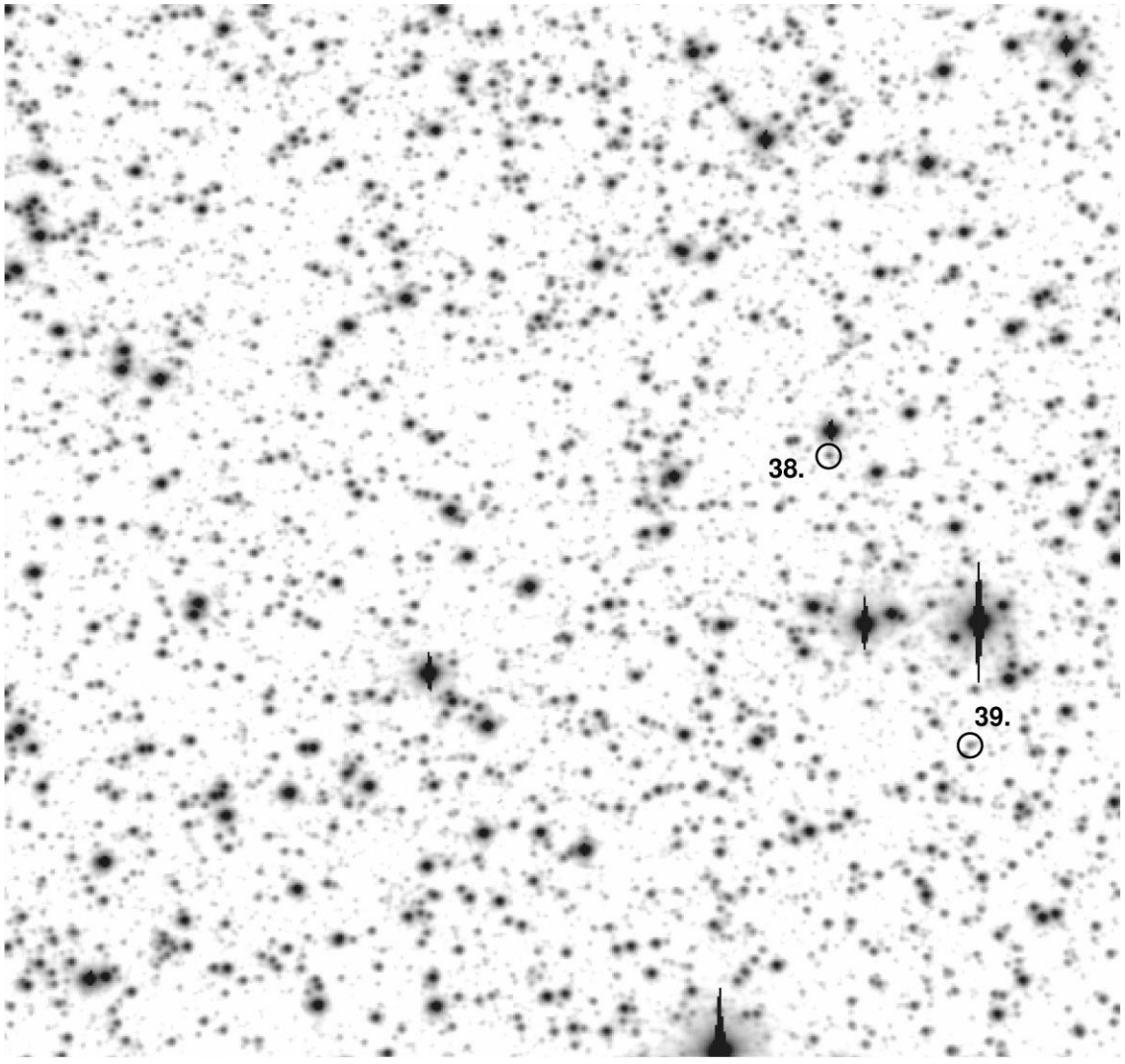

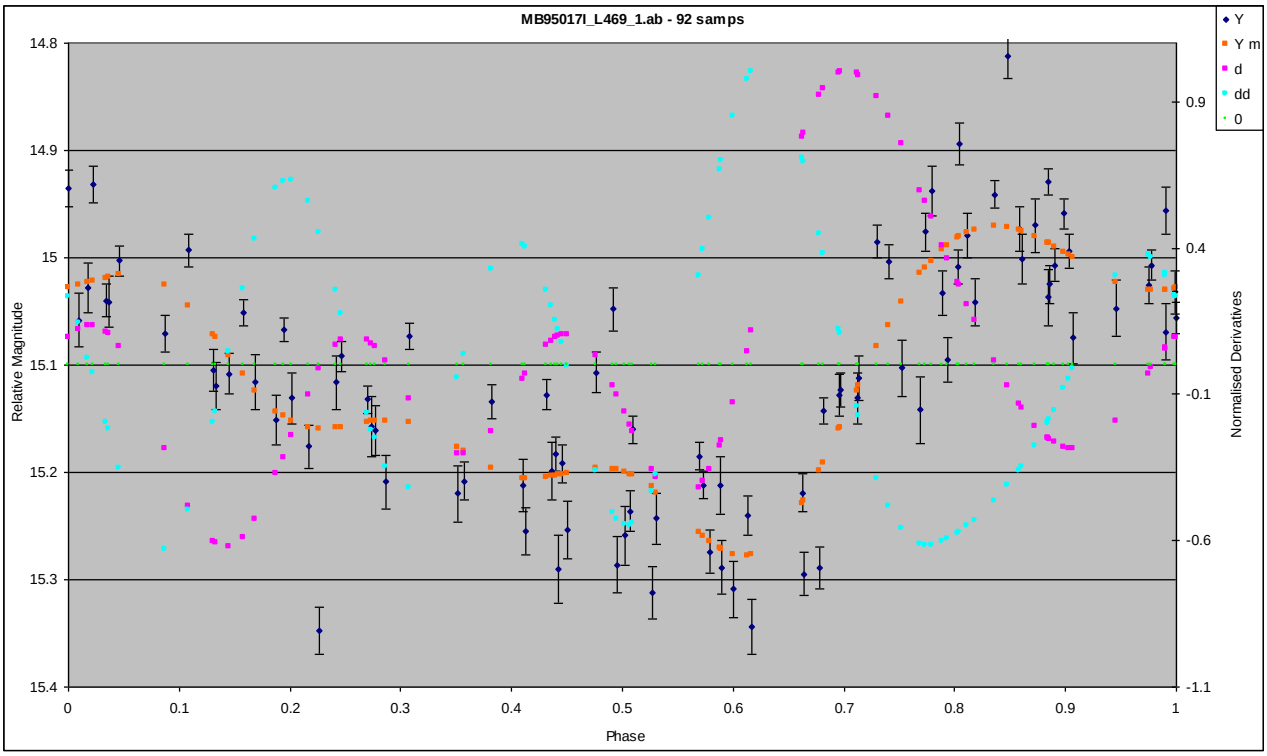
MB95017I_L469_1.ab - 92 samps
Y
Y m
d
dd
0
Relative Magnitude
Normalised Derivatives
Phase
14.8
14.9
15
15.1
15.2
15.3
15.4
0.9
0.4
-0.1
-0.6
-1.1
0
0.1
0.2
0.3
0.4
0.5
0.6
0.7
0.8
0.9
1

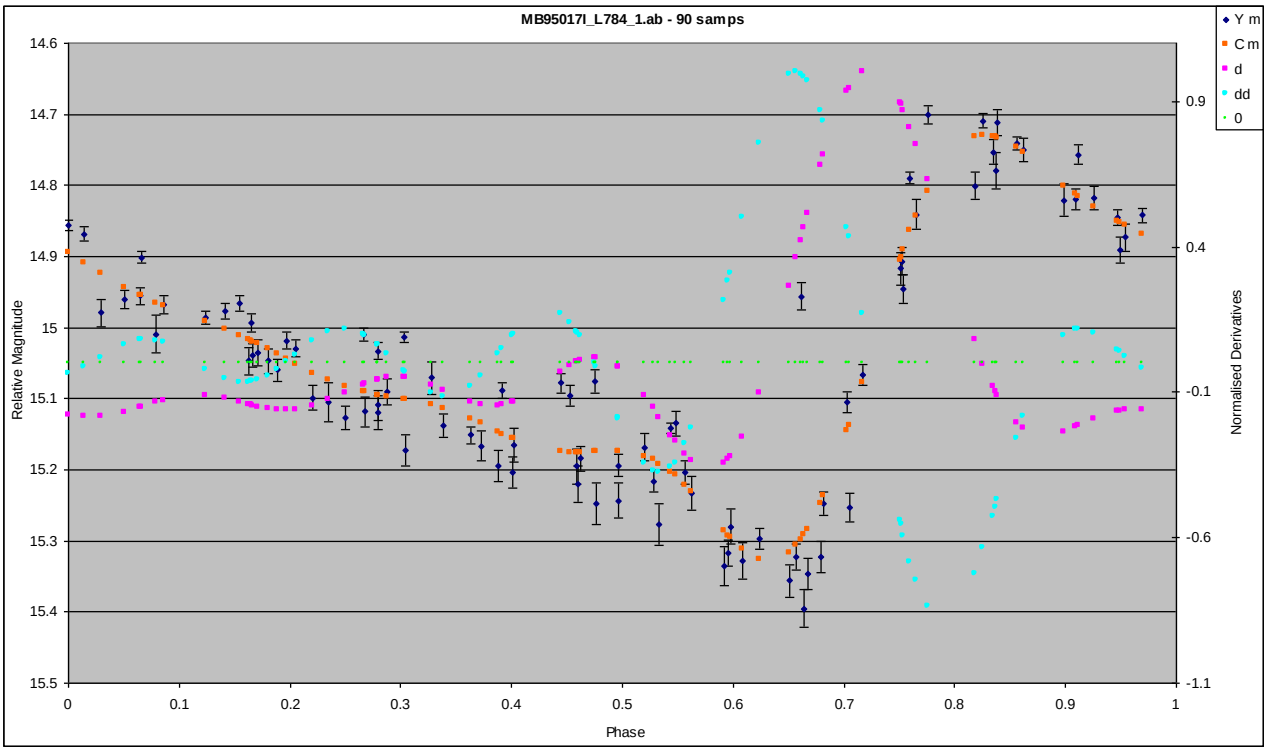
MB95017I_L784_1.ab - 90 samps
Y m
C m
d
dd
0
Relative Magnitude
Normalised Derivatives
Phase
14.6
14.7
14.8
14.9
15
15.1
15.2
15.3
15.4
15.5
0.9
0.4
-0.1
-0.6
-1.1
0
0.1
0.2
0.3
0.4
0.5
0.6
0.7
0.8
0.9
1

TMB96020I for event MB96020I ~ 5.54’ by 4.18’

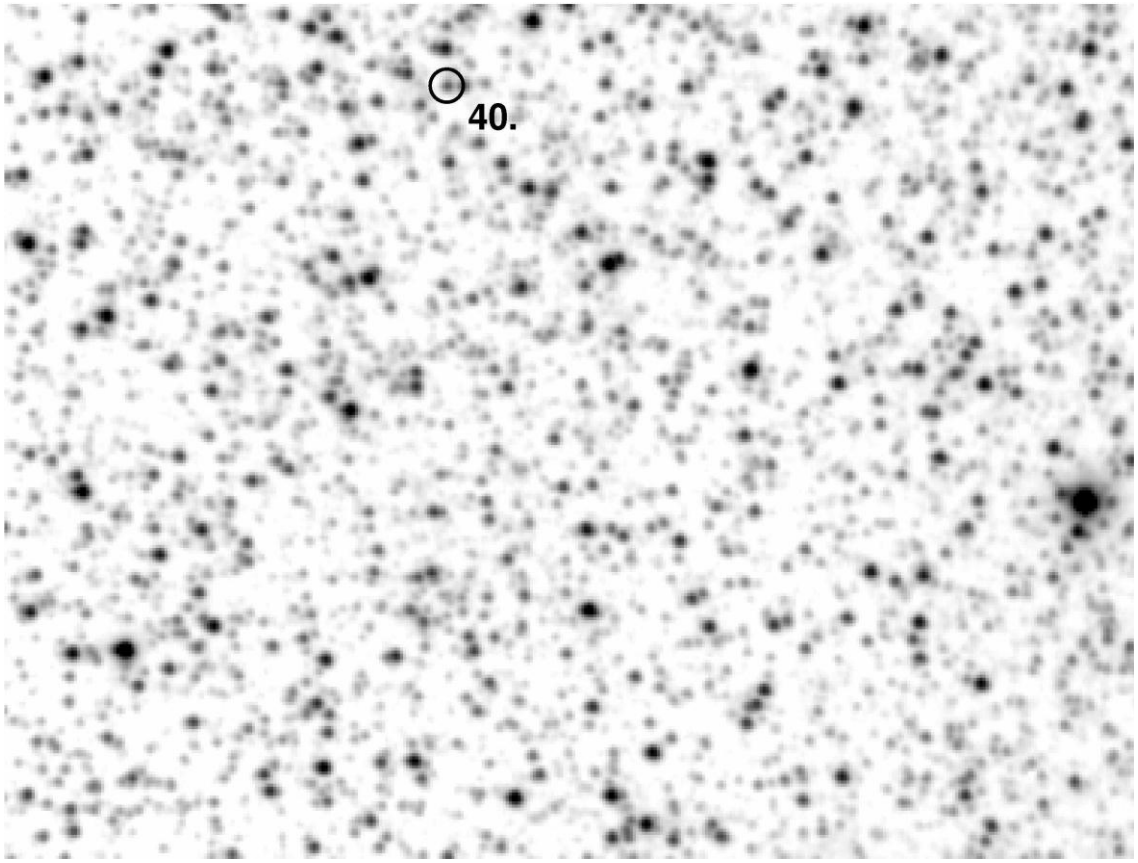

SMS98001I for event MS98001I ~ 2.99’ by 2.99’

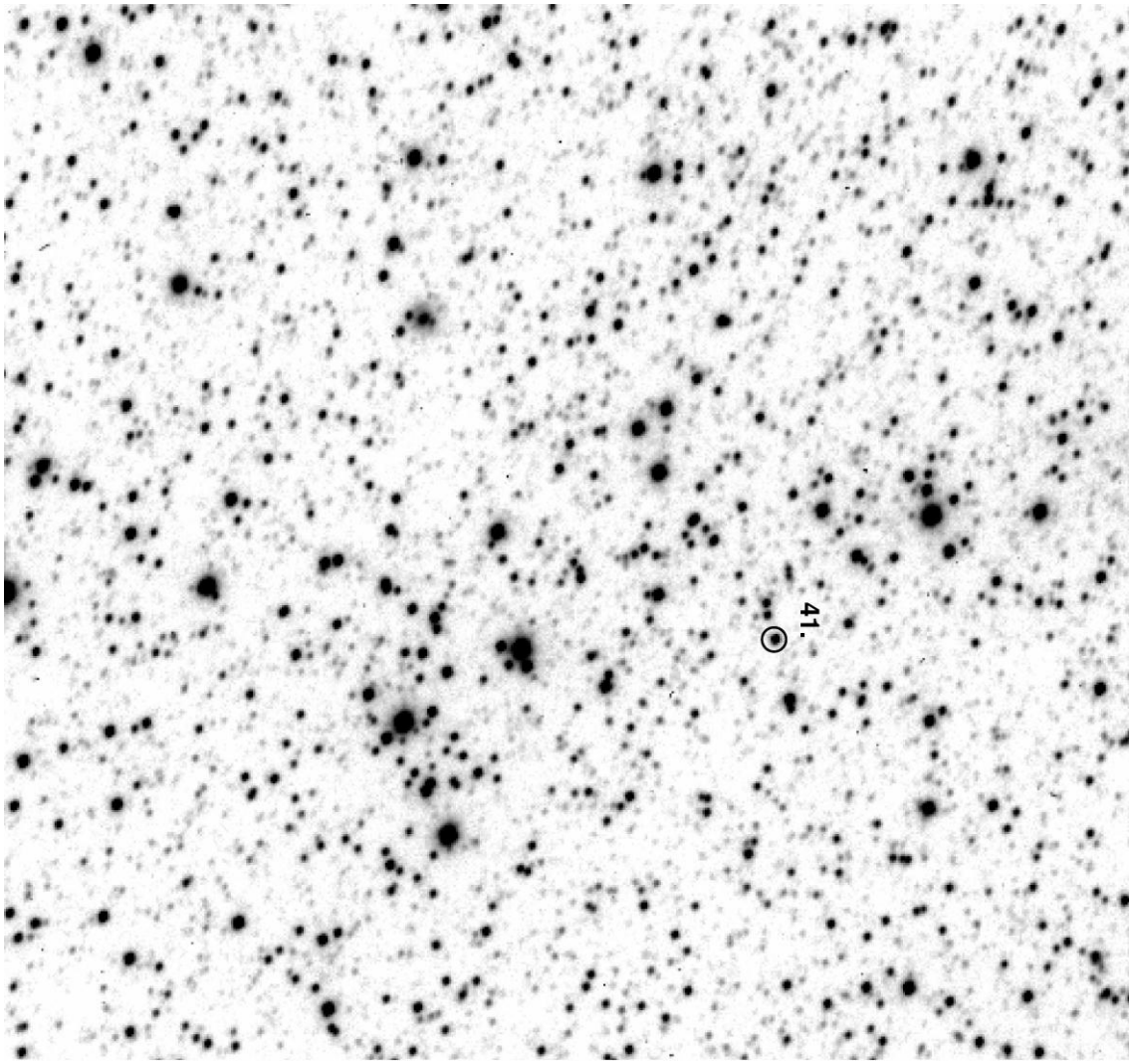

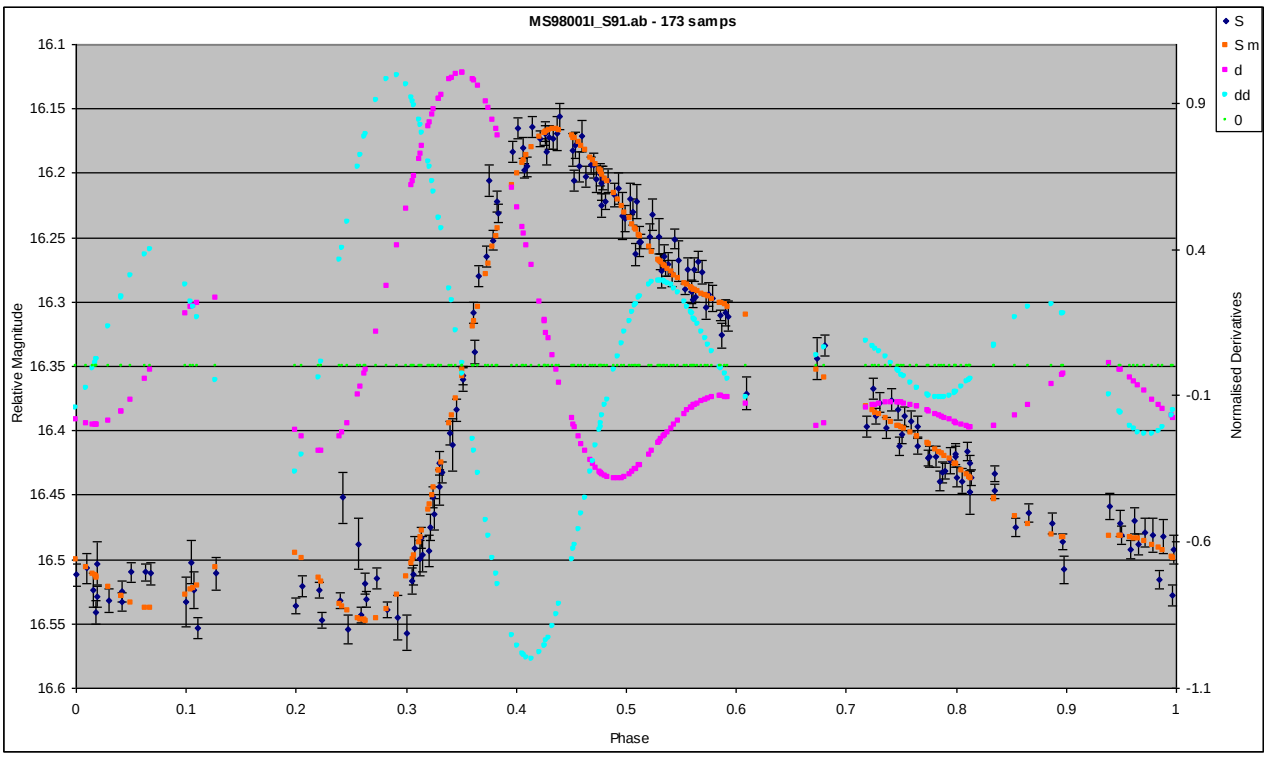

YMB99008I for event MB99008I ~ 5.01’ by 5.01’

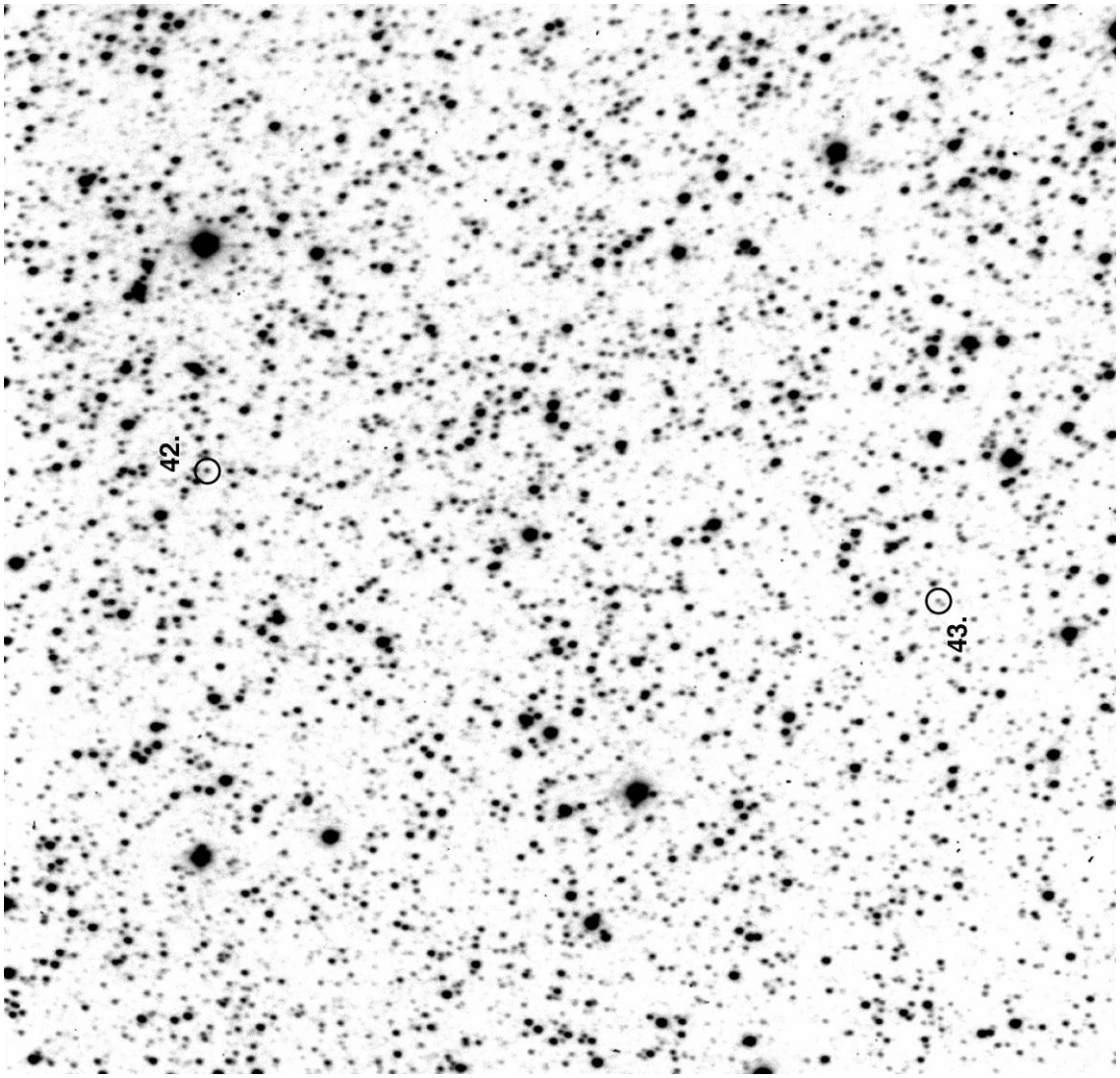

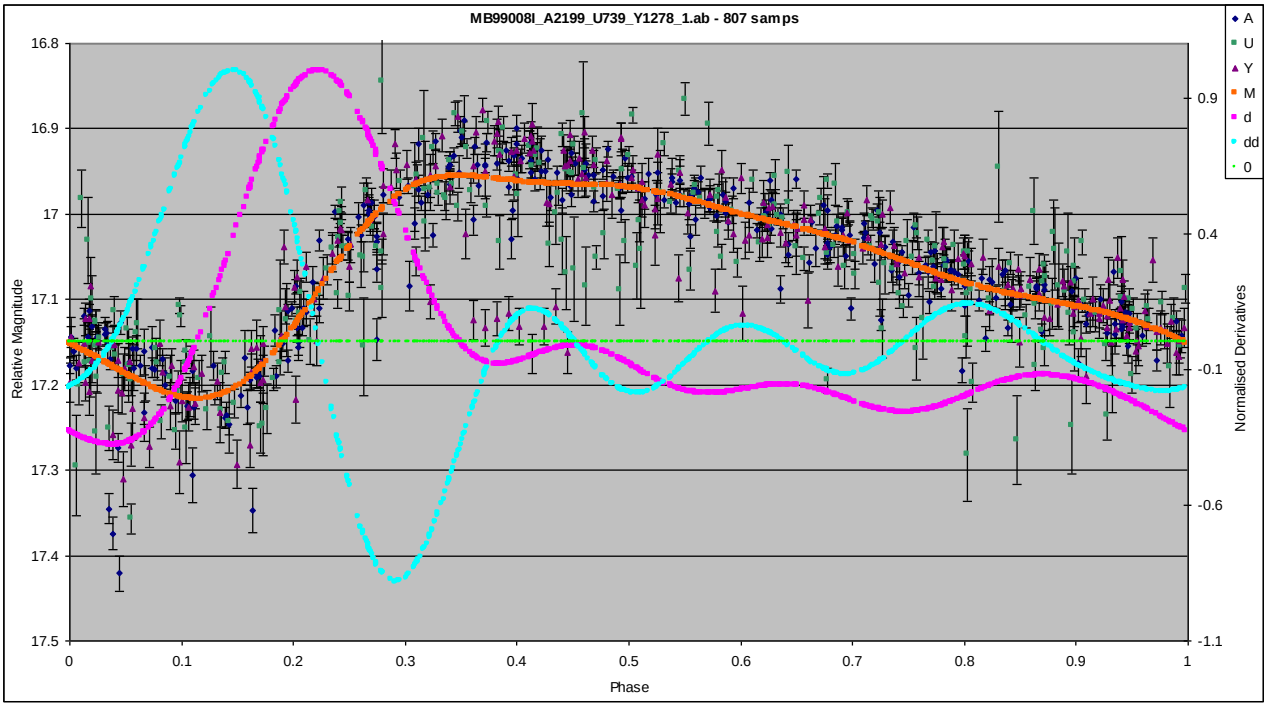

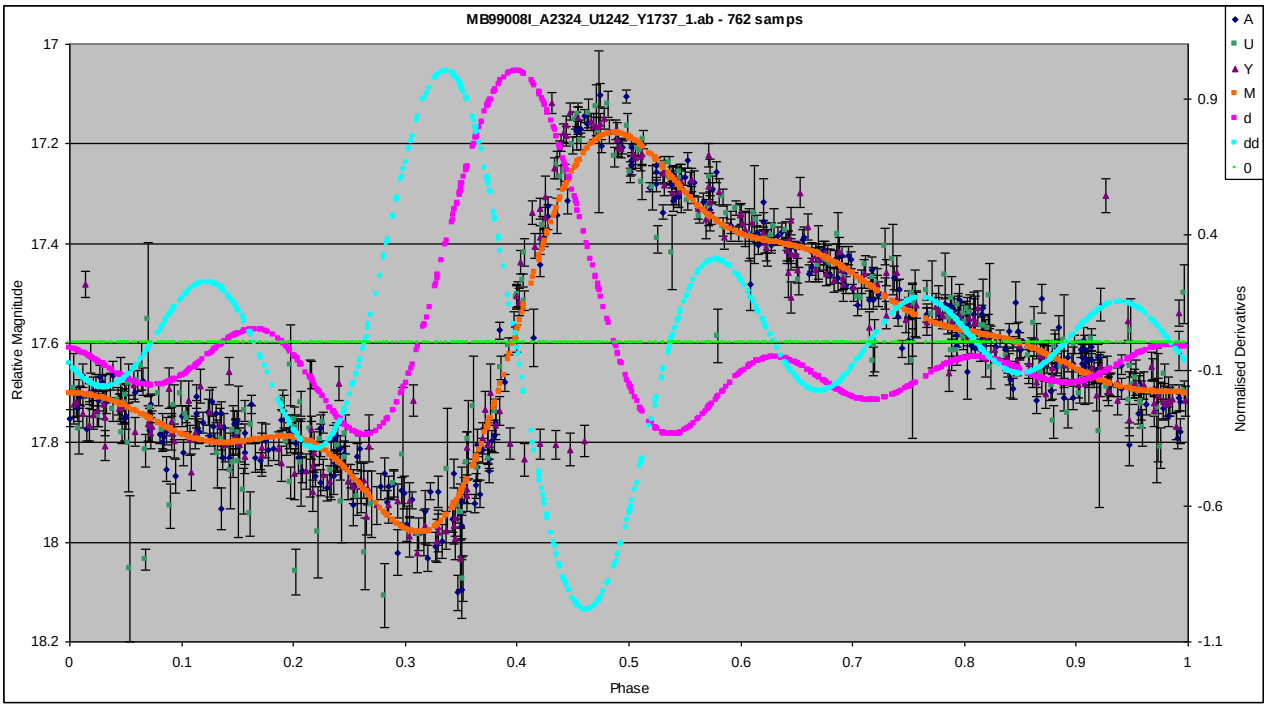

YMB99018I for event MB99018I ~ 5.01’ by 5.01’

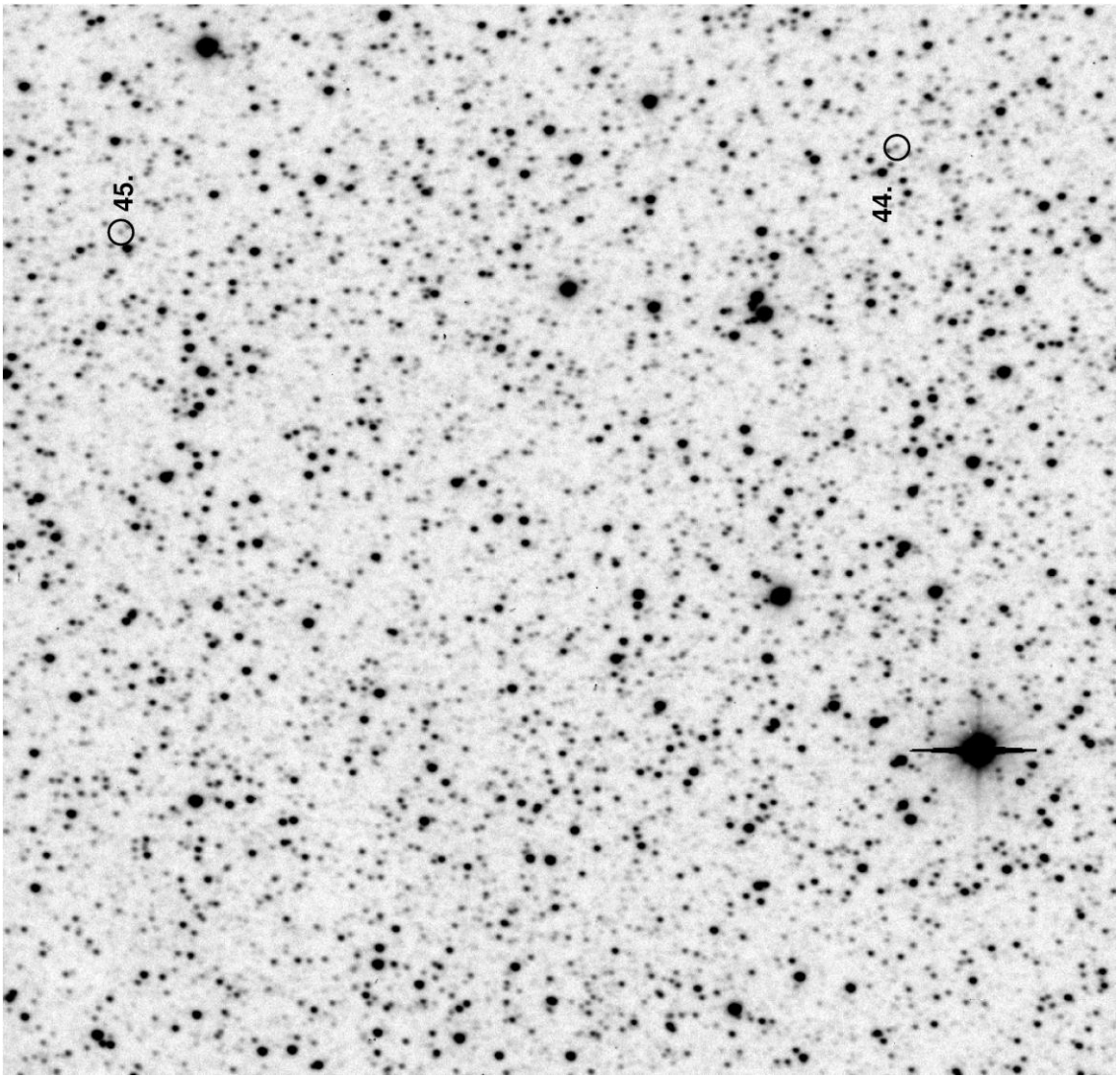

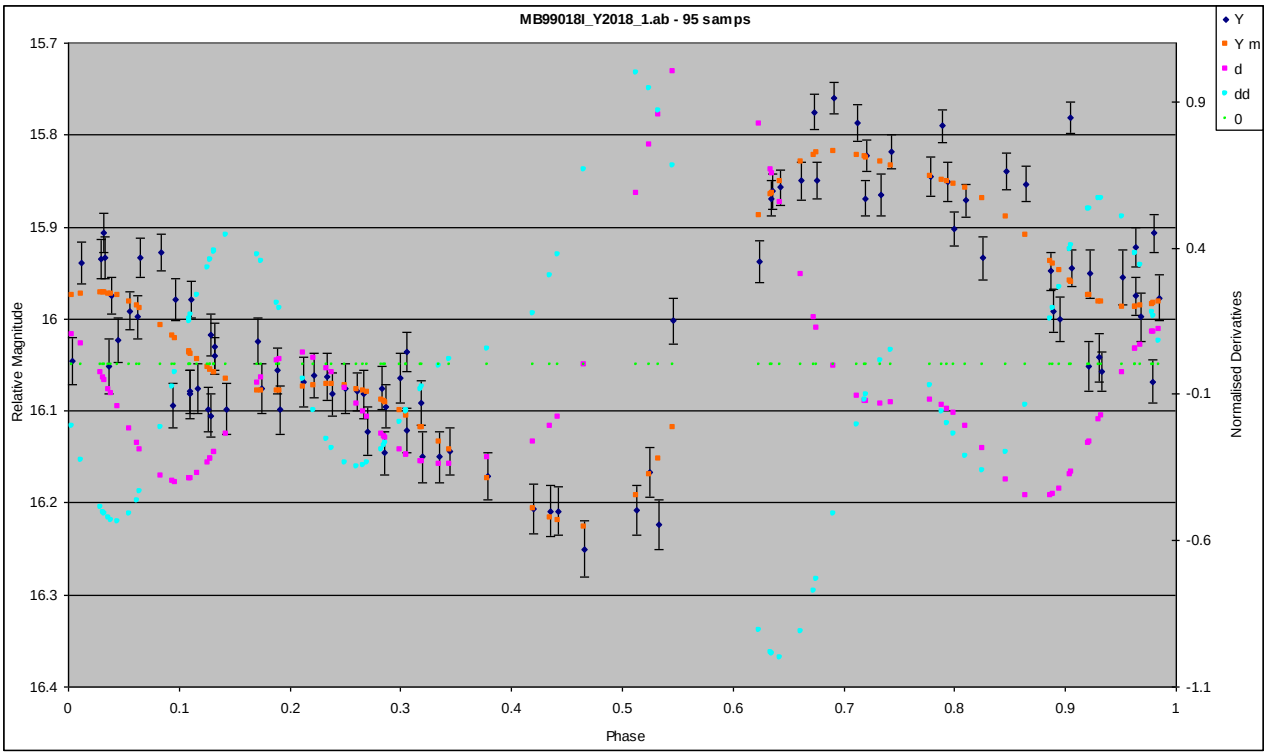
MB99018I_Y2018_1.ab - 95 samps
Y
Y m
d
dd
0
Relative Magnitude
Normalised Derivatives
Phase
15.7
15.8
15.9
16
16.1
16.2
16.3
16.4
0.9
0.4
-0.1
-0.6
-1.1
0
0.1
0.2
0.3
0.4
0.5
0.6
0.7
0.8
0.9
1

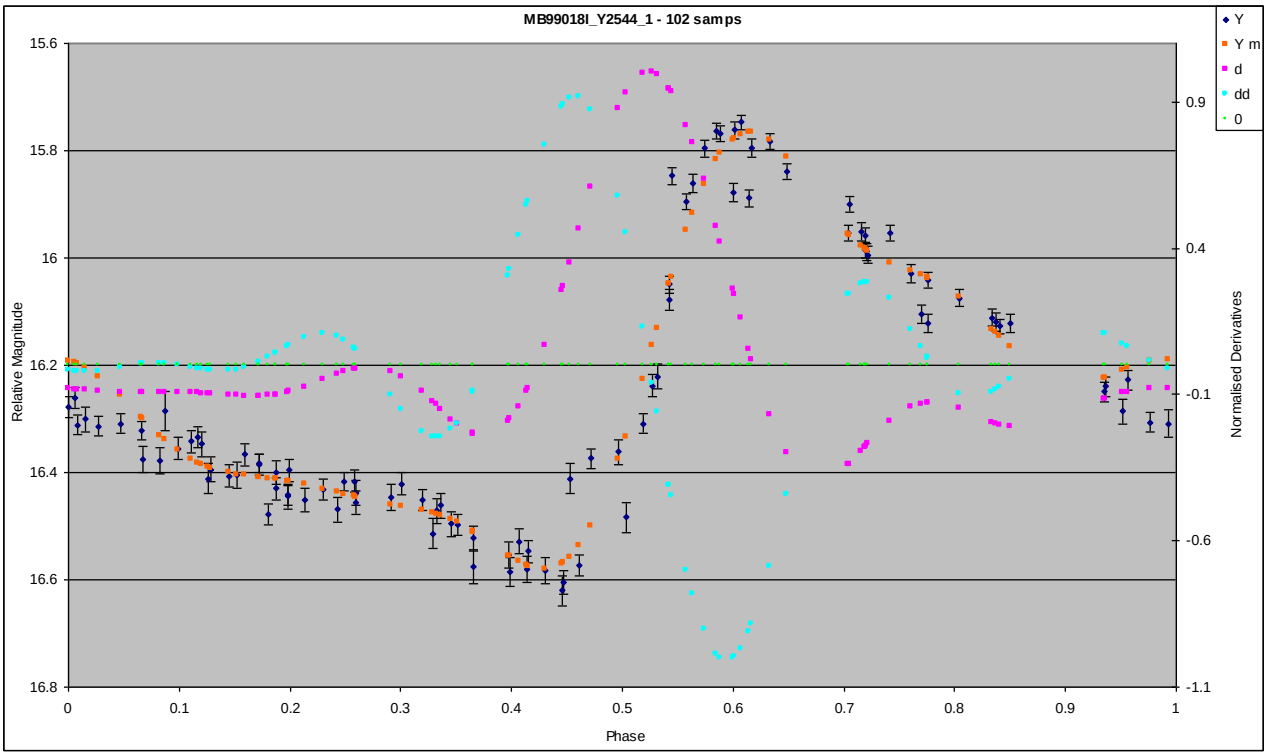
MB99018I_Y2544_1 - 102 samps
Y
Y m
d
dd
0
Relative Magnitude
Normalised Derivatives
Phase
15.6
15.8
16
16.2
16.4
16.6
16.8
0.9
0.4
-0.1
-0.6
-1.1
0
0.1
0.2
0.3
0.4
0.5
0.6
0.7
0.8
0.9
1

AOB99035I for event OB99035I ~ 5.48’ by 5.48’

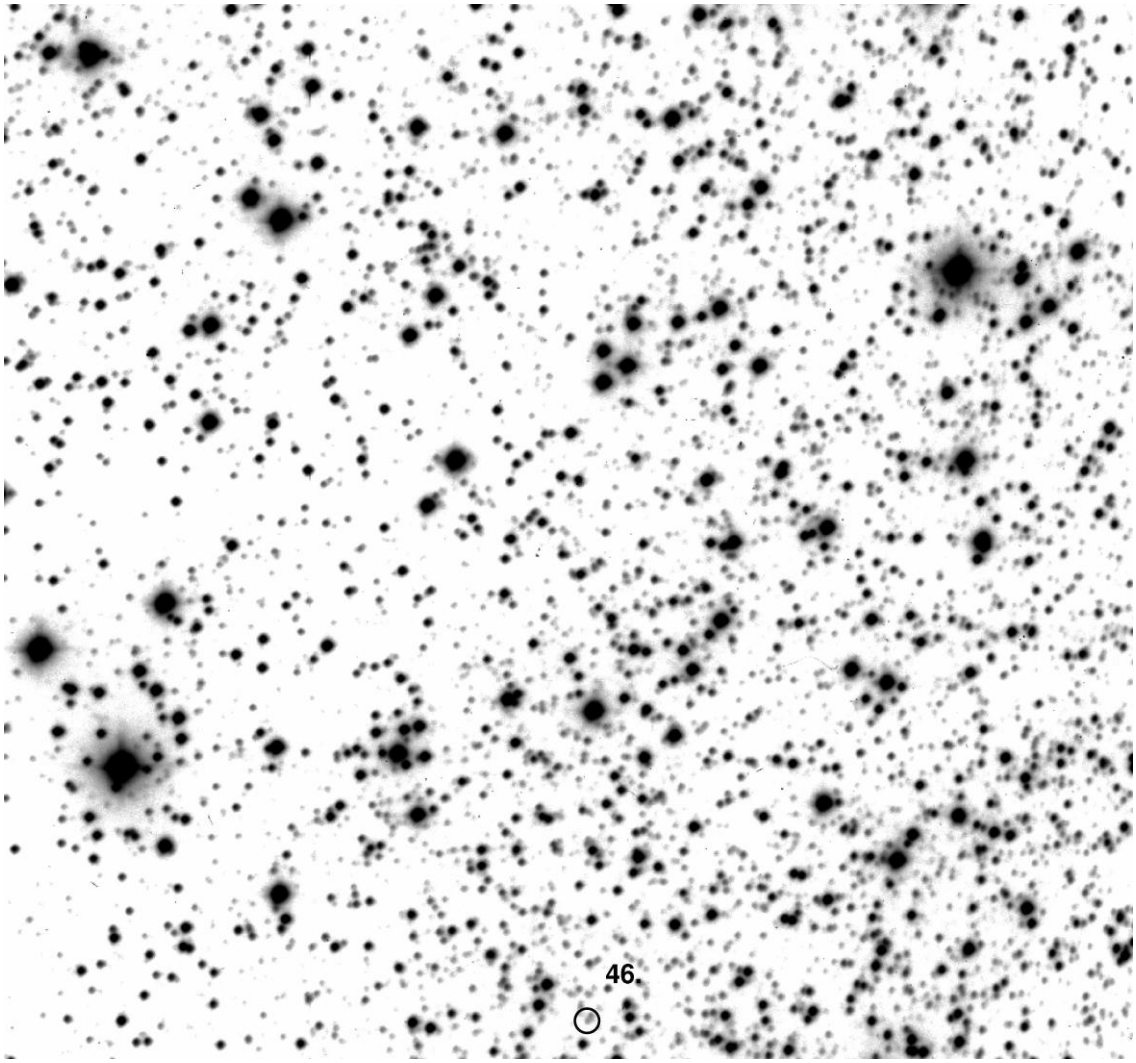

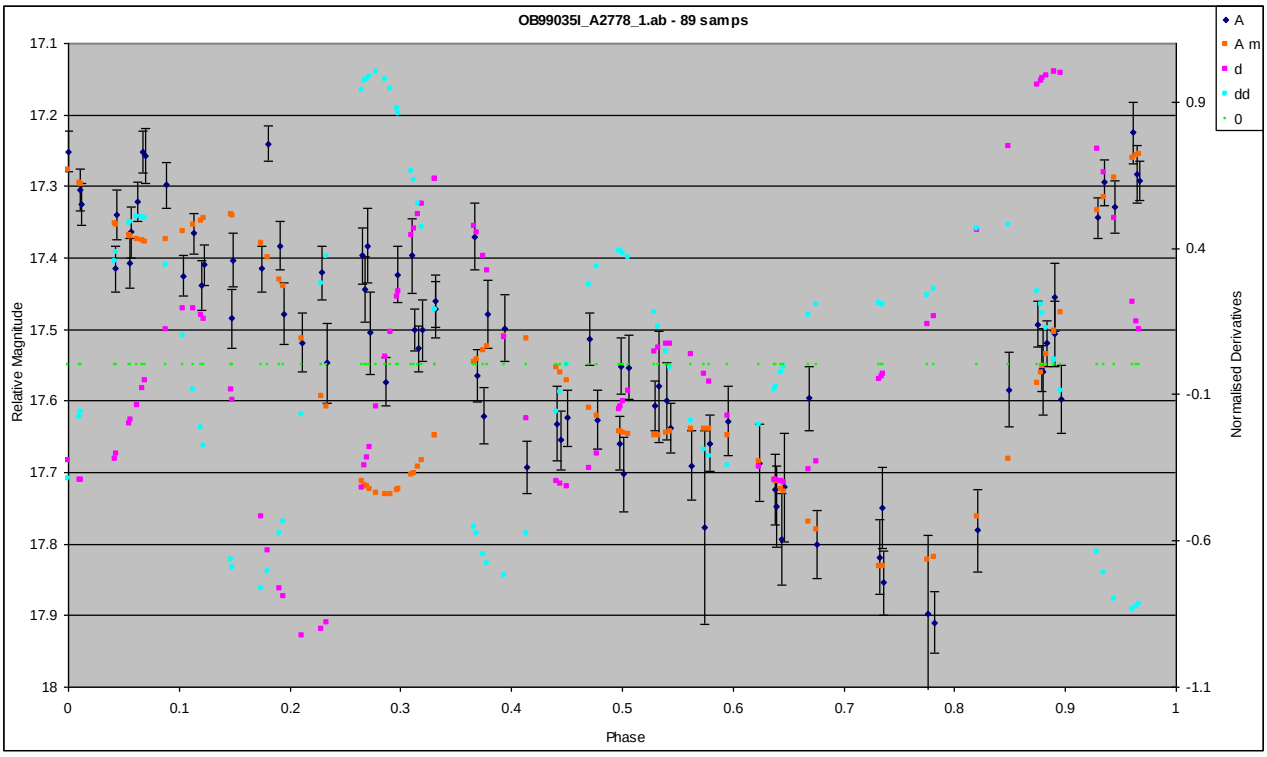

YOB99036I for event OB99036I ~ 5.01’ by 5.01’

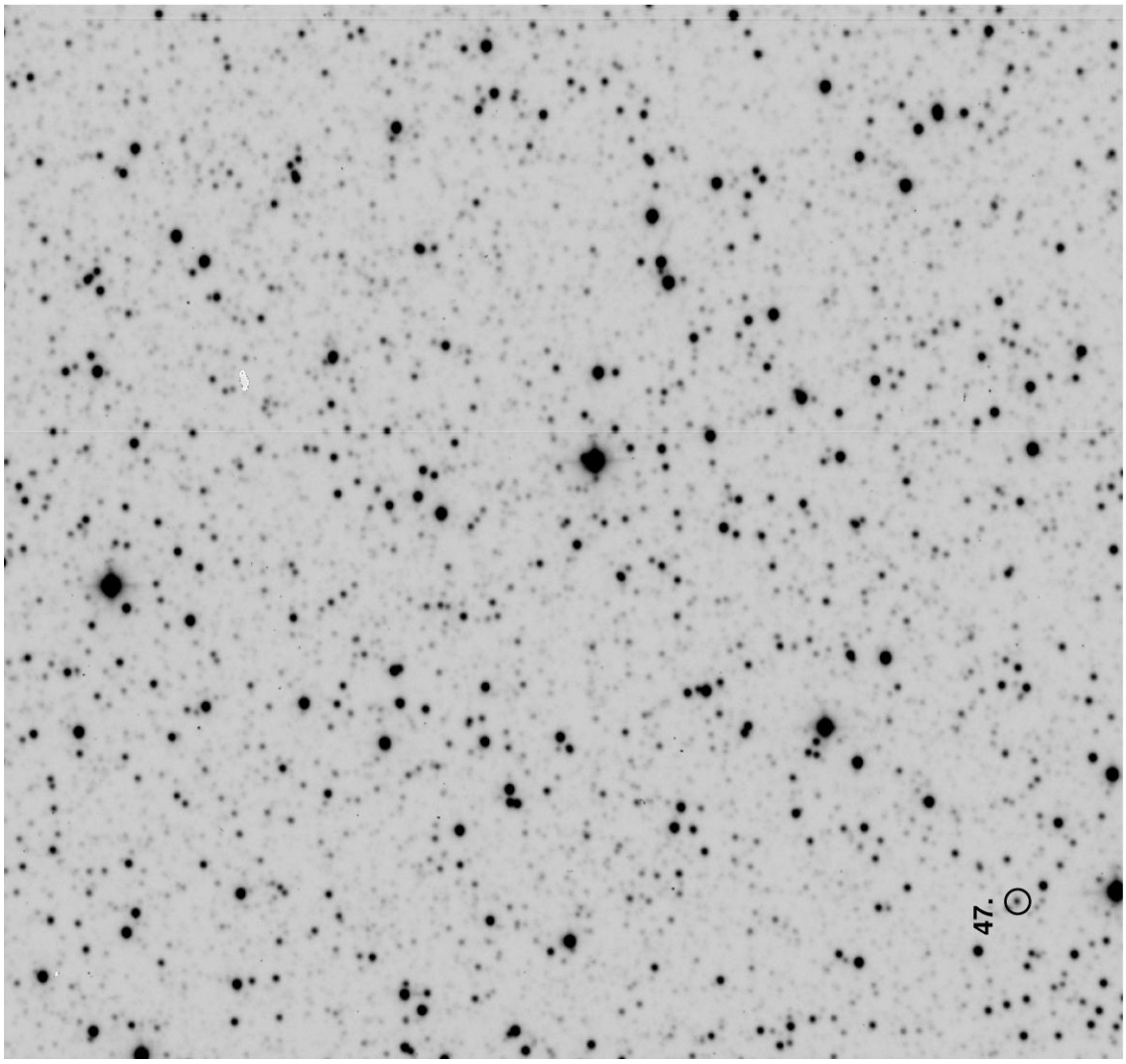

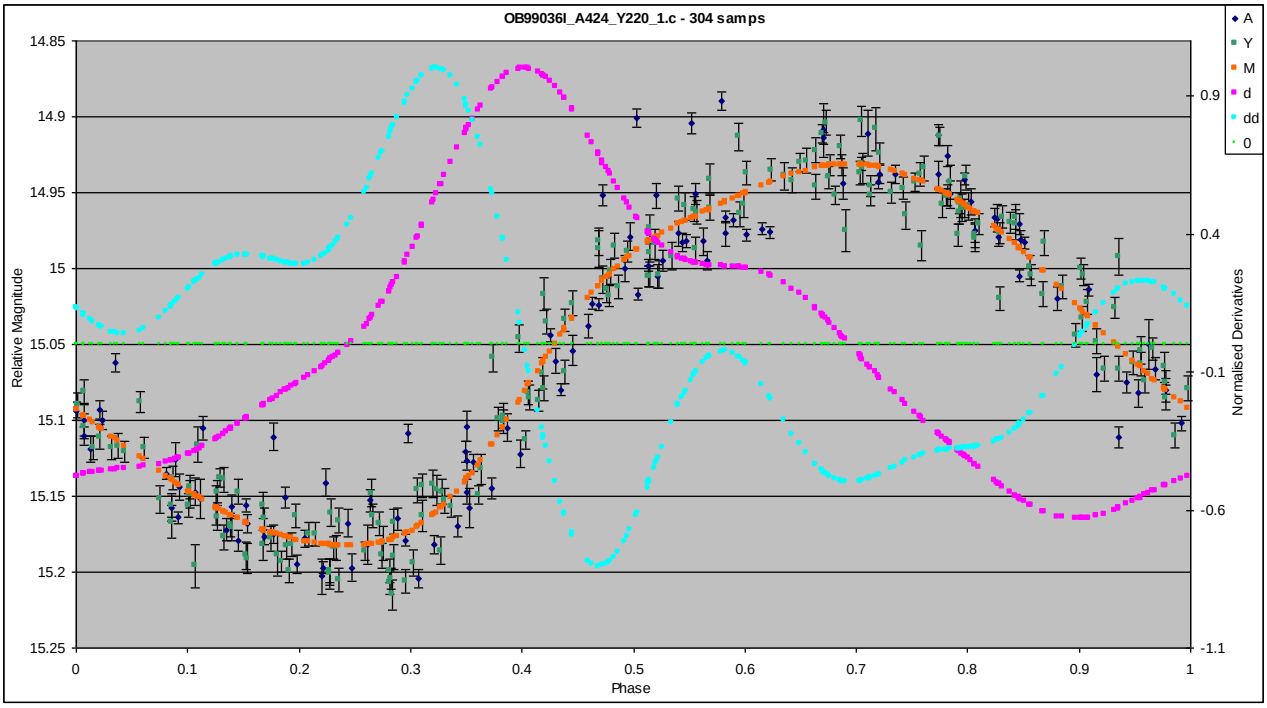

AOB99005I for event OB99005I ~ 5.48’ by 5.48’

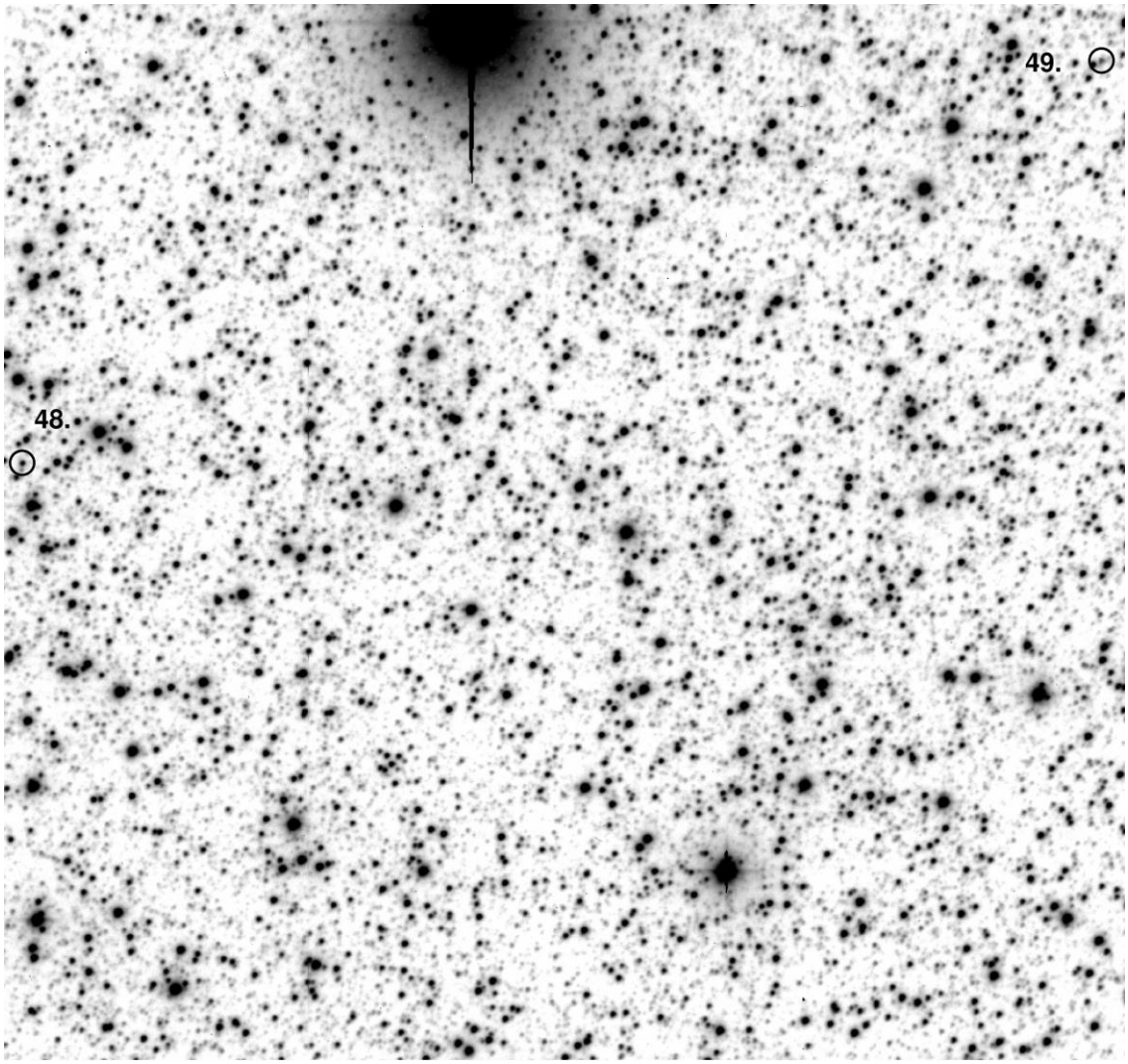

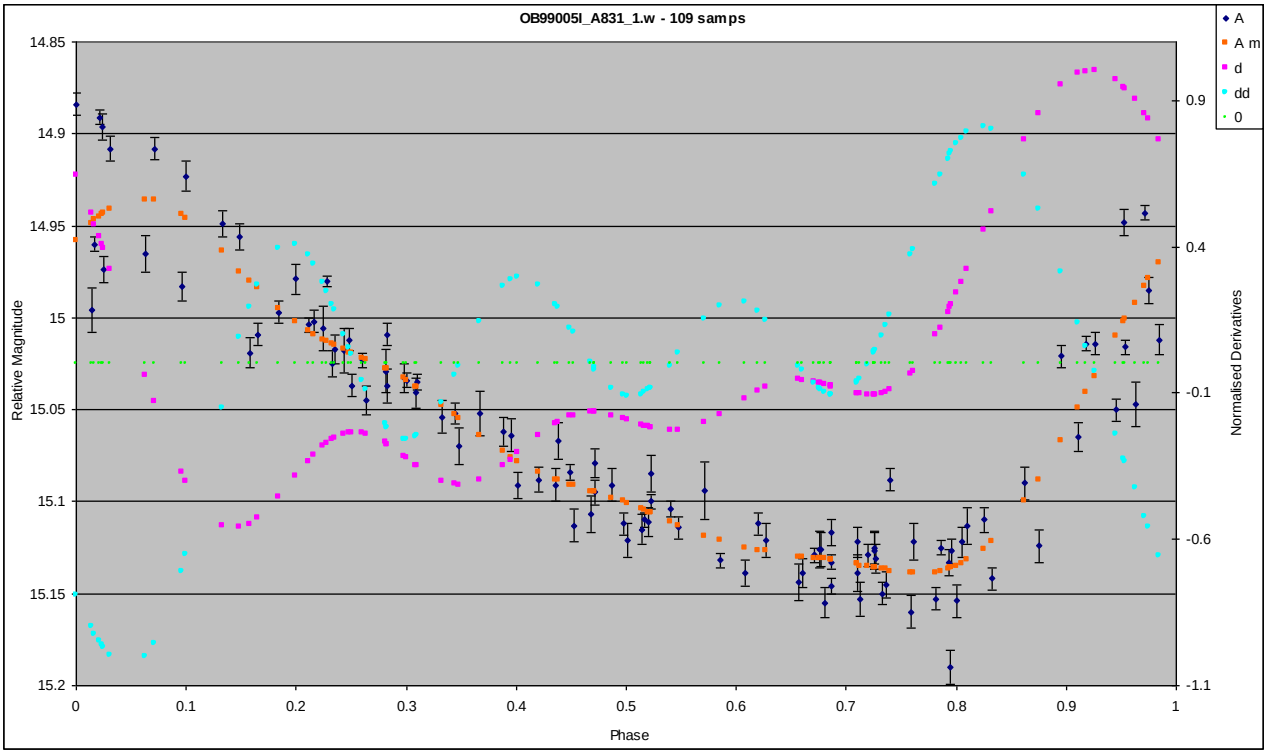

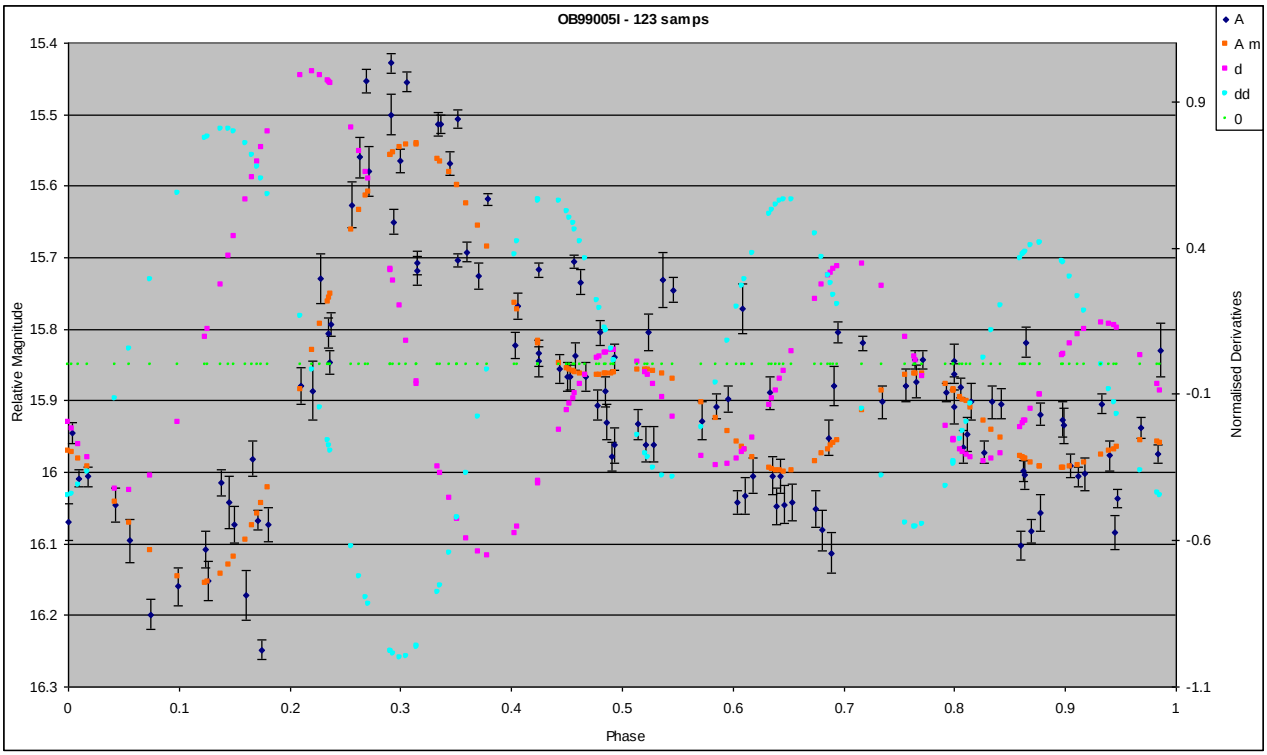

LMB97018I for event MB97018I ~ 3.77' by 3.77'

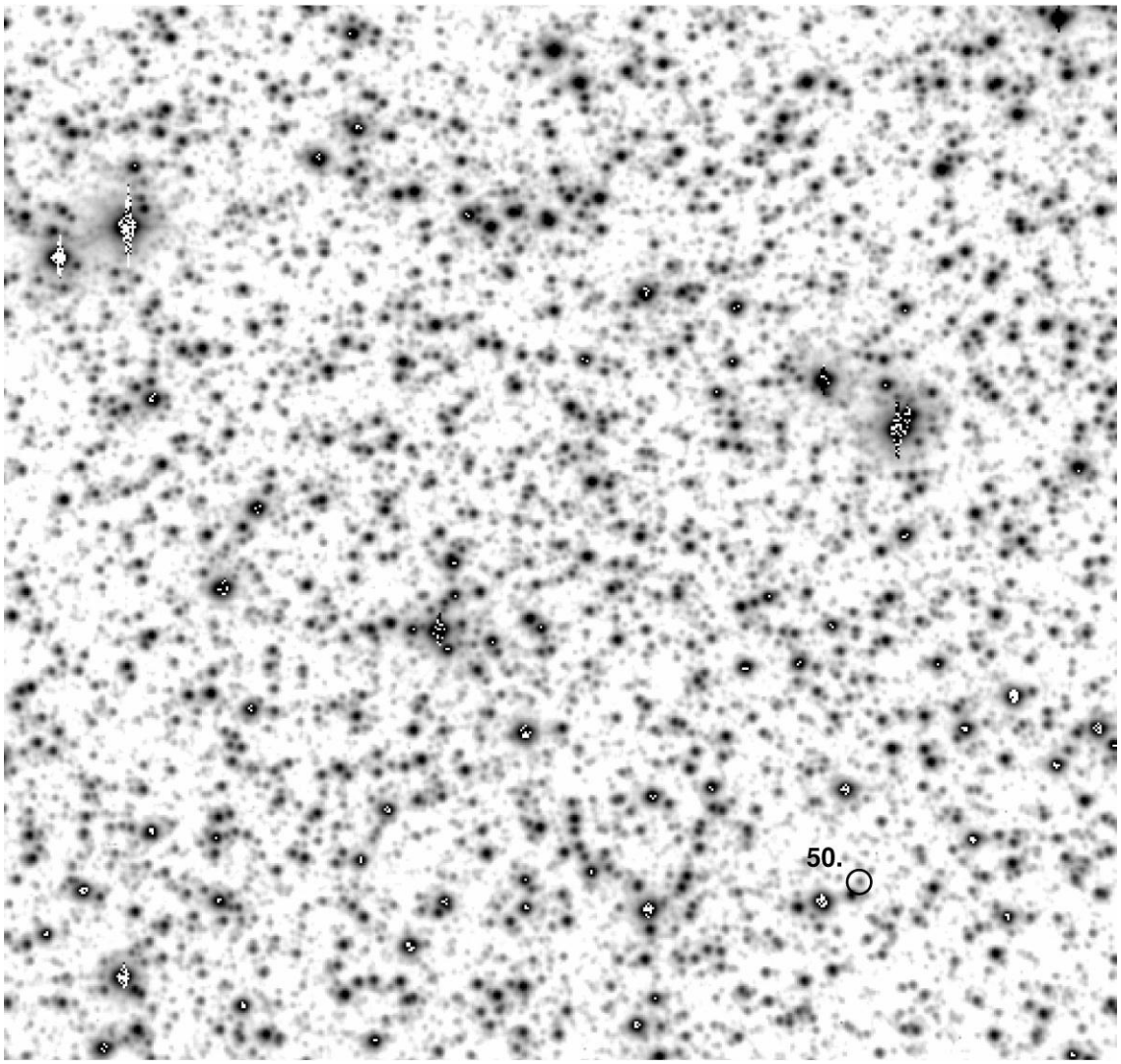

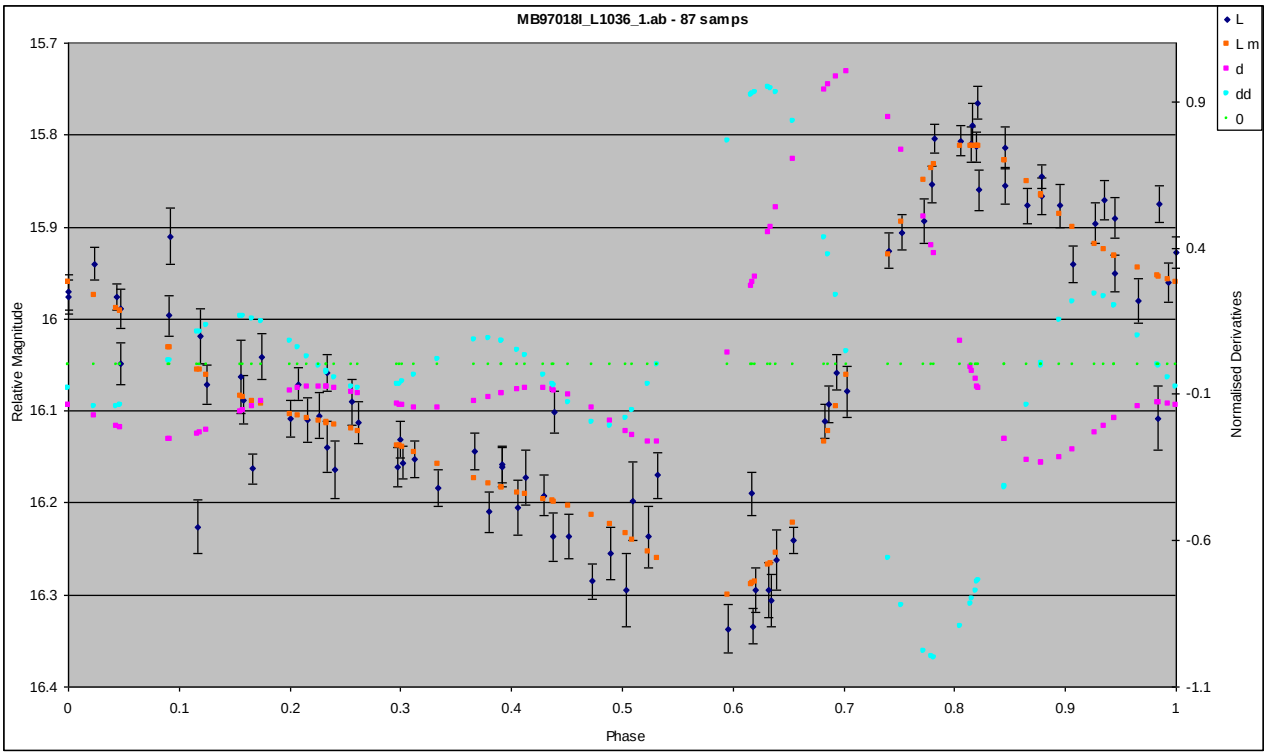

LMB97028I for event MB97028I ~ 3.77’ by 3.77’

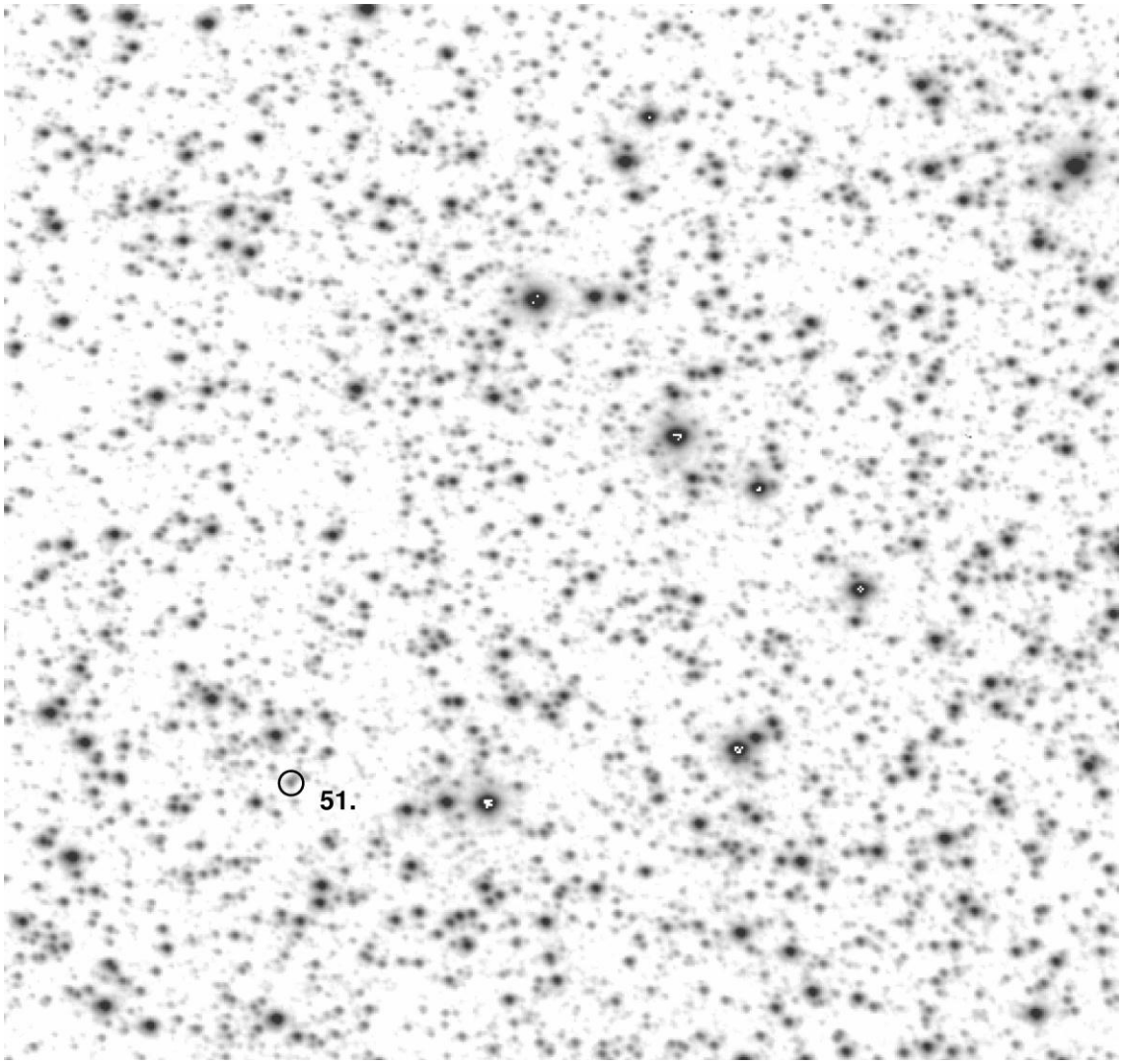

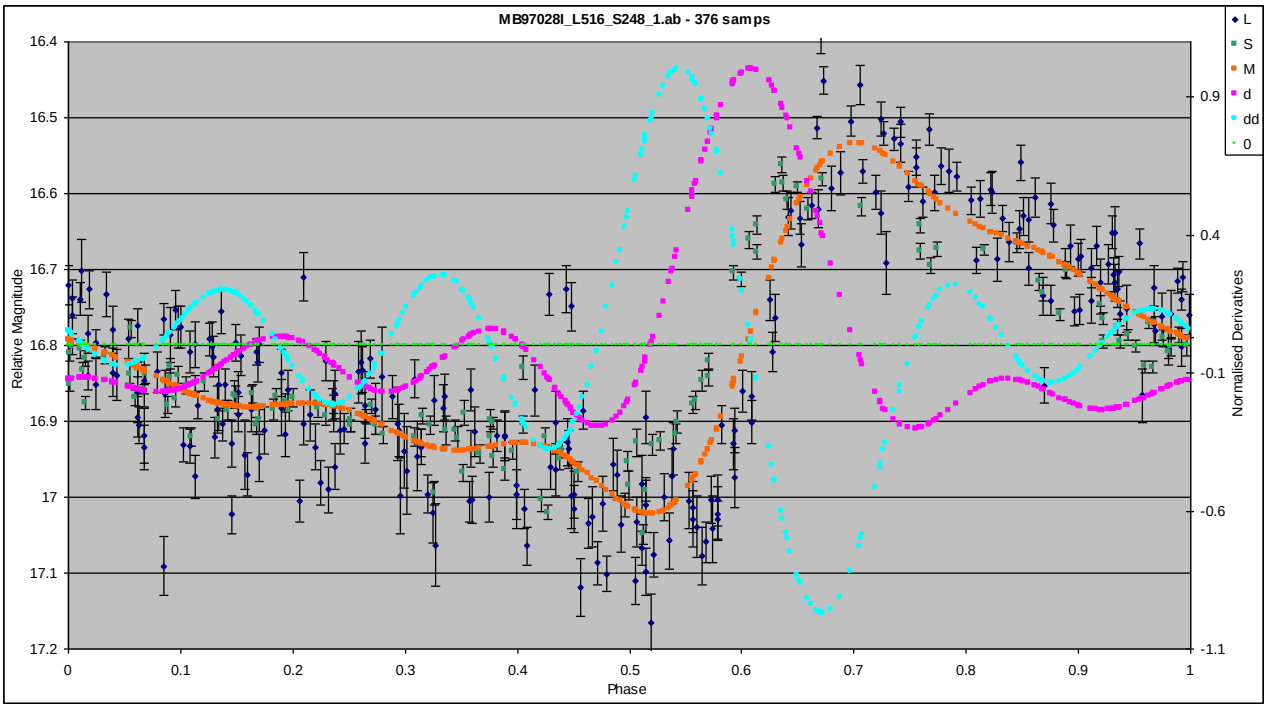

YKB01002I for event KB01002I ~ 5.13’ by 5.13’

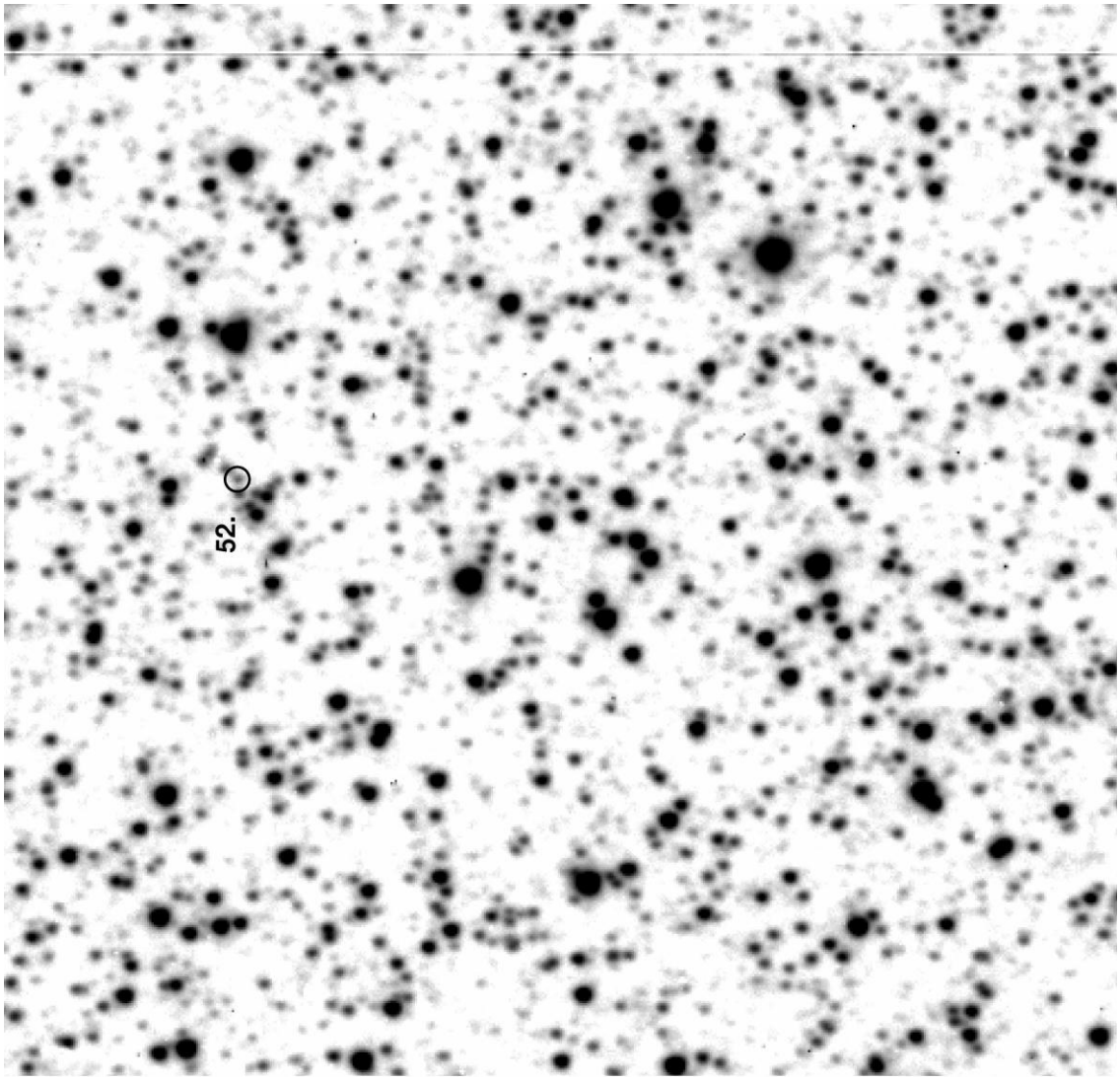

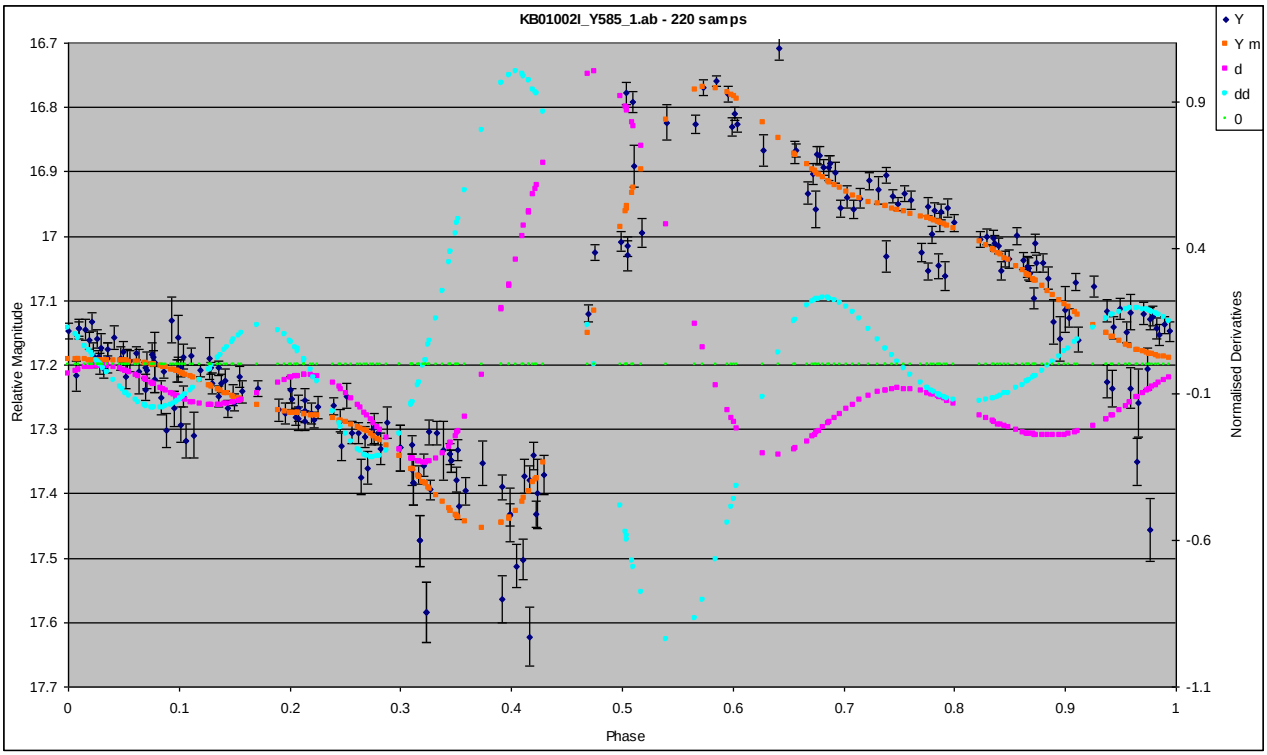

WKB01012I for event KB01012I ~ 5.15’ by 5.15’

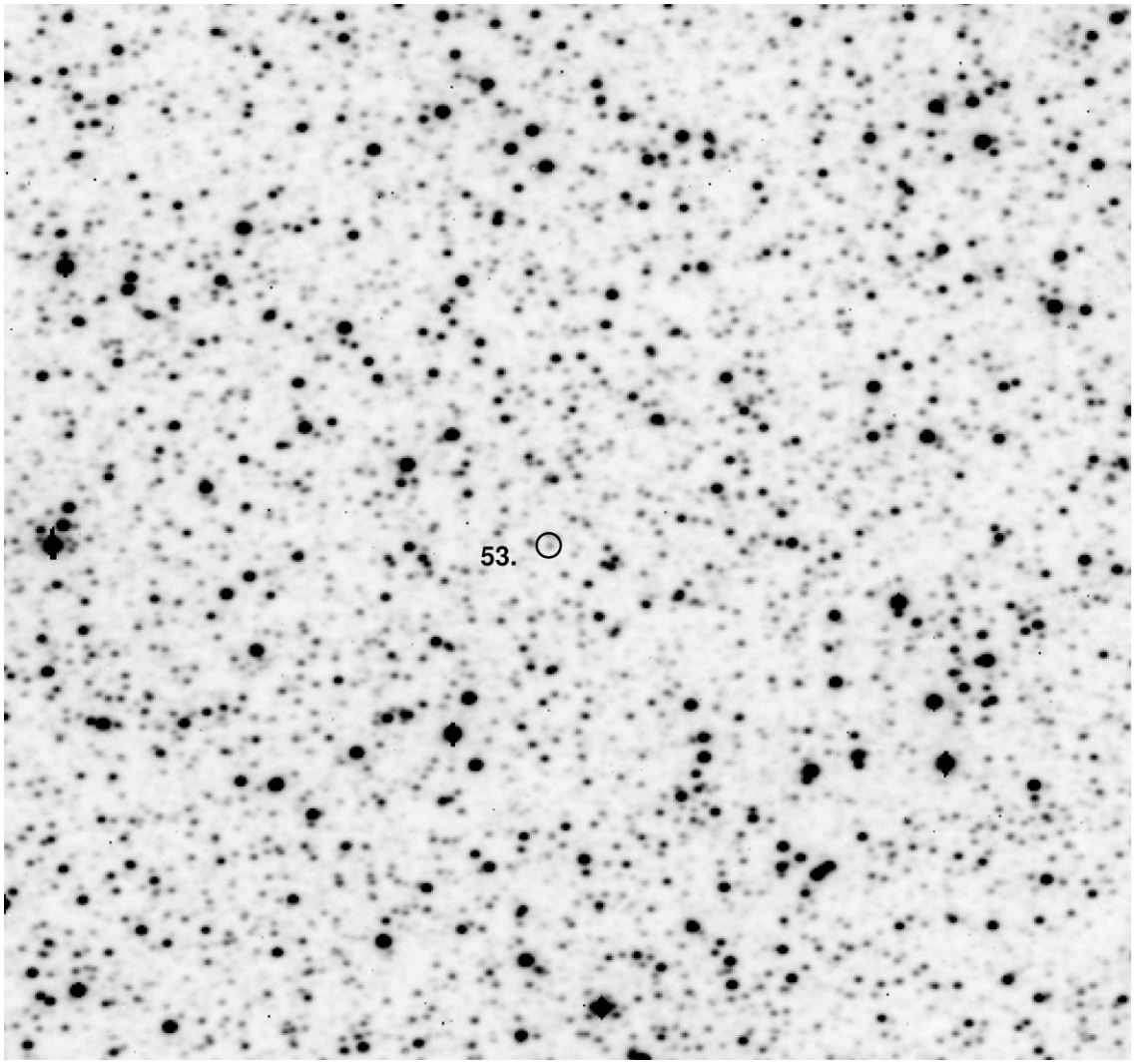

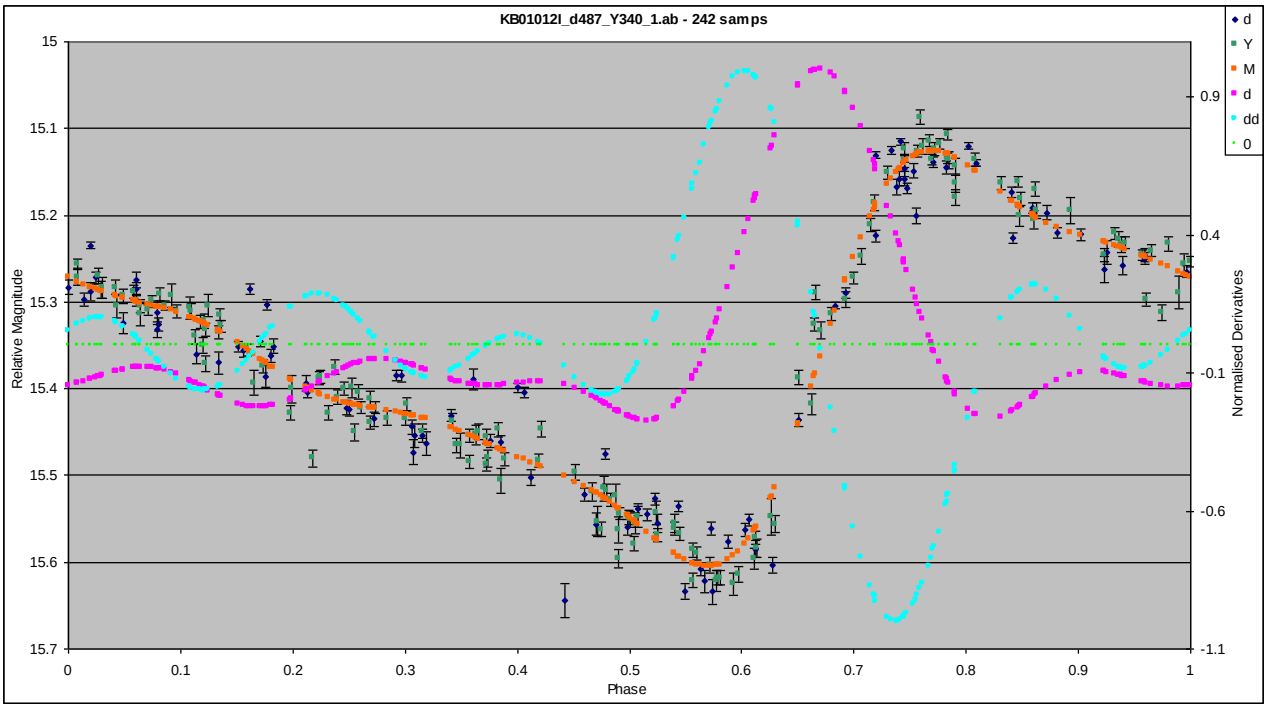

WOB03167I for event OB03167I ~ 5.15’ by 5.15’

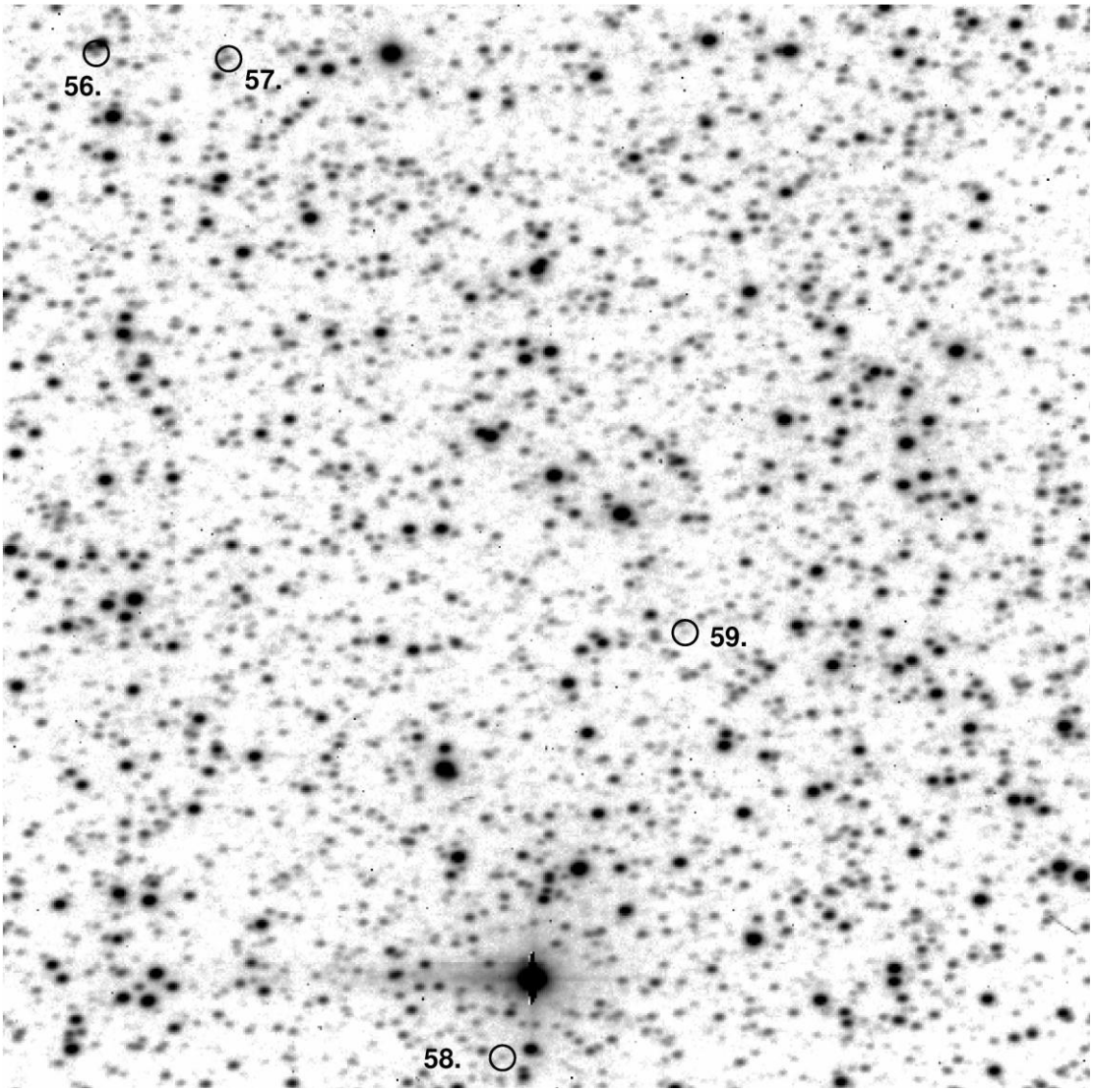

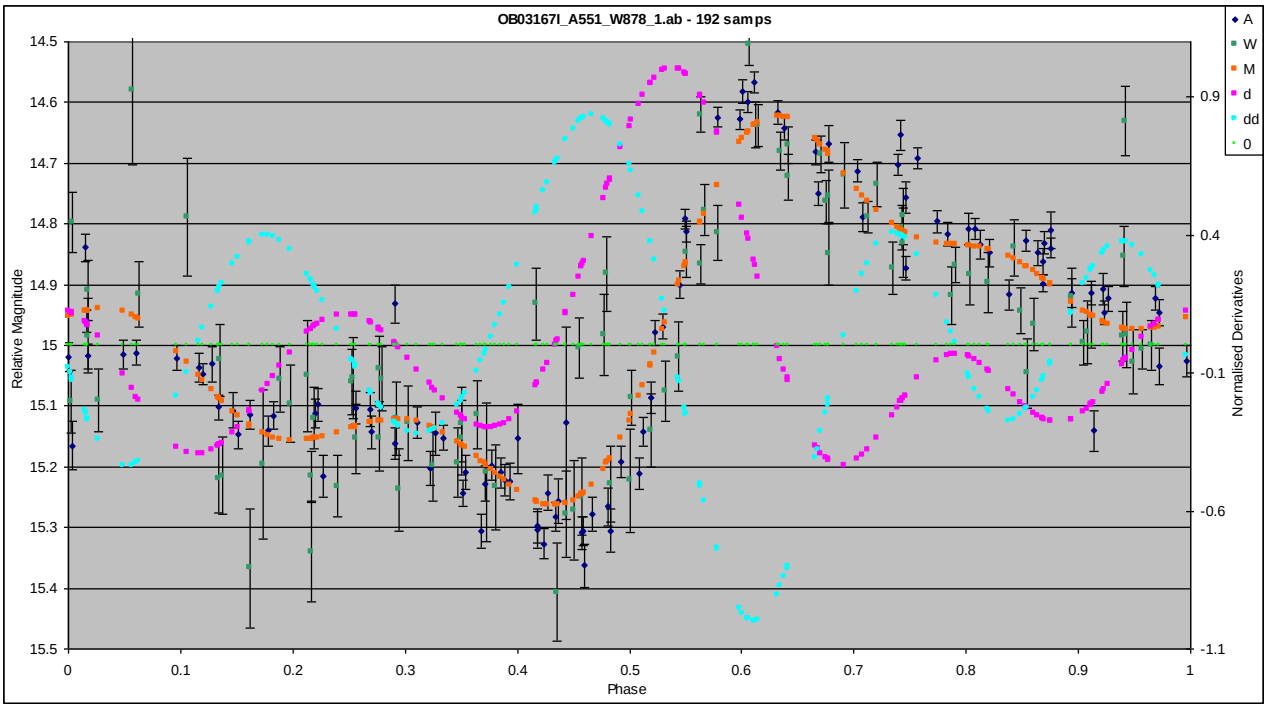
OB03167I_A551_W878_1.ab - 192 samps
A
W
M
d
dd
0
Relative Magnitude
Normalised Derivatives
Phase
14.5
14.6
14.7
14.8
14.9
15
15.1
15.2
15.3
15.4
15.5
0.9
0.4
-0.1
-0.6
-1.1
0
0.1
0.2
0.3
0.4
0.5
0.6
0.7
0.8
0.9
1

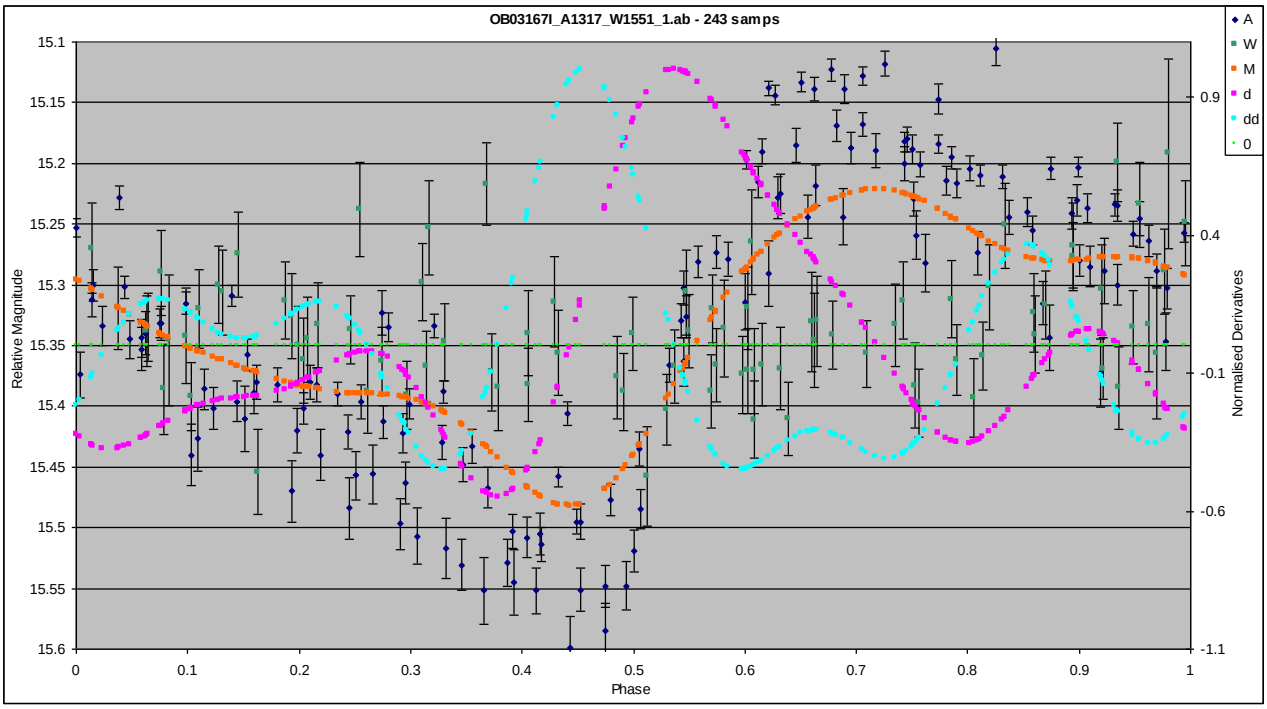
OB03167I_A1317_W1551_1.ab - 243 samps
A
W
M
d
dd
0
Relative Magnitude
Normalised Derivatives
Phase
15.1
15.15
15.2
15.25
15.3
15.35
15.4
15.45
15.5
15.55
15.6
0.9
0.4
-0.1
-0.6
-1.1
0
0.1
0.2
0.3
0.4
0.5
0.6
0.7
0.8
0.9
1

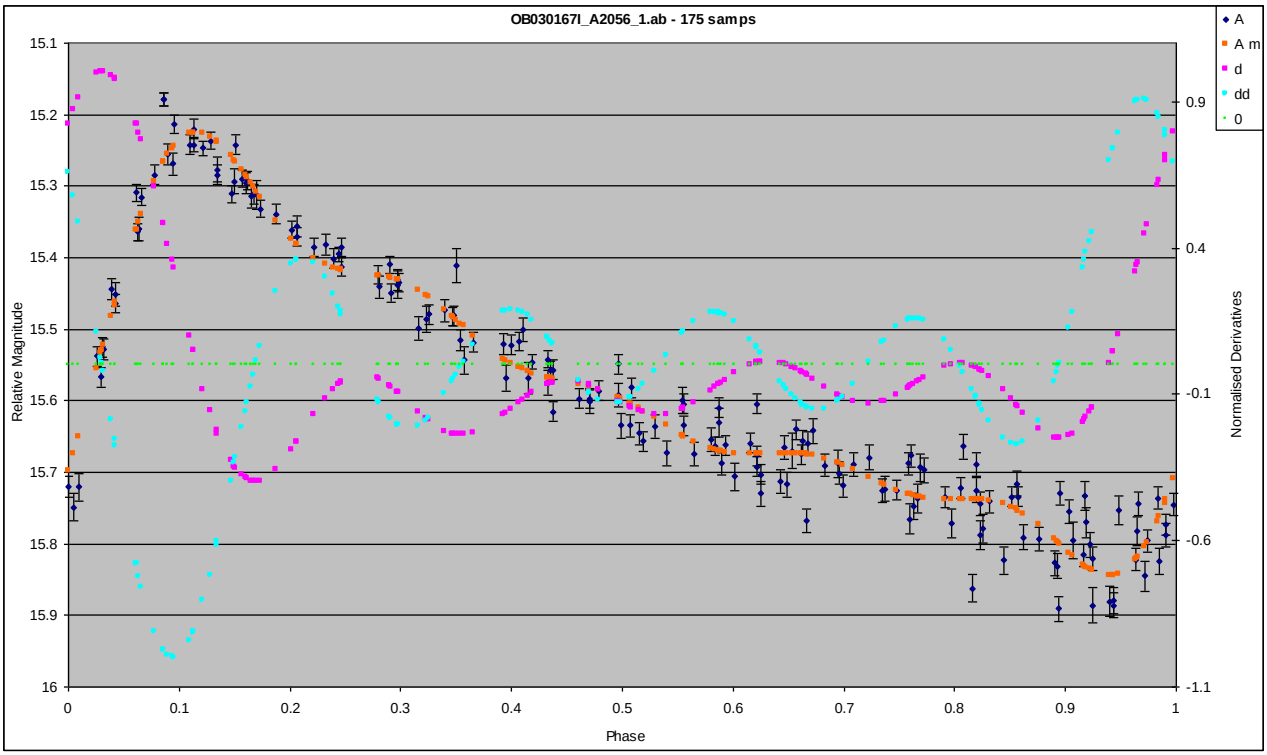
OB030167I_A2056_1.ab - 175 samps
A
A m
d
dd
0
Relative Magnitude
Normalised Derivatives
Phase
15.1
15.2
15.3
15.4
15.5
15.6
15.7
15.8
15.9
16
0.9
0.4
-0.1
-0.6
-1.1
0
0.1
0.2
0.3
0.4
0.5
0.6
0.7
0.8
0.9
1

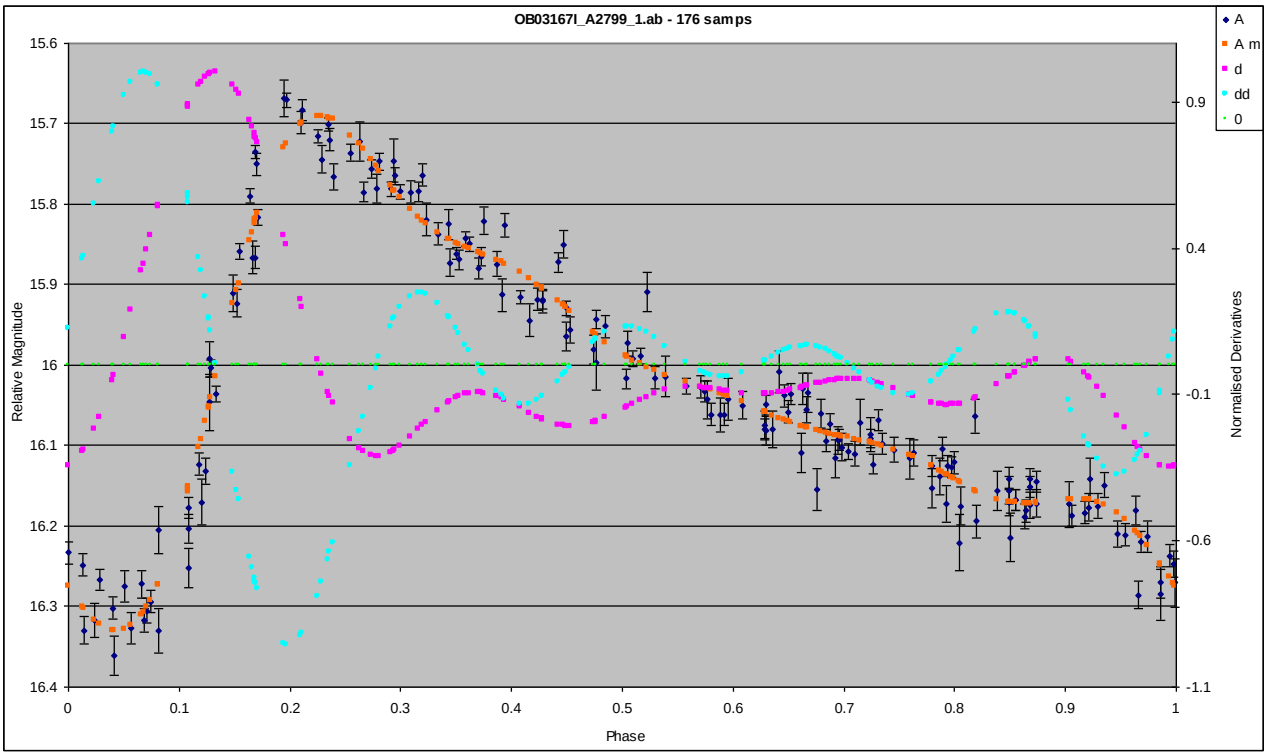
OB03167I_A2799_1.ab - 176 samps
A
A m
d
dd
0
Relative Magnitude
Normalised Derivatives
Phase
15.6
15.7
15.8
15.9
16
16.1
16.2
16.3
16.4
0.9
0.4
-0.1
-0.6
-1.1
0
0.1
0.2
0.3
0.4
0.5
0.6
0.7
0.8
0.9
1

For event OB03177I the fits image for telescope A, source of the data, is missing from the PLANET archive. An image and a co-ordinate transformation is available from telescope W for the same event, but the star 60 lies outside of the observing field in this case. Thus no finder chart or Gaia co-ordinate calibration has been accomplished.

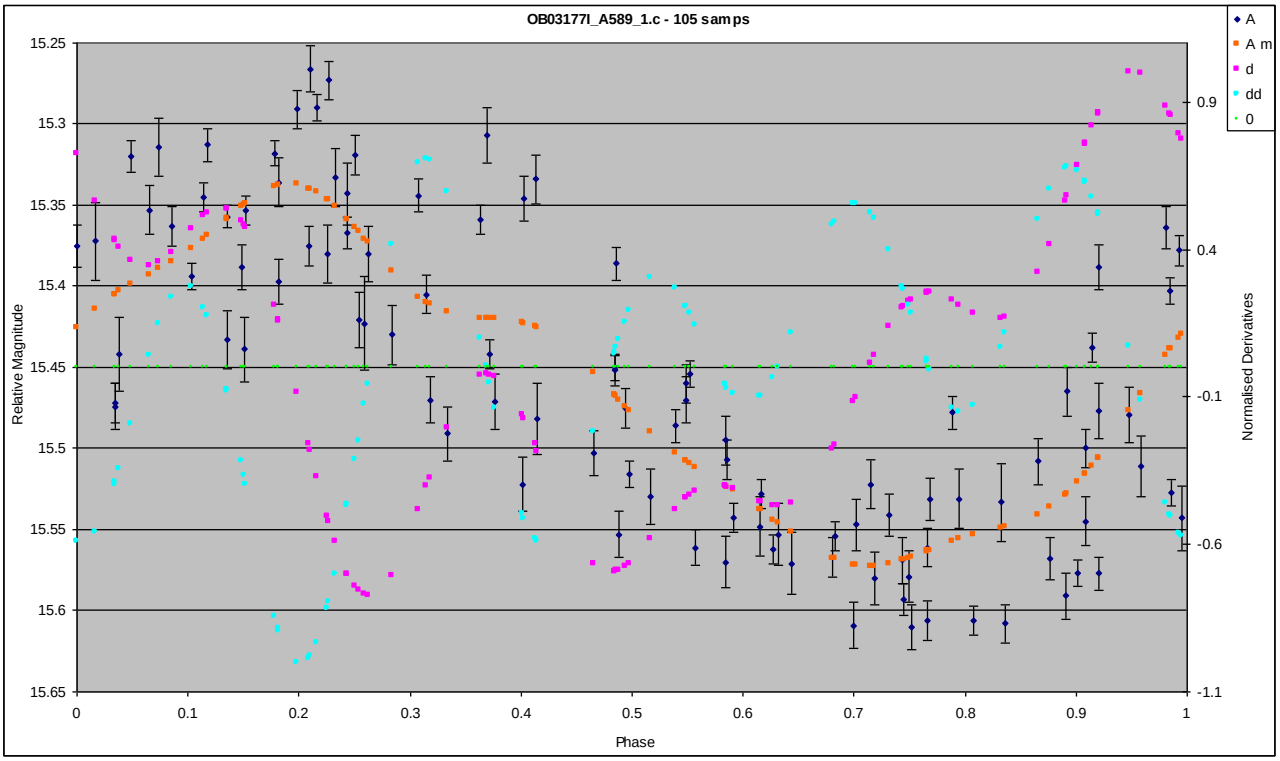

WOB03200I for event OB03200I ~ 5.15’ by 5.15’

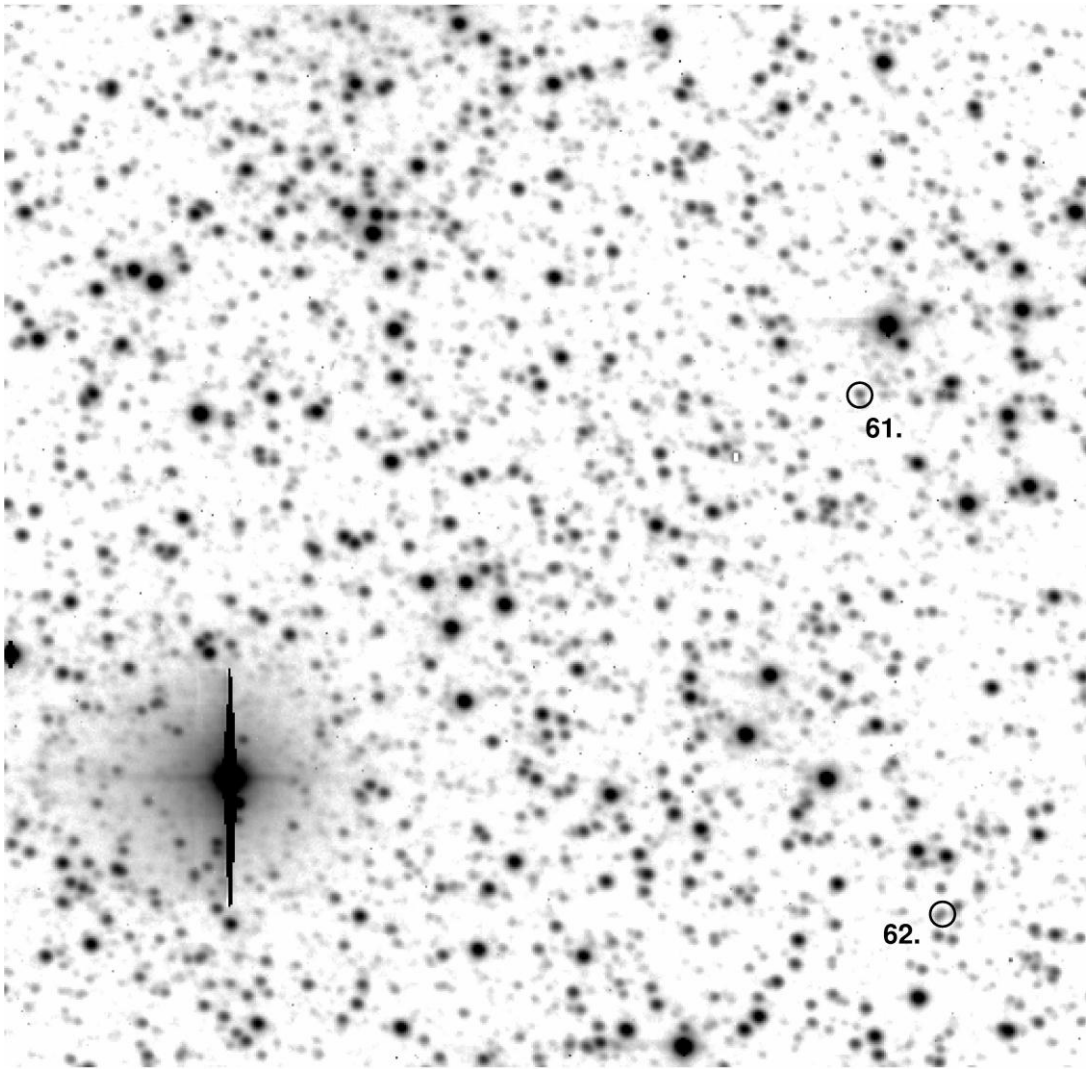

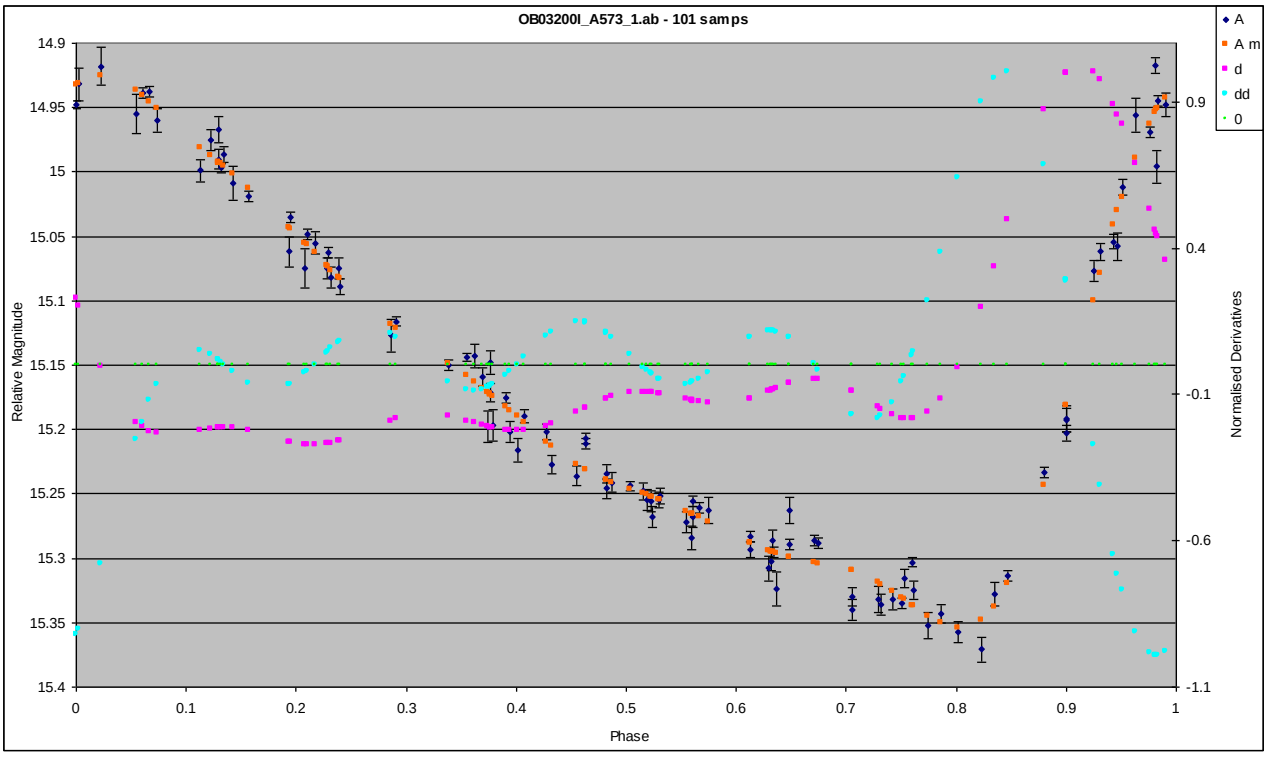

WOB03208I for event OB03208I ~ 5.15’ by 5.15’

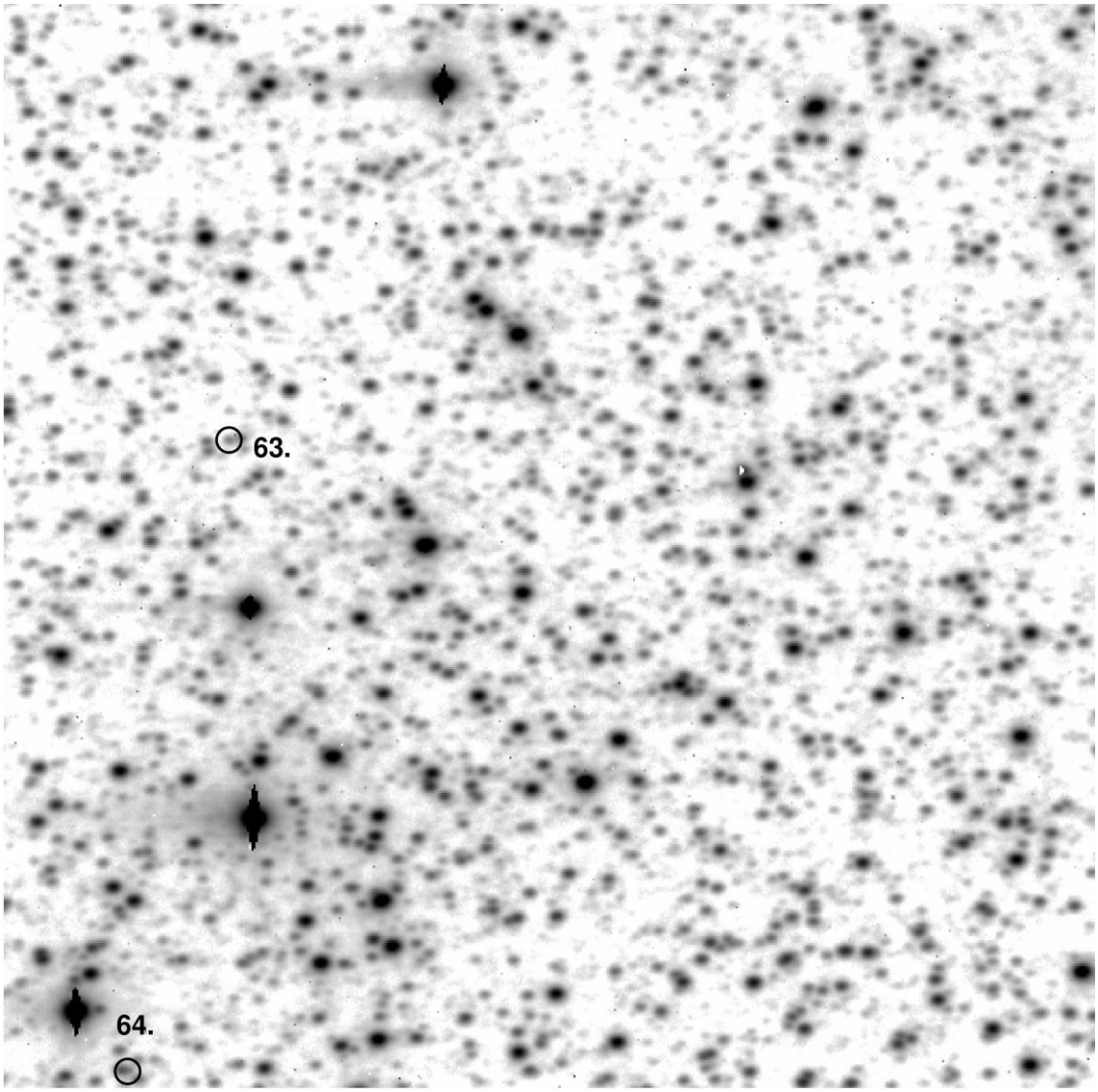

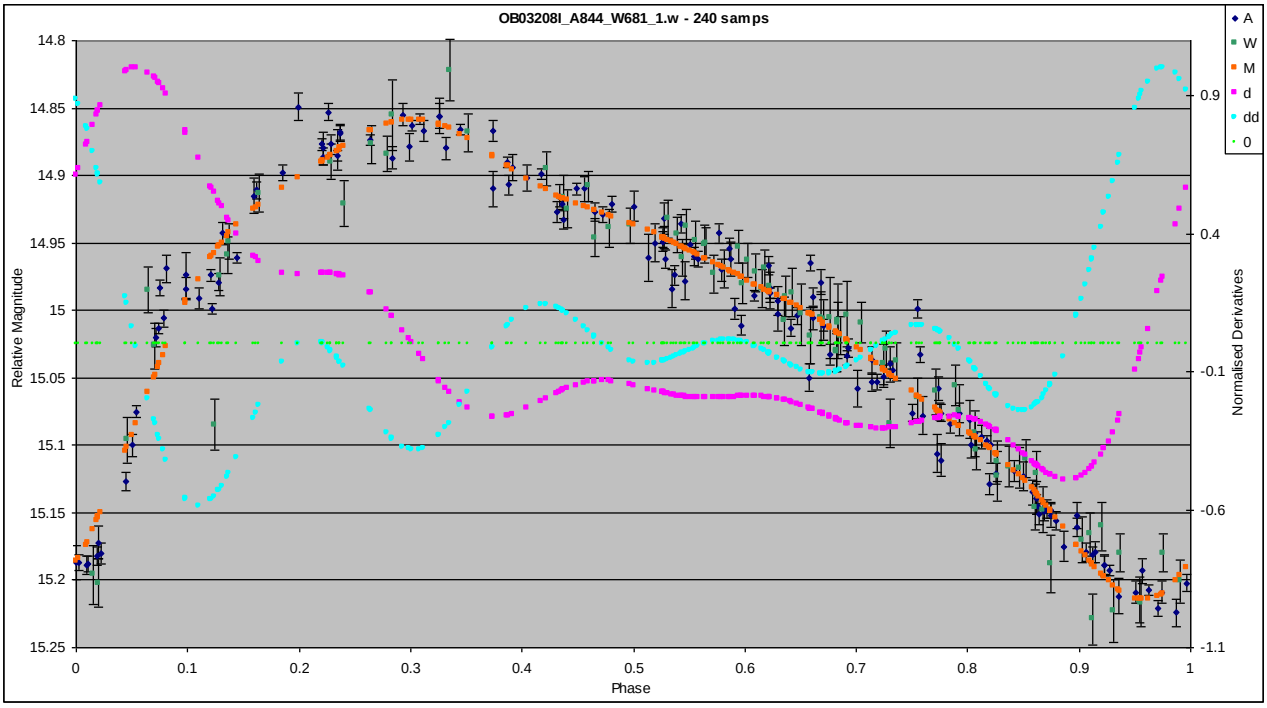

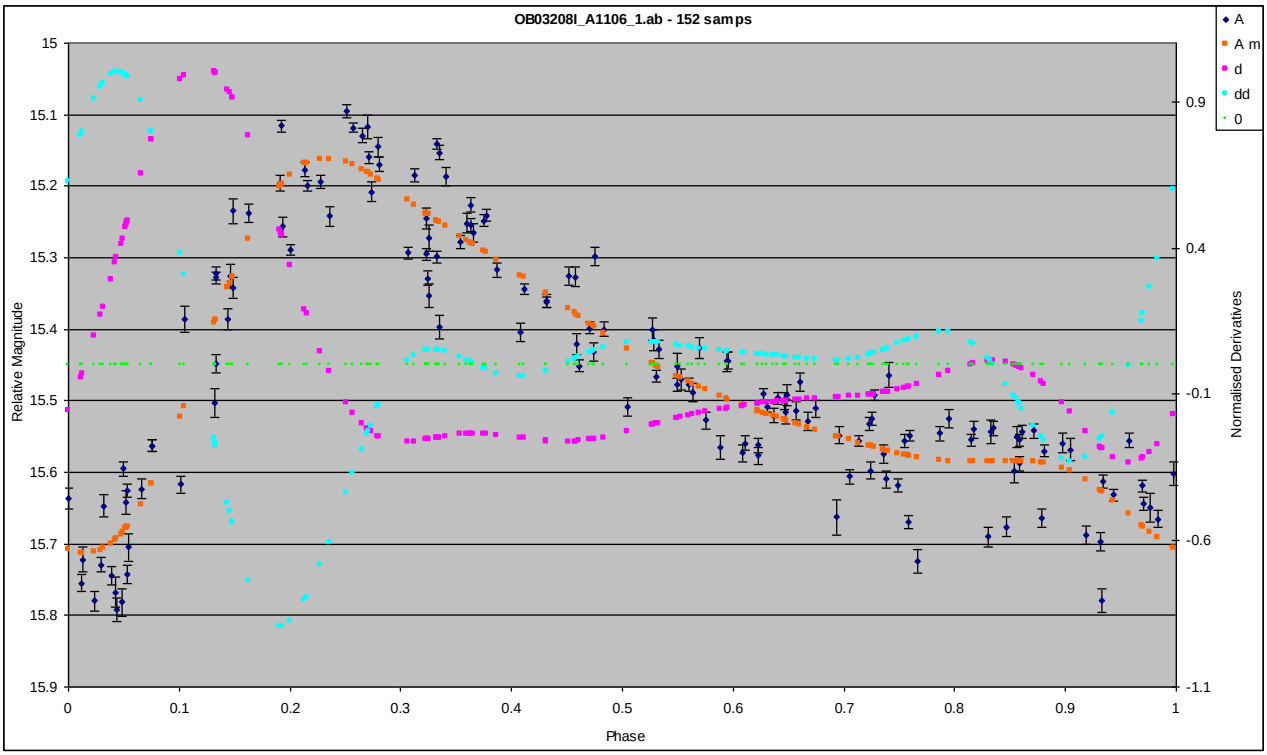

WOB03262I for event OB03262I ~ 5.15’ by 5.15’

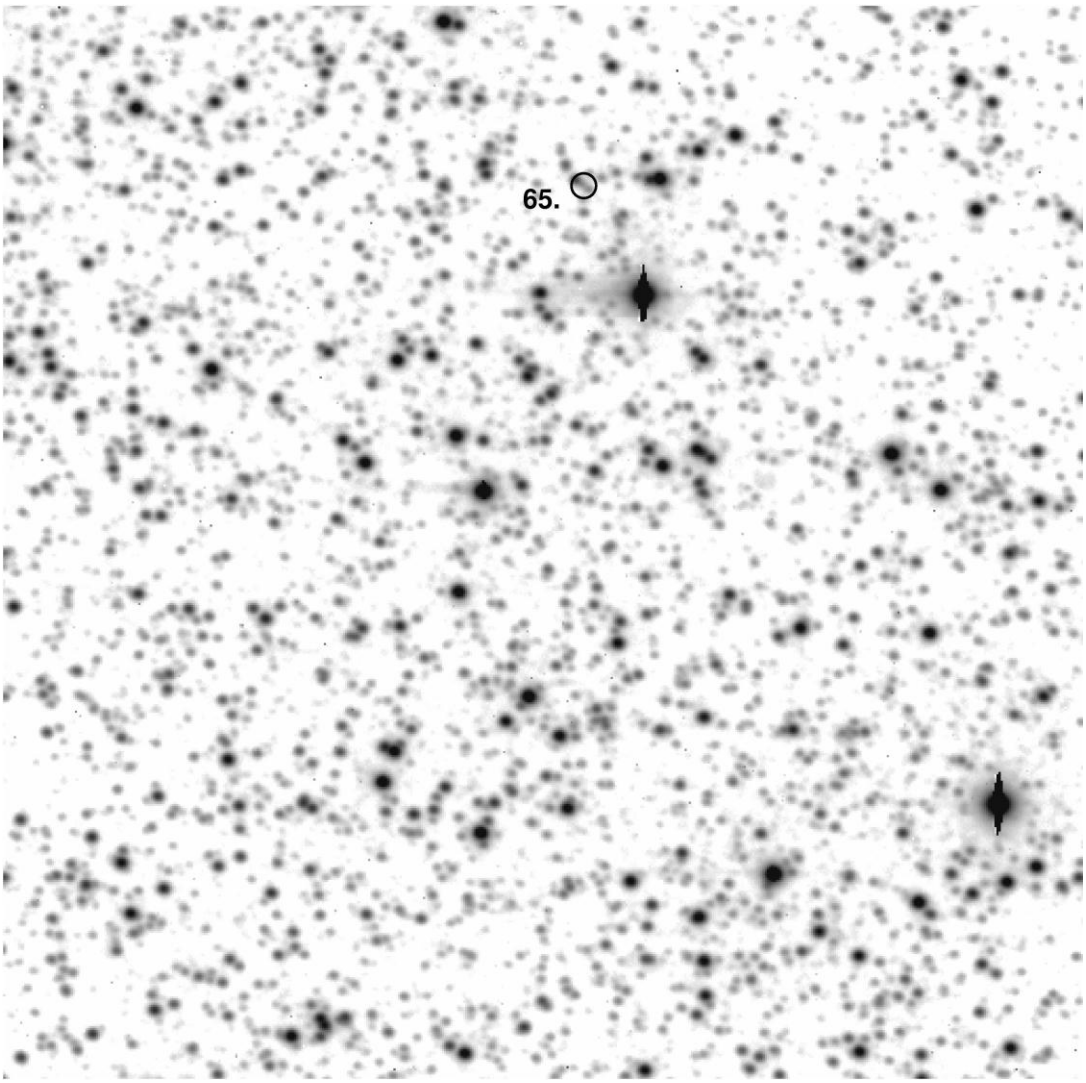

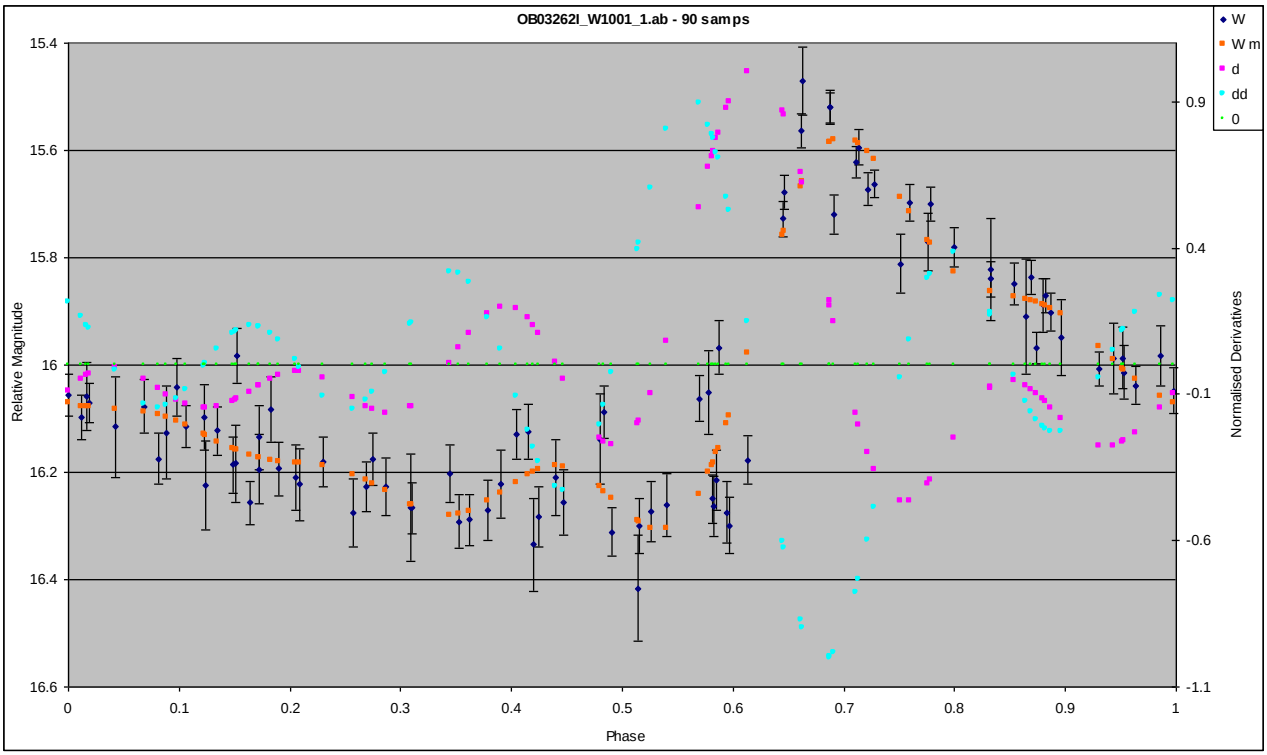

WKB02033I for event KB02033I ~ 5.15’ by 5.15’

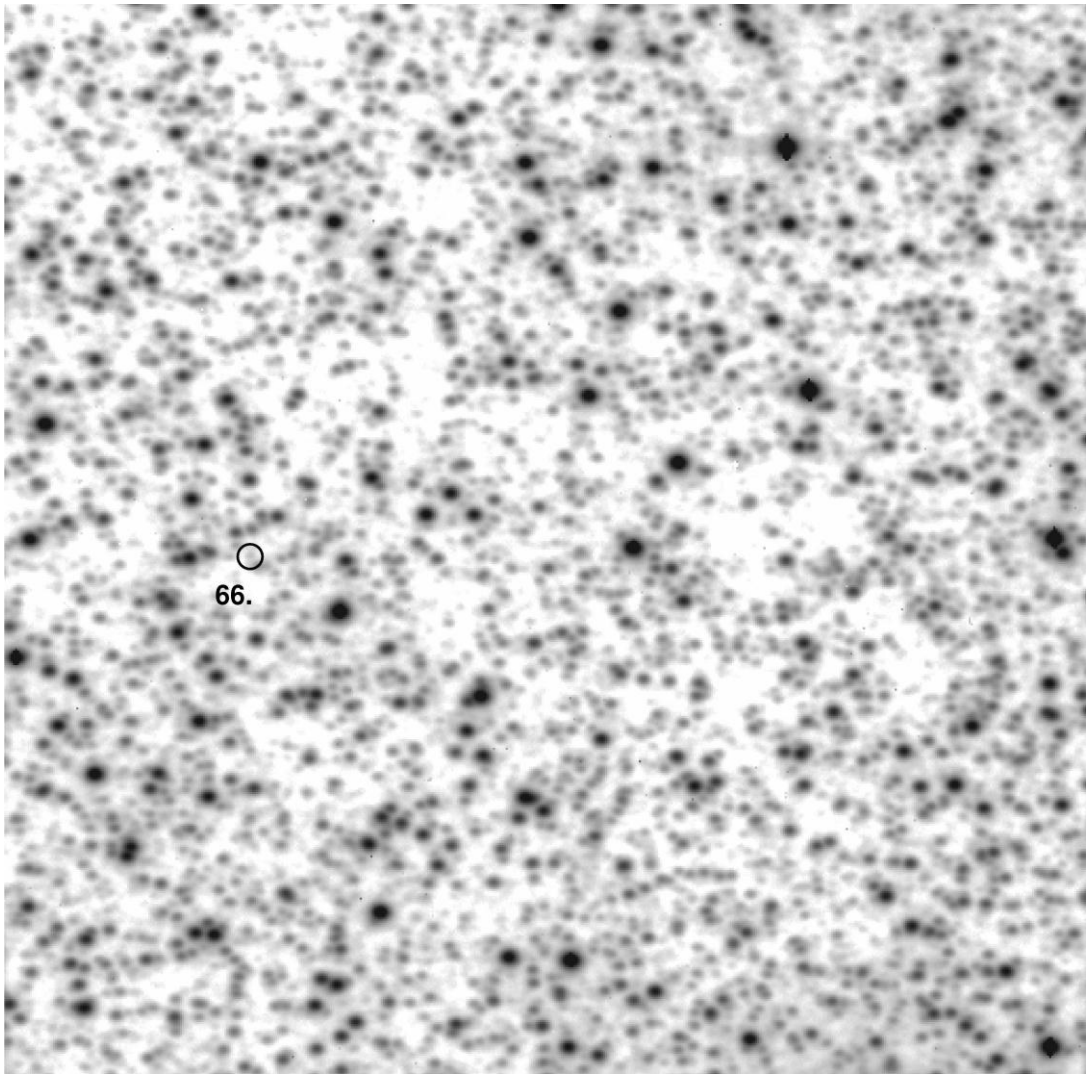

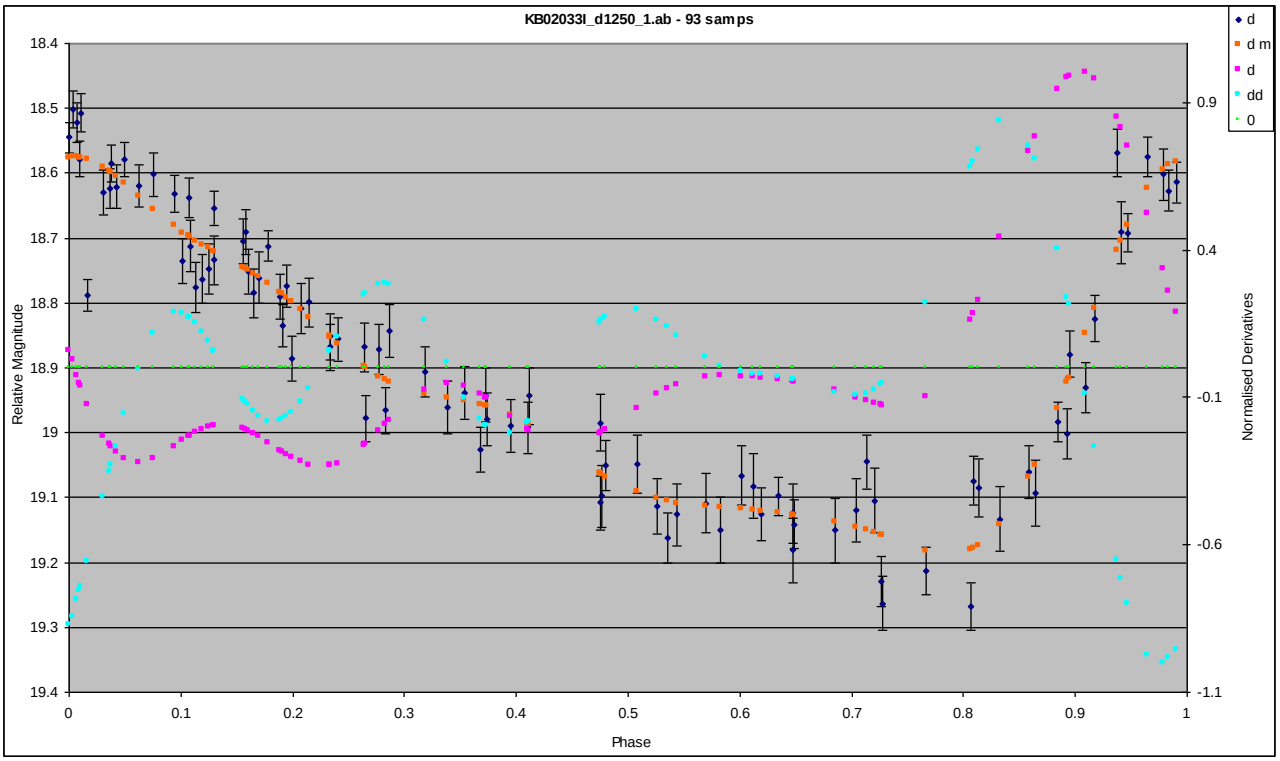

WOB02181I for event OB02181I ~ 5.15' by 5.15'

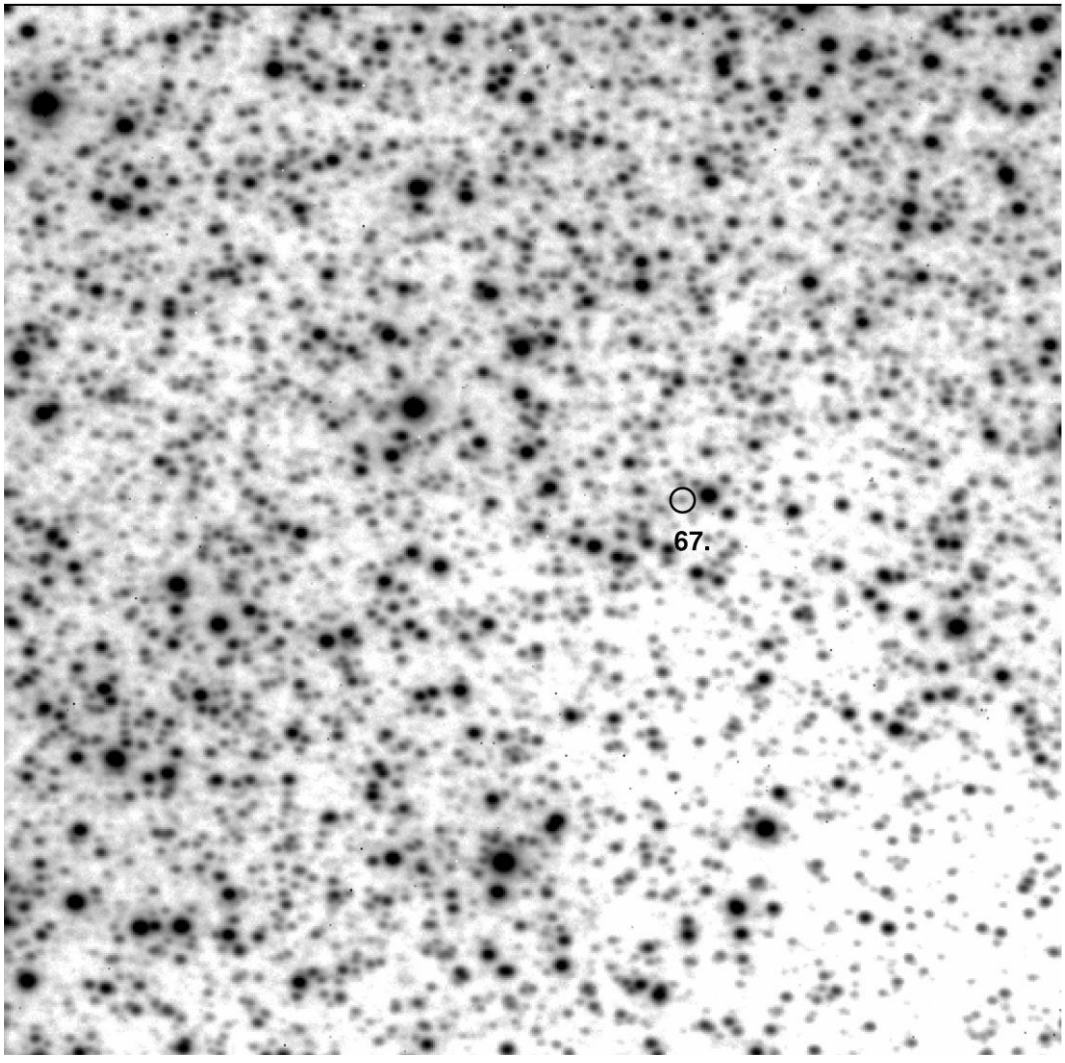

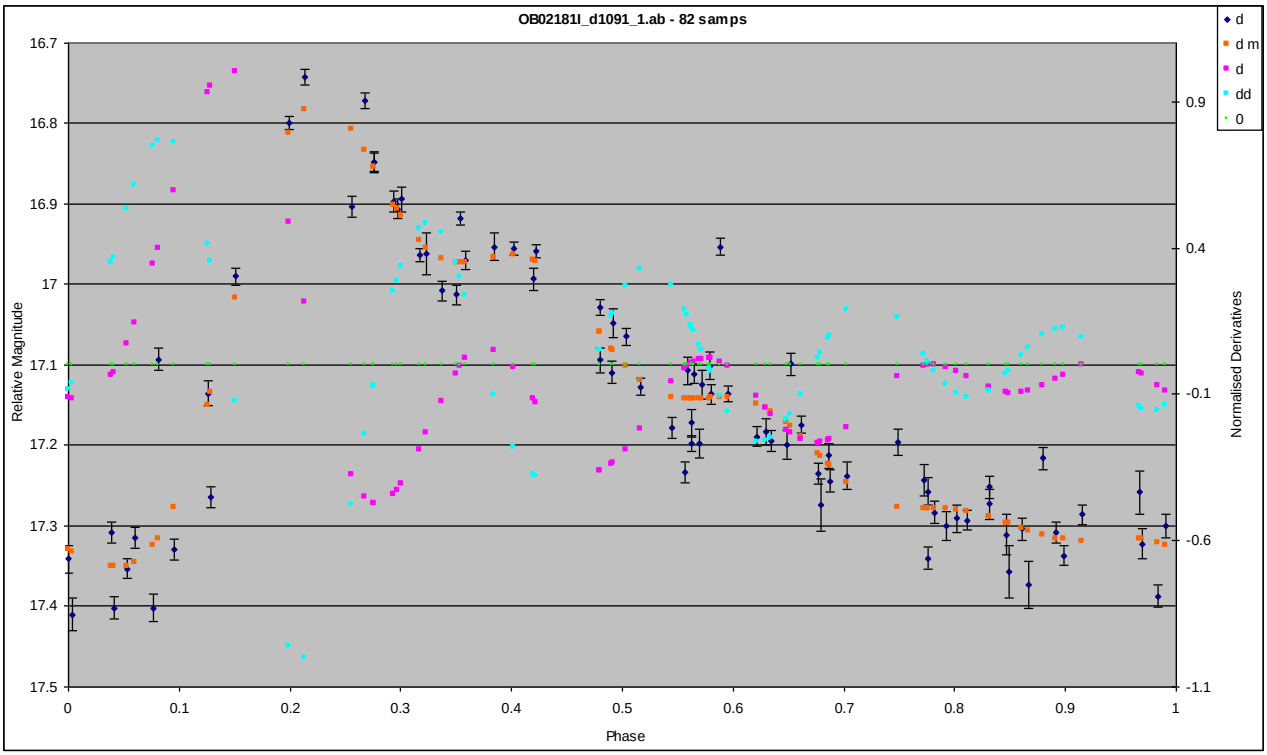
OB02181l_d1091_1.ab - 82 samps
d
d m
d
dd
0
Relative Magnitude
Normalised Derivatives
Phase
16.7
16.8
16.9
17
17.1
17.2
17.3
17.4
17.5
0.9
0.4
-0.1
-0.6
-1.1
0
0.1
0.2
0.3
0.4
0.5
0.6
0.7
0.8
0.9
1

ZOB05153I for event OB05153I ~ 3.91’ by 3.91’

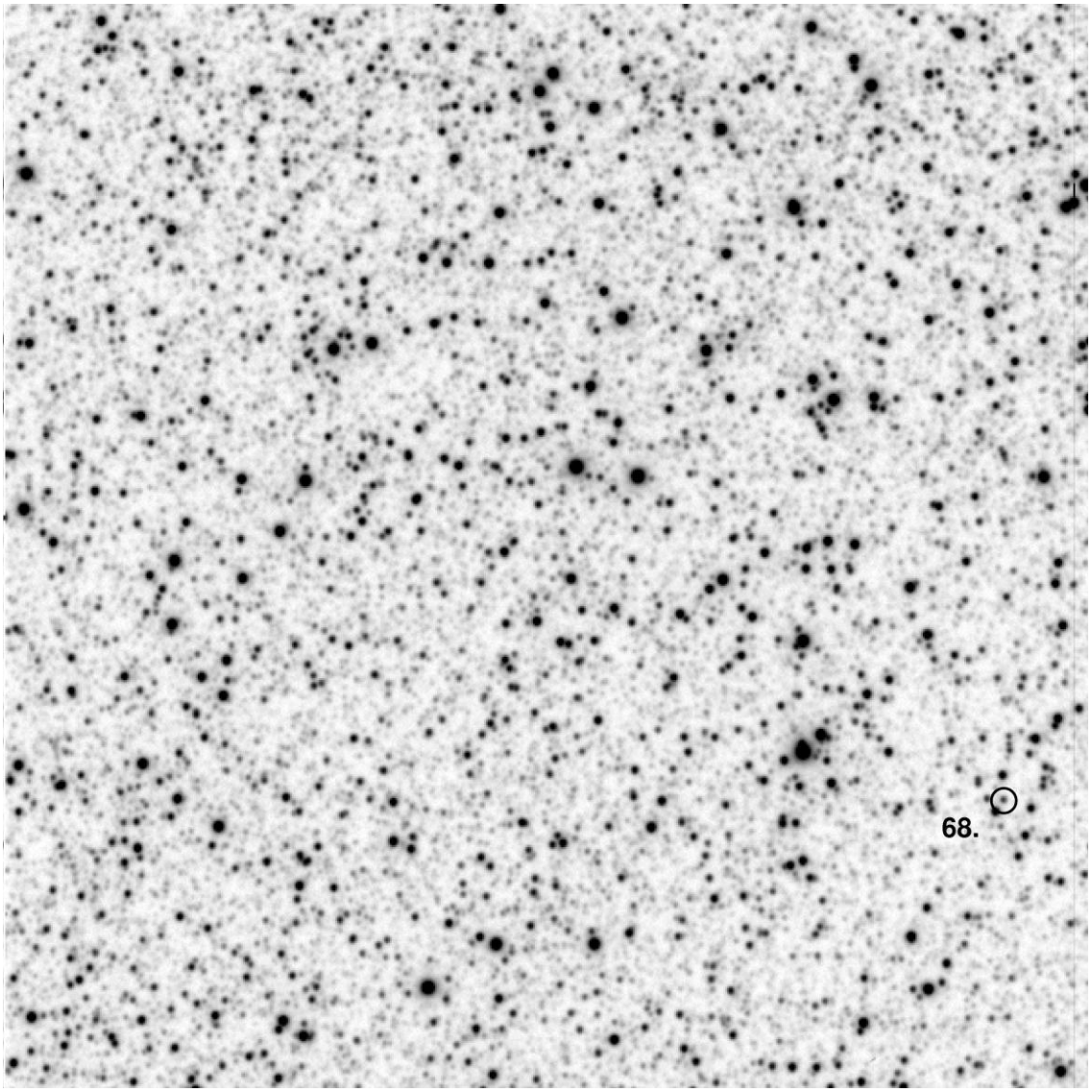

WOB05099I for event OB05099I ~ 5.15’ by 5.15’

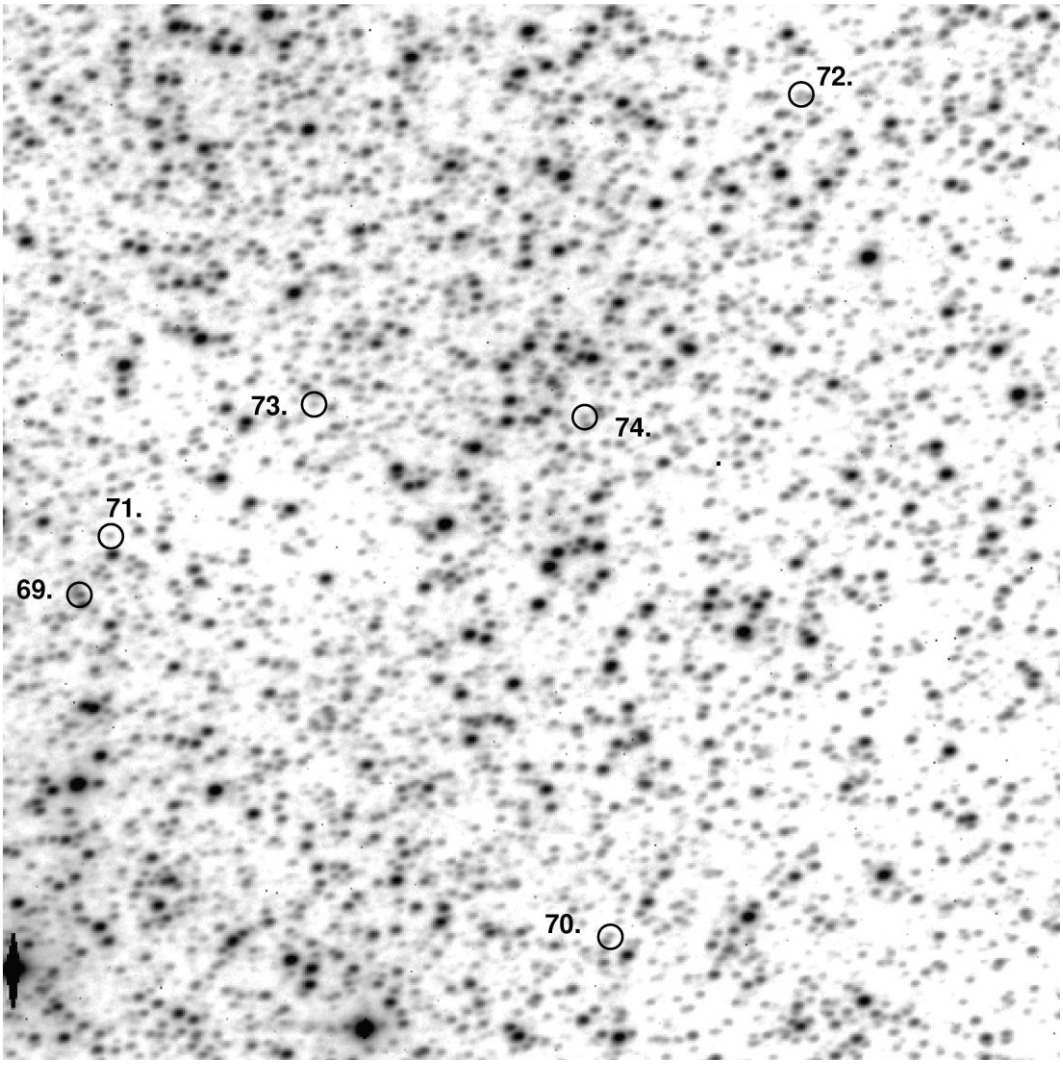

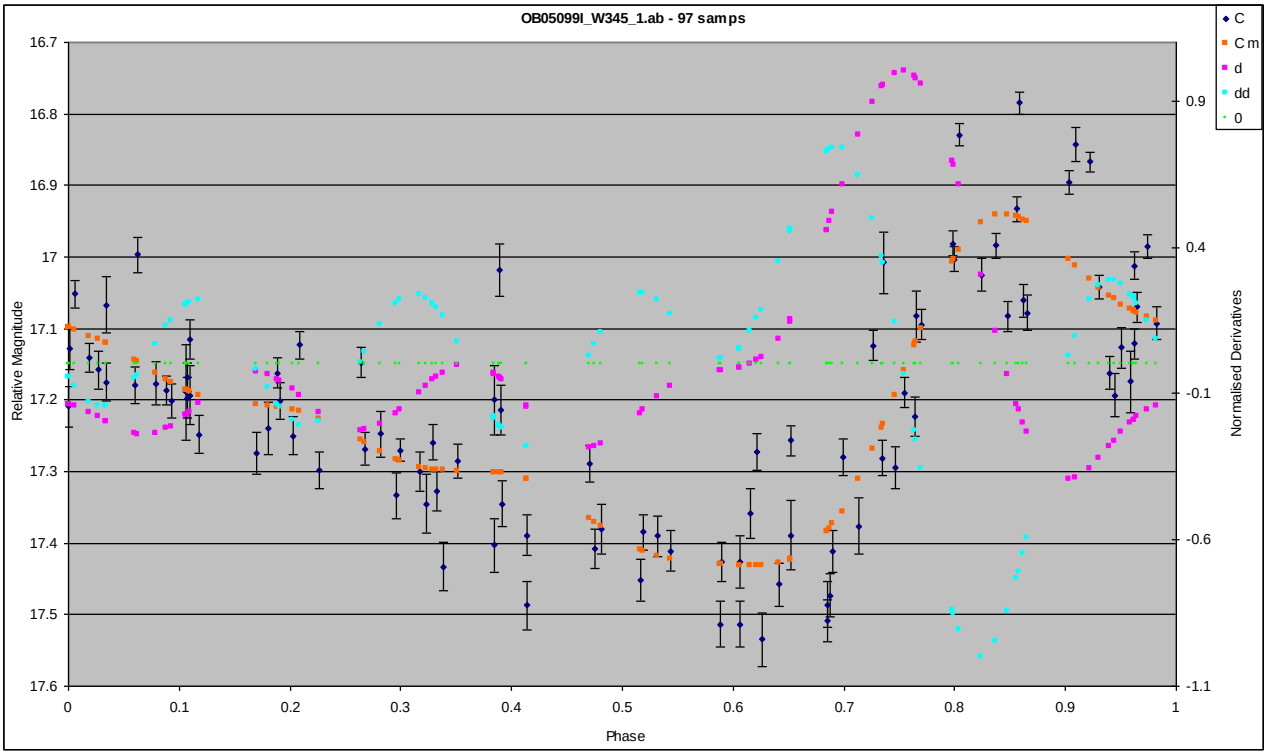

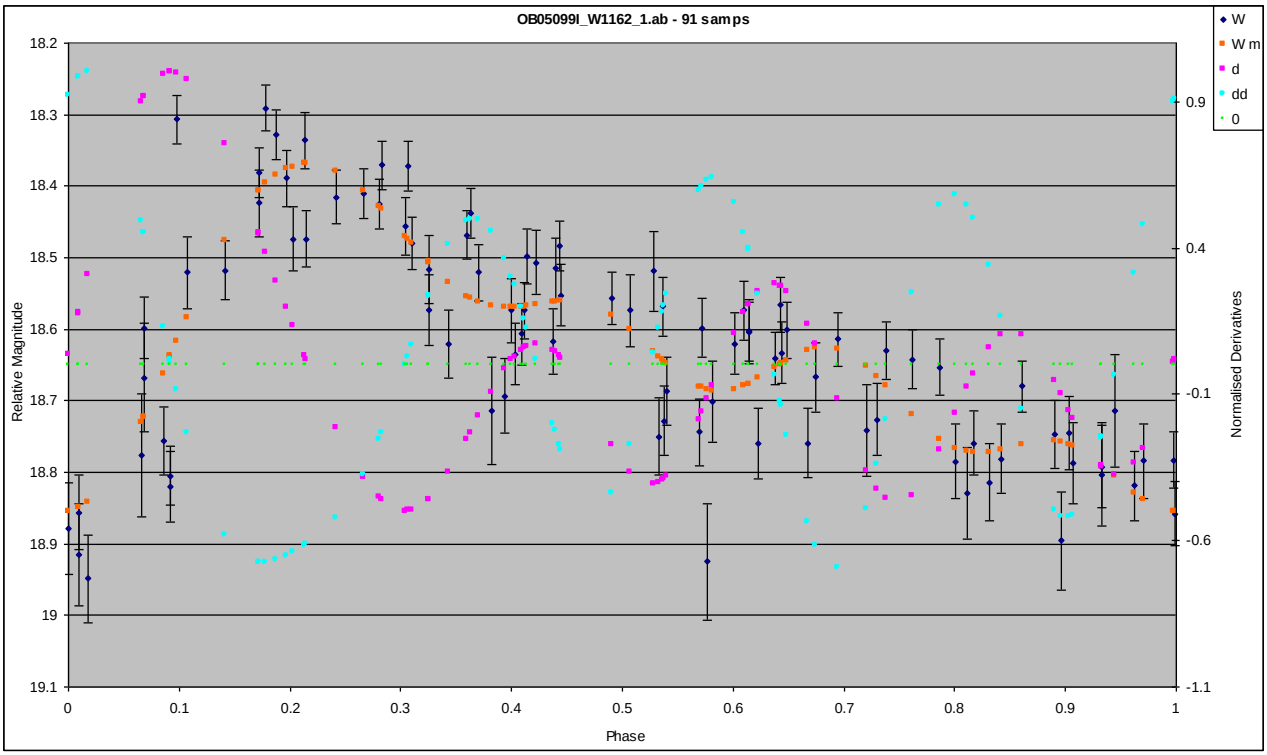
OB05099I_W1162_1.ab - 91 samps
W
W m
d
dd
0
Relative Magnitude
Normalised Derivatives
Phase
18.2
18.3
18.4
18.5
18.6
18.7
18.8
18.9
19
19.1
0.9
0.4
-0.1
-0.6
-1.1
0
0.1
0.2
0.3
0.4
0.5
0.6
0.7
0.8
0.9
1

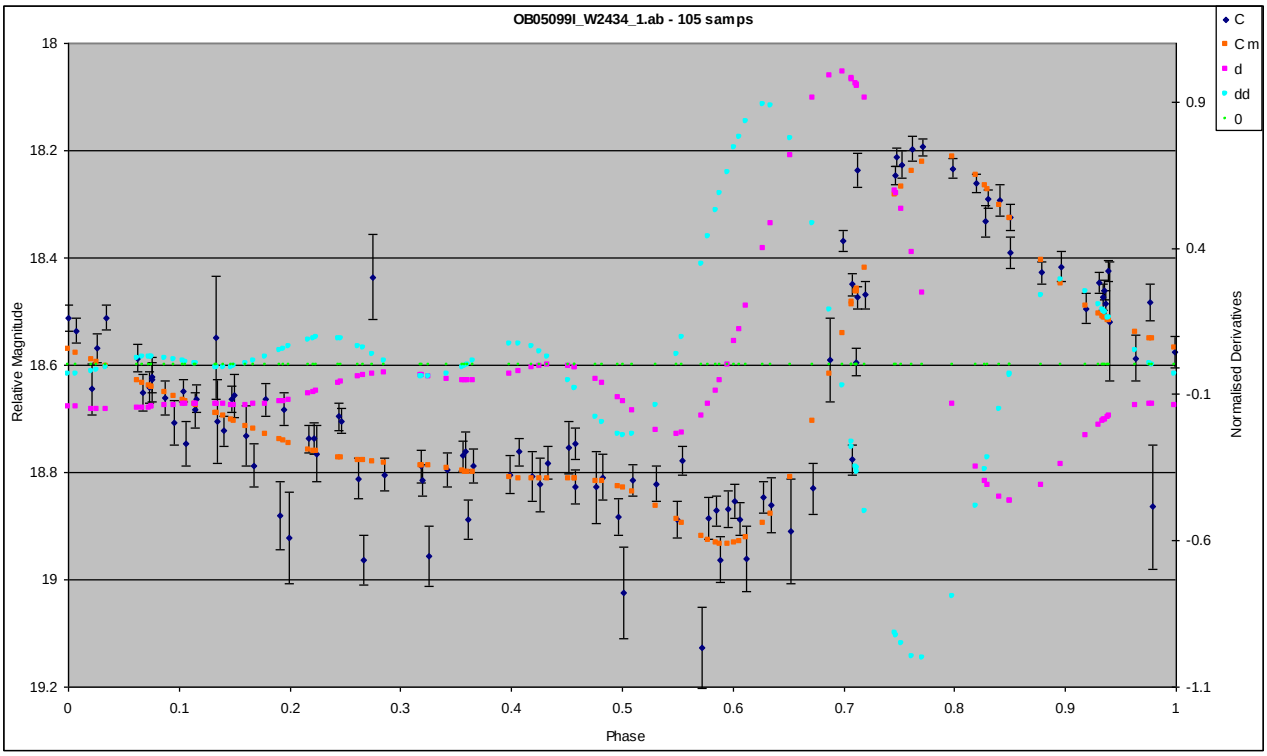
OB05099I_W2434_1.ab - 105 samps
C
C m
d
dd
0
Relative Magnitude
Normalised Derivatives
Phase
18
18.2
18.4
18.6
18.8
19
19.2
0.9
0.4
-0.1
-0.6
-1.1
0
0.1
0.2
0.3
0.4
0.5
0.6
0.7
0.8
0.9
1

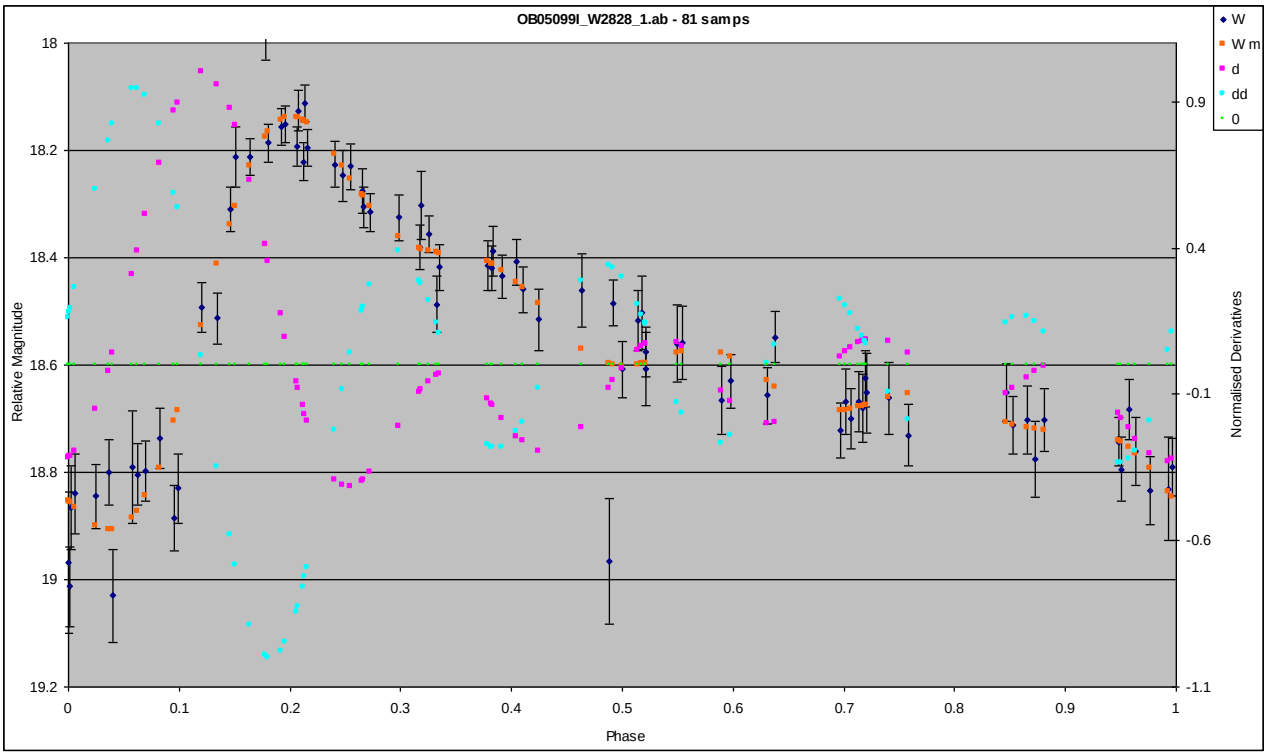
OB05099I_W2828_1.ab - 81 samps
W
W m
d
dd
0
Relative Magnitude
Normalised Derivatives
Phase
18
18.2
18.4
18.6
18.8
19
19.2
0.9
0.4
-0.1
-0.6
-1.1
0
0.1
0.2
0.3
0.4
0.5
0.6
0.7
0.8
0.9
1

ZOB05304I for event OB05304I ~ 3.91’ by 3.91’

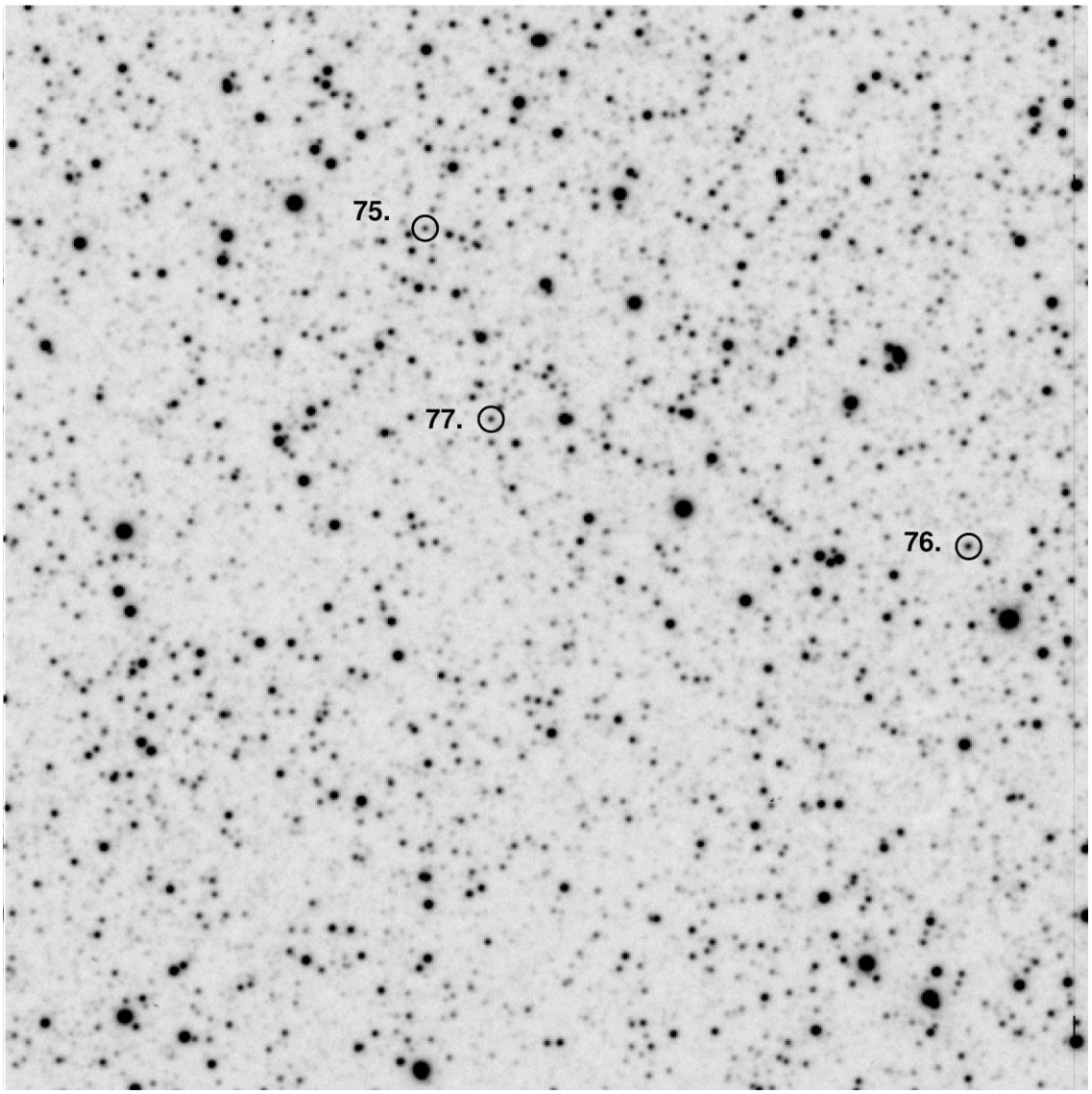

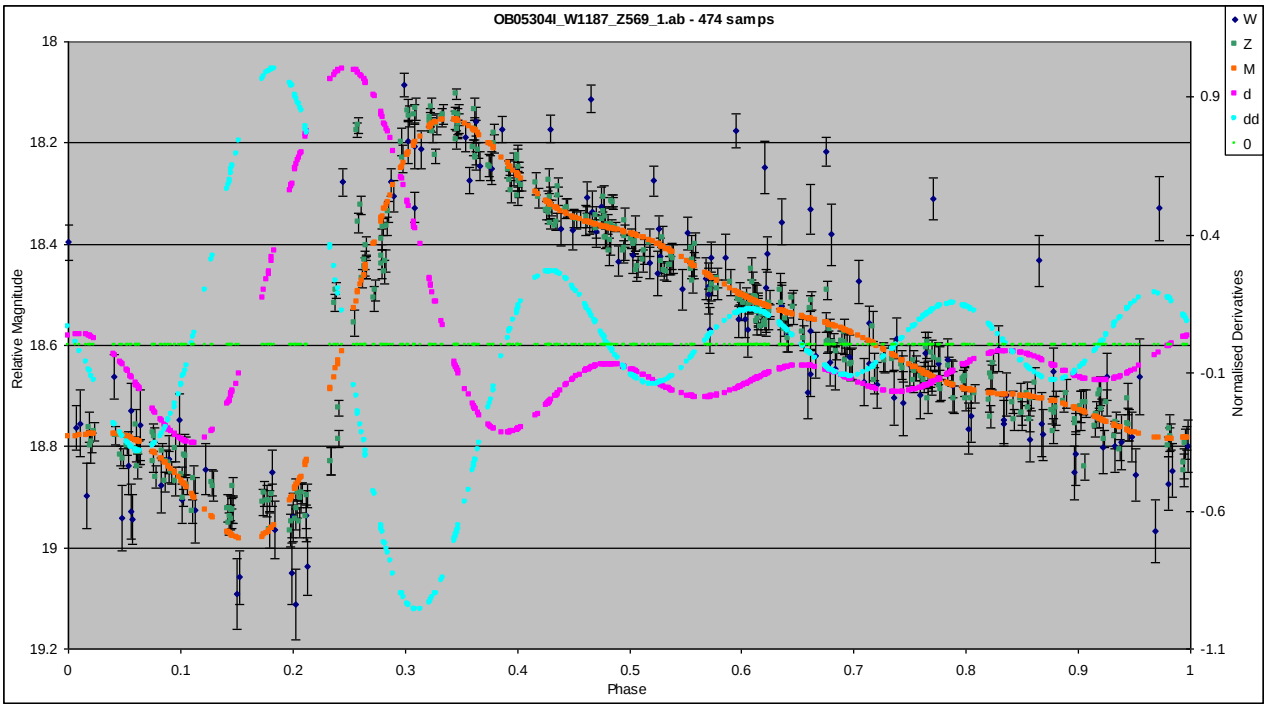
OB05304I_W1187_Z569_1.ab - 474 samps
W
Z
M
d
dd
0
Relative Magnitude
Normalised Derivatives
Phase
18
18.2
18.4
18.6
18.8
19
19.2
0.9
0.4
-0.1
-0.6
-1.1
0
0.1
0.2
0.3
0.4
0.5
0.6
0.7
0.8
0.9
1

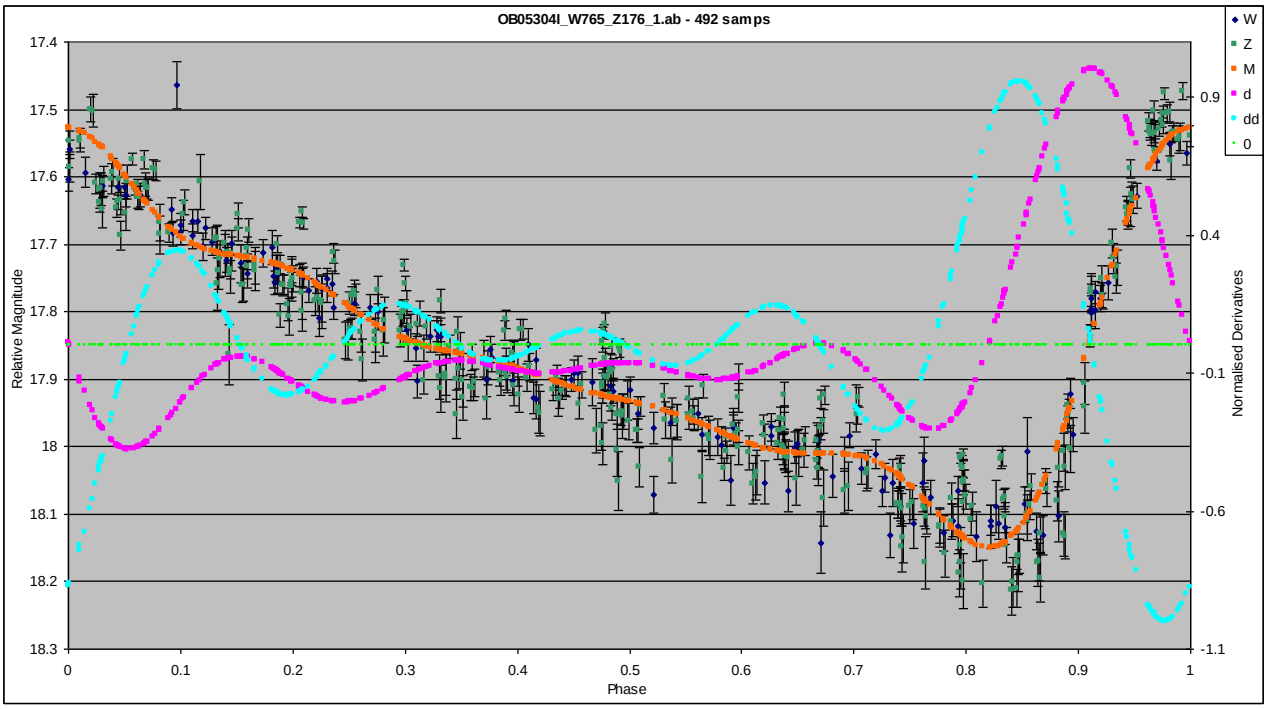
OB05304I_W765_Z176_1.ab - 492 samps
W
Z
M
d
dd
0
Relative Magnitude
Normalised Derivatives
Phase
17.4
17.5
17.6
17.7
17.8
17.9
18
18.1
18.2
18.3
0.9
0.4
-0.1
-0.6
-1.1
0
0.1
0.2
0.3
0.4
0.5
0.6
0.7
0.8
0.9
1

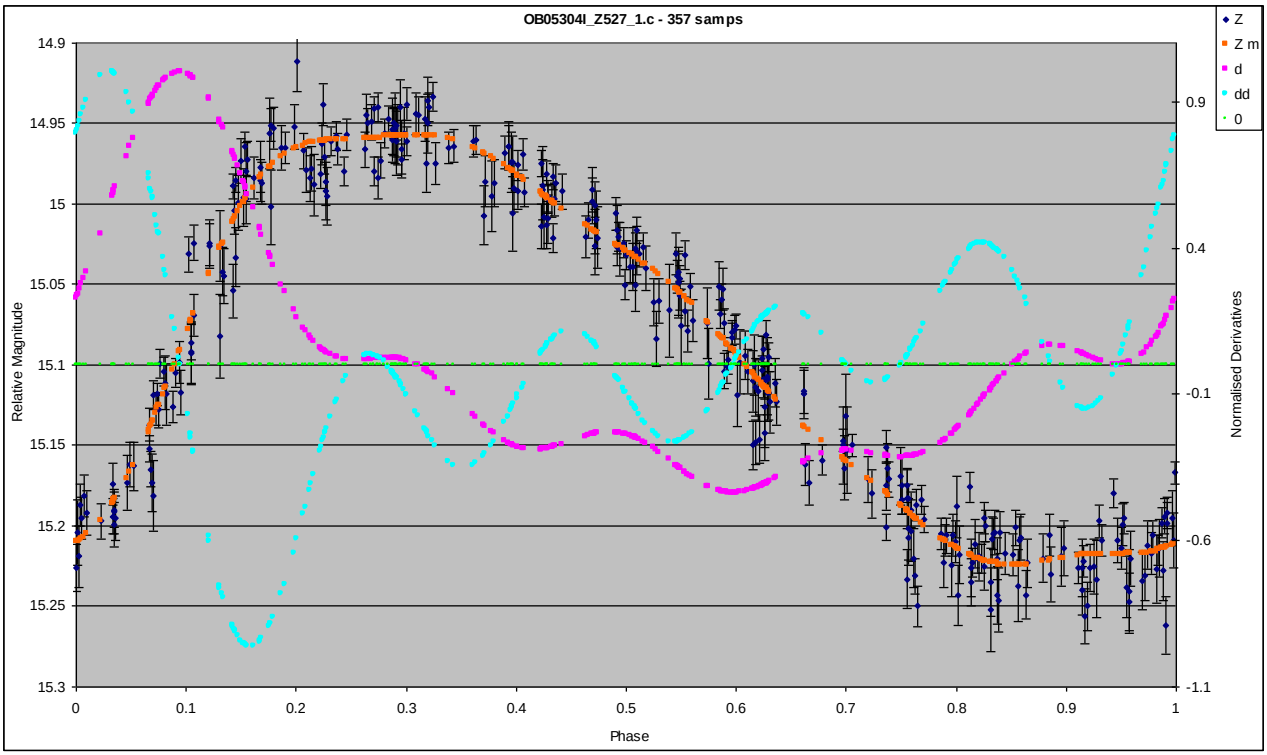

ZOB05018I for event OB05018I ~ 3.91’ by 3.91’

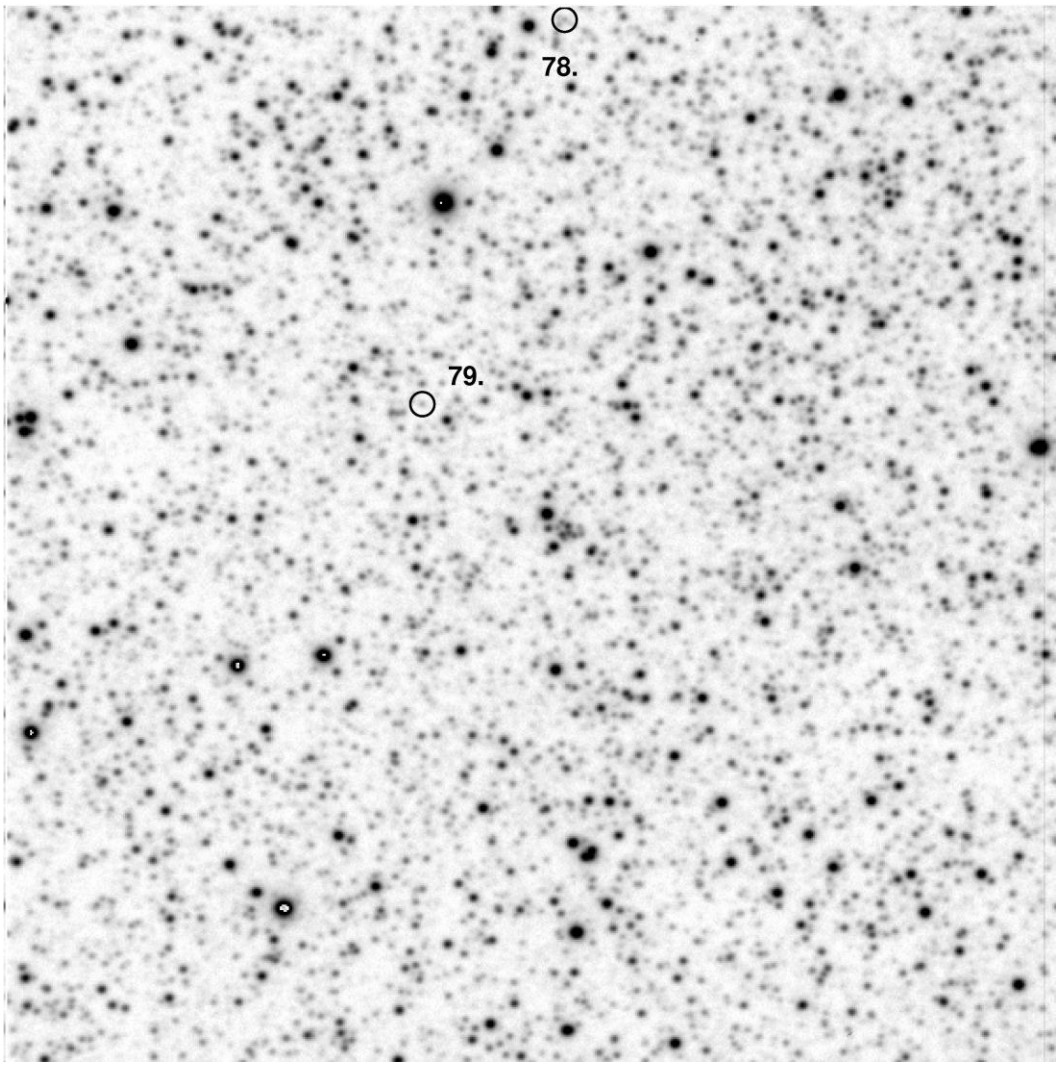

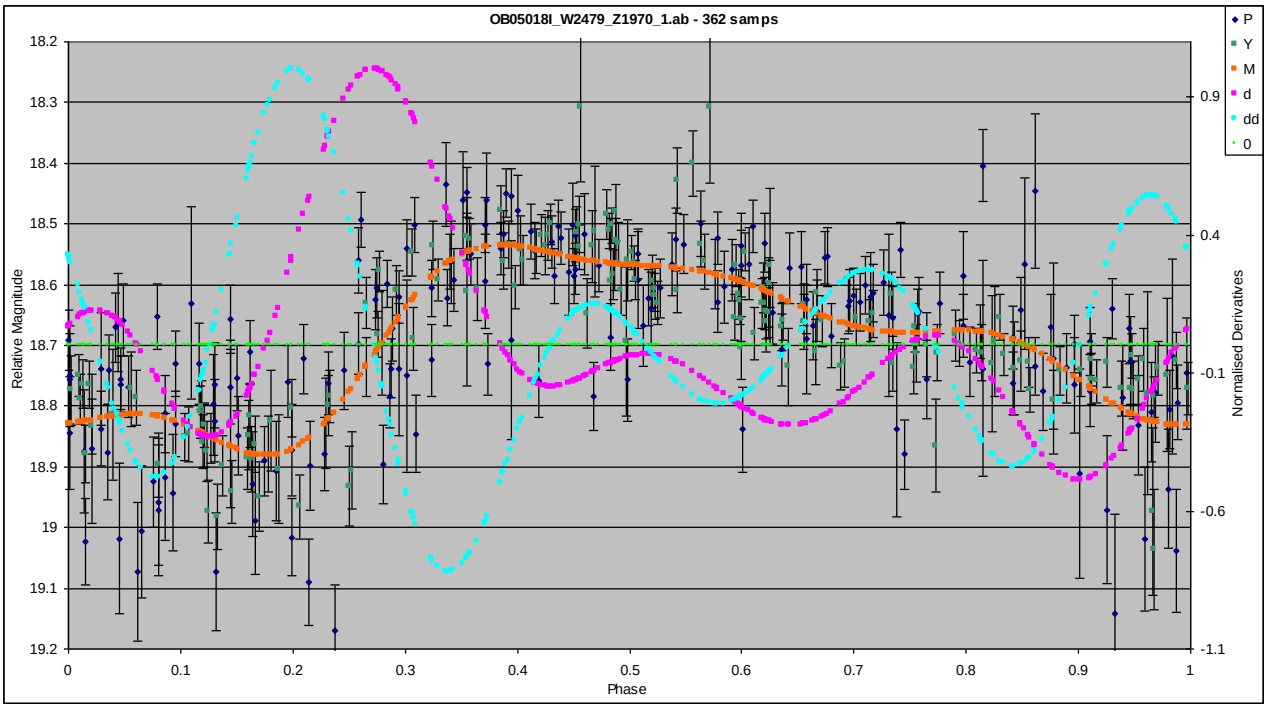
OB05018I_W2479_Z1970_1.ab - 362 samps
Relative Magnitude
Normalised Derivatives
Phase
P
Y
M
d
dd
0

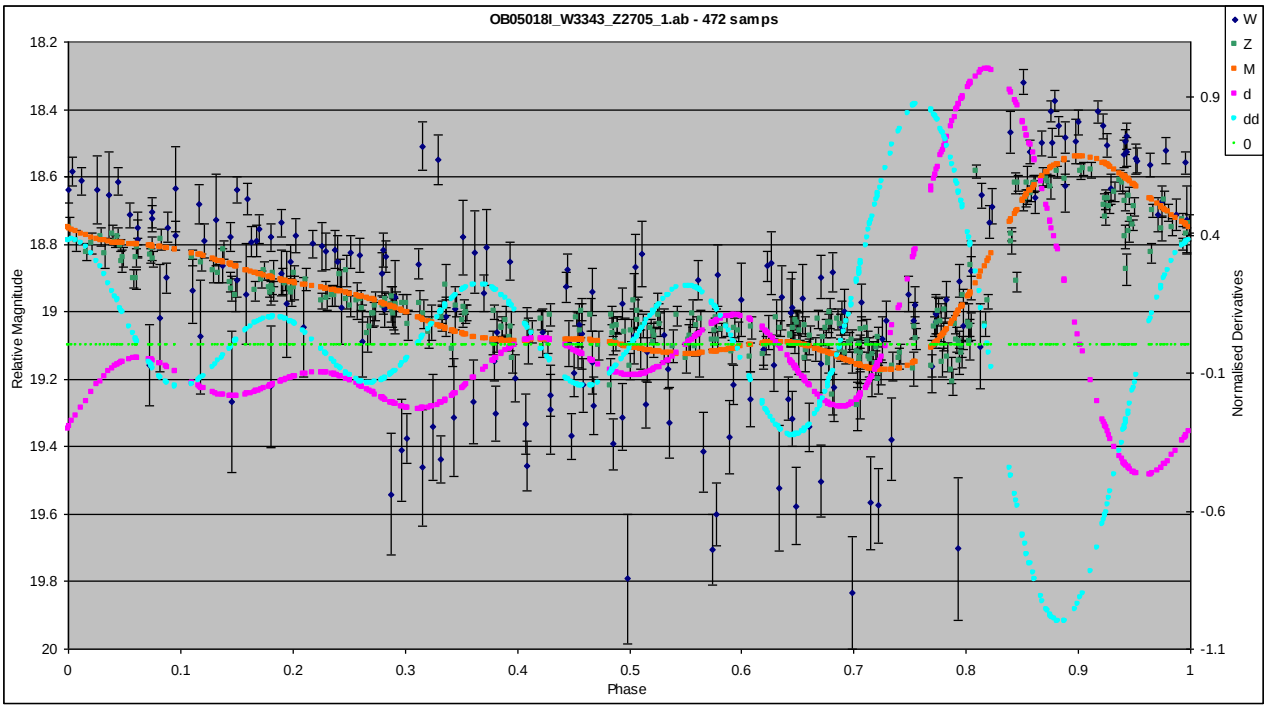
OB05018I_W3343_Z2705_1.ab - 472 samps
Relative Magnitude
Normalised Derivatives
Phase
W
Z
M
d
dd
0

ZOB05216I for event OB05216I ~ 3.91’ by 3.91’

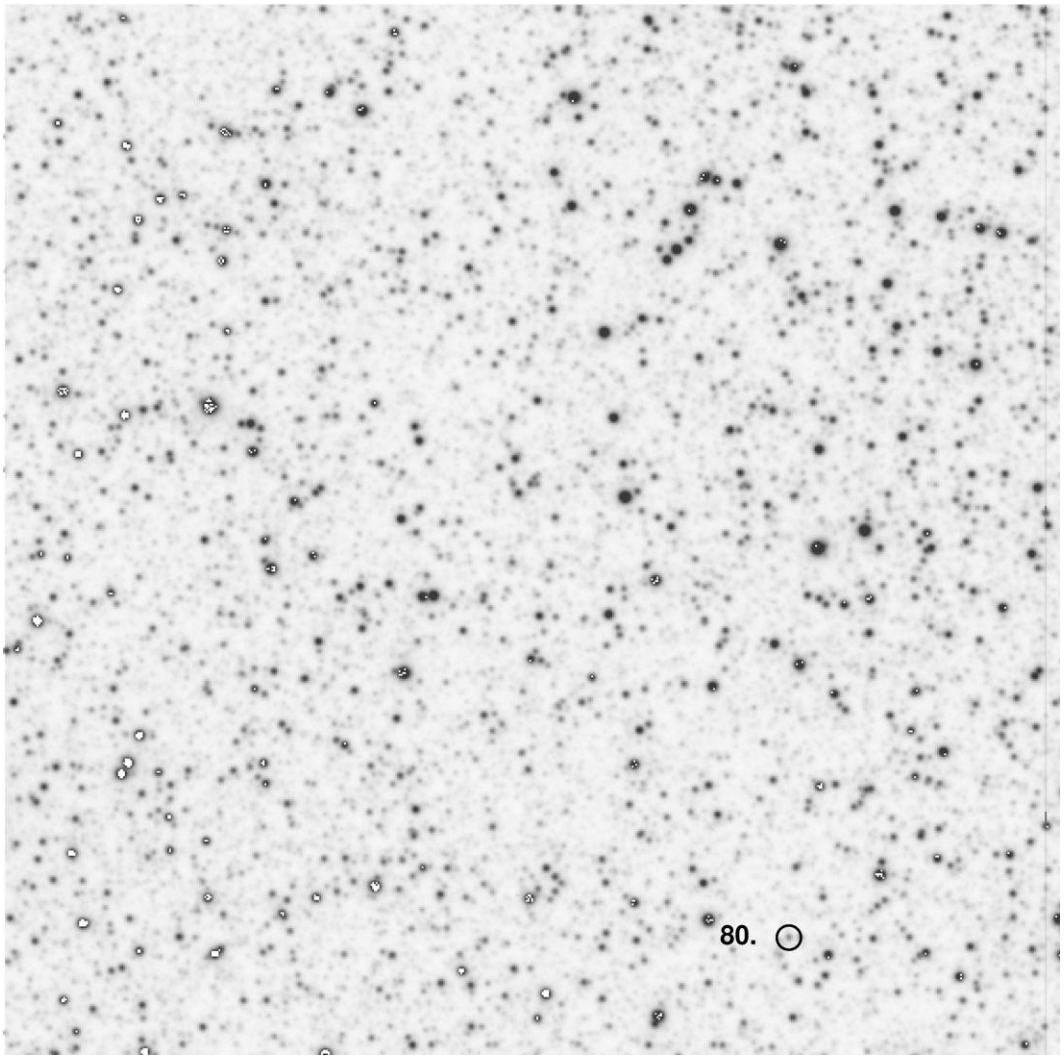

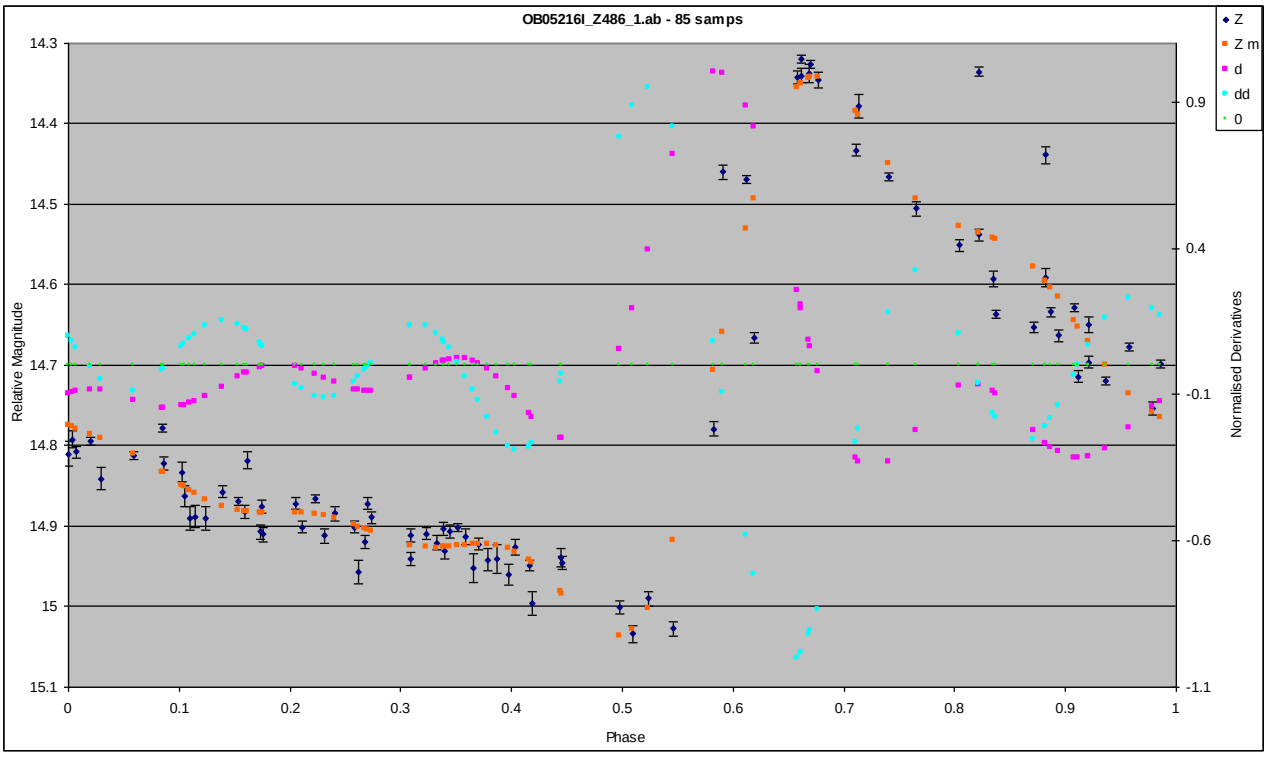

WOB05226I for event OB05226I ~ 5.15’ by 5.15’

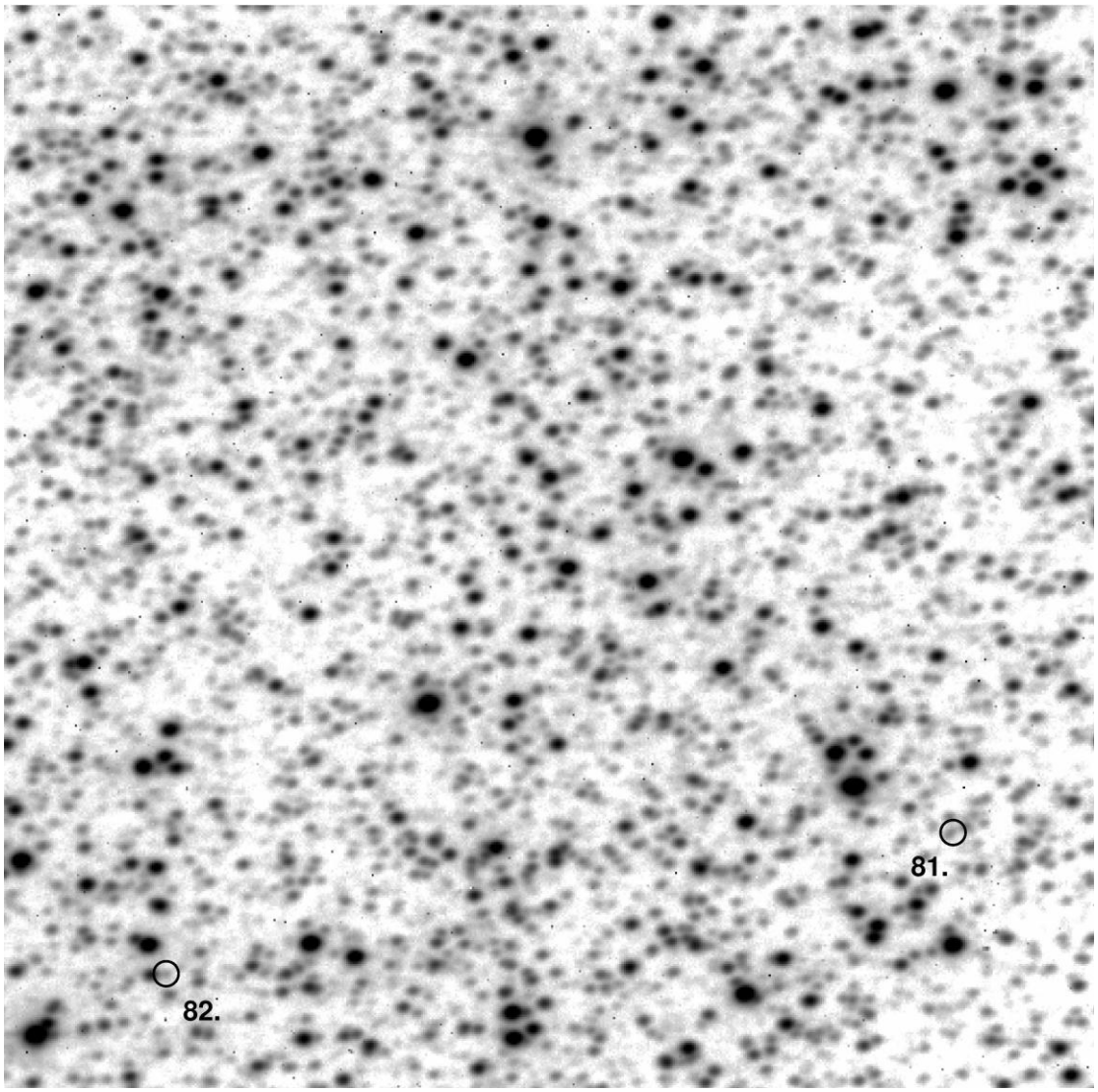

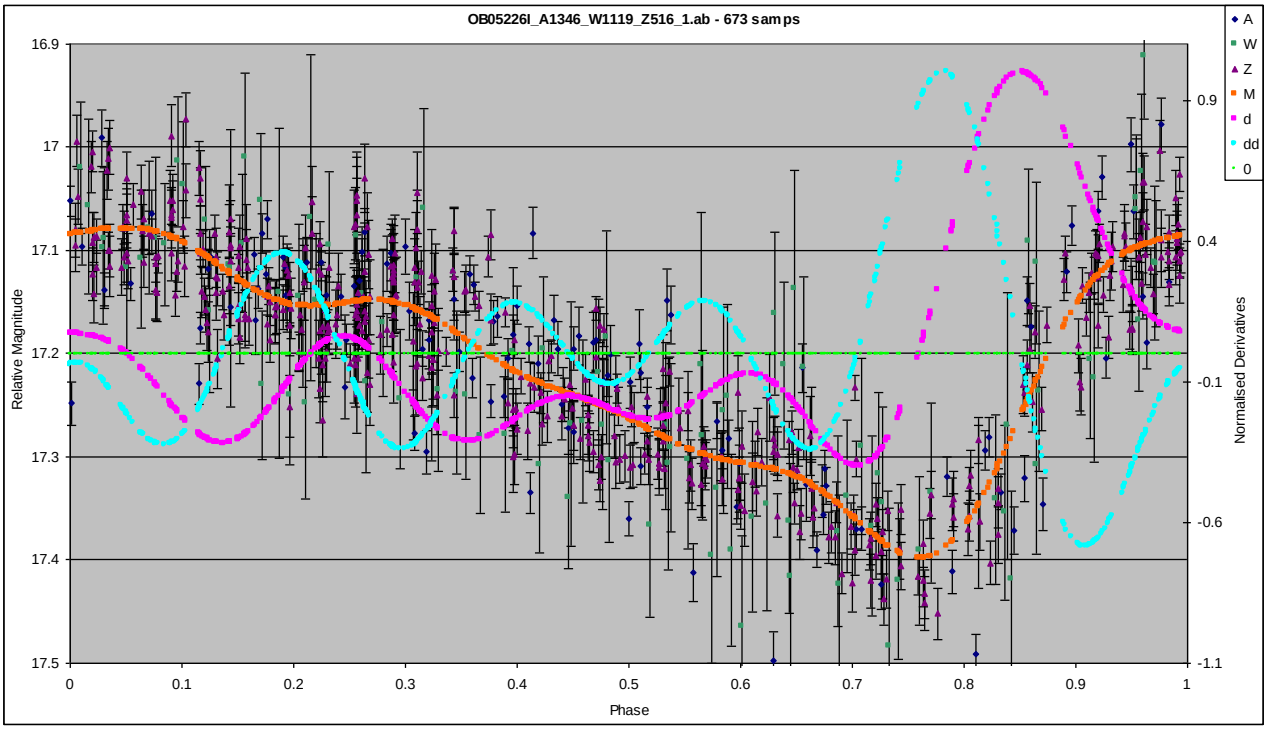

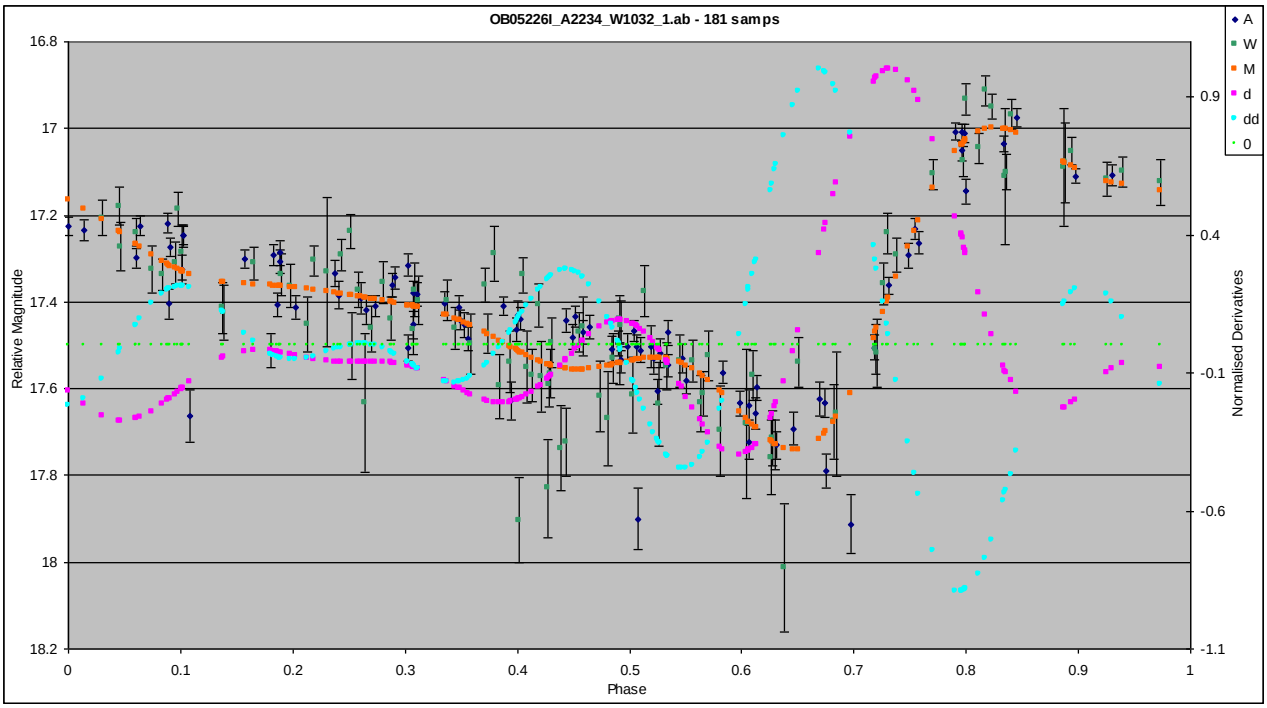

ZOB05259I for event OB05259I ~ 3.91’ by 3.91’

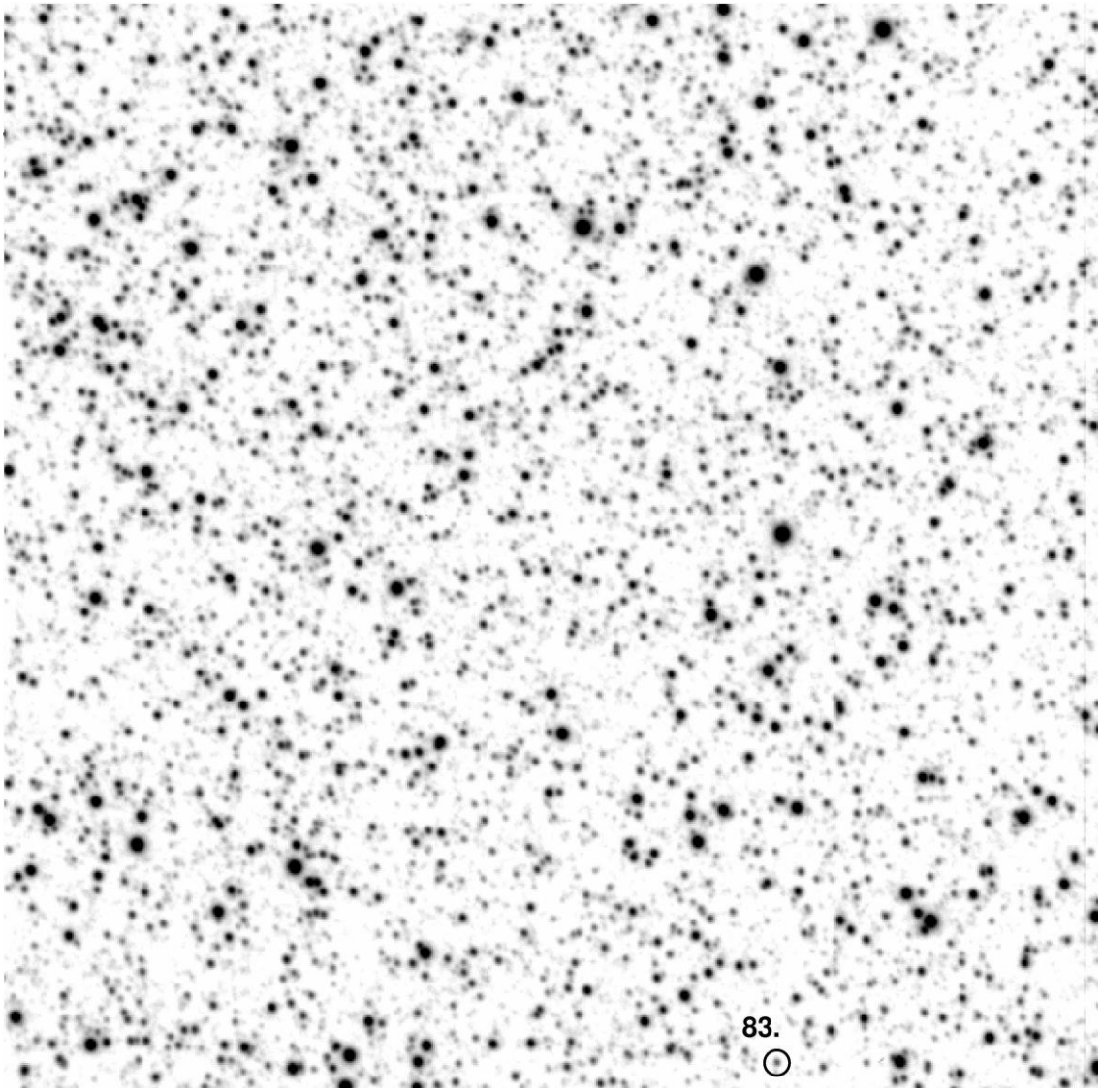

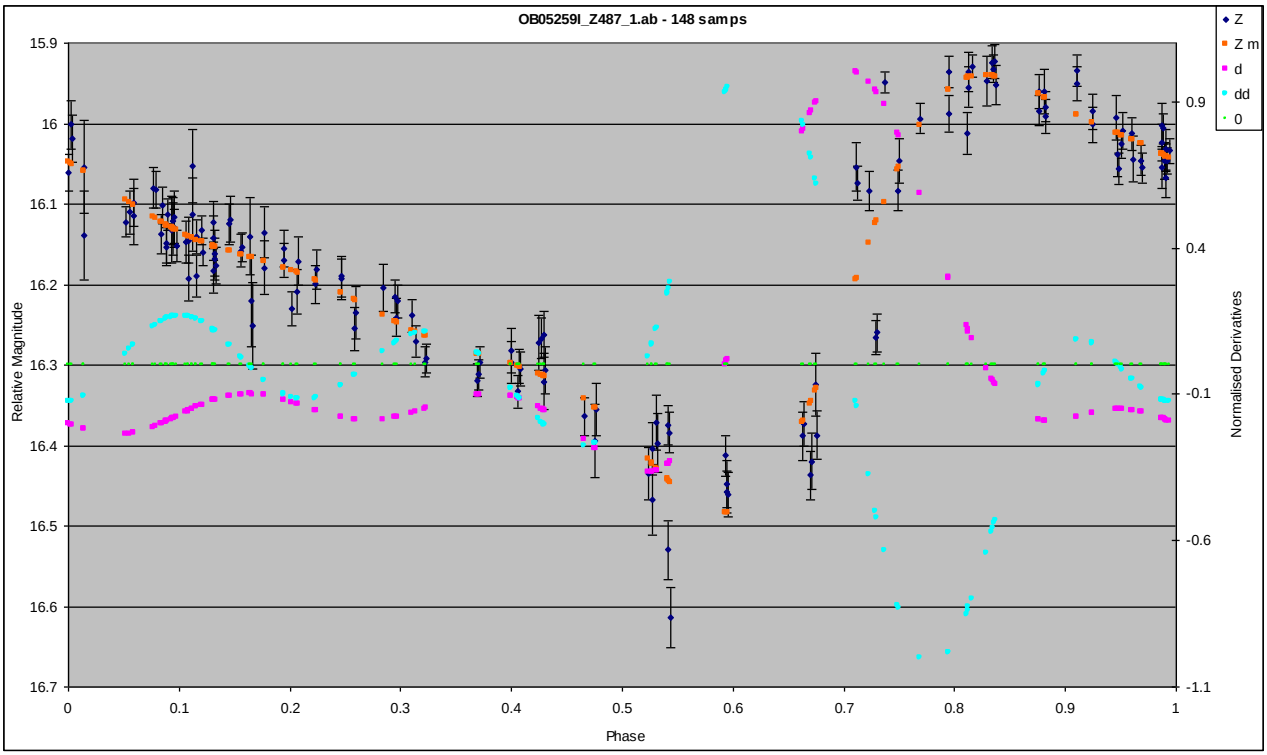

AOB05327I for event OB05327I ~ 5.31’ by 5.31’

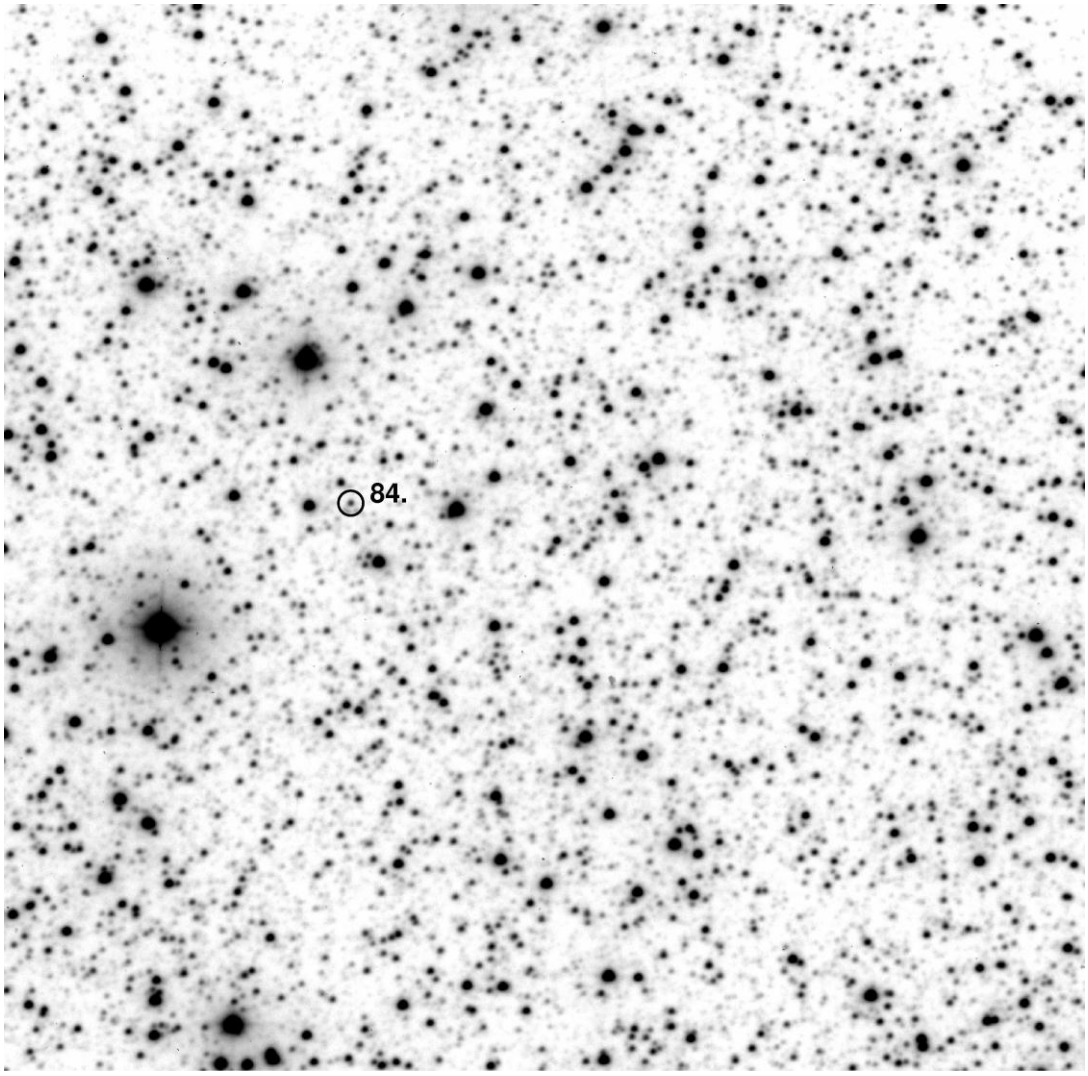

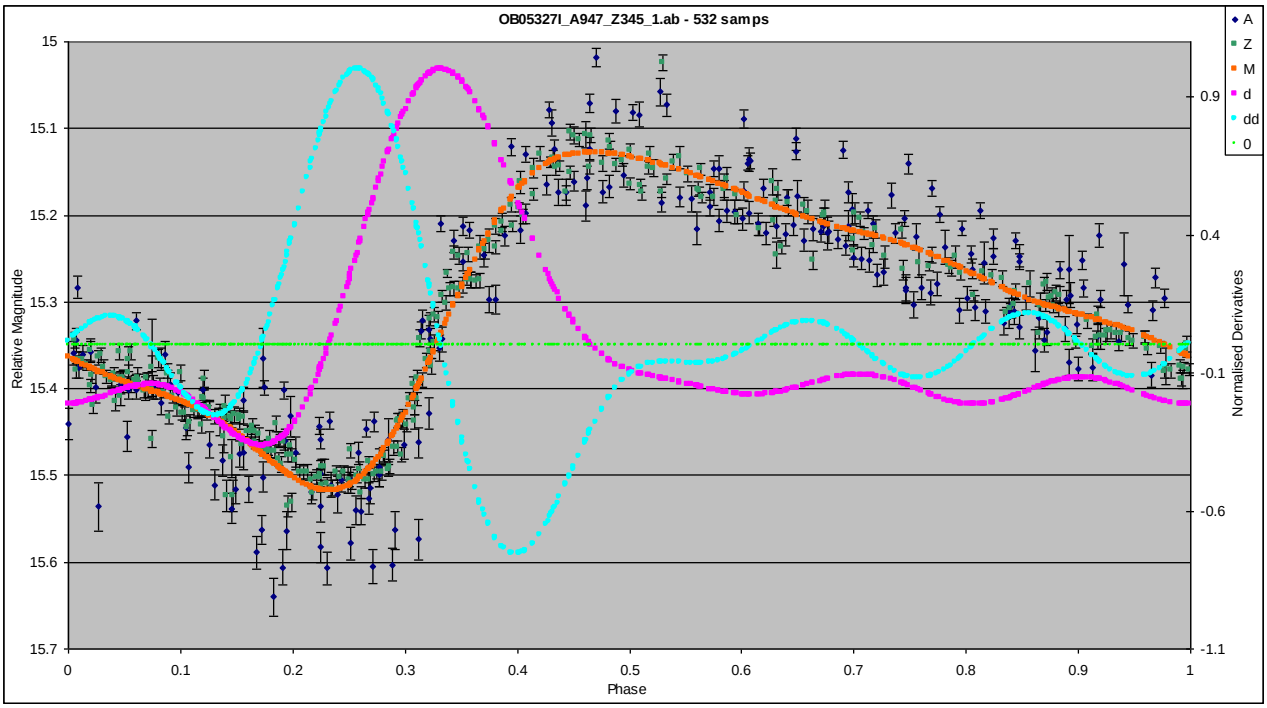

ZOB05331I for event OB05331I ~ 3.91’ by 3.91’

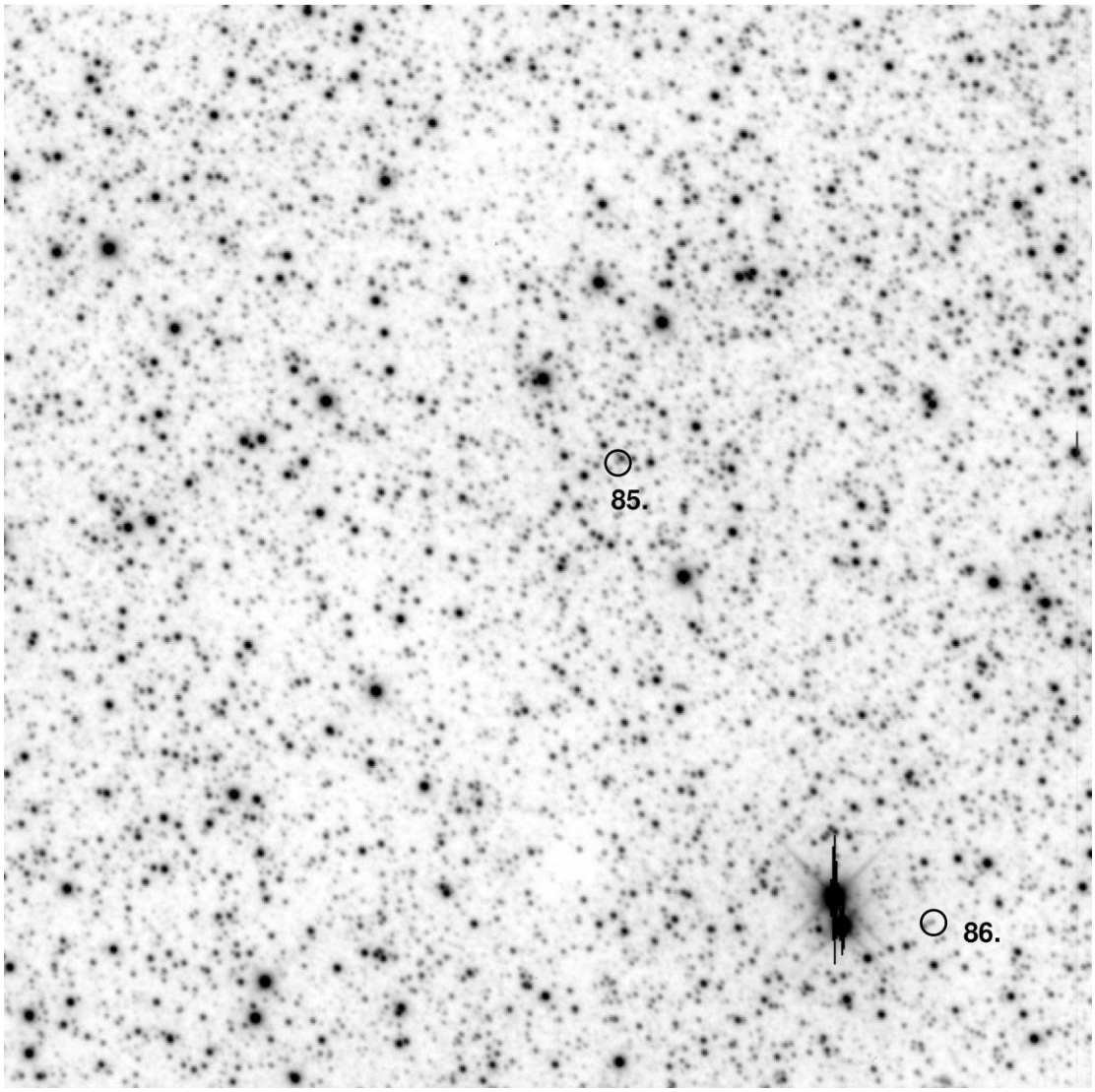

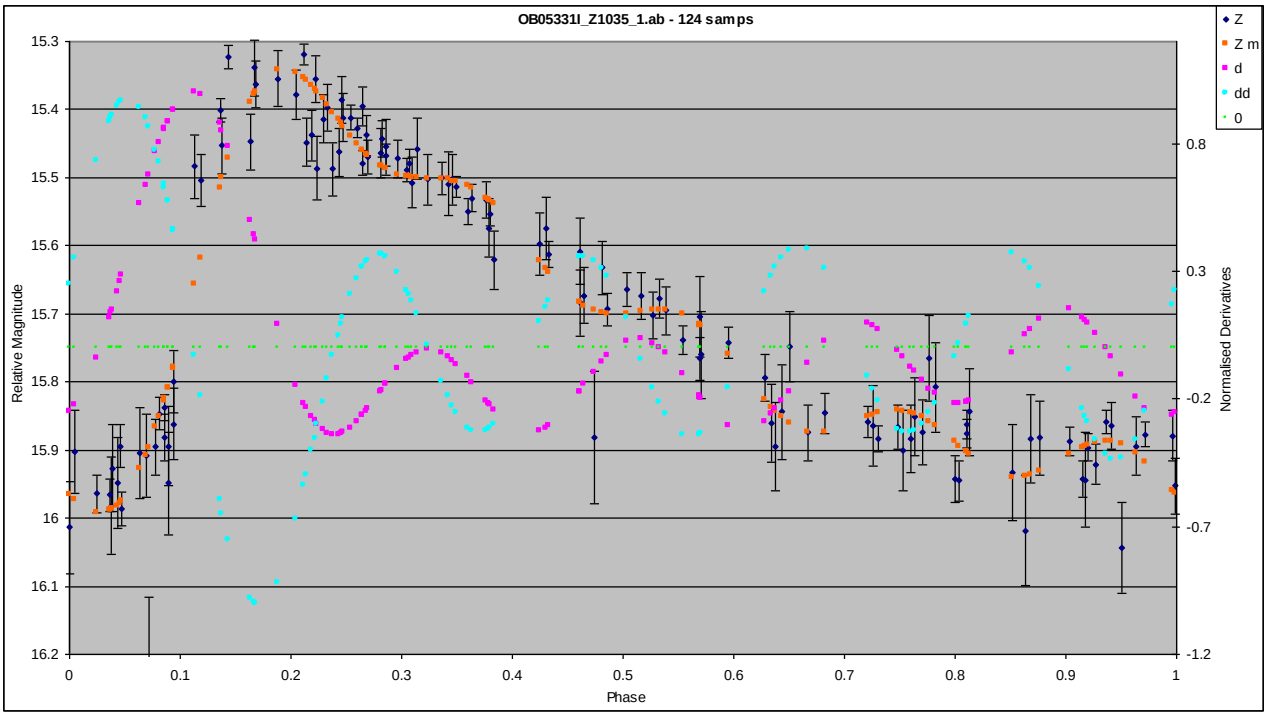
OB05331l_Z1035_1.ab - 124 samps
Z
Z m
d
dd
0
Relative Magnitude
Normalised Derivatives
Phase
15.3
15.4
15.5
15.6
15.7
15.8
15.9
16
16.1
16.2
0.8
0.3
-0.2
-0.7
-1.2
0
0.1
0.2
0.3
0.4
0.5
0.6
0.7
0.8
0.9
1

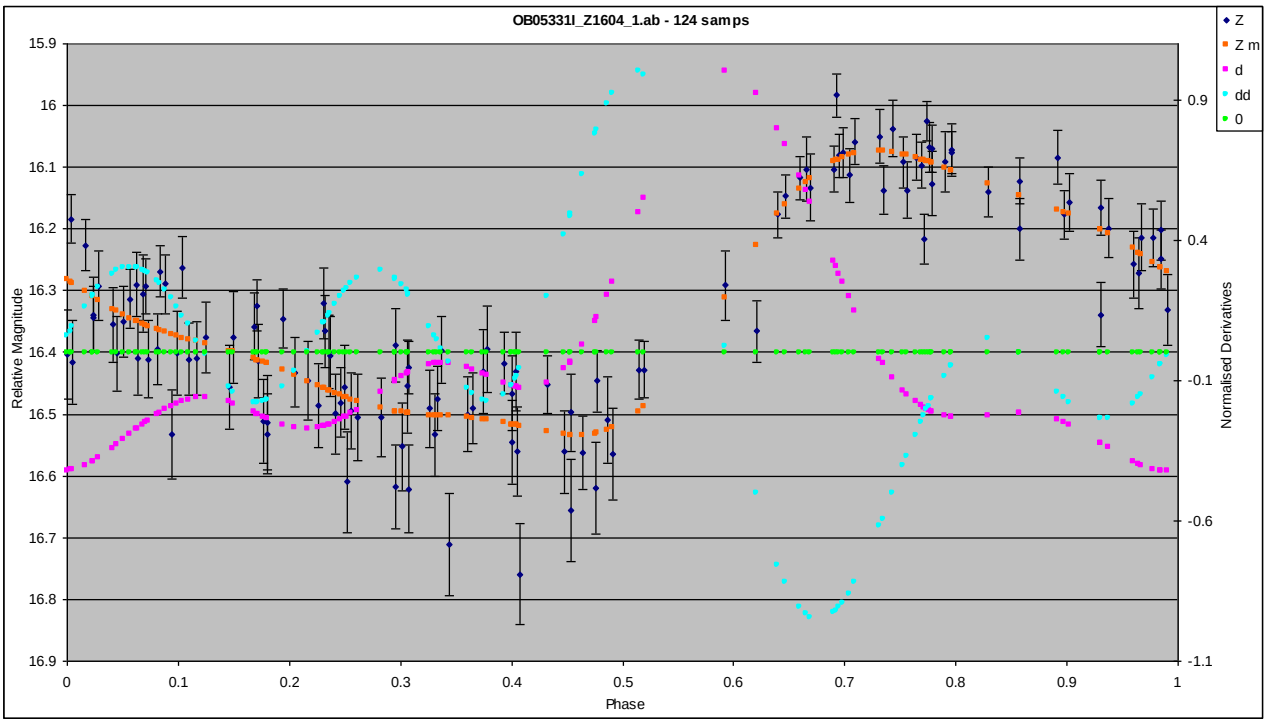
OB05331l_Z1604_1.ab - 124 samps
Z
Z m
d
dd
0
Relative Magnitude
Normalised Derivatives
Phase
15.9
16
16.1
16.2
16.3
16.4
16.5
16.6
16.7
16.8
16.9
0.9
0.4
-0.1
-0.6
-1.1
0
0.1
0.2
0.3
0.4
0.5
0.6
0.7
0.8
0.9
1

WOB05390I for event OB05390I ~ 5.15’ by 5.15’

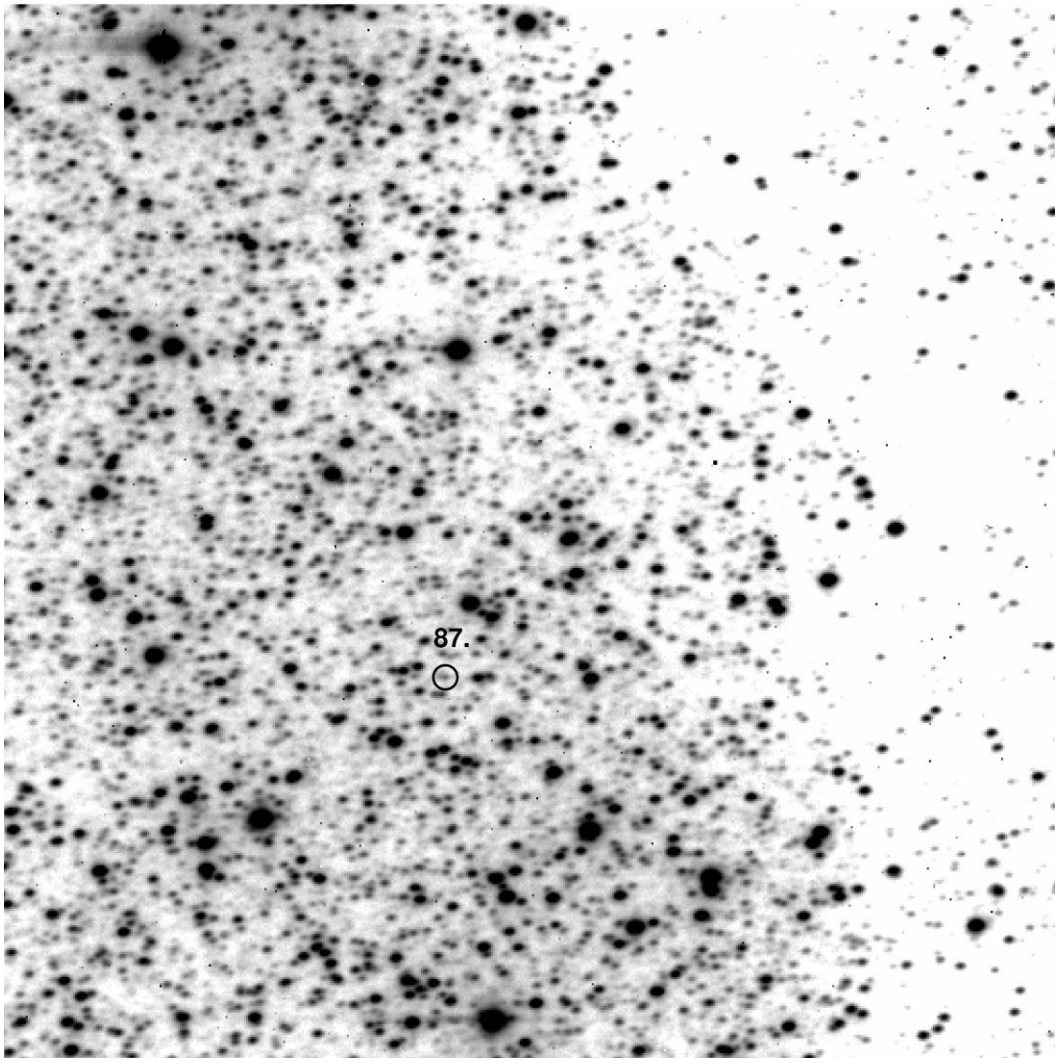

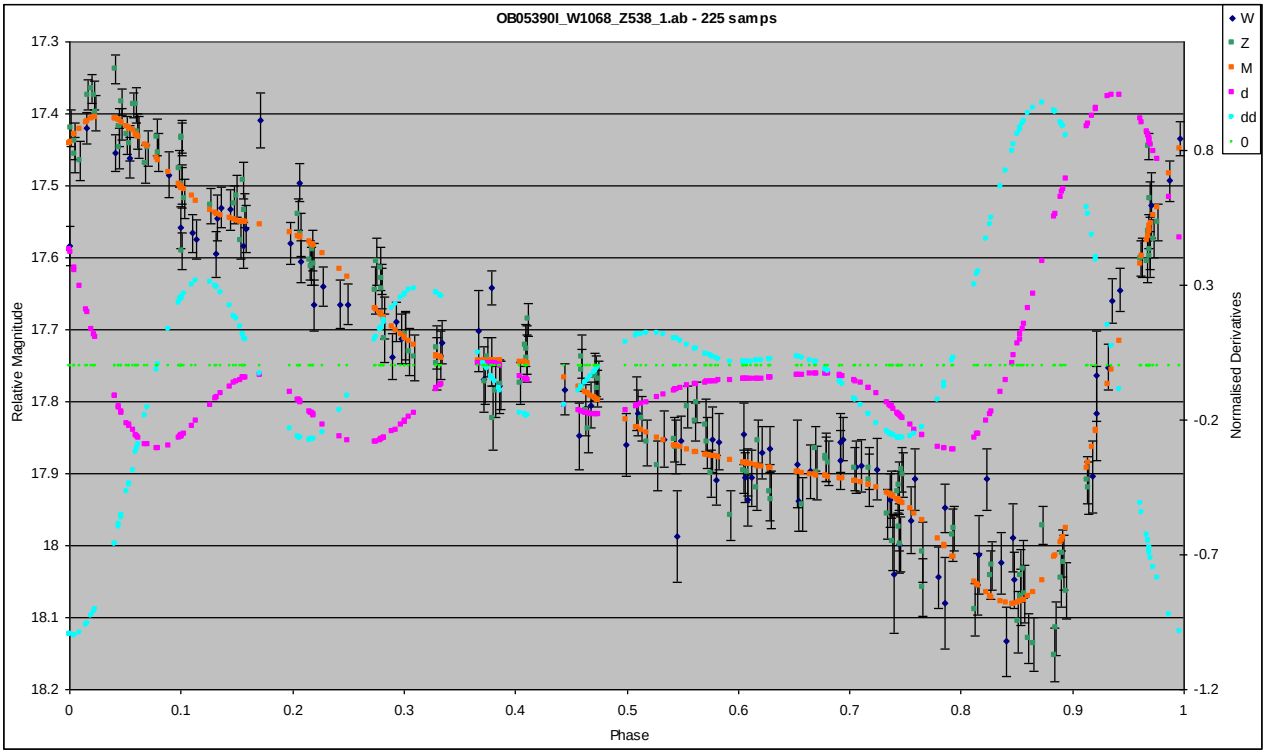

9 High resolution frequency analysis

The motivation for the work presented in section 9 grew out of the results and conclusions obtained from identifying RR Lyrae and in particular Blazhko stars from PLANET data as presented in the preceding sections of this thesis. New data has been obtained and analysed while the background and theory on Blazhko stars has been revisited in more detail and with different emphasis.

9.1 Summary

This section presents the discovery of new equidistant frequency quintuplets in the lightcurves of two Blazhko stars. Such frequency quintuplets are a requirement of the magnetic models attempting to explain the Blazhko effect. The Blazhko effect has remained unexplained for over 100 years and represents a well known and persistent puzzle in variable star research. Competing models explaining this effect have been developed but all lack conclusive support from observations. In recent years six other detections of a frequency quintuplet in a Blazhko star have been published (Hurta et al 2008, Jurcsik et al 2008, Kolenberg et al 2009, Jurcsik et al 2009, Chadid et al 2010, Kolenberg et al 2011). This work adds to the removal of the objection against the magnetic model explanation of the Blazhko effect based on lack of frequency quintuplets by showing that they are relatively common and are not an analysis or data artefact. It is shown that the previous absence of frequency quintuplet detections in Blazhko stars was caused by the lack of data suitable for their detection and that this has fundamental implications for the explanation of the Blazhko effect. It can no longer be said that the absence of frequency quintuplets in Blazhko stars is an inconsistency with the magnetic models. Preliminary results in this area are presented and specific future research is described that in combination with the detection of frequency quintuplets should further constrain which models for the Blazhko effect agree with observations.

9.2 Introduction

The Blazhko effect was first noticed by S. Blazhko (Blazhko 1907) who found dispersion in the lightcurve of the RR Lyrae star RW Dra that could not be described by the main period alone. The addition of a 41.6 day variation in the maxima of the RR Lyrae pulsation fitted the observations. In this way the original definition of a Blazhko star was set.

The Blazhko modulation is typically a combination of varying amounts of amplitude and phase modulations of the dominant radial pulsation in RR Lyrae stars. Blazhko stars are known in which either phase or amplitude modulations are almost absent. The amplitude modulations appear as cyclical changes in the light output of the radial pulsation although the amount of the change varies with the phase of this radial pulsation. Typically the parts of the lightcurve around the maximum light output are changed the most. The phase modulation appears as shifts in the positions of the light output maxima and minima but without change in the period of radial pulsation. In this case the shape of the lightcurve varies between more and less asymmetric. The lightcurves of Blazhko stars exhibit changes and features in addition to amplitude and phase modulations. For example a shifting bump is often present on the rising branch of the lightcurve. Overall the light output from Blazhko stars changes in multiple and complex patterns.

The Blazhko effect has been described with increasing detail through a period of close to 100 years after its discovery in terms of cyclic modulations in the lightcurves of RR Lyrae stars. The accumulation of larger numbers of increasingly accurate observations of RR Lyrae stars produced a growing number of Blazhko stars identified through the presence of a periodic modulation in the shape and amplitude of the main radial pulsation. This description was finessed and expanded in details but the essentially qualitative definition of the Blazhko effect remained while a proven theoretical explanation of the processes producing it eluded researchers. The

observations of Blazhko stars concentrated on single stars chosen as case studies and were often conducted with different telescopes by different observers as parts of unrelated projects. This typically resulted in uncontrolled and thus highly uneven data sampling. Combining data from unrelated sources probably introduced additional uncertainties to this type of observations. During the same time various attempts at explaining the Blazhko effect have been made (see summary in Stothers 2006) and were contradicted by additional considerations or lack of sufficient observational proof. A full and detailed review of all the proposed explanations for the Blazhko effect and their strengths and weaknesses is too large to be included here but the common theme of work in this area is the lack of sufficient observational constraints to conclusively accept, reject or appropriately modify the existing models. The practical difficulties with gathering observational data on Blazhko stars resulted in lack of observations sufficiently detailed to better explain their nature.

More recently as better sampled photometric observations of RR Lyrae stars became available the Blazhko effect started to be described in terms of all the frequency components detectable in the lightcurves. The periodic modulation of main RR Lyrae pulsation in Blazhko stars was associated with the presence of additional frequency components closely spaced around the strongest one. The first detections of additional frequencies in close proximity to the frequency associated with the fundamental radial pulsation in Blazhko stars were published by Borkowski (1980) and Kovács (1995). This approach to looking at Blazhko stars started expanding with the use of microlensing survey data for variable star research (Olech *et al* 1999a and 1999b, Alcock *et al* 2000, Kurtz 2000, Moskalik 2000). The observations from microlensing surveys were conducted for extended periods of time over regular and relatively wide observing fields, resulting in multi-year lightcurves for very large numbers of stars. In a relatively short time hundreds of RR Lyrae stars exhibiting the Blazhko effect and light output changes with frequency multiplet structures

around the radial pulsation frequency were identified and well described (Mizerski 2003, Moskalik and Poretti 2002, Moskalik and Poretti 2003).

Initially Blazhko stars were subdivided into two main groups based on the presence of either a frequency doublet (a single additional frequency close in value to the radial pulsation frequency) or a frequency triplet (two additional frequencies close in value and on opposite sides of the radial pulsation frequency). The strengths of the frequencies in these multiplets are unequal or asymmetric to varying degrees but as expected the radial frequency is always the strongest. Some RR Lyrae stars with Blazhko modulation contain frequency triplets with unevenly spaced components and additional frequencies not part of the multiplet structures (Mizerski 2003). The spacing between the components of frequency multiplets corresponds to the frequency of the Blazhko modulation as expected. Thus the photometric data from microlensing surveys like PLANET and OGLE II has sufficient observations and accuracy to reliably detect frequency multiplets down to the level of triplets.

The PLANET data used in this work is sufficient for the detection of frequency multiplets in RR Lyrae stars at the shorter end of modulation period range provided the modulation is strong in amplitude. The combined OGLE II and OGLE III data is sufficient to detect a wider range of frequency multiplets in Blazhko stars. In order to fully study the complex frequency structures which are being discovered in Blazhko stars the observations require sufficient frequency resolution and thus sufficiently long time span. Judging qualitatively from the results of this work the minimum number of well spaced observations to provide new results is on the order of a thousand. The accuracy of the photometry makes a difference to the results – DOPHOT photometry in the original PLANET observations allowed only a single detection of a frequency doublet in a very strongly modulated Blazhko star. The image subtraction photometry used for the OGLE data provided substantially more and clearer detections of frequency multiplets in a variety of Blazhko

stars. For similar reasons as with photometry knowing accurate magnitude shifts caused by the specifics of different sets of instruments will improve the ability to detect the weaker frequencies in combined observations – for example as demonstrated in this work with the combined OGLE II and III data. Thus the optimal lightcurves for the detection and a good quality description of multiplet frequency structures in Blazhko stars satisfy the following criteria: all the observations are obtained with a single unchanged instrument; the lightcurve is frequently sampled over the duration of multiple Blazhko cycles; the photometry is of good accuracy; the number of observations is in the range of a few thousand. The potential changes in the radial pulsation and Blazhko periods should also be considered when planning this type of observations. These changes may accumulate over very long term observations, enough to make frequency analysis problematic for at least some Blazhko stars. Provided that observations satisfy the above requirements, relatively small, 0.6 to 1 m terrestrial based telescopes are sufficient for the detection of new frequency structures in Blazhko stars as demonstrated with the more recent detections of frequency quintuplets in these stars (Jurcsik et al 2008, Kolenberg et al 2009, Jurcsik et al 2009). Combined with the earlier detection of the first frequency quintuplet by Hurta et al (2008) the new detections describe four terrestrially observed Blazhko stars containing frequency quintuplets. The most recent observations use space based photometry to explore the frequency structure of Blazhko stars: one description of a frequency quintuplet from the CoRoT space mission (Convection Rotation and Planetary Transits) by Chadid et al (2010); and one description by Kolenberg et al (2011) based on data from the Kepler space telescope. The space based observations have the advantages of highly accurate photometry undistorted by the atmosphere and the ability to observe Blazhko stars continuously without the interruption of day time. These advantages have produced previously unknown features in the frequency spectra of Blazhko stars indicating that frequency quintuplets alone are not sufficient to fully describe the pulsation. Overall in order to further increase our knowledge about Blazhko stars very specific and effort intensive observations are required. Equally, new results cannot be derived without appropriate data.

Upon the detection of the closely spaced frequency multiplets in Blazhko stars their presence was described as indicating non-radial modes in RR Lyrae stars that occurr through resonance with the dominant radial pulsation mode. This connection was made through the well established presence of similar multiple frequency structures indicating non-radial pulsation in other variables such as δ Scutti stars (for example Nowakowski and Dziembowski 2003). Dziembowski and Mizerski (2004) present some evidence for the presence of this type of resonance in Blazhko stars by pointing out that the only available source of energy needed to maintain non-radial modes involves energy transfer from the radial mode and a reduction in its amplitude. This reduction in the amplitude of the main radial pulsation is observed on average in Blazhko stars but to a smaller extent than predicted by the paper, leaving the argument for the presence of radial and non-radial mode resonance unproven. In addition the expected reduction in the amplitude of the radial pulsation is not seen in RRc Blazhko stars and as pointed out by the authors no theoretical models have been developed to account for this absence.

Shibahashi (2000) explains the Blazhko effect in terms of an Oblique Pulsator Model without the mention of non-radial modes but requiring the presence of a "substantial" magnetic field in the star. This model requires in the star a power spectrum with a quintuplet fine structure around the radial pulsation frequency with the spacing between all the components being the same and equal to the rotational frequency of the star. To a first order description the period of the Blazhko modulation is derived from the rotation of the star. The model does not develop any additional effects which may modify the primary modulation. In addition the relative ratios among side-peak frequency amplitudes are dependent on the geometrical configuration of the star in terms of its magnetic and rotation axes with respect to the line of sight. For some geometric configurations the predicted quintuplet will be detectable as an equally spaced triplet with separation equal to double the rotational frequency. Thus this model does not require the lightcurves

of all Blazhko stars to contain frequency quintuplets, but it does require that any triplets they contain have equally spaced components.

Chadid (2004) describes 27 magnetic field measurements from spectropolarimeter observations of RR Lyrae, the brightest Blazhko star and the prototype for RR Lyrae stars, over almost 4 years which do not detect any strong photospheric magnetic fields in this star. Chadid (2011) presents observations of the Blazhko star RV UMa, the same Blazhko star for which Hurta et al (2008) found the first frequency quintuplet, over two nights that show the absence of a strong magnetic field. The earlier detections of strong magnetic fields in RR Lyrae (Romanov et al 1987, 1994 and Babcock 1958) are suggested to be incorrect by Chadid (2004) due to problems with the use of photographic plates for the detection of magnetic fields and/or the confounding effects of shocks on spectroscopic line profiles. Both papers (Chadid 2004 and 2011) describe unambiguous detections of magnetic fields in different Ap stars, young, hot and known magnetic stars, with the same instruments as are used for observing the Blazhko stars, as a control for the validity of the methods used.

The method used by Chadid (2004) and (2011) is derived from the Zeeman-Doppler imaging technique (ZDI) (Semel 1989, Donati *et al* 1989, Semel *et al* 1993, Semel 1995 and Semel and Li 1996). The technique permits polarimetric detection of magnetic fields on rapidly rotating stars. Magnetic fields are heterogenous on the surfaces of the studied stars and located in spots or areas, possibly at multiple locations and with opposing polarities. Their orientation with respect to the observer affects how well they can be detected (Brown et al 1991, Donati et al 1992, Donati and Collier Cameron 1997b among others). Integrated over the surfaces of these stars magnetic field effects from areas of opposing polarities are very difficult to detect as they cancel out each other. ZDI relies on sufficiently fast rotation of the star to separate absorption lines from distinct magnetic areas when some of them are on the side of the star rotating towards the observer while the others

are rotating away from the observer. Essentially the spectroscopic lines shift and the opposing magnetic effects no longer cancel out precisely, making it possible to detect them at least some of the time, depending on the phase of the star's rotation. ZDI provides a reduced in strength line of sight component of the magnetic field and the amount of the reduction depends on the structure of the star's magnetic field and the orientation to the observer. During the star's rotation different parts of the magnetic field lie along the line of sight to the observer and can be potentially detected, but again this depends on the orientation of the observer. Magnetic field lines perpendicular to the line of sight to the observer are not detected. The size of the Zeeman signatures detectable in the spectral lines is very small, typically 0.1 percent of the unpolarised continuum. In order to detect these small changes multiple spectral lines in the observed stars are scaled and summed together relying on the fact that they have the same shape to within the uncertainties and assumptions used in detecting the Zeeman signatures. Least Square Deconvolution (LSD) is a recent and highly sensitive method for summing spectral lines to increase the detectability of magnetic signatures (Donati et al 1997b). This process results in the construction of an LSD spectral line profile that is compared to an appropriate spectral line mask constructed for the type of star being observed from standard spectral lines unaltered by magnetic signatures.

The proof of the absence of strong magnetic fields in RR Lyrae stars is a crucial result in the study of the Blazhko effect as it would invalidate some models including that of Shibahashi (2000). However, the requirements for the proof of absence go beyond presenting the non-detection of magnetic field in one or two stars. Instead it has to be shown that if strong magnetic fields were present in the observed stars, they would have been detected. Several questions on the presence or absence of strong magnetic fields in Blazhko stars remain to be settled. Could the orientation of a magnetic field reduce its detectability in some stars? In this case it would be useful to observe strengths of magnetic fields in a larger sample of Blazhko stars. What is the detectability of a magnetic field with multiple zones of opposing polarities on a slowly rotating star? Do Blazhko

stars rotate fast enough for the ZDI method to separate magnetic fields from zones of opposing polarities? Does the pulsating nature of the photosphere of a Blazhko star and the presence of shocks affect the profiles of the spectral lines used for the detection of magnetic fields in such a way as to reduce or fully hide the signature of a magnetic field? How would potential non-radial pulsation modes (in which case the light would be coming from a mixture of areas moving both away and towards the observer) affect the separation of spectral lines in the ZDI method? The applicability of the ZDI and LSD methods has to be demonstrated specifically for RR Lyrae stars.

Currently the detections of frequency quintuplets outnumber the non-detections of magnetic fields in Blazhko stars. Though until relatively recently the absence of frequency quintuplet detections in Blazhko stars had been used as an argument against the magnetic Oblique Pulsator Model of Shibahashi (2000). More extensive spectroscopic observations of different Blazhko stars along with a full understanding of how photospheres and shocks in low mass pulsating red giants (i.e. RR Lyrae and Blazhko stars) affect spectroscopic line profiles used for the detection of magnetic fields are required to finalise the answer to the question of whether Blazhko stars contain strong magnetic fields distorting their pulsation.

The magnetic model of Shibahashi (2000) assumes a dipole filed for the calculations but does not exclude the possibility that magnetic fields of different configurations can be present. The dipole formulation of Chadid (2011) points out Stothers (2006, 2010) suggestion that in some RR Lyrae stars turbulent/rotational dynamo mechanism generates magnetic fields that grow and decay over the Blazhko cycle while inducing changes in the period of the fundamental radial pulsation. At the same time Chadid (2011) argues that slow convective cycles are not enough to explain Blazhko modulation in the hypersonic atmospheres of RR Lyrae stars. Preston (2011) points out that both Stothers (2006, 2010) and Jurcsik et al (2009) agree that “phase modulations during the Blazhko cycle may simply reflect the oscillations of the pulsation period, while the amplitude changes are

due to periodic alterations in the atmospheric structure of the star". In Stothers (2006, 2010) hypothesis the magnetic fields suppress turbulent convection and thus produce small changes in the fundamental pulsation, but as Preston (2011) points out the magnetic fields "could be replaced by any cyclic process that alters the convective transport of energy through the envelope". Thus no current explanation requiring either stable or changing strong magnetic fields in RR Lyrae stars fully addresses all the objections made against them.

The excitation of non-radial pulsation modes with frequencies close to the dominant radial pulsation frequency in RR Lyrae stars forms the basic premise of current Resonant Mode models of the Blazhko effect. In addition the presence of non-radial pulsation modes is a part of all the currently dominant models for the Blazhko effect, as presented by Kovács (1995), and thus their presence alone is not sufficient for choosing an explanation that agrees the most with observations. The potentially observable quantity that differs between the models is the predicted strength of the higher order frequency multiplets. The overall prediction is that a triplet (or doublet) is the detectable frequency structure in resonance models since the frequencies making up the higher order parts of the multiplets have very low amplitudes, and a quintuplet structure (or higher order) is allowed by and detectable in the "oblique rotator-pulsator model" (see Kovács 1995 for a discussion, Dziembowski and Cassisi 1999, and Hurta *et al* 2008 for additional details)

A Blazhko star with a triplet in which the two side-peaks have different frequency offsets from the radial frequency is not explained by Shibahashi (2000). Through extension of the argument and equations in the paper in some cases the inner components of quintuplets can have amplitudes lower than the outer ones, possibly to the point where the quintuplet turns into a triplet with spacing equal to double the rotational frequency of the star. This last argument provides an additional testable prediction of the model if quintuplets are found with these amplitude ratios or if a bi-modal distribution in the frequency spacing of triplets in Blazhko stars is established. In either

case precise frequency structures for a sufficiently large group of Blazhko stars have to be determined in order to check this prediction.

Non-equidistant frequency triplets have been detected in multiple Blazhko stars in an apparent contradiction to the magnetic model of Shibahashi (2000) (Moskalik and Poretti 2003, Mizerski 2003, Dziembowski and Mizerski 2004). However, at the same time equidistant frequency triplets have been detected in most Blazhko stars. In the OGLE II group of Blazhko stars described by Mizerski 2003 the equidistant triplets form the more numerous group. This contradiction has potential explanations that can preserve the magnetic model as a possible description of the Blazhko effect. For example as Mizerski (2003) suggests the stars with a non-equidistant triplet may not be typical Blazhko stars or they may form a separate group within Blazhko stars. Or it is possible that the non-equidistant triplets are misidentifications caused by the inaccuracies inherent in the quality of the lightcurves being analysed. This type of misidentification of frequency triplet structures became apparent in this work when OGLE II and OGLE III data for the same stars was compared. Some stars that were labelled as having a non-equidistant triplet in OGLE II data turned out to have an equidistant triplet in OGLE III data. In the same manner that quintuplets had not been detected in Blazhko stars prior to Hurta et al (2008), due to the limitations of the data rather than their absence, the non-equidistant triplets may be caused by inaccurately resolved components, perhaps complicated by the occasional changes in the RR Lyrae radial pulsation frequencies. The existence of exclusively equidistant frequency triplets based on the analysis of sufficiently accurate data for a large group of stars or the opposite case is another testable prediction that can help judge the correctness of the various models of the Blazhko effect.

The search for an explanation of the Blazhko effect has produced the above predictions of clearly defined frequency patterns in the power spectra of their lightcurves as associated with the various models. To date there has been only six detections of the quintuplet fine structure required

by the Oblique Pulsator Model (Hurta et al 2008, Jurcsik et al 2008, Kolenberg et al 2009, Jurcsik et al 2009, Chadid et al 2010, Kolenberg et al 2011). In each case the detections describe a single star. Further confirmations of the presence of these patterns in Blazhko stars, or otherwise, depend on the availability of accurate lightcurves with high frequency resolution even if not all characteristics of the data fit the suggestions presented above. Apart from a reasonable phase coverage of the variations being observed high frequency resolution requires the longest possible time-span of observations. Combining data from multiple sources will increase the time-span of observations. This work presents the results of high resolution frequency analysis of the lightcurves of a group of Blazhko stars based on OGLE II and OGLE III data and informed by RR Lyrae stars detected in data gathered by the PLANET collaboration.

9.3 Observations

The choice of the set of stars analysed for this work originates with the 87 RR Lyrae stars identified in this thesis from the PLANET group's microlensing data. The PLANET RR Lyrae stars are compared to RR Lyrae and Blazhko stars from the OGLE II microlensing survey database (Udalski et al 1997) as analysed by Mizerski (2003). This comparison produced a set RR Lyrae stars common to PLANET and OGLE II as described in the previous chapters of this thesis. In a natural step the lightcurves of the RR Lyrae stars common to both surveys were combined but initial analysis quickly established the need for an even greater frequency resolution to establish the desired details of frequency structures in Blazhko stars.

The increased time span needed for better frequency resolution was obtained when data from the OGLE III microlensing survey database became available (Soszyński 2011). Where possible PLANET, OGLE II and III RR Lyrae stars were matched up to produce lightcurves with the highest available number of observations and the best possible frequency resolution. However,

when the more than 2700 RR Lyrae stars detected in the OGLE II observations are compared to the 87 RR Lyrae stars in PLANET observations the stars analysed in this section of the thesis are dominated by OGLE identifications. For this reason the two detections of frequency quintuplets presented here are both based on the OGLE data alone.

This sample selection result was extended by choosing around 100 additional Blazhko stars with frequency triplets among the type ab RR Lyrae identified in OGLE II data and matching them with OGLE III data where possible. These selection criteria were chosen to match the RR Lyrae and Blazhko types of RV UMa in which Hurta et al 2008 detected the first frequency quintuplet. The list of Galactic Bulge type ab RR Lyrae stars with the Blazhko effect identified in the OGLE II data was automatically sorted to choose stars with predicted modulation periods between 20 to 150 days. The predicted modulation period was determined from the frequency spacings in the triplets determined from the OGLE II data. The choice of the modulation period range was done iteratively – the period range was increased until about 100 Blazhko stars were chosen. These selection criteria included most of the slightly over 100 Blazhko stars of this specific type found in the Galactic Bulge in the OGLE II data but excluded stars that are outliers in the Blazhko modulation period. Finally six stars were analysed for the presence of frequency quintuplets. The targets for analysis were chosen from the larger group based on the presence of relatively large amplitudes for the frequency triplet components. The original aim was to analyse a larger number of these stars but the work ended up being limited by time constraints. Crucially frequency quintuplets were detected in the lightcurves of some of these additional Blazhko stars: the two new Blazhko stars with frequency quintuplets described in this thesis. Thus it is demonstrated that these frequency features can be found in terrestrial microlensing observations at probably a high occurrence rate.

Hence while the selection of data and stars for analysis was made on the basis of maximising the likelihood of additional detections of frequency quintuplets the sample is

representative of RRab stars with the Blazhko effect and thus frequency triplets. The single caveat being that the frequency triplet detections are based on only OGLE II data which will have lower frequency resolution than combined observations and thus some of the triplet detections may not be as precise as from the combined data. This imprecision is suggested by relatively small differences in the separation of the observed triplet frequency components whereas they should be exactly equal. However, this potential discrepancy does not affect the analysis used to derive the results presented here. The more accurate determination of triplet frequencies in the combined data happens as one step in looking for the quintuplet frequencies.

Both PLANET and OGLE have conducted extended observations through the standard I-band filters and this is the main reason for originally choosing to combine data from these two microlensing surveys. The correct addition of variable star lightcurves produced by different telescopes requires a sufficient number of observations to specify the variability in such a way that the precise shift needed to “line up” the data in magnitudes can be determined. This requirement is fulfilled by data from both surveys. In practice the addition of variable star lightcurves from different telescopes introduces an error between the two sets of magnitudes equal to the error of the model fit used to “line up” the observations. Thus this step of data analysis is a potential source of uncertainties in magnitudes and can ever be only as accurate as the model fit. Blazhko stars contain complicated sets of frequencies in their lightcurves and fitting accurate models for the same star observed at different location with different phase coverage will always produce some amount of imprecision. The same principle applies to combining OGLE II and III data which in theory is magnitude calibrated and could simply be joined together but in practice may require small constant magnitude adjustments introduced due to instrumental changes between the two phases of the survey. The changes in instrumentation between OGLE II and III were small and in this analysis it is assumed that any resulting magnitude shifts were small and thus they are not corrected for. The

use of the same colour filter in all these surveys removes the need for transforming observations between different colour systems and avoids introducing the associated inaccuracies.

The stars are matched between the different surveys initially through location. This match is confirmed by a precise agreement of the frequency of radial pulsation – the strongest frequency in RR Lyrae stars that should be very closely the same irrespective of in which survey the data was gathered. The radial pulsation frequency is determined separately for each set of observations to be combined. If these frequencies do not agree for all surveys, all the sets of observations are discarded as an incorrect star match. In this analysis the matching of stars through location produced very reliable overall results and only a single incorrect match. In the case of the single incorrect match one set of observations was very sparse and noisy perhaps causing a bad frequency determination. Finally each star match was confirmed through the presence of matching triplet frequencies in observations from the different surveys. Following this star matching procedure it is effectively impossible that observations from the surveys were combined for different stars.

The above effort results in lightcurves based on combined data that are suitable for a high frequency resolution study of Blazhko stars. All of the combined data is based on image subtraction photometry. The time span of the combined data varies slightly between the different stars but is around 12 years for most of them. Greater variability occurs in the number of observations contained in each combined lightcurve as this varies from a few hundred up to about three thousand. Typically well over 1000 observations spread out over 12 years are available per star.

9.4 Analysis of the lightcurves of Blazhko stars

The aim of this analysis is to determine the frequency spectra of an extended sample of Blazhko stars with the highest possible resolution in frequency. The motivation for this task is to

find and describe in detail additional frequency quintuplets in Blazhko stars and compare these to the predictions made by the models attempting to explain the Blazhko effect. The analysis of a larger group of Blazhko stars is used to establish the occurrence of frequency quintuplets and to explore how their properties vary.

This analysis also presents the possibility of finding higher order frequency multiplets, where a multiplet is defined by Equation 9.1:

$$f_0 \pm n \times f_m$$

f_0 – is the frequency of the radial pulsation

f_m – is the frequency of modulation

n > 0 and is an integer and corresponds to the order of the multiplet

The frequency series composed for n=0, 1, 2 in the above equation defines the positions of all the peaks in a quintuplet. The frequency series for n=0, 1 by itself corresponds to the positions of an equidistant triplet. Definitions of higher order multiplets follow the same pattern.

This analysis searches for frequencies forming parts of quintuplets at well predicted positions. The frequency of the main radial pulsation and those corresponding to the triplet are determined through standard frequency analysis of the combined lightcurves. The modulation frequency is obtained from the separation of frequency components of the triplet. The positions of the frequencies that extend a triplet into quintuplet detection should be located on each side of the triplet an additional distance away equal to the frequency of modulation. Frequency analysis is carried out around the quintuplet frequency positions calculated in this way and detections are compared to the predictions.

The TiFrAn data analysis package (Kolláth and Csubry 2006) is used to initially identify those Blazhko stars that contain frequency quintuplets. The results are confirmed and analysed in detail with the Period04 software (Lenz and Breger 2005). The dominant frequency corresponding to the radial pulsation is obtained through a Discrete Fourier Transform algorithm (DFT) for unequally spaced data. This and all subsequent frequencies are found using a frequency step rate of 1×10^{-8} cd^{-1} (cycles per day is the frequency corresponding to the inverse of a period specified in units of days). The frequency stepping is determined by testing for the point at which the frequencies determined from the current data do not change at the sixth decimal place upon further reduction in the step rate. The radial frequency and its harmonics are used to construct a model of the lightcurve through a non-linear least square best fit of the data as implemented in Period04. The model is subtracted from the data and the residuals are analysed for the frequencies corresponding to a frequency triplet. In an iteration of the previous step a model is constructed using all the triplet frequencies, including the radial pulsation frequency, and their harmonics and subtracted from the residual data. All the models are fitted in Period04 by keeping the frequencies fixed while the amplitudes and phases are optimised. The model is composed of 36 frequencies: up to the 12^{th} harmonic for the main radial oscillation period and the corresponding 2 triplet frequencies for each harmonic. The second iteration residual data is searched for any additional frequencies that may belong to the quintuplet part of the pattern.

Formally: f_0 and f_m were determined as described in the paragraph above. Frequencies for both $k\,f_0$ and $k\,f_0 \pm 2\,f_m$ for an integer k = 1 to 12 were predicted and simultaneously fitted to the lightcurves with a non-linear least square routine. The fitted model was subtracted from the observed lightcurve to produce the residual lightcurves in which the quintuplet frequencies were detected.

The presence and accuracy of all frequency determinations is confirmed with the standard Lomb-Scargle method as implemented in Peranso software (http://www.peranso.com). The frequencies obtained through the DFT method in Period04 agree very well in all cases with the frequencies determined with the Lomb-Scargle method. For example, the small differences between the two methods are given for the detected frequency quintuplet components in Table 9.2. The frequencies obtained with the L-S method and their significance levels as determined through False Alarm Probability (FAP) as an independent confirmation of their nature. This differs to the analysis described in section 5.3 in which the significance of likely artefacts was being determined through FAPs. Finding a frequency does not determine its identity as a true variation or an artefact. Similarly FAPs determine the significance above the general noise or randomness in the data and an artefact can be significant in this fashion without representing a true variation in the data. Thus, rather than through a fault with a particular method, a frequency analysis can be stopped through a lack of sufficient information to identify the artefacts contained in the signal being analysed.

The lightcurves from the available surveys are initially combined by a simple concatenation in time of the various observations and thus the initial analysis assumes that there is no additional constant magnitude shifts required to account for instrumental difference between surveys. This is a reasonable assumption because all the surveys use the same I-Band colour filters but the possibility exists for further fine tuning of this data combination. However, combining the lightcurves on the basis of average magnitudes over the time period for the surveys involved is strongly inadvisable in the presence of multiple variabilities and varying phase coverage.

9.5 Detection of additional frequency quintuplets in Blazhko stars

The distinguishing feature in the frequency spectra of the Blazhko stars presented here is the appearance of equidistant quintuplet frequencies closely fitting the positions predicted by $k f_0 \pm$

$2 f_m$. The same stars also exhibit equidistant triplet frequencies predicted by $k f_0 \pm f_m$ where, as expected, f_0 and f_m.have the same values for both quintuplets and triplets. Thus, both frequency multiplets are determined by the same underlying set of physical parameters in each star. This regularity and consistency identifies and confirms the presence of the frequency quintuplets.

The stars s2366 and a3 (internal identification numbers) represent two new detections of frequency quintuplets in Blazhko stars in addition to the recent six detections (Hurta et al 2008, Jurcsik et al 2008, Kolenberg et al 2009, Jurcsik et al 2009, Chadid et al 2010, Kolenberg et al 2011). Table 9.1 gives the predicted and detected frequencies for both stars. As indicated in the table the frequency of modulation f_m is set to half the frequency separation between the two measured triplet components. The corresponding predicted triplet components are calculated from the measured f_0 and the derived f_m. Due to all the measured frequencies following very closely the distribution of equidistant triplets and quintuplets there is no value in calculating an average f_0 and f_m from all the detected harmonics as both ways produce about the same range of differences between the predicted and measured frequencies. The differences between measured and predicted values are on the order of 0.00001 cd^{-1} for the star s2366 and 0.0001 cd^{-1} for the star a3.

This shows that the agreement between the detected frequencies and the predicted frequencies is well within the errors estimated from the time span of the data and compares to the errors from the detected positions of the harmonics of the main period. In this sense the detected frequencies are found exactly at the values predicted by the harmonics of the main period, equidistant triplet and equidistant quintuplet positions. All the clearly detected quintuplet frequencies are included in Table 9.1.

However the main frequency and its harmonics as well as the triplet frequencies given in Table 9.1 for the two stars do not represent all the detectable frequencies in these series, but rather

are examples to demonstrate that these patterns fit the predictions of equidistant triplet and quintuplet frequency positions.

The high accuracy in positions of the detections of multiple parts of both equidistant triplet and quintuplet patterns confirms the classification of these patterns. This combination of coherent details could not have arisen by chance.

The Figures 9.1 – 9.13 show the frequency spectra around the measured values and follow the progression of the data analysis. The fundamental radial pulsation mode frequency is followed by the first set of triplet frequencies and all the measured quintuplet components as specified. These spectra show that while the quintuplet frequency components are clearly distinguishable from the noise they only clearly appear after the subtraction of the main frequency with harmonics and the triplet frequencies. Formal determinations of signal to noise ratios and significances for all the measured frequencies are presented below**.**

The quintuplet series of frequencies is different between the stars s2366 and a3. For the star s2366 only the quintuplet frequencies formed by $k f_0 + 2 f_m$ are detectable. For the star a3 frequencies formed by $k f_0 \pm 2 f_m$ are detectable. This difference can be in agreement with the features of the magnetic model based explanations for the Blazhko effect stating that the relative strengths of the multiplets frequencies can vary with the relative orientation of the observer towards the star. Such variations are predicted and allowed by the magnetic models. Strictly speaking all the quintuplet frequencies are present but some may have relatively low amplitudes that make them undetectable. It is fortunate to detect such a distinct variation in the two stars presented here as it adds support to magnetic models as the explanation of the Blazhko effect through being consistent with more than one aspect of their predictions.

Star	Type	Order	Predicted	Measured	Difference	Details
s2366	Main period harmonics	f_0	na	2.282328	na	f_m = 0.008336
		$2f_0$	4.564655	4.564661	0.000006	
		$3f_0$	6.846983	6.846974	0.000008	
		$4f_0$	9.129310	9.129318	0.000008	Timespan =
	Triplet harmonics	$f_0 - f_m$	2.273991	2.273991	0.000001	4404.0 days
		$f_0 + f_m$	2.290663	2.290663	0.000001	
	Quintuplet harmonics	$f_0 - 2f_m$	2.265656	nd	na	
		$f_0 + 2f_m$	2.298999	2.298980	0.000009	Theoretical
		$2f_0 - 2f_m$	4.547984	nd	na	Frequency
		$2f_0 + 2f_m$	4.581327	4.581326	0.000001	resolution =
		$3f_0 - 2f_m$	6.830311	nd	na	
		$3f_0 + 2f_m$	6.863654	6.863686	0.000032	0.000227 cd^{-1}
a3	Main period harmonics	f_0	na	2.039675	na	f_m = 0.009095
		$2f_0$	4.079349	4.079354	0.000005	
		$3f_0$	6.119024	6.119044	0.000020	
		$4f_0$	8.158699	8.158714	0.000015	Timespan =
	Triplet harmonics	$f_0 - f_m$	2.030580	2.030572	0.000008	4405.0 days
		$f_0 + f_m$	2.048770	2.048762	0.000008	
	Quintuplet harmonics	$f_0 - 2f_m$	2.021485	2.021422	0.000086	
		$f_0 + 2f_m$	2.057865	2.057900	0.000035	Theoretical
		$2f_0 - 2f_m$	4.061159	4.061080	0.000079	Frequency
		$2f_0 + 2f_m$	4.097539	4.098028	0.000489	resolution =
		$3f_0 - 2f_m$	6.100834	6.100745	0.000089	
		$3f_0 + 2f_m$	6.137214	6.137685	0.000471	0.000227 cd^{-1}

Table 9.1: Predicted and detected multiplet frequencies. *Star* is an internal identification number for stars. *Type* specifies the multiplet type. *Order* stands for the definitions of the first few frequencies in the multiplet – used to confirm the type of the multiplet but not providing a full listing of all the detectable frequencies. *Predicted* is the estimated position of the specified frequency derived from the spacing between the main period and the lowest order triplet frequencies. *Measured* is the measured position of the frequency in the power spectrum of the star. *Difference* is the difference between the *Predicted* and *Measured* frequencies. The frequencies and their differences are given in units of cycles per day (cd^{-1}). The 'nd' entries mean that a frequency was not detected close to the predicted position.

The figures presented below are plots of frequency in units of cd^{-1} (cycles per day) versus amplitude in units of magnitude.

9.6 Frequency spectra

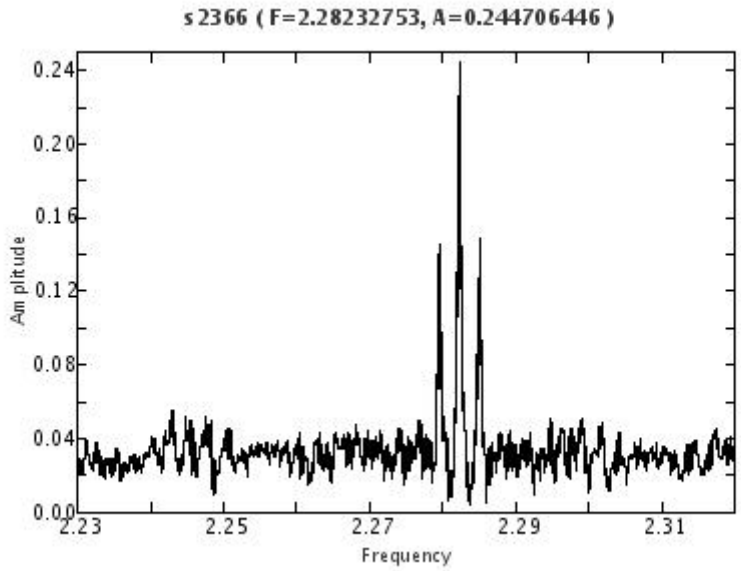

Figure 9.1: The main period f_0 = 2.282327 for star s2366 surrounded by a relatively clean frequency spectrum.

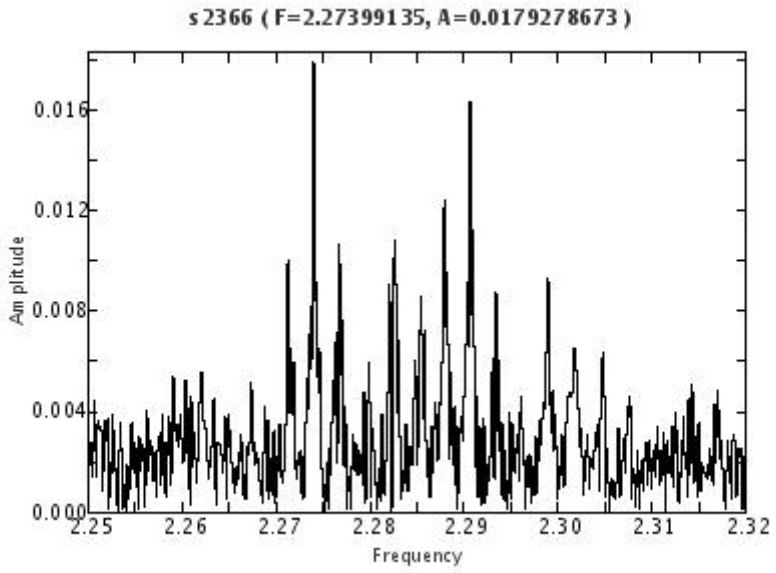

Figure 9.2: The first harmonic of the triplet structure for star s2366, $f_0 \pm f_m$ with frequency values of 2.273991 and 2.290665.

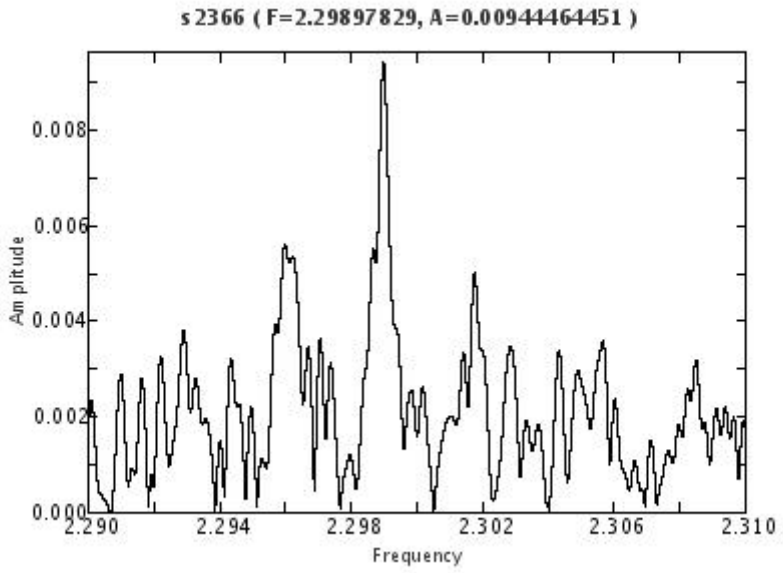

Figure 9.3: Frequency detection in the quintuplet in star s2366, $f_0 + 2f_m = 2.298978$.

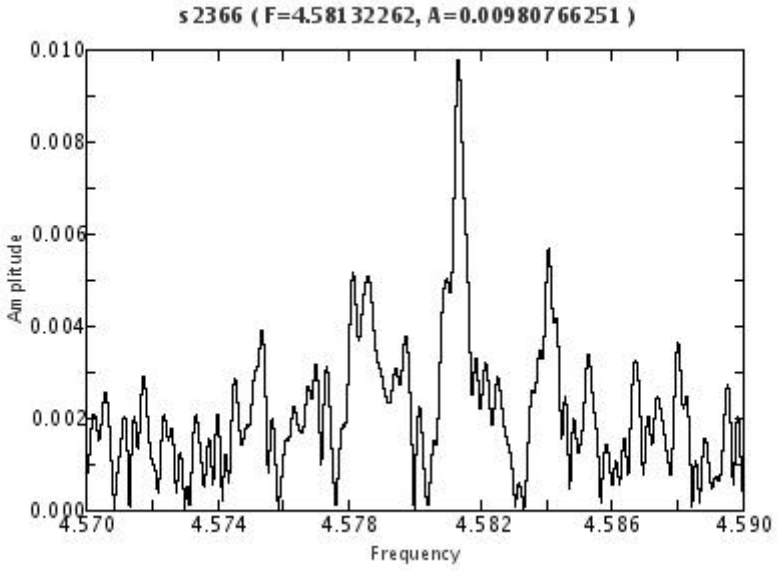

Figure 9.4: Frequency detection in the quintuplet in star s2366, $2f_0 + 2f_m$ = 4.581323

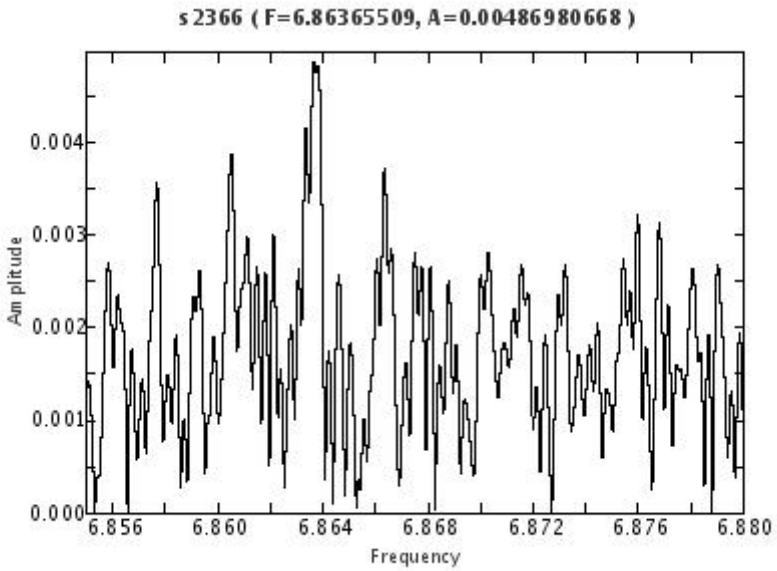

Figure 9.5: Frequency detection in the quintuplet in star s2366, $3f_0 + 2f_m$ = 6.863655. This is the highest frequency detectable in the quintuplet series for this star.

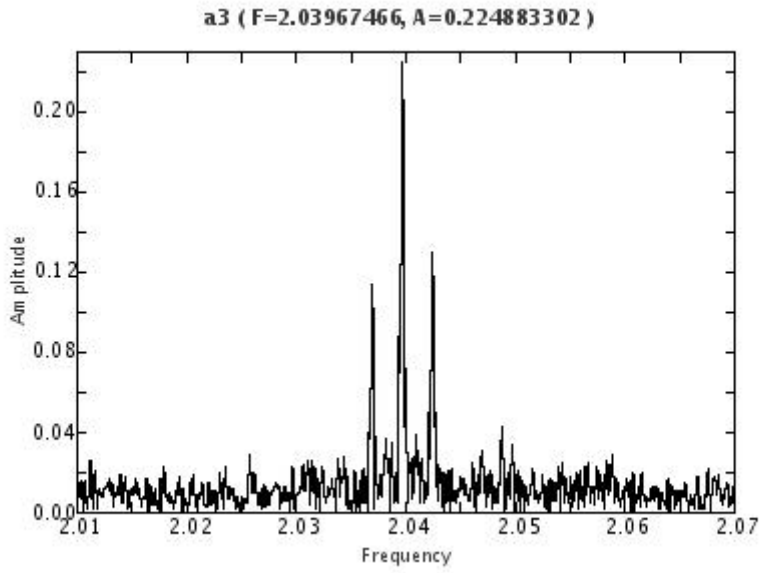

Figure 9.6: The main period f_0 = 2.039675 for star a3, strong and surrounded by a relatively clean frequency spectrum.

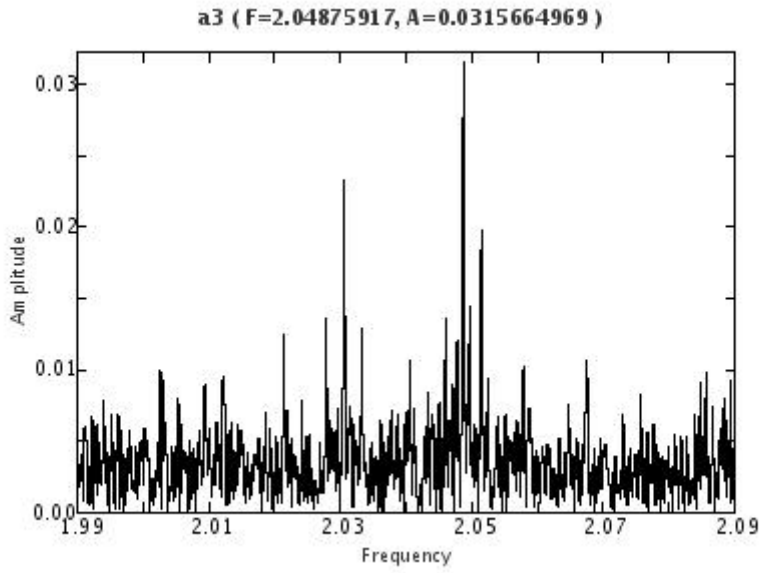

Figure 9.7: The first harmonic of the triplet structure for star a3, $f_0 \pm f_m$. A significant asymmetry is visible in the amplitudes of the triplet components.

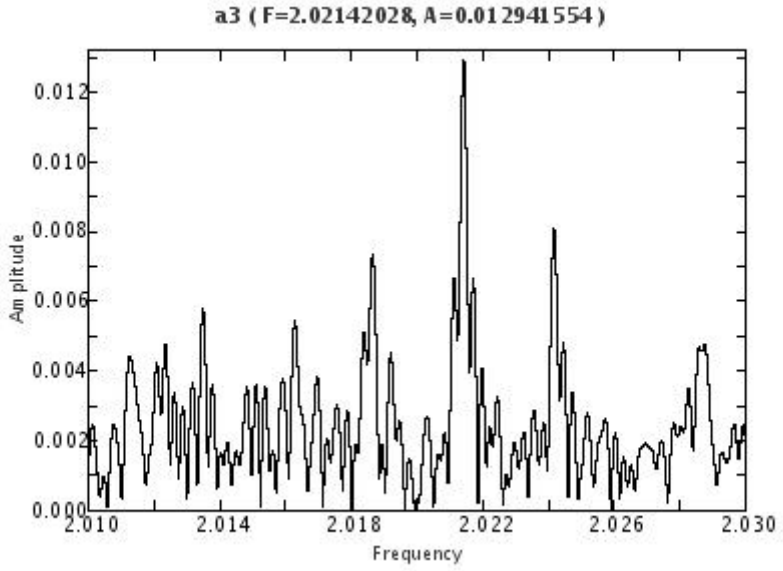

Figure 9.8: Frequency detection in the quintuplet in star a3, $f_0 - 2f_m = 2.021420$

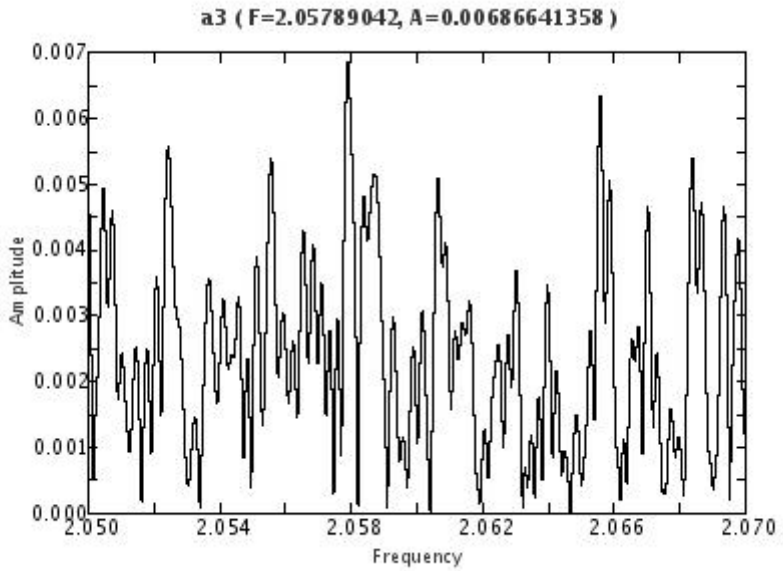

Figure 9.9: Frequency detection in the quintuplet in star a3, $f_0 + 2f_m = 2.057890$.

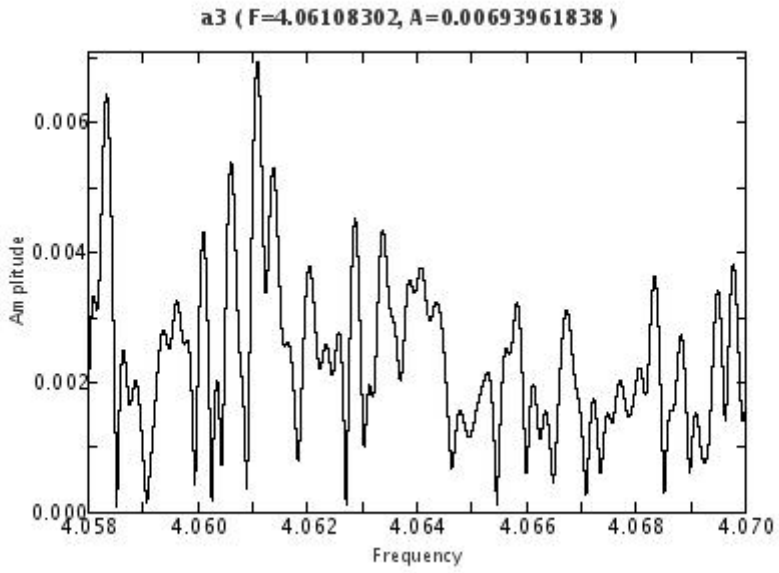

Figure 9.10: Frequency detection in the quintuplet in star a3, $2f_0 - 2f_m = 4.061083$.

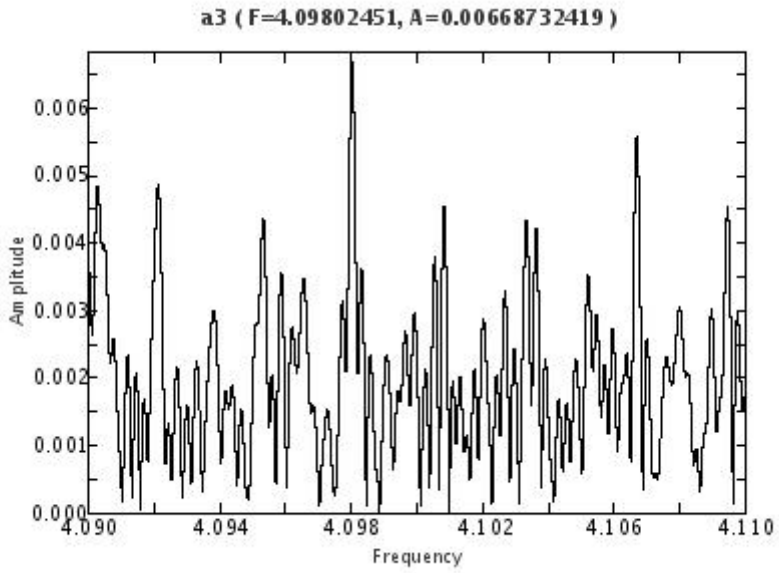

Figure 9.11: Frequency detection in the quintuplet in star a3, $2f_0 + 2f_m = 4.098025$.

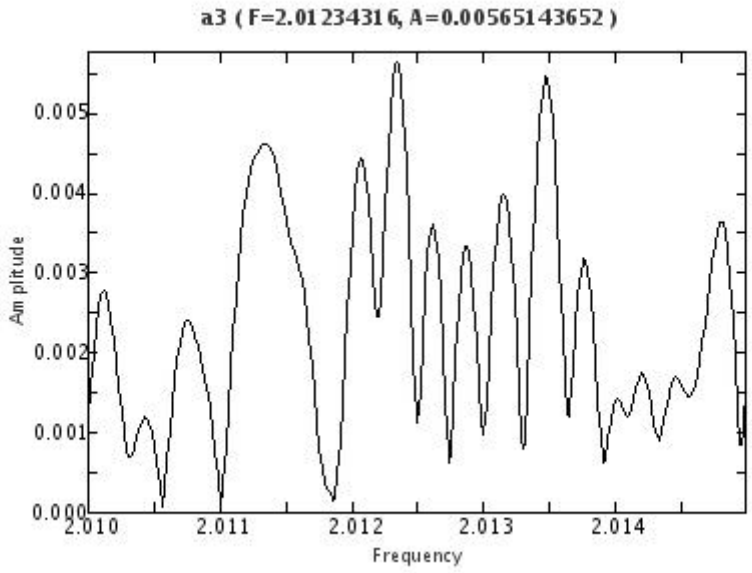

Figure 9.12: Frequency detection at 2.012343 in the star a3 that fits well the frequency predicted by $f_0 - 3f_m$. The amplitude is relatively low but the peak is distinguishable. Thus this is a potential detection of a part of a frequency septuplet.

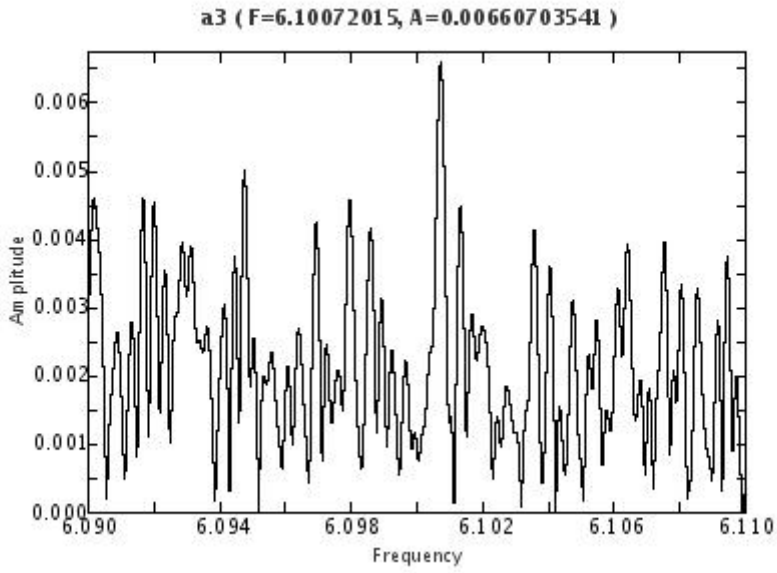

Figure 9.13: Frequency detection in the quintuplet in star a3, $3f_0 - 2f_m$ = 6.100720. This is the highest frequency clearly detectable in the quintuplet series for this star.

9.7 Frequency spectra for stars with complicated 'fine structure'

The majority of Blazhko stars checked for frequency multiplets had frequency spectra that were 'noisy' in frequencies around the f_0. In particular the frequency spectra around the fundamental had additional structure overlaid on the main peak. The difference between these stars and those in which frequency quintuplets were detected becomes immediately clear after the first least-square fitting and removal of the fundamental frequency and its harmonics. The characteristic of these Blazhko stars is that the residual frequency spectra show remaining frequencies with values close to f_0. Moreover, this process has to be repeated several times before the first set of triplet frequencies has amplitudes higher than any remaining frequencies with values close to f_0. As an example this type of frequency spectrum is shown below for one star, see Figures 9.14 – 9.16. Several stars with this type of frequency spectra were found in this analysis but their details are not included.

A simple check for the stability of the primary radial pulsation period in star a6 has been carried out. Subsets containing 200 observations were chosen from the beginning, middle and end of the timespan of the whole set of observations. Frequency analysis was carried out for each subset with exactly the same settings as for the whole set. The resulting frequencies for the subsets specified in this paragraph were 2.211921, 2.212053 and 2.212199 cd^{-1} resepctively. The corresponding timespans are 1117, 571 and 681 days, respectively. The differences between these frequencies themselves and or the frequency calculated for the whole set of observations are very small. The biggest difference between a combination of two these frequencies equals 0.01% of their values. This suggests that at least over the timespans inspected the primary radial pulsation frequency is stable. Furthermore this suggests that any variations in period implied by the 'noisy' frequency spectrum around the main frequency occur on shorter timescales. This simple result should not be used as a 'proof of absence' of variations in the main radial pulsation period because

it may also be biased by phase coverage. The lightcurve for star a6 qualitatively shows a well mixed timespan coverage over the phase like variation (see section 9.9).

This is a topic that needs additional investigation concentrating on this specific type of Blazhko stars. These spectra may relate directly to the detection of a subgroup of Blazhko stars with claimed non-equidistant triplet frequency structures. Specifically the non-equidistant frequency structures are not compatible with magnetic models for the Blazhko effect but these could be explained if they are not truly non-equidistant but an artefact of 'noisy' frequency spectra. In the presence of such a complicated frequency structure different peaks may be picked out by DFT analysis depending on variations in sampling and model fitting and different peaks again when these parameters change. Thus non-equidistant frequency multiplets can be an artefact of such complicated frequency spectra and not a counter-argument to magnetic models for the Blazhko effect.

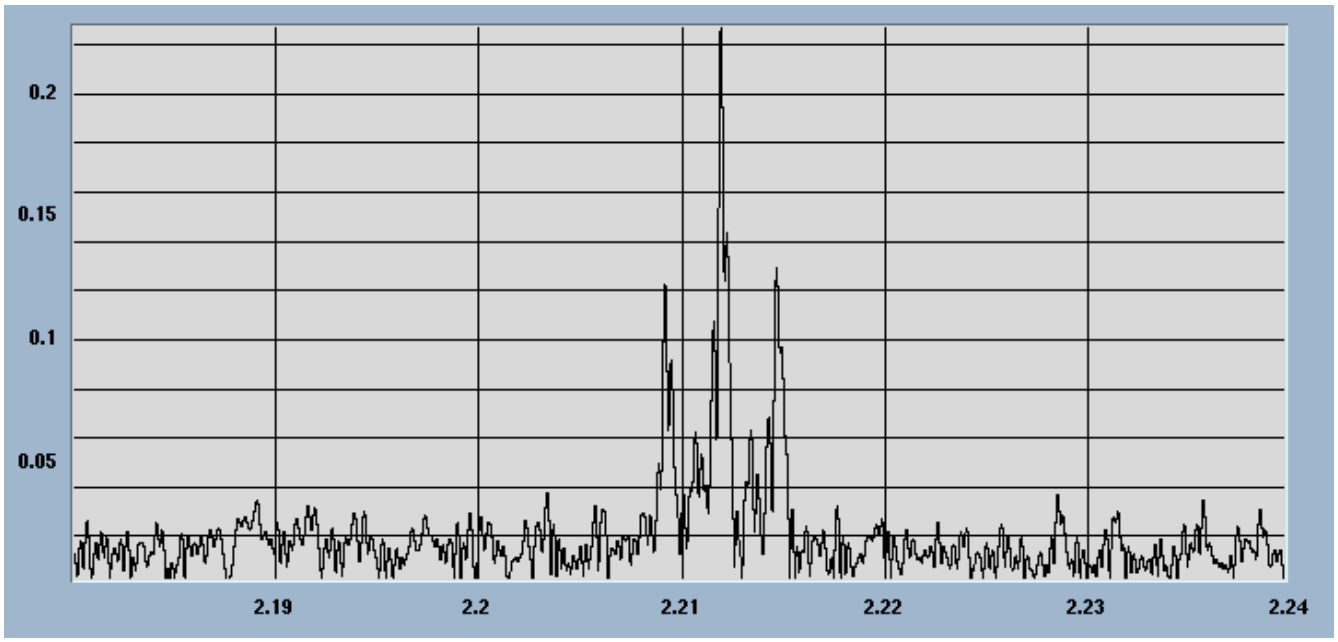

Figure 9.14: Frequency spectrum for star a6 around the main period f_0 = 2.212066. This spectrum shows more fine structure around the main frequency than the stars s2366 and a3 with the quintuplet detections.

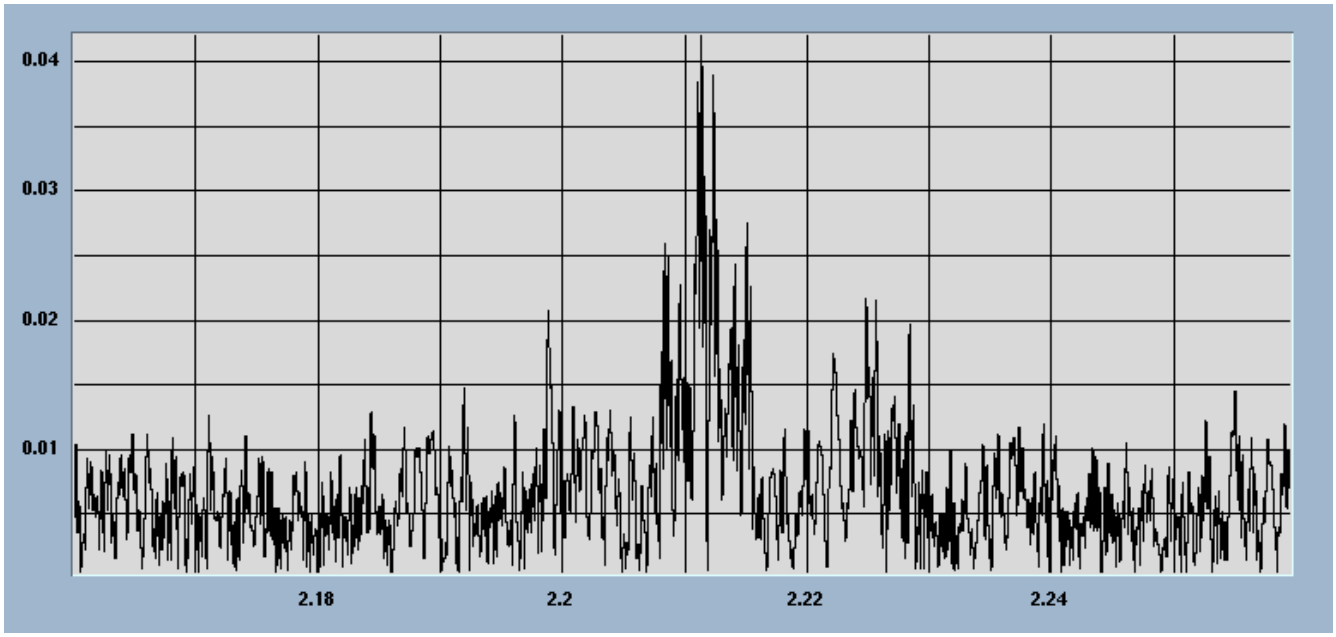

Figure 9.15: The residual frequency spectrum for star a6 with main frequency removed still shows a peak close to the original frequency at 2.211582. This is in contrast to the frequency spectra for the two quintuplet detections in which a triplet is immediately detectable after the removal of the main period and its harmonics.

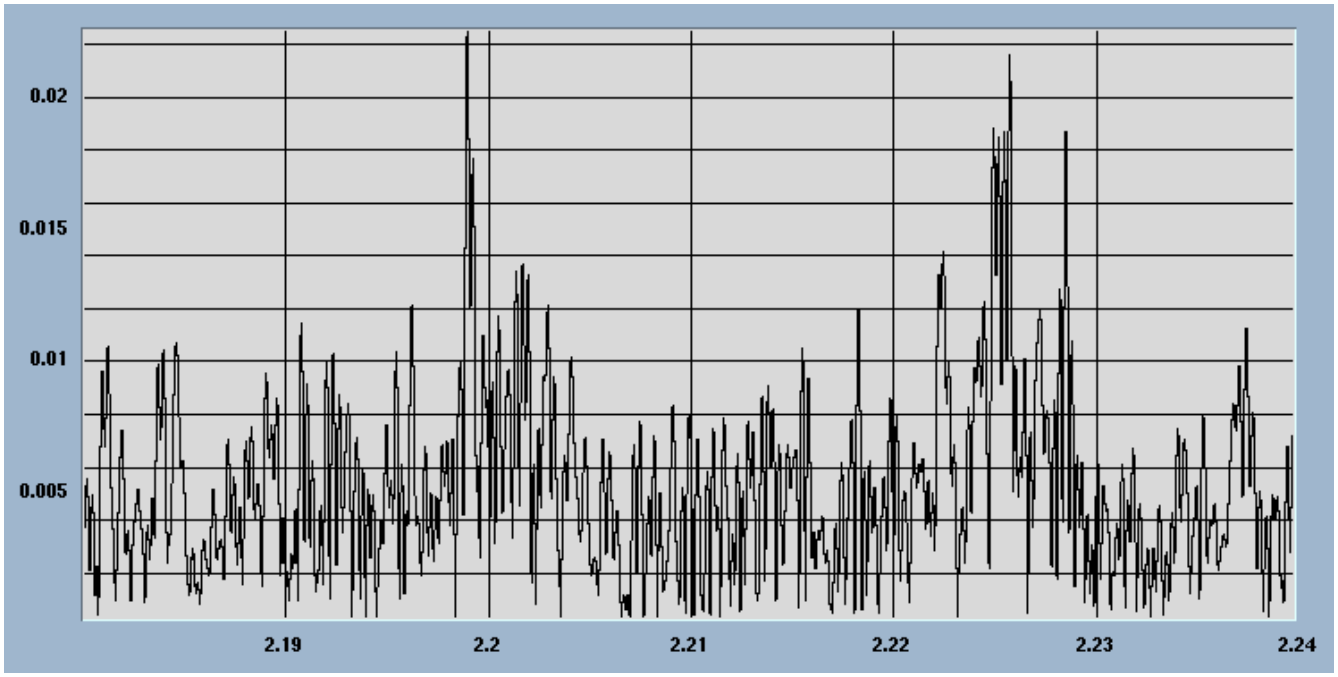

Figure 9.16: Frequency spectrum of star a6 after several iterations removing periods close to the main period. This reveals a triplet structure at frequencies of 2.199042 and 2.225898. Compared to

the central period of 2.212066 the frequency differences of the two triplet components are -0.013024 and +0.013832. These differences make it a slightly asymmetric triplet suggesting that it is incompatible with the magnetic models of the Blazhko effect. The predicted Blazhko modulation from the two different separations is 76.8 and 72.3 days, close but significantly different. However, a quintuplet structure could not be extracted from the spectrum because higher harmonics of the main frequency still appear in it and most likely cover any existing quintuplet components. The plethora of very closely spaced and most likely not fully resolved frequencies makes the job of modelling and removing frequency components problematic in this and similar stars.

9.8 Confirming the frequency detections

The Monte Carlo based method for finding frequency errors as implemented in Period04 is not appropriate for this data and does not provide information on significance levels of the frequencies (see the histogram in Figure 9.17). One iteration of the method implemented in Period04 adds randomly up to one sigma noise to the data and re-analyses the lightcurve for frequencies. The approach conflicts with data analysis in this section in two ways: it is not clear how the level of noise is determined and how adding it to the data relates to errors in the frequencies; the implementation does not always pick the same frequencies in a multiplet series and thus overestimates the errors. The significance of the detected quintuplet frequencies is obtained in ways alternate to those provided by Period04.

The Lomb-Scargle method is used to confirm the detections of all the frequency quintuplets. The Peranso software calculates Lomb-Scargle periodograms around the detected quintuplet frequencies. The resolution of 4000 steps over a range of 0.02 cd^{-1} is used in all cases. The resulting frequencies are compared to the DFT based frequencies as obtained above. The DFT and Lomb-Scargle derived frequencies agree to within small differences. These differences are in the

same range as the differences in Table 9.1. This result confirms that the frequency detections are independent of the method used to obtain them.

The signal to noise (SN) ratios are calculated for the detected quintuplet frequencies using the Period04 inbuilt procedure and given in Table 9.2. The frequency range over which the SN ratio is calculated is 0.04 cd^{-1} centered on the frequency in question. The same frequency step rate of 1×10^{-8} cd^{-1} is used for these calculations as is used for the frequency detections. The SN ratios indicate weak but real quintuplet frequencies. The significance of the S/N to noise ratio has to be assessed for each set of quintuplet frequencies as a whole and not just individually. Some of the frequencies occur at the expected quintuplet positions but are relatively weaker. These weaker frequencies become more reliable or significant when detected as part of a set at predicted positions by for example following one of the rules of combining probabilities: when tossing a coin the probability of getting 3 heads in a row is 1/8 and it is not ½ just because the chance of getting a head is ½ at each throw. Similarly because the S/N to noise ratios occur for an interdependent set of frequencies the combined reliability of getting them together is higher than can be judged from each detection independently. Determining precisely how S/N ratios indicate reliability for Blazhko frequency multiplets is an interesting area for future work but is beyond the scope of this thesis. The manual for Peranso states that FAP values less than 0.01 indicate significant detection (method as per Linnel Nemec and Nemec 1985). Similarly to the argument on the S/N values the FAPs have to be interpreted as part of set of frequencies and not independently. Equally as for S/N ratios it would be a fascinating project in statistics to construct a simultaneous FAP determination for a set of quintuplet frequencies.

Quintuplet Frequency	Frequency (cd^{-1})			S/N	FAP1	FAP2
	DFT	Lomb-Scargle	Δ ($\times 10^{-6}$)			
s2366 $f_0 + 2f_m$	2.298980	2.298980	1	3.9	0.000	0.000
s2366 2 $f_0 + 2f_m$	4.581326	4.581330	4	4.4	0.000	0.000
s2366 3 $f_0 + 2f_m$	6.863686	6.863805	119	2.8	0.005±0.002	0.000
a3 $f_0 - 2f_m$	2.021422	2.021425	3	4.8	0.000	0.000
a3 $f_0 + 2f_m$	2.057900	2.057895	5	2.5	0.012±0.003	0.001±0.001
a3 2 $f_0 - 2f_m$	4.061080	4.061080	1	2.9	0.013±0.004	0.000
a3 2 $f_0 + 2f_m$	4.098028	4.098020	8	1.9	0.004±0.002	0.000
a3 3 $f_0 - 2f_m$	6.100745	6.100755	10	2.2	0.005±0.002	0.000

Table 9.2: The significance of frequency quintuplet detections.

The False Alarm Probability (FAP) is a metric to express the significance of a frequency. The lower the FAP for a given frequency, the more likely it is that the frequency is significant. As a rule of thumb guide FAPs below 0.01 (1%) should indicate a very secure frequency identification, while FAPs above 0.2 most likely indicate data artefacts and not true frequencies (Peranso user manual). Peranso uses Fisher Randomisation to calculate FAP1 and FAP2 as per the method in Linnel Nemec and Nemec 1985. This method is specific to assessing the significance of frequency detections in variable star lightcurves and fully suited to this data analysis. The FAPs are calculated for the frequency quintuplet detections and given in Table 9.2. For each frequency 1000 permutations or iterations are used in the Monte Carlo simulation. The frequency range in the simulation is the same as in the Figures showing the frequency spectrum for a given detection and is 0.02 cd^{-1} in almost all cases (except where the range is truncated through the presence of another

close significant frequency). For each permutation the data is randomised and the frequency spectrum computed over the specified range.

The FAP1 of a frequency *f* represents the proportion of permutations that contain a frequency with a peak higher than *f* had in the original data. It is the probability that there is no frequency in the specified range equal to *f*.

The FAP2 of a frequency *f* represents the proportion of permutations that contain a peak at *f* higher than in the original data. It is the probability that the data contains a true frequency that is different from *f*.

All the FAP metrics for the quintuplet detections listed in Table 9.2 are low enough to indicate significant frequencies. The Monte Carlo simulations for the star a3 show somewhat higher probabilities of incorrect frequency detection but still within limits for real frequency detections.

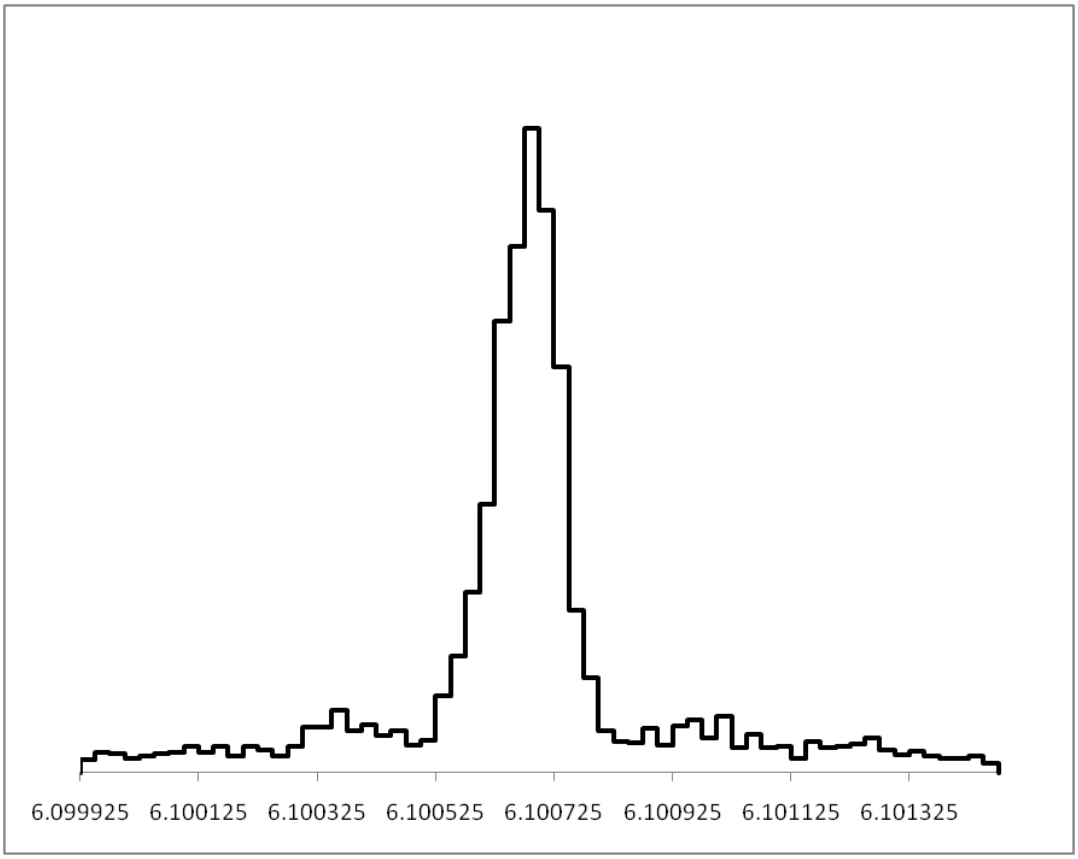

Figure 9.17: Histogram of Monte Carlo simulations for the $3f_0 - 2f_m$ frequency for star a3. The routine in Period04 for error estimation in frequencies produced simulated frequenices for 5000 iterations. In each iteration random noise is added to the fitted lightcurve model and the best matches to the model frequencies are sought in this simulated data. The specified quintuplet frequency is chosen as an example and its simulated values are plotted in the histogram above. Only the 80% of frequencies detected in simulated data closest to the real frequency detection are chosen for the histogram. The 80% bound is required to demonstrate the shape of the main distribution through the removal of a low frequency of relatively distant outliers. The shape of the distribution is asymmetric around the real frequency and contains additional peaks. This suggests that the distribution is not Gaussian and the Monte Carlo simulation implemented in Period04 is not a good predictor of frequency errors in the data analysed here.

Spectral windows for both stars are produced using the inbuilt procedure of Period04. These calculations use a frequency step rate of 1×10^{-8} cd^{-1} keeping them consistent with other steps of

this analysis. The frequency range inspected is centered on the dominant radial pulsation frequency and has a width of eight times the respective modulation frequency. The spectral windows are plotted in this range because it corresponds to the frequency range searched for frequency multiplets. The spectral window for the star s2366 shown in Figure 9.18 does not contain significant peaks corresponding to any true frequency detections in this analysis. In addition the spectral window for s2366 contains a similar double peaked feature as seen in Figure 9.19 around 2 cd^{-1} not shown here because it lies outside the chosen frequency range.

The spectral window for the star a3 shown in Figure 9.19 contains small peaks slightly above the noise level in the vicinity of two frequencies judged significant, at 2.021891 and 2.039347 cd^{-1} and the two frequencies detected in star a3 that are closest to these are f_0 and f_0 - $2f_m$, respectively. The f_0 is detected correctly in the original and this is confirmed by detecting the same frequency in data subsections where the spectra window lacks a similar feature, folding of the data at this frequency and producing a clear RR Lyrae lightcurve and the self consistency of all steps in this analysis. In both cases the two frequencies in the spectral window are very weak and their differences from the corresponding true frequencies are much larger than the typical differences derived above. For these reasons these two spectral window features for a3 are noted but it is decided that they are not significant because the radial frequency is shown as being real and the other feature is weak.

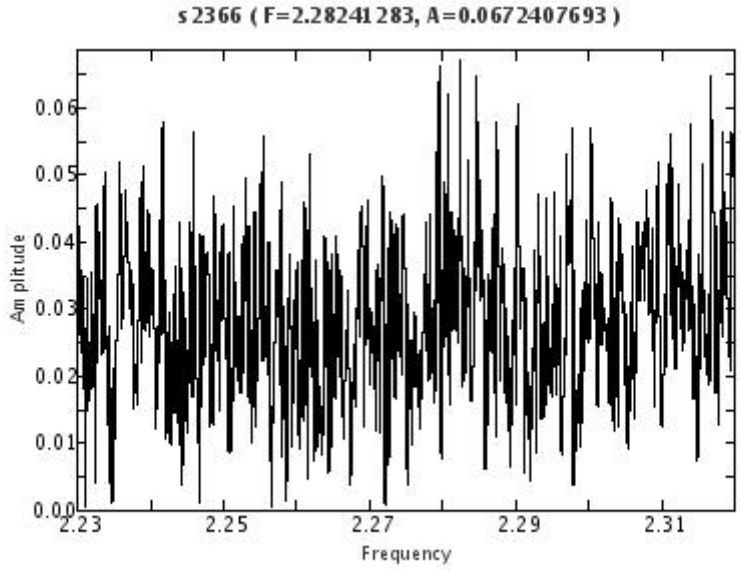

Figure 9.18: The spectral window for star s2366 in the frequency span of approximately $f_0 \pm 4 f_m$.

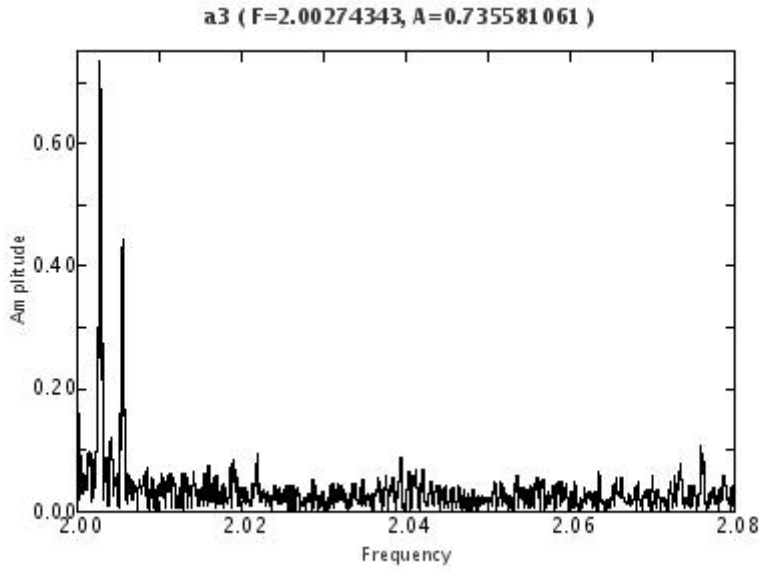

Figure 9.19: The spectral window for star a3 in the frequency span of approximately $f_0 \pm 4 f_m$.

The results in this section confirm the accuracy and significance of the frequency detections for both the stars described. The positions of the frequencies are determined accurately and while some are relatively weak when compared to the surrounding noise level they are all significant.

9.9 Lightcurves

Lightcurves of the stars analysed in section 9 at high resolution for residual frequencies are presented below. The lightcurves plotted in blue show observations for the two stars in which frequency quintuplets have been detected. The lightcurves plotted in brown show stars with frequency spectra that are ‘noisy’ around the main pulsation frequency as discussed in section 9.7. Table provides the identifications and locations for these stars. Observations for each star are plotted in two complementary ways:

- in single colour for all observation and with error bars to clearly demonstrate the density of the observations and the accuracy of the magnitudes.
- without error bars but in a range of colours that represent when the observations were taken. The colours are scaled by how many cycles of the radial pulsation occurred since the earliest observation for each star.

These multi-coloured lightcurves qualitatively show how the Blazhko modulation relates to a given time and that the observations are well distributed over phase for all the stars. Both types of plots suggest that the stars with the ‘noisy’ frequency spectra around the main pulsation period exhibit a pronounced movement over time in the position of the lightcurve maxima with respect to phase in addition to amplitude modulation. In contrast the two stars in which frequency quintuplets have been detected appear to lack a strong component of phase modulation while still showing the amplitude modulation. A quantitative assessment of this distinction is a potential area for further study.

Star	OGLE II ID	Co-ordinates	Main frequency (d^{-1})	Blazhko Period (days)
s2366	bul sc34 607633	17:58:19.17 -29:05:47.4	2.282328	119.4
a3	bul sc1 59431	18:02:15.88 -30:05:09.2	2.039675	110.0
a6	bul sc2 783422	18:04:48.66 -28:30:50.0	2.212066	77.4 and 76.7
a20	bul sc4 601095	17:54:53.69 -20:06:58.3	2.216807	116.2 and 117.3
a33	bul sc18 578891	18:07:28.61 -27:37:42.1	2.128610	134.3 and 149.2
a1	Bul sc1 587412	18:02:49.22 -30:12:54.7	2.029399	68.5 and 68.2

Table 9.3: Identifications and co-ordinates for the stars processed with detailed high resolution frequency analysis. The *Main frequency* in this table is the frequency for the main and strongest pulsation cycle of the star (the radial pulsation). The *Blazhko Period* is derived from the frequency separation of the triplet, in the case of stars s2366 and a3 it is based on the combined OGLE II and OGLE III data and for the rest of the stars on OGLE II data from Mizerski 2003. The pairs of Blazhko periods correspond to the detection of uneven frequency triplets and are a further indication of the complex and 'noisy' frequency structures around the fundamental radial pulsation frequency.

The available OGLE III data for star a1 contained only 114 observations not adding as much information on its frequency components as is the case for other stars in the set. Thus star a1 was rejected at an early stage of the search for a quintuplet frequency structure and its lightcurve is not presented below. Similarly star s2366 is the same as PLANET star KB02033I_d1250.ab but the PLANET data is not included in the combined lightcurve due to containing only 93 observations on a relative magnitude scale making combining the data impractical.

The lightcurves are presented in the same order as in Table 9.3:

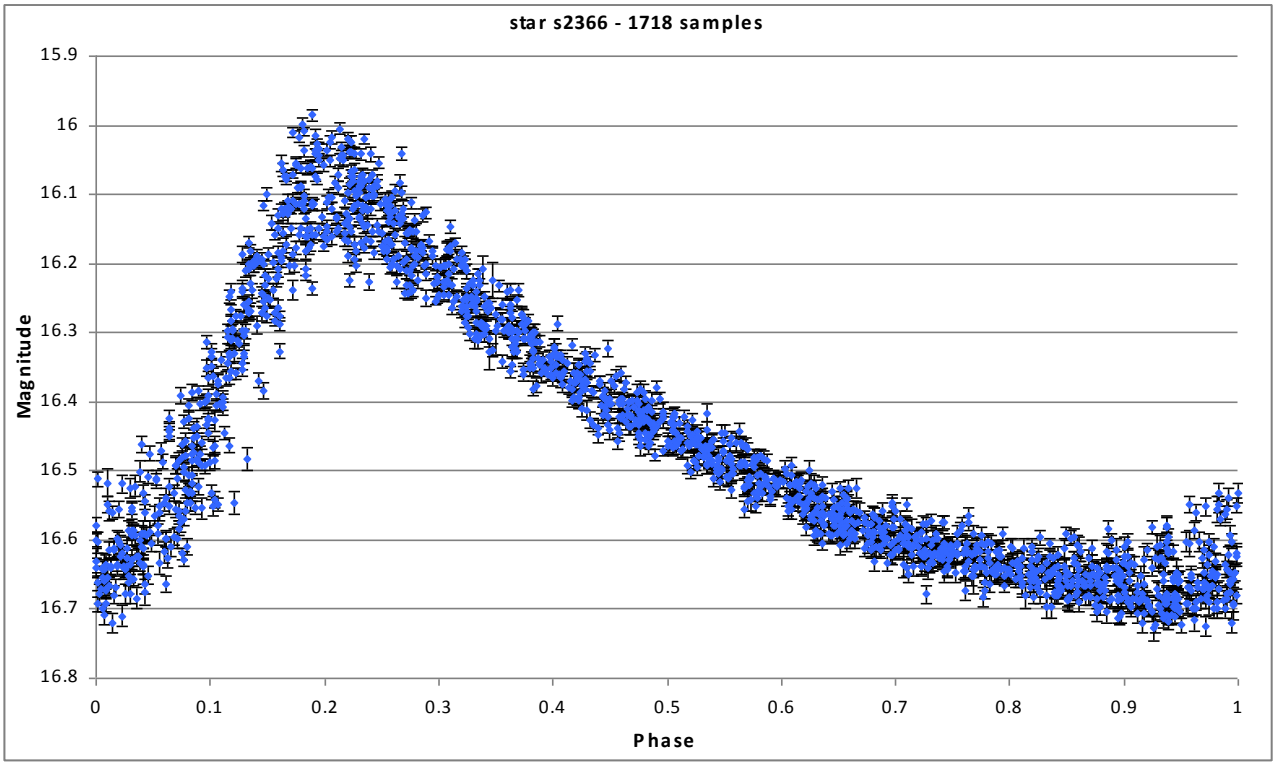

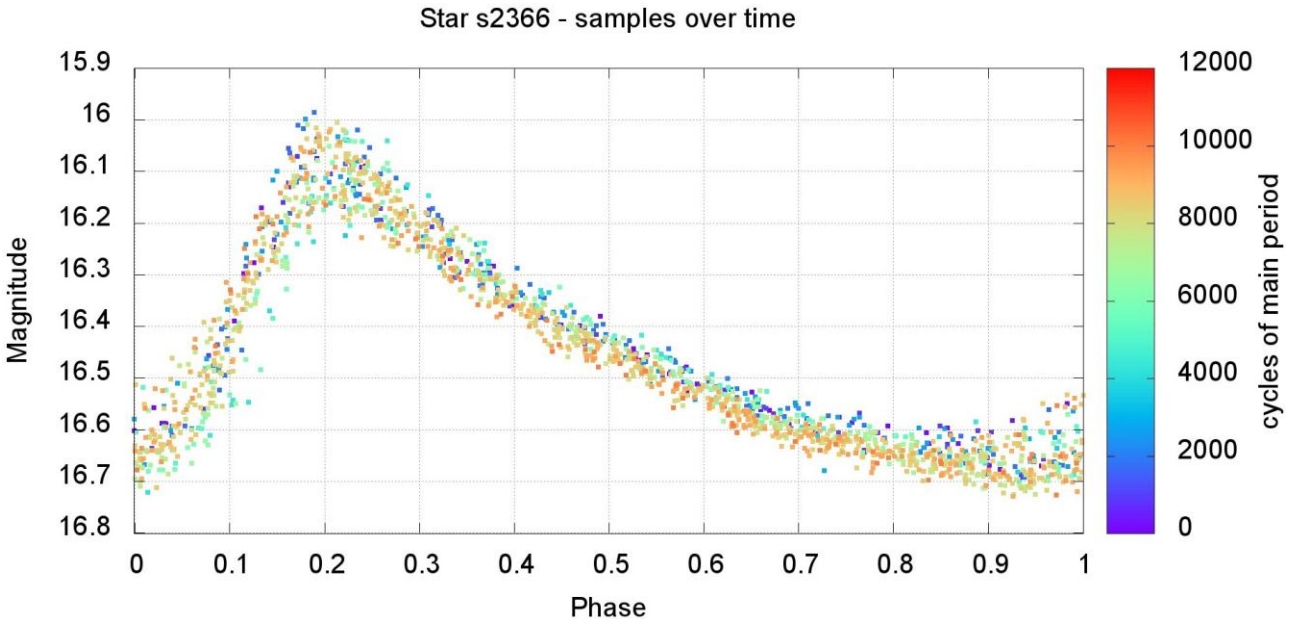

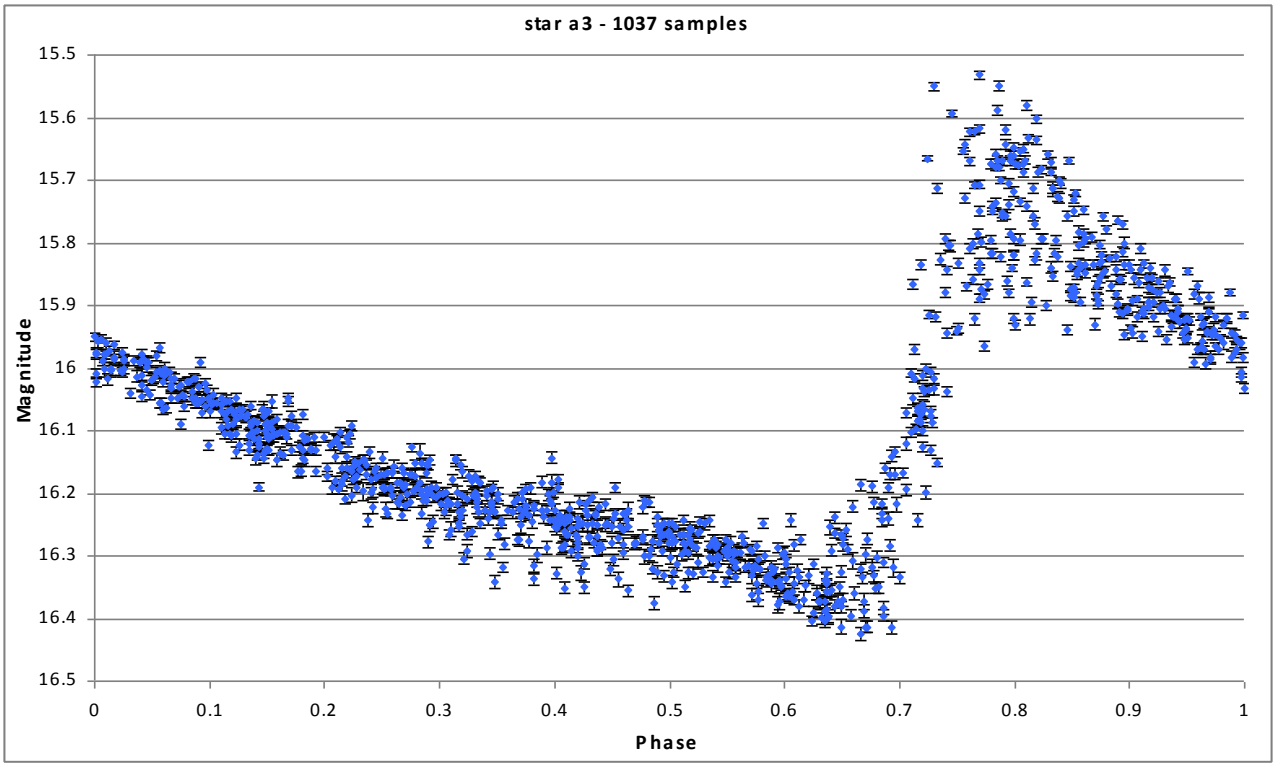
star a3 - 1037 samples
Magnitude
15.5
15.6
15.7
15.8
15.9
16
16.1
16.2
16.3
16.4
16.5
0
0.1
0.2
0.3
0.4
0.5
0.6
0.7
0.8
0.9
1
Phase

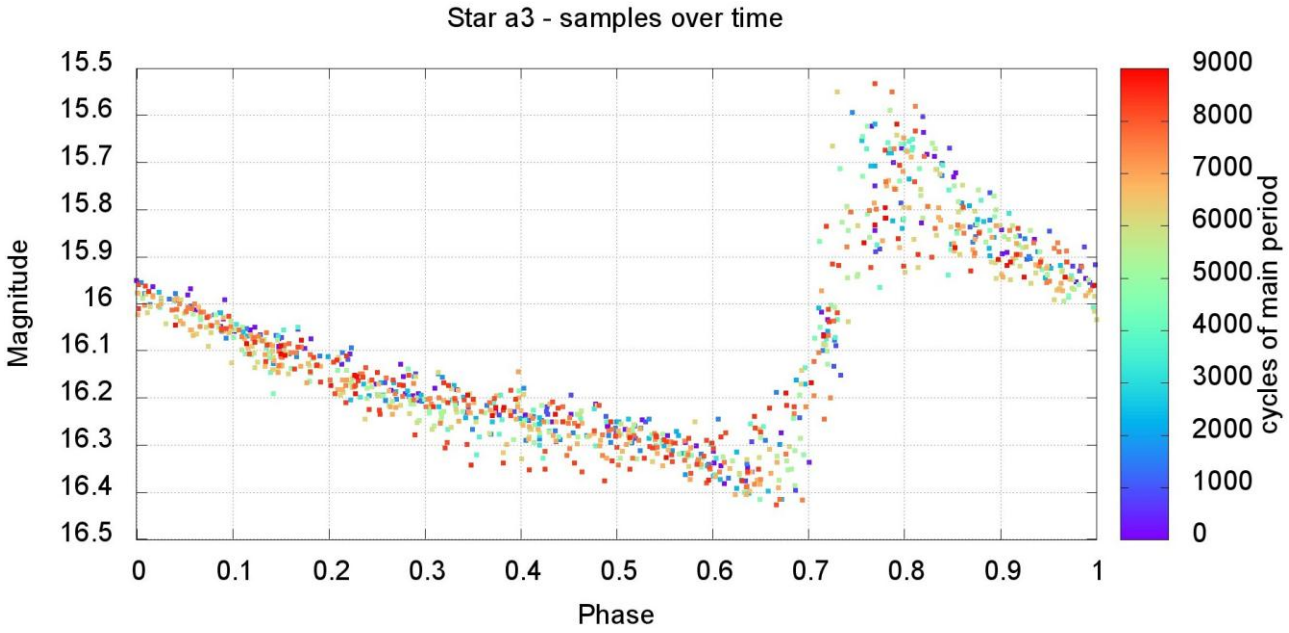
Star a3 - samples over time
Magnitude
15.5
15.6
15.7
15.8
15.9
16
16.1
16.2
16.3
16.4
16.5
0
0.1
0.2
0.3
0.4
0.5
0.6
0.7
0.8
0.9
1
Phase
9000
8000
7000
6000
5000
4000
3000
2000
1000
0
cycles of main period

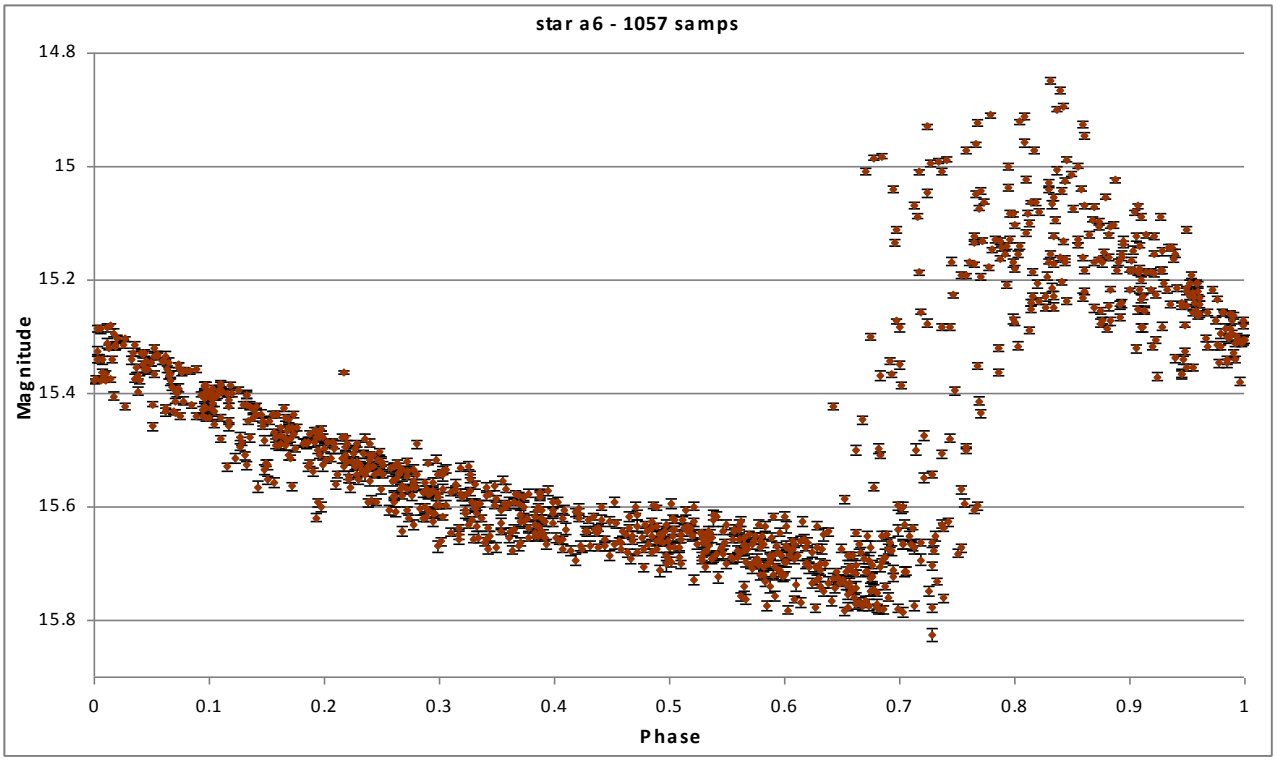
star a6 - 1057 samps
Magnitude
14.8
15
15.2
15.4
15.6
15.8
0
0.1
0.2
0.3
0.4
0.5
0.6
0.7
0.8
0.9
1
Phase

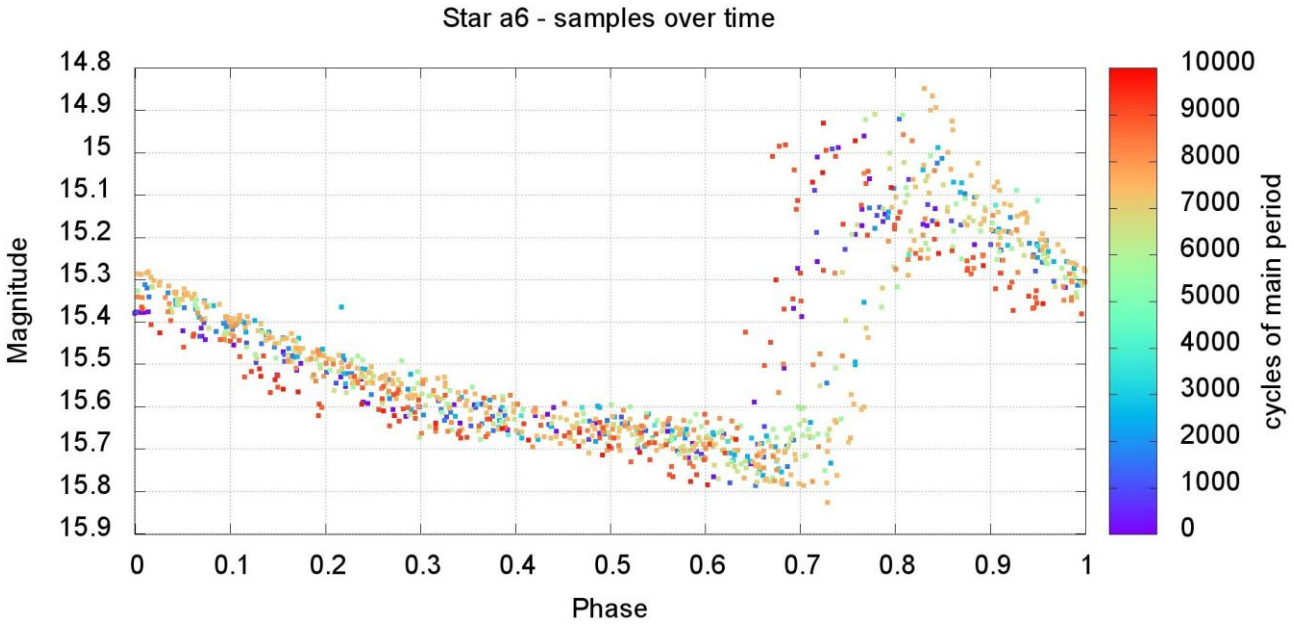
Star a6 - samples over time
Magnitude
14.8
14.9
15
15.1
15.2
15.3
15.4
15.5
15.6
15.7
15.8
15.9
0
0.1
0.2
0.3
0.4
0.5
0.6
0.7
0.8
0.9
1
Phase
10000
9000
8000
7000
6000
5000
4000
3000
2000
1000
0
cycles of main period

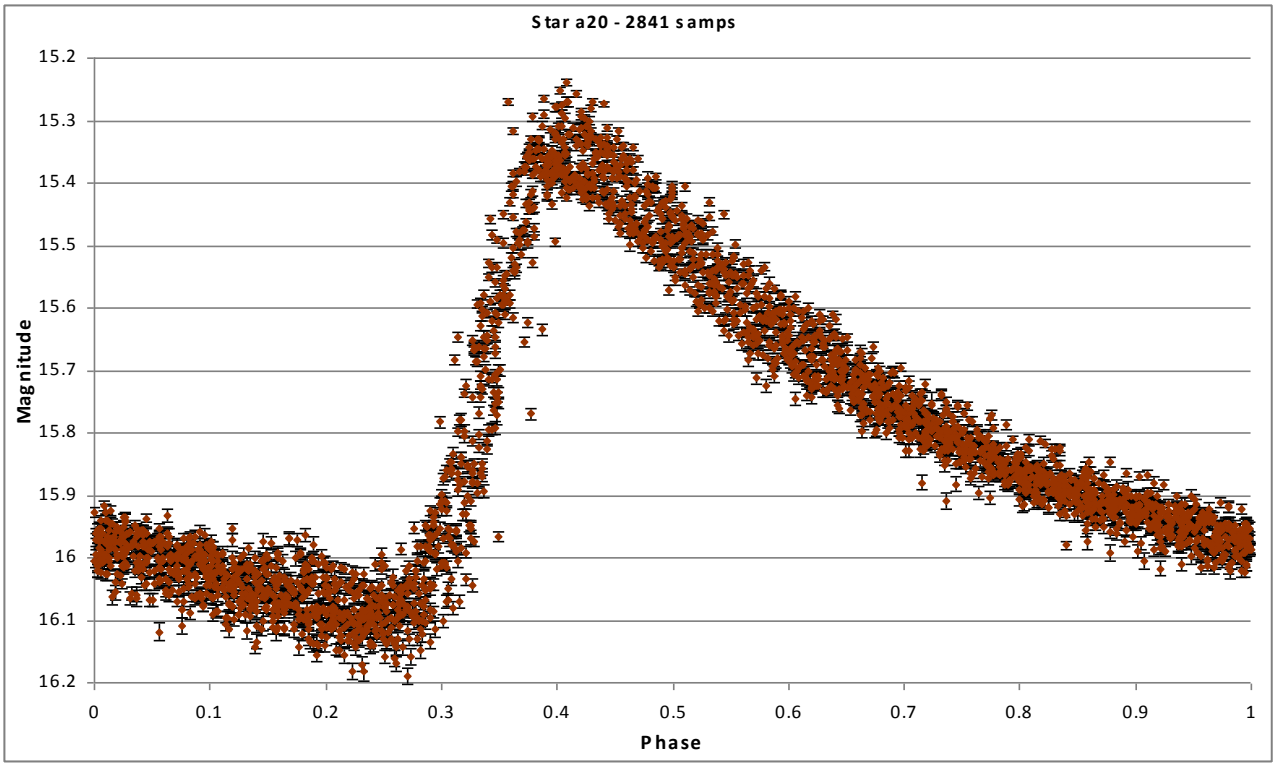
Star a20 - 2841 samps
Magnitude
15.2
15.3
15.4
15.5
15.6
15.7
15.8
15.9
16
16.1
16.2
0
0.1
0.2
0.3
0.4
0.5
0.6
0.7
0.8
0.9
1
Phase

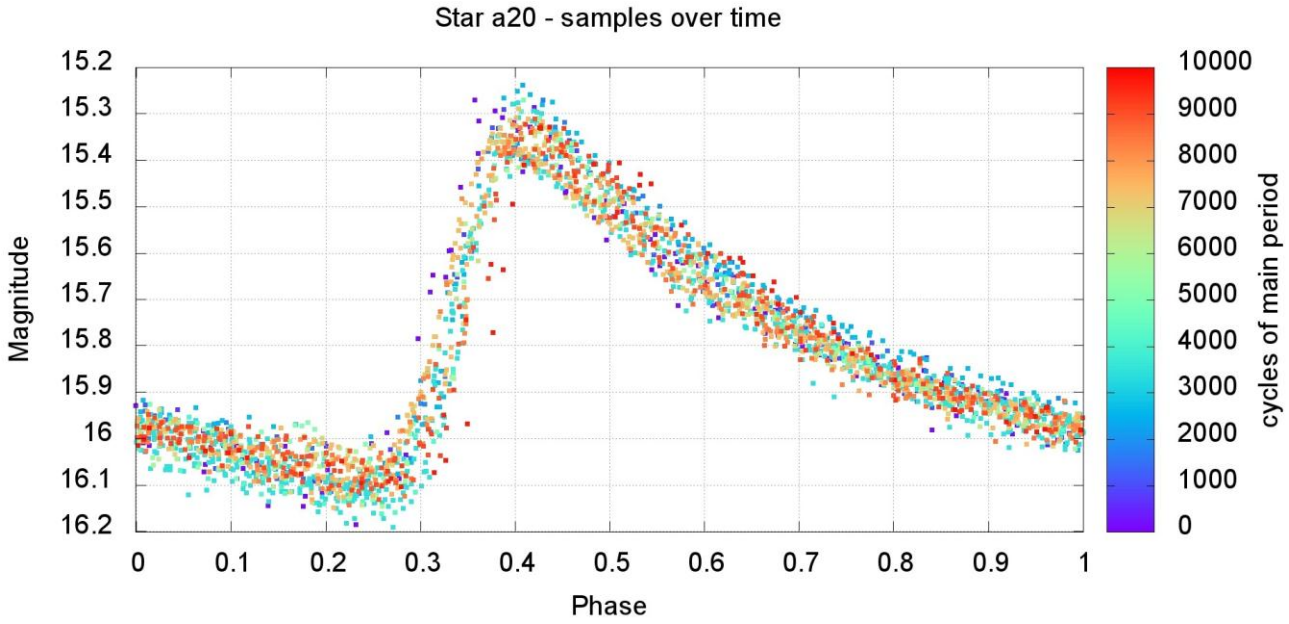
Star a20 - samples over time
Magnitude
15.2
15.3
15.4
15.5
15.6
15.7
15.8
15.9
16
16.1
16.2
0
0.1
0.2
0.3
0.4
0.5
0.6
0.7
0.8
0.9
1
Phase
10000
9000
8000
7000
6000
5000
4000
3000
2000
1000
0
cycles of main period

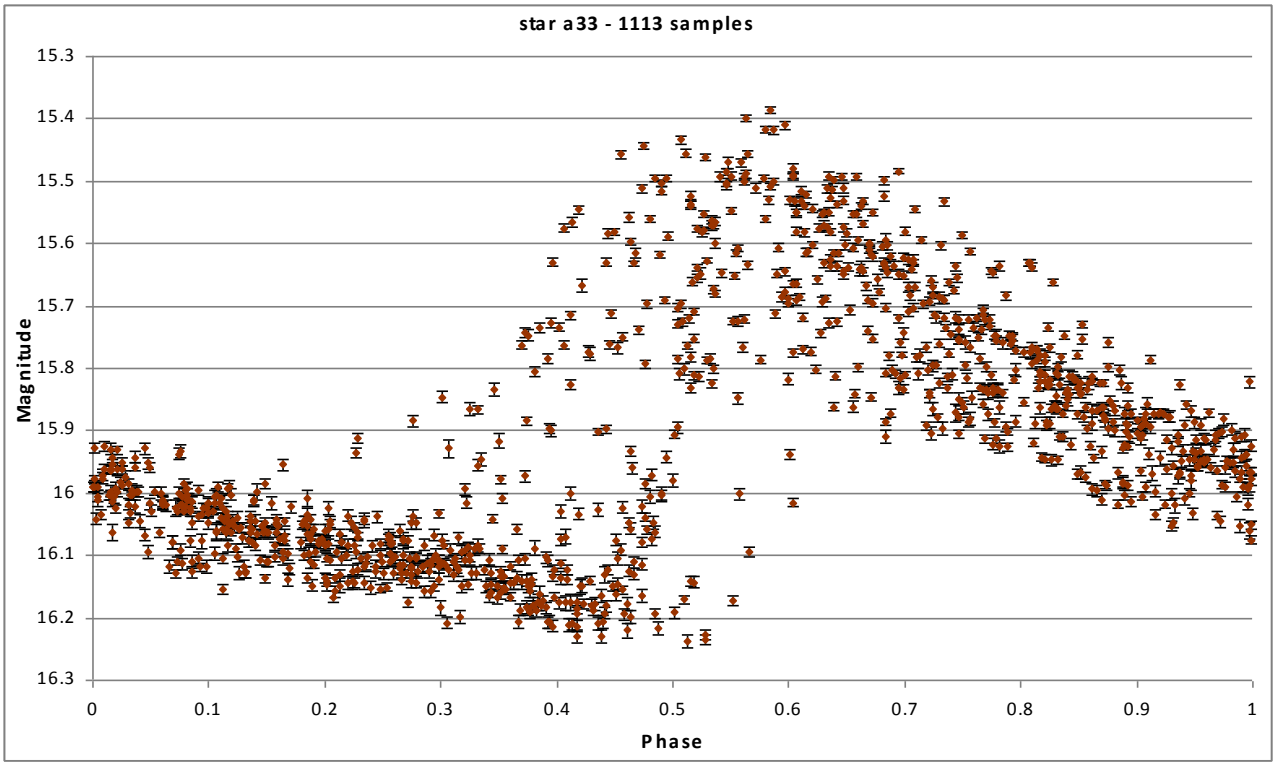
star a33 - 1113 samples
Magnitude
15.3
15.4
15.5
15.6
15.7
15.8
15.9
16
16.1
16.2
16.3
0
0.1
0.2
0.3
0.4
0.5
0.6
0.7
0.8
0.9
1
Phase

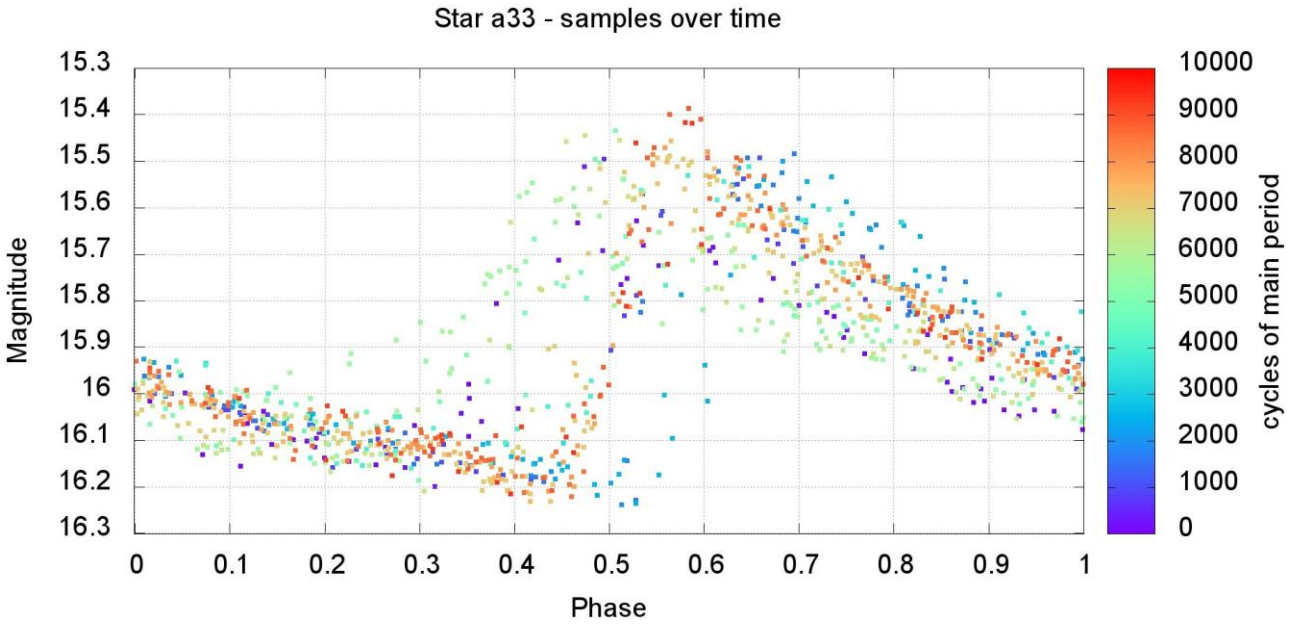
Star a33 - samples over time
Magnitude
15.3
15.4
15.5
15.6
15.7
15.8
15.9
16
16.1
16.2
16.3
0
0.1
0.2
0.3
0.4
0.5
0.6
0.7
0.8
0.9
1
Phase
10000
9000
8000
7000
6000
5000
4000
3000
2000
1000
0
cycles of main period

9.10 Discussion and future work

From the stars selected for this work the power spectra of six Blazhko stars have been analysed in additional detail. The lightcurves of this sample are from a group sufficiently well sampled over a long time interval to test the predictions of models for the modulation mechanism in Blazhko stars. In the sub-sample of six stars two new stars with frequency quintuplets in their power spectra have been identified and described in detail. Only six other detections of a frequency quintuplet have been made so far (Hurta et al 2008, Jurcsik et al 2008, Kolenberg et al 2009, Jurcsik et al 2009, Chadid et al 2010, Kolenberg et al 2011). This analysis provides additional support for the magnetic model of the Blazhko effect but as discussed the model remains unproven and requires further work to establish how it agrees with the recent high quality observations of Blazhko stars. The positions of the frequency detections lie precisely at values predicted by the pattern of frequency quintuplets and this supports their identifications. The varying relative strengths of the frequency components for different stars are consistent with predictions of the magnetic models that these will vary dependent upon the spatial orientation of the magnetic field in Blazhko stars (Shibahashi 2000). These results add further proof that the previous absence of frequency quintuplet detections in Blazhko stars was caused by the lack of data suitable for their detection and this has important implications for the explanation of the Blazhko effect. It can no longer be said that the absence of frequency quintuplets in Blazhko stars is a reason for rejecting the magnetic models as an explanation of the effect. The four Blazhko stars for which analysis was carried out in this thesis but for which frequency quintuplets were not identified do not demonstrate the absence of frequency quintuplets but are a case of frequency spectra with a lot of fine structure which makes identifying residual periods very difficult.

In addition, through the exploration of the available data, evidence for the need to reclassify Blazhko types has been presented. Similarly to the recent lack of frequency quintuplets the current

classification of Blazhko stars that includes non-equidistant frequency triplets may be based on data lacking sufficient frequency resolution. Instead it seems that some Blazhko stars have dense and complicated frequency structures possibly caused by changing period of radial pulsation. However, firm conclusions on this specific issue require an assessment of more Blazhko stars showing such frequency structures and thus this is a topic for future work.

Period changes in the Blazhko modulation contradict magnetic models which rely on a modulation caused purely by the rotation of the star (for example see Kolenberg et al 2011 and Stothers 2006). The rotation rate of a star is stable on the relatively short time scales over which Blazhko stars have been observed. Detections of period changes in the Blazhko modulation over the long term are well known. More recently Kolenberg et al (2011) and Chadid et al (2010) show that the Blazhko modulation does not repeat precisely from one cycle to the next and this result is used to support the argument that the period of the modulation may be variable. However, so far these short term variabilities in the "shape" of the Blazhko modulation have not been shown to equate to changes in the period of the modulation. These results do conclusively demonstrate that in Blazhko stars both the radial pulsation and modulation are changeable through some as yet undetermined causes. Thus the existing magnetic models for the Blazhko effect need to be expanded or adapted to describe all the observed features of the modulation.

It should be kept in mind that RR Lyrae stars are post main sequence red giants with outer layers which expand and contract on the very short time scales of their radial pulsation. These stars will rotate at various rates and the radial pulsation will involve changes in angular momentum for the outer layers involved in the radial pulsation. Differential rotation in these stars will occur. These two effects are highly likely to occur in RR Lyrae stars and alone will be able to distort both radial pulsation and the Blazhko modulation. For example, on the assumption that the modulation is connected with stellar rotation it would be interesting to examine if the shorter period Blazhko stars

exhibit larger or smaller changes in the radial pulsation period. In this case faster rotating stars should have a shorter period of Blazhko modulation and larger differential rotation and if in turn the distortions in radial pulsation and Blazhko modulation are larger as well, this would suggest a connection between these processes.

A large fraction of the stars in the Galaxy exists in binary star systems. Simply by chance some RR Lyrae and Blazhko stars are likely to be part of binaries although so far no Blazhko stars have been identified in a binary. A Blazhko star in a binary orbit would present the same orientation to a very distant observer and thus for non-eclipsing and non-interacting binaries would appear the same as a single star. However, it is possible that in some cases Blazhko stars in binary system are either eclipsing or interacting. If the magnetic field, a binary companion or another effect distorts the mass distribution in a Blazhko star asymmetrically from the rotation axis, it becomes possible that a precession or wobble is induced in the star. Thus in the case of the Blazhko modulation being explained by the magnetic Oblique Pulsator model, a binary orbit may further affect the perceived amplitude and period of the effect.

Some Blazhko stars show clearly measurable changes in both primary radial pulsation periods and Blazhko periods and two examples AR Her and XZ Cyg are described in detail by Smith *et al* (1999) and LaCluyzé *et al* (2004) respectively. LaCluyzé *et al* (2004) also points out that RV UMa the Blazhko star with the first detected frequency quintuplet (Hurta et al 2008) also shows changes over time in the primary radial pulsation period and the Blazhko period but this result is based on photoelectric observations by Kanyó (1976). The authors suggest that due to its unusually blue colour AR Her is a potential binary system though not containing two RR Lyrae stars but rather a Blazhko star and a nonvariable component. The evidence for the binary nature of AR Her is not developed but the idea is offered with suggestions for follow up work. The behaviour of XZ Cyg is discussed in terms of the timing of decreases and increases in the primary radial

pulsation and Blazhko periods. The period changes in XZ Cyg occur in opposite directions, the primary radial pulsation period decreased when the Blazhko period increased and LaCluyzé *et al* (2004) point out that if the star's rotational period changed accordingly to the Blazhko period the opposite should have happened. Smith *et al* (1999) and LaCluyzé *et al* (2004) argue that models which require the Blazhko period to be always equal to the rotation of the Blazhko star are excluded by their results but, as pointed out in this section of the thesis, differential rotation in the star can potentially modify this conclusion. The lightcurves of stars a6, a20 and a33 in this thesis, the stars with frequency spectra that are 'noisy' around the main pulsation frequency, are qualitatively similar to the lightcurves of AR Her and XZ Cyg. The Blazhko modulation in these stars shows phase like changes of the radial pulsation. The lightcurves of stars s2366 and a3 in this thesis, the two stars with frequency quintuplet detections, are qualitatively similar to the lightcurve of RV UMa, containing the first detected frequency quintuplet in a Blazhko star, as all of these stars show changes in amplitude with relatively little movement in phase.

The first RR Lyrae star in a binary system has been identified in the OGLE III survey data see Figure 6 in Soszyński (2011). Type ab RR Lyrae star shows a lightcurve overlaid with the modulation of an eclipsing detached binary. Soszyński (2011) mentions several other RR Lyrae stars that are potentially located in binary star systems. Thus, while no Blazhko star has been so far identified as belonging to a binary star system, this possibility should be remembered as a potential explanation for those variations in Blazhko or RR Lyrae behaviour that may exist in some of these stars but be absent in others. The influence of a binary star companion on the Blazhko modulation would mostly depend on the details of the orbit. The size of the orbits would determine the strength of tidal interactions and whether the stars end up tidally locked or just in distorted shapes. Some tidal distortions may affect pulsation. Orbits with higher eccentricities may allow resonant orbital periods and intermittent changes in pulsation as the strength of tidal effects varies over the orbit. It has to be kept in mind that RR Lyrae stars are relatively old and a careful consideration is needed of

whether orbits can retain high eccentricity in such systems. Precession effects may add another layer of variability to Blazhko stars in binary star systems. One observable prediction for changes in RR Lyrae pulsation due to a stellar companion would be their regularity. For example, if the changes in the primary radial pulsation are not strongly regular, they are not likely to be caused by orbital motion. Future work in this area and an examination of these hypotheses for Blazhko stars could start with modelling of the strengths of tidal interactions over a range of likely orbits along with long term observations to determine the precise patterns of changes in pulsation periodicities.

None of the above hypotheses are developed for Blazhko stars and it is not known how strongly these distortions would contribute to the observed light variability. They are presented here to suggest that dismissing the magnetic Oblique Pulsator model on the basis of changes in the modulation period is premature. Rather as Kolenberg et al (2011) suggest none of the current models for the Blazhko effect satisfactorily explain all the features of the observed lightcurves. The models need to be re-examined and adapted. This is not surprising considering the recent nature of the very high quality lightcurves now available for Blazhko stars.

In analysis of the data for the presence of frequency quintuplets other significant results were derived which are interesting areas for future work:

(a) A substantial fraction of the Blazhko stars have lightcurves that produce frequency spectra with a ‘forest’ of frequencies around the standard triplet. This prevents the derivation of clean residual data and the subsequent search for frequency quintuplets. This type of fine frequency structure seems to be a common feature of Blazhko stars and it hints at period instabilities or changes in Blazhko stars over the 12 years of observations. Changes in the radial pulsation period can be checked for in these stars and if they become associated with the presence of these

structures, this would offer an explanation for the underlying cause. The multi survey data used in this study may be suitable for such a project.

(b) All the frequency triplets cleanly identified in the data so far are of the variety where the side frequencies are equally spaced around the central one. The stars that were previously identified as triplets with unequally spaced frequencies turn out in this analysis to be misidentified. The unequal triplets are either doublets with noise over-resolved into a false frequency detection or they have the 'forest' of frequencies one of which gets incorrectly picked. If a larger number of Blazhko stars with exclusively equidistant triplets are described, this would offer strong support for this conclusion. Similarly to the point above, the multi survey data used in this study is suitable to derive this conclusion. Exploring this question is particularly important to a full understanding of the Blazhko effect because clearly established non-equidistant triplets represent a strong counter argument to the magnetic models.

(c) In some stars there is an indication of frequency multiplets of an order higher than quintuplets. However, a few more detections of this type are needed to confirm this result and to establish the significance and accuracy of the detections.

(d) During the search for frequency quintuplets in Blazhko stars several non-equidistant frequency triplet detections were identified where the separation between one of the side frequencies and the main frequency was very close to double that of the other separation. These stars fit well the case predicted by magnetic models where the quintuplet frequencies have stronger amplitudes than triplet frequencies. In effect one side of the triplet frequencies is not detected and instead a frequency with a $2 f_m$ offset is found. Since the frequencies offset by $2 f_m$ are part of a frequency quintuplet, the 'triplet' detections of this type are in fact quintuplets with different relative strengths of frequency components. It should be kept in mind that the magnetic models for the Blazhko effect not only require the presence of frequency quintuplets but also require a

variation in the relative strengths of components in frequency multiplets due to varying orientations of Blazhko stars with respect to the observer. The data used for this work is suitable to present a few examples of such ‘hidden’ frequency quintuplets among the Blazhko stars but this question was not followed up due to time constraints.

References

Alard C., 1997, *"Variable Stars and the Astrophysical Returns of the Microlensing Surveys"*, editors Ferlet R., Maillard J-P., and Raban B., Editions Frontieres, p 273

Albrow M. *et al*, 1997, *"Variable Stars and the Astrophysical Returns of the Microlensing Surveys"*, editors Ferlet R., Maillard J-P., and Raban B., Editions Frontieres, p 135

Albrow M. *et al*, 1998, *ApJ*, 509, 687

Albrow M. *et al*, 2000, *"The Impact of Large-Scale Surveys on Pulsating Star Research",* editors Szabados L., and Kurtz D. W., ASP Conference Series, Vol 203, p 25

Alcock C. *et al*, 1996, *AJ*, 111, 1146

Alcock C. *et al*, 2000, *ApJ*, 542, 257

Alcock C. *et al*, 2000, *ApJ*, 542, 257

Arp H. C., 1955, *AJ*, 60, 317

Baade W., Hubble E. P., 1939, *PASP*, 51, 40

Babcock H. M., 1958, *ApJS*, 3, 141

Bailey S. I., 1902, *Harv. Coll. Observ. Annals*, 38, 1

Beaulieu J-P *et al*, 2006, *Nature*, 439, 437

Benedict G. F. *et al*, 2002, *AJ*, 123, 473

Bersier D., Wood P. R, 1999, *IAUS*, 192, 161

Blanco V., 1992, *AJ*, 104, 734

Blazhko S., 1907, *Astron. Nachr.*, 175, 325

Bonatto C., Bica E., Ortolani S., Barbuy B., 2007, *MNRAS*, 381, L45

Bono G., 2003, *LNP*, 635, 85

Borkova T. V., Marsakov V. A., 2003, *A&A*, 398, 133

Borkowski K. J., 1980, AcA, 30, 393

Brown S. F., Donati J.-F., Rees D. E., Semel M., 1991, *A&A*, 250, 463

Brown T. M. *et al*, 2004, *AJ*, 127, 2738

Butler D., 1975, *ApJ*, 200, 68

Cacciari C., Clementini G., 2003, *LNP*, 635, 105

Cacciari C., Clementini G., Fernley J. A., 1992, *ApJ*, 396, 219

Caputo F., 1985, *Rep. Prog. Phys.*, 48, 1235

Carney B. W. *et al*, 1992, *PASP*, 104, 44

Castellani V., Maceroni C., Tosi M., 1981, *A&A*, 102, 411

Chadid M., *et al*, 2010, *A&A*, 510, A39

Chadid M., 2000, *A&A*, 359, 991

Chadid M., 2011, *Carnegie Observatories Astrophysics Series*, Vol. 5, 29

Chadid M., Kolenberg K., Aerts C., Gillet D., 1999, *A&A*, 352, 201

Chadid M., Wade G. A., Shorlin S. L. S., Landstreet J. D., 2004, *A&A*, 413, 1087

Christensen-Dalsgaard J., 2003, Lecture Notes on Stellar Oscillations, fifth edition, Institut for Fysik og Astronomi, Aarhus Universitet Teoretisk Astrofysik Center, Danmarsk Grundforskningsfond, (http://owww.phys.au.dk/~jcd/oscilnotes/)

Christy R. F., 1966, *ApJ*, 144, 108

Clement C. M. *et al*, 2001, *AJ*, 122, 2587

Clement C. M., Rowe J. F., 2001, *AJ*, 122, 1464

Clementini G., Corwin T. M., Carney B. W., Sumerel A. N., 2004, *AJ*, 127, 938

Cousins A. W. J., 1976, *Memoirs of the Royal Astronomical Society*, 81, 25

Cumming A. M., Marcy G. W., Butler R. P., 1999, *ApJ*, 526, 890

Da Costa G. S., 1992, pp 90-104 in *Astronomical CCD Observing and Reduction Techniques*, ASP Conference Series, Vol. 23, Steve B. Howell, ed.

Del Principe *et al*, 2006, *ApJ*, 652, 362

Dominik M. *et al*, 2002, *P&SS*, 50, 299

Donati J.-F. *et al*, 1992, *A&A*, 265, 682

Donati J.-F. *et al*, 1997b, *MNRAS*, 291, 658

Donati J.-F., Collier Cameron A., 1997a, *MNRAS*, 291, 1

Donati J.-F., Semel M., Praderie F., 1989, *A&A*, 225, 467

Dziembowski W. A, Cassisi S., 1999, *AcA*, 49, 371

Dziembowski W. A., Mizerski T., 2004, *AcA*, 54, 363

Dziembowski W. A., and Cassisi, S., 1999, *AcA*, 49, 371

Dziembowski W., 1997, *AcA*, 27, 95

Feast *et al*, 2008, 2008arXiv0803.0466F

Feast M., 1999, *PASA*, 111, 775

Feast M., 2003, *LNP*, 635, 45

Fields D. L. *et al*, 2003, *ApJ*, 572, 1031

Foster G., 1996, *AJ*, 112, 1709

Gilmore G., King I. R., van der Kruit P. C., 1990, "*The Milky Way as a Galaxy"*, Mill Valley: University Science Books

Gouda N. *et al*, 2007, *AdSpR*, 40, 664

Harris W. E., 1996, *AJ*, 112, 1487

Hawley S. L., Jeffreys W. H., Barnes III T. G., Lai W., 1986, *ApJ*, 302, 626

Held E. V. *et al*, 2001, *ApJ*, 562, 39

Hurta *et al*, 2007, arXiv:0712.0479v1

Hurta Zs. *et al*, 2008, *AJ*, 135, 957

Ibata R. A., Gilmore G., Irwin M. J., *Nature*, 370, 194

Jerzykiewicz M., 1995, *ASPC*, 78, 265

Jesper S., 2006, *MmSAI*, 77, 188

Johnson H. L., Morgan W. W., 1953, *ApJ*, 117, 313

Jones R. V. *et al*, 1992, *ApJ*, 386, 646

Jurcsik J. *et al*, 2008, *MNRAS*, 391, 164

Jurcsik J. *et al*, 2009, *MNRAS*, 393, 1553

Jurcsik J. *et al*, 2009, *MNRAS*, 397, 350

Kanyó S., 1976, *Commun. Konkoly Obs. Budapest*, 7(69), 1

Kemper E., 1982, *AJ*, 87, 1395

King D. S., Cox J. P., 1968, *PASP*, 80, 365

Kinman T. D. *et al*, 1991, *PASP*, 103, 1279

Kinman T. D., Brown W. R., 2010, *AJ*, 139, 2014

Kirkpatrick J. D., *ARA&A*, 2005, 43, 195

Klaus B., Wils P., 2006, *IBVS*, 5698, 1

Kolenberg K. *et al*, 2009, *MNRAS*, 396, 263

Kolenberg K. *et al*, 2011, *MNRAS*, 411, 878

Kolenberg K., Guggenberger E., and the Blazhko collaboration, 2007, *Comm. In Astroseismology*, 150, 381

Kolláth Z., Csubry Z., 2006, *MemSAIt*, 77, 109

Korn A. J. *et al*, 2007, accepted for publication in the *ApJ*

Kovács G., 1994, *Annals of New York Academy of Science*, 295, 693

Kovács G., 1995, *A&A*, 295, 693

Kovács G., 1998, *ASPC*, 135, 52

Kovács G., 1993, "Stochastic Processes in Astrophysics", *Annals of New York Academy of Sciences*, 706, Eds. J. R. Buchler and H. E. Kandrup, p. 70

Kovács G., Buchler J. R., 1988, *ApJ*, 324, 1026

Kurtz D. W. *et al*, 2000, *ASPC*, 203, 291

LaCluyzé A. *et al*, 2004, *ApJ*, 127, 1653

Lee Y. –W., 1992, *AJ*, 104, 1780

Lenz P., Breger M, 2005, *CoAst.*, 146, 53

Linnell Nemec A. F., Nemec J. M., 1985, *AJ*, 90, 2317

Mackey A. D., Gilmore G. F., 2003, *MNRAS*, 343, 747

Martin N. F. *et al*, 2004, 348, 12

McWilliam A., 2011, *Carnegie Observatories Astrophysics Series*, Vol. 5, "RR Lyrae Stars, Metal-Poor Stars, and the Galaxy"

Mizerski T., 2003, *AcA*, 53, 307

Morgan W. W., Keenan P. C., 1973, *ARA&A*, 11, 29

Moro D., Munari U., 2000, *A&AS*, 147, 361

Moskalik P., 1986, *AcA*, 36, 333

Moskalik P., 2000 *ASPC*, 203, 315

Moskalik P., Poretti E., 2002, *ASPC*, 259, 392

Moskalik P., Poretti E., 2003, *A&A*, 398, 213

Muzzin *et al*, 2004, *ASPC*, 310, 180

Nowakowski, R. M., Dziembowski, W. A., 2001, *AcA*, 51, 5

Nowakowski, R. M., Dziembowski, W. A., 2003, *ApSS*, 284, 273

Olech A. *et al*, 1999a, *AJ*, 118, 442

Olech A. *et al*, 1999b, *MNRAS*, 310, 759

Petersen J. O., 1973, *A&A*, 27, 89

Preston G. W., 1959, *ApJ*, 130, 507

Preston G. W., 2011, *AJ*, 141, 6

Pritchet C. J., 1988, in "*The Extragalactic Distance Scale*", ed van den Bergh S., and Pritchet C. J., San Francisco: ASP, p. 120

Pritchet C. J., van den Bergh S., 1987, *ApJ*, 316, 517

Renzini A., *Ap&SS*, 1999, 267, 357

Romano D. *et al*, 2007, *MNRAS*, 376, 405

Romanov Y. S. *et al*, 1987, *Sov. Astron. Lett.*, 13, 29

Romanov Y. S. et al, 1994, *Bul. Spec. Astrophys. Obs.*, 38, 169

Sackett P. D. *et al* 2004, "*Bioastronomy 2002: Life Among the Stars*", Proceedings of IAU Symposium #213. Edited by R. Norris, and F. Stootman. San Francisco: Astronomical Society of the Pacific, p.35

Sandage A., Katem B., Sandage M., 1981, *ApJS*, 46, 41

Sandage A., Saha A., 2002, *AJ*, 123, 2047

Santolamazza P., 1998, *MemSAI*, 69, 307

Sarajedini A., Barker M. K., Geisler D., Harding P., Schommer R., 2006, *AJ*, 132, 1361S

Scargle J. D., 1982, *ApJ*, 263, 835

Schmidt E. G. *et al*, 1990, *ApJ*, 360, 604

Schwarzenberg-Czerny A., 1989, *MNRAS*, 241, 153

Schwarzschild M., 1940, *Harvard College Observ. Circ.*, No. 437

Semel M., 1989, *A&A*, 225, 456

Semel M., 1995, *ASPC*, 71, 340

Semel M., Donati J.-F., Rees D. E., 1993, *A&A*, 278, 231

Semel M., Li J., 1996, *Solar Physics*, 164, 417

Shibahashi H., 2000, *ASPC*, 203, 299

Silberman, N. A. et al, 1998, ApJ, 515, 1

Smith H. A., 1985, *AJ*, 90, 1242

Smith H. A., 1995, *"RR Lyrae Stars"*, Cambridge University Press

Smith H. A. *et al*, 1999, *ApJ*, 118, 572

Soszyński I. *et al*, 2003, *AcA*, 53, 93

Soszyński I. et al, 2011, *AcA*, 61, 1

Sozzetti A., 2009, *Highlights of Astronomy*, 15, 716

Spergel D. N. *et al*, 2003, *ApJS*, 148, 175

Stellingwerf R. F., 1978, *ApJ*, 224, 953

Storm J., 2006, *MemSAI*, 77, 188

Stothers B. R., 2006, *ApJ*, 652, 643

Stothers B. R., 2010, *PASP*, 122, 536

Strugnell P., Reid N., Murray C. A., 1986, *MNRAS*, 220, 413

Suntzeff N. B., 1992, *ASPC*, 30, 161

Suntzeff N. B., Kinman T. D., Kraft R. P., 1991, *ApJ*, 367, 528

Szczygieł D. M., Fabrycky D. C., 2007, *MNRAS*, 377, 1263

Szczygieł D. M., Pojmański G., Pilecki B., 2009, AcA, 59, 137

Szeidl, B., 1988, in *Multimode Stellar Pulsations*, ed. G. Kovacs, L. Szabados, and B. Szeidl, Budapest, Konkoly Observatory, p 45

Szymański M. K., 2005, *AcA*, 55, 43

Taam R. E., Kraft R. P., Suntzeff N., 1976, *ApJ*, 207, 201

Talon S., 2007, arXiv:0708.1499v1 [astro-ph]

Thackeray A. D., Wesselink A. J., 1953, *Nature*, 171, 693

Udalski A., Kubiak M., Szymański M., 1997, *AcA*, 47, 319

Van Hoolst T., Dziembowski W.A., Kawaler S.D., 1998, *MNRAS*, 297, 536

Van Hoolst, T., 1992, "Nonlinear, Non-radial Oscillation of Stars. Resonance Between Two Modes with Nearly Equal Frequencies", PhD thesis, Katholike Universiteit, Leuven

Van Hoolst, T., Dziembowski, W., and Kawaler, S. D., 1998, *MNRAS*, 297, 536

Vauclair S., 2003, *Ap&SS*, 284, 205

Wesselink A. J., 1969, *MNRAS*, 144, 297

Wozńiak P. R., 2000, *AcA*, 58, 69

Zinn R., 1980, *ApJ*, 241, 602

Zinn R., 1985, *ApJ*, 293, 424